Mechanism of damage to fibronectin by myeloperoxidase derived oxidants

Author: Siriluck Vanichkitrungruang

Supervisors: Prof. Michael J. Davies & Dr. Christine Y. Chuang

A thesis submitted in fulfilment of the requirements for the degree of Doctor of Philosophy

Faculty of Medicine

University of Sydney

2018

Declaration

The work contained in this Thesis is original work conducted by the author at the Heart Research Institute, Sydney, and Panum Institute, Copenhagen. It has not been submitted to any other institution for a higher degree and does not contain any materials previously published or written by another person except where due reference is made in the text.

Siriluck Vanichkitrungruang

Bachelor of Medical Science (First Class Honours)

"I try to best every previous defining moment with a new one. In that way you don't live in the past, you live for the future."

- Neil deGrasse Tyson

Abstract

Atherosclerosis is characterised by the deposition of lipids in the arterial wall, which triggers an inflammatory response. Leukocytes migrate into the area of injury and release heme-peroxidase myeloperoxidase (MPO) into the extracellular matrix (ECM) milieu, which converts hydrogen peroxide (H_2O_2) in the presence of halides or pseudohalides, chloride (Cl^-) and thiocyanate (SCN^-), to generate oxidants hypochlorous acid (HOCl) and hypothiocyanous acid (HOSCN), respectively. There is considerable evidence that these oxidants, particularly HOCl, modify and damage surrounding cells and ECM proteins at the site of inflammation, and therefore have been suggested to play a role in the pathophysiology of cardiovascular disease (CVD). HOCl is a highly reactive oxidant and has been observed to modify and oxidise lipids, proteins, DNA, and RNA, which subsequently leads to cellular dysfunction. In contrast, HOSCN is much less reactive compared to HOCl and has a high specificity for cysteine (Cys) residues. Oxidation by HOSCN is generally reversible by endogenous antioxidant mechanisms but can be irreversibly damaging at high concentrations. The ECM harbours several important proteins including fibronectin (FN), which plays a role in matrix assembly, remodelling, and assists in cell functions. FN possesses functionally important epitopes including: cell binding fragment (CBF), heparin binding fragment (HBF), and extra domain A (EDA). The proximity between FN and MPO-derived oxidants makes it a likely target for oxidation and modifications. Therefore, this project aims to elucidate the effects of HOCl, and HOSCN on ECM protein, FN, and whether SCN^- concentrations can modulate the extent of modifications causes by HOCl.

In the first study, commercially-derived human plasma FN was exposed to increasing concentrations of reagent HOCl for 2 hr at 37°C. Human plasma FN exposed to

HOCl resulted in fragmentation and aggregation (or formation of altered species) of FN, particularly at greater than 50x molar ratios as seen with sodium dodecyl sulfate polyacrylamide gel electrophoresis (SDS-PAGE), silver staining and Western blotting. HOCl targets methionine (Met) and tryptophan (Trp) residues in a dose dependent manner, but not tyrosine (Tyr) residues. Methionine sulfoxide (MetSO), a by-product of Met oxidation, was observed to be present in native FN and treatment with HOCl. MetSO was likely to be further oxidised with treatment of higher concentrations of HOCl. The FN CBF and HBF epitopes were targeted and modified by HOCl as seen with loss of antibody recognition using enzyme-linked immunosorbent assay (ELISA) and Western blotting. Human coronary artery endothelial cells (HCAEC) exposed to HOCl-modified FN were observed to lose adhesion with impaired cell spreading, and a reduction in cell metabolic activity. Furthermore, HCAEC exposed to HOCl-modified FN were observed to up- and down-regulate genes associated with ECM and adhesion molecules. HOCl was also observed to target and modify cellular-derived FN in HCAEC-derived whole ECM extract causing loss of antibody recognition for the CBF, HBF and cellular-derived FN EDA epitopes. These data support the hypothesis that HOCl targets and modifies FN, which subsequently leads to biological dysfunction of HCAEC exposed to HOCl-modified FN.

In the second study, commercially-derived human plasma FN was exposed to increasing concentrations of reagent HOSCN derived from lactoperoxidase (LPO)/SCN^-/H_2O_2 and incubated for 2 hr at 37°C. Modifications by HOSCN to human plasma FN were observed to be less extensive than what was observed with HOCl. HOSCN was observed to structurally modify human plasma FN starting at 10x molar ratio with minor formations of fragments and aggregates (or altered species). HOSCN was observed to target and oxidize Cys (thiol) residues as examined using a ThioGlo assay, which is in-line with the knowledge that HOSCN has a specificity for Cys residues. The functional CBF epitope on FN was observed to be modified by HOSCN but to a lesser extent compared to HOCl. Subsequent biological functional assays for cell adhesion and metabolic activity

for HCAEC exposed to HOSCN-modified FN showed no changes. However, these HCAEC were observed to up- and down-regulate certain ECM and adhesion molecules, although fewer changes were examined when compared to HCAEC exposed to HOCl-modified FN. Exposure of HCAEC-derived whole ECM extract to HOSCN resulted in no significant changes to the functional CBF, HBF, and EDA epitopes, and no major structural changes were observed in Western blots. These data support the hypothesis that HOSCN does modify FN but to a lesser extent compared to HOCl, suggesting that the presence of HOSCN over that of HOCl may lead to less FN damage.

In the third study, human plasma FN was exposed to an enzymatic MPO/Cl^-/H_2O_2 or MPO/SCN^-/H_2O_2 system, which would better simulate the reaction that occurs *in vivo*. Exposure of human plasma FN to the enzymatic MPO/Cl^-/H_2O_2 system resulted in extensive modifications to the structure of FN as observed with silver staining and Western blotting. The functional CBF and HBF epitopes on FN were both observed to be targeted and modified by the enzymatic MPO/Cl^-/H_2O_2 system. Furthermore, a HOCl-generated epitope was observed with increasing concentration of H_2O_2. A decrease in HCAEC adhesion and proliferation were observed when HCAEC were exposed to FN modified by the enzymatic MPO/Cl^-/H_2O_2 system. In contrast, exposure of human plasma FN to the enzymatic MPO/SCN^-/H_2O_2 system resulted in minor modifications to the protein structure and functional CBF, and HBF epitopes. HCAEC adhesion and proliferation were not significantly affected when incubated on treated FN. These data support that oxidants derived from the enzymatic MPO/Cl^-/H_2O_2 modifies the structure of human plasma FN resulting in loss biological function. The extent of modification by MPO/SCN^-/H_2O_2 system on human plasma FN was minor compared to the MPO/Cl^-/H_2O_2 system and resulted in no changes to cell adhesion or metabolic activity.

The final study examined the competition between Cl^- and SCN^- as a substrates for MPO and their modifications on human plasma FN. At physiologically relevant concentrations of 100 mM of Cl^- and absent or low concentrations of SCN^-, FN is

modified resulting in protein fragmentation and aggregation (or altered species), and loss of antibody recognition of the functional CBF and HBF epitopes on FN. Furthermore, a formation of HOCl-generated epitopes were also observed. Addition of increasing concentrations of SCN^- resulted in a shift of structural modifications that were specific to $MPO/Cl^-/H_2O_2$ to those observed with treatment using the enzymatic $MPO/SCN^-/H_2O_2$ system. The addition of increasing concentration of SCN^- also mitigated the loss of antibody recognition, returning it back to levels similar to control. This supports the hypothesis that addition of SCN^- assists in mitigating damage derived from the enzymatic $MPO/Cl^-/H_2O_2$ system.

Acknowledgements

I would first like to humbly thank my supervisors Prof. Mike Davies and Dr. Christine Chuang for the opportunity to work alongside them over the last five years. It has been an honour and an absolute pleasure to be taken under your wings and to learn the wonders of science and research.

Prof. Mike Davies, you have been a wonderful supervisor and mentor. Thank you for the opportunity to be your student, and the great opportunities to explore the world. It has ignited a passion in me to seek and experience more every day. Your constant reassurance, support and guidance have gotten me through many difficulties along the way. You have truly made this a memorable journey that I will fondly look back on.

Dr. Christine Chuang, you have made such an impact on me over the period of my candidature. Your upbeat attitude and passion in research have left an everlasting impression on me. When you and Mike made the move to Copenhagen, I couldn't help but follow in pursuit. The difficulties of moving to a new country on the other side of the world were easily overcome with the support from both you and Fred. I am so ever grateful for everything.

Associate Prof. Clare Hawkins, thank you for your support and advice particularly during my time at HRI prior to moving to Copenhagen.

Thank you to Prof. Ernst Malle and Astrid Hammer as collaborators for the immunohistochemistry studies.

Thank you to everyone at the Heart Research Institute, particularly the Free Radical and Immunobiology Group. Special thanks to Georg Degendorfer for his help on experimental

procedures, and Pat Pinsansarakit for all his work in Tissue Culture.

Thank you to the Protein Oxidation Group at Panum Institute at the University of Copenhagen for being so welcoming. It was wonderful getting to know you all over the last few years.

Special thanks to Luke Carroll, my work wife Kelly Gardiner, and Song Huang. You have been most supportive over the last five years. The crossword breaks and board game nights has always filled me with energy and laughter to keep me going.

Thank you to all my friends in Australia, especially Mustafa Agha, Betty Wong, Oliver Jones, Jimmy Yu, Michael Camden, and Grace Abou Abdallah, for their constant support.

Thank you to all my friends in Denmark. Special thanks to Jacob Merrild and Mikkel Rasmussen for their friendship and technical help using LaTeX.

Lastly, thank you to my parents (Piyavee and Tom), my brother (Bobby), and my girlfriend (Lovis Hakala) for your unconditional love and support. Thank you for picking me up when I may have faltered, and guiding me through to the end.

Contents

List of Abbreviations

3,5-chloroTyr	3,5-chloroTyrosine
3-chloroTyr	3-chloroTyrosine
3-nitroTyr	3-nitroTyrosine
6-nitroTyr	6-nitroTyrosine
o-Tyr	*ortho*-Tyrosine
ADAMTS	a disintegrin and metalloproteinase with a thrombospondin motif
AP	Alkaline phosphatase
Arg	Arginine
Asn	Asparagine
Br^-	Bromide
CAD	Coronary artery disease
CBF	Cell binding fragment
CHD	Coronary heart disease
CHO	Chinese Hamster Ovary cells
Cl^-	Chloride
Co-IP	Co-immunoprecipitation
CO_2	Carbon Dioxide
CS	Chrondroitin sulfate
CTGF	Connective Tissue Growth Factor
CTNN	Catenin
CVD	Cardiovascular disease
Cys	Cysteine
dG	2'-deoxyguanosine
di-Trp	di-Tryptophan

di-Tyr	di-Tyrosine
dilDTNB	diluted DTNB
DOPA	L-3,4-dihydroxyphenylalanine
DTNB	5,5′-dithiobis-(2-nitrobenzoic acid)
EC	Endothelial cells
ECM	Extracellular matrix
EDA	Extra domain A
EDB	Extra domain B
EDTA	Ethylenediaminetetraacetic acid
ELISA	Enzyme-linked immunosorbent assay
Endo-Basal	Endothelium cell basal media without phenol red
eNOS	Endothelial nitrix oxide synthase
EPO	Eosinophil Peroxidase
FN	Fibronectin
GAG	glucosaminoglycan
GlcNAc	N-acetylglucosamine
$GlcNSO_3$	glucosamine-N-sulphate
Gln	Glutamine
$GlnNH_2$	N-substituted glucosamine
GSH	Glutathione
H_2O_2	Hydrogen peroxide
HBF	Heparin binding fragment
HBGF	Heparin binding growth factor
HCAEC	Human coronary artery endothelial cells
His	Histidine
$HO^{\bullet}$	Hydroxyl radical
HOBr	Hypobromous acid
HOCl	Hypochlorous acid

HOI	Hypoiodous acid
HOSCN	Hypothiocyanous acid
HRP	Horse peroxidase
HS	Heparin/Heparan sulfate
HUVEC	Human umbilical vein endothelial cell
I^-	Iodide
IHC	Immunohistochemistry
iNOS	Cytokin-inducible nitric oxide synthase
LDL	Low density lipoprotein
LOX	Lysyl oxidase
LPO	Lactoperoxidase
Lys	Lysine
Met	Methionine
MetSO	Methionine sulfoxide
MMP	Matrix metalloproteinase
MPO	Myeloperoxidase
NaCl	Sodium chloride
NADPH	Nicotinamide adenine dinucleotide phosphate
NaOH	Sodium hydroxide
NaSCN	sodium thiocyanate
NO_2^-	Nitrite
$NO_2^\bullet$	Nitrogen dioxide radical
$NO^\bullet$	Nitric Oxide
$O_2^{\bullet-}$	Superoxide
$ONOO^-$/ONOOH	Peroxynitrite
OPA	*o*-Phthaldialdehyde
PBS	Phosphate buffer saline
PBST	0.1% (w/v) tween-20 in PBS

PTAH	Phosphotungstic acid haemotoxylin
PVDF	Polyvinylidene fluoride
QCM	Quartz Crystal Microbalance
RS-OH	Sulfenic acid
RS-SCN	Thiosulfenyl thiocyanate
RSO_3H	Cysteic acid
RT	Reverse-Transcriptase
SCN^-	Thiocyanate
SDS-PAGE	Sodium dodecyl sulfate polyacrylamide gel electrophoresis
SEL*	Selectin L, Selectin P, Selectin E
SeMet	Seleno-methionine
SeMetO	Selenoxide
SMC	Smooth muscle cells
SPG7	Paraplegin Matrix AAA Peptidase Subunit
SPR	Surface Plasmon Resonance
TBS	Tris-buffered saline
TBST	0.1% (w/v) Tween 20 in TBS
THBS	Thrombospondin
THBS-1	Thrombospondin-1
THF	Tetrahydrofuran
TIMP	Tissue inhibitor of metalloproteinases
TNB	5-thio-2-nitrobenzoic acid
Trp	Tryptophan
Tyr	Tyrosine
$Tyr^\bullet$	Tyrosine radical
v/v	Volume/Volume
VCAN	Versican
VEGF	Vascular endothelial growth factor
w/v	Weight/Volume

List of Figures

List of Tables

Chapter 1

Introduction

1.1 General Overview

This chapter will provide background information on myeloperoxidase (MPO), extracellular matrix (ECM), and their role in the immune response and in the basement membrane. It will also include a literature review on the current knowledge of the relationship between MPO and ECM proteins, and their role in the inflammatory disease atherosclerosis.

1.2 Chronic inflammatory disease and atherosclerosis

Atherosclerosis is a common chronic inflammatory disease that is characterized by the accumulation of lipids in the arterial wall, in particular those derived from low density lipoprotein (LDL) (Figure 1.1) [1]. LDL is necessary for lipid transport and is derived endogenously in small quantities within the body, but high levels can occur with poor dietary intake, leading to increased risk of cardiovascular disease [2]. Increased circulating levels of LDL leads to increase occurrences of LDL deposits in the arterial walls with evidence of extensive LDL modifications by enzymatic mechanisms (lipoxygenase, myeloperoxidase, NADPH oxidases, and nitric oxide synthase), reactive nitrogen/oxygen species, free radicals and two-electron oxidant [3–5]. Such modifications have been suggested to contribute to LDL retention [3, 4, 6]. An inflammatory response occurs against modified LDL, with un-regulated uptake by macrophages leading to formation of foam cells [7–9]. Oxidised LDL is seen to express a number of pro-atherogenic and atherosclerotic effects including changes to the arterial wall proteins [5].

MPO is a leukocyte-derived haem-peroxidase that produces reactive oxidants during inflammation [11]. These oxidants are proposed to structurally modify the ECM of the arterial wall basement membrane. Structurally modified ECM protein may lose its function, which can alter metabolism and cause endothelial dysfunction. Further changes can occur when MPO and its oxidants, interacts with smooth muscle cells (SMC) during the development of atherosclerosis [12, 13]. Inflammatory cell and SMC infiltration [14], accumulation of intracellular/extracellular lipids [1, 15], and endothelial dysfunctions [16] are all hallmark characteristics of plaque formation in atherosclerosis.

Moreover, occlusion of the vessel in combination with arterial calcification results in hardening and inflexibility in advanced lesions, which leads to an increased pressure on arterial walls [17]. As with any wound healing or formation of lesions, the process of fibrosis occurs, which is highly dependent on the basement membrane (and corresponding ECM) to generate a fibrous cap for a more stable lesion. Mortalities and complications

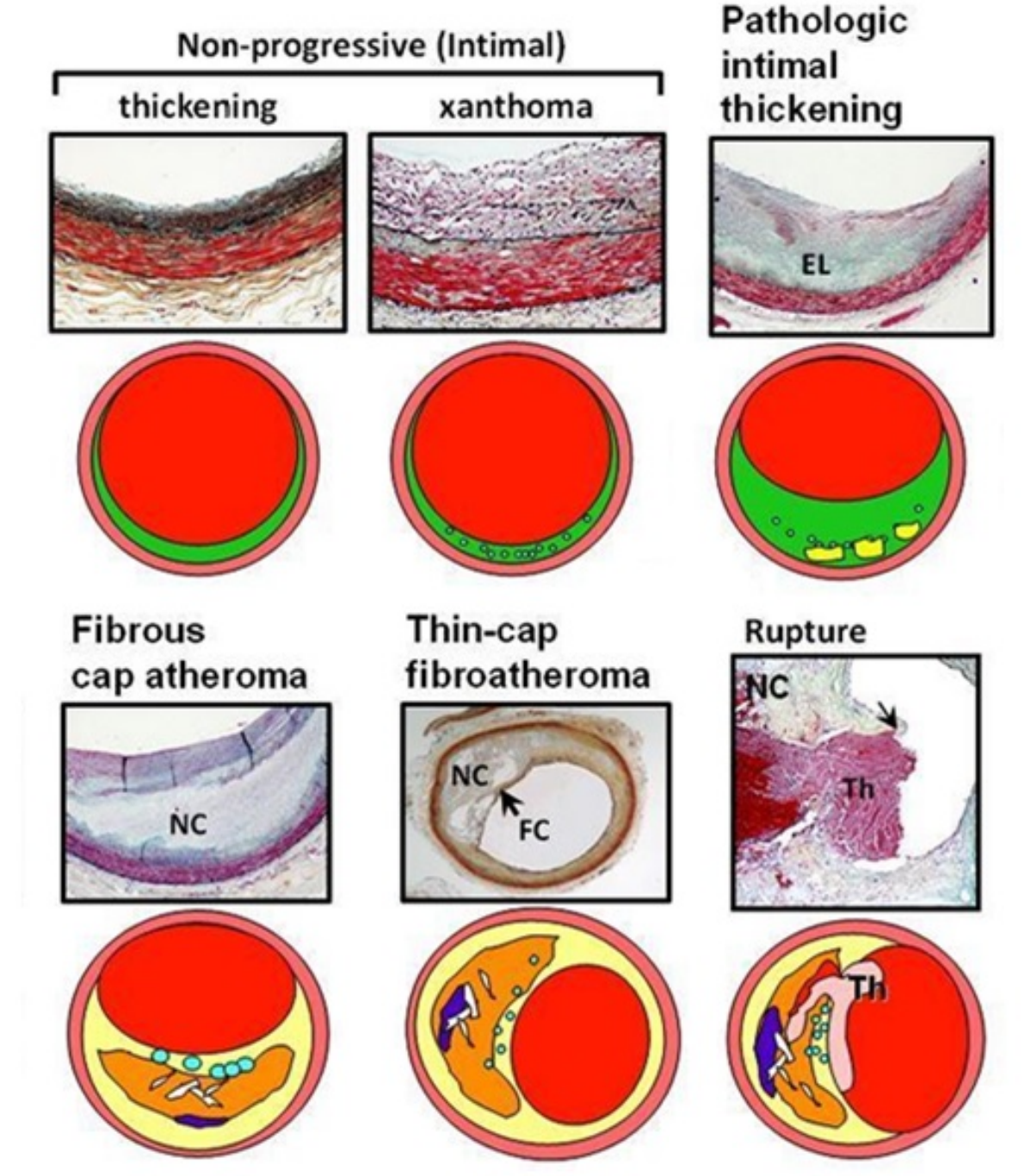

Figure 1.1: **Schematic diagram demonstrating the progression of atherosclerosis. EL is extracellular lipid, NC is necrotic core, FC is fibrous cap, and Th is luminal thrombi.** Adapted from Virmani, 2000 [10]

from chronic heart disease (CHD), as well as cerebrovascular disease (i.e. myocardial infarction and stroke, respectively) have been associated with rupture of lesions and subsequent stenosis of the blood vessels, rather than the presence of an atherosclerotic lesion itself [18]. The likelihood of rupture is determined by the composition of the plaque; thin fibrous caps with higher levels of inflammatory cells are more likely to rupture than a plaque with a thick fibrous cap [1]. Thus, structural modifications and/or damage to the basement membrane and the associated ECM can make the plaque prone to rupture. Therefore, it is pertinent to understand how such modifications may come about and there is substantial evidence that oxidants produced during inflammation (notably those derived from MPO) contribute to this damage.

1.3 Myeloperoxidase and its oxidative reactions

During the "respiratory burst", activated leukocytes convert diatomic oxygen to superoxide radical ($O_2^{\bullet-}$) [19, 20]. $O_2^{\bullet-}$ can subsequently undergo spontaneous or catalytic (by superoxide dismutase enzyme) dismutation to generate the antimicrobial agent hydrogen peroxide (H_2O_2) (Figure 1.2) [19, 20]. MPO is also released extracellularly into the extracellular milieu (via degranulation of activated leukocytes) or are transcytosed from plasma through the endothelium, and has been found to co-localise with fibronectin (FN) in the ECM [21, 22].

MPO is a dimeric protein of approximately 146 kDa, made up of two monomers of 73 kDa linked by a disulfide bond. Each identical monomer are functionally independent and are composed of a heavy (58.5 kDa) and a light (14.5) chain [23]. The active site on MPO is only easily accessible to H_2O_2 and small anions [24]. Reaction between H_2O_2 and ferric MPO converts the enzyme to compound I by two electron oxidation (Figure 1.3) [25]. MPO compound I, in the presence of H_2O_2 and halides (chloride - Cl^-, bromide - Br^-, iodide - I^-) or pseudohalides (thiocyanate - SCN^-) catalytically converts these substrates to hypohalous acids, hypochlorous (HOCl), hypobromous (HOBr), hypoiodous (HOI), and hypothiocyanous (HOSCN) acid, respectively via a two electron reduction [26]. This process reverts MPO back to the ferric enzyme state [26]. MPO have reactivity rates for substrates in the preference order of $I^- \sim SCN^- > Br^- > Cl^-$ (Table 1.1) [27]. Other heme enzymes also exist such as eosinophil peroxidase (EPO) and lactoperoxidase (LPO). EPO is an eosinophil-derived granule that play a role in allergies and parasitic infections [28], and LPO is found to be present in higher concentrations in saliva, milk and tears [29]. LPO preferentially generates HOSCN, while EPO has previously been found to preferentially generate both HOBr and HOSCN over HOCl [26, 30].

Hypohalous acids generated via the MPO halogenation cycle are one of many reactions that can cause oxidation. MPO is also capable of generating radicals via its peroxidase cycle to produce other reactive species. MPO compound I, via a one electron oxidation,

Table 1.1: **Second-order rate constant of halide and pseudohalide substrates.**

Substrate	Second-order rate constant
SCN^-	$9.6 \pm 0.5 \times 10^6\ M^{-1}\ s^{-1}$
I^-	$7.2 \pm 0.7 \times 10^6\ M^{-1}$
Br^-	$1.1 \pm 0.7 \times 10^6\ M^{-1}$
Cl^-	$2.5 \pm 0.3 \times 10^4\ M^{-1}\ s^{-1}$

converts to compound II, oxidizing free radical $O_2^{\bullet-}$ and nitric oxide ($NO^{\bullet}$). The MPO peroxidase cycle generates nitrogen dioxide radical ($NO_2^{\bullet}$) tyrosyl radicals from the oxidation of nitrite (NO_2^-) and Tyr, respectively [26]. $O_2^{\bullet-}$ is particularly known to react with Tyr residues (free or present on peptides) to form crosslinks such as di-Tyr [31].

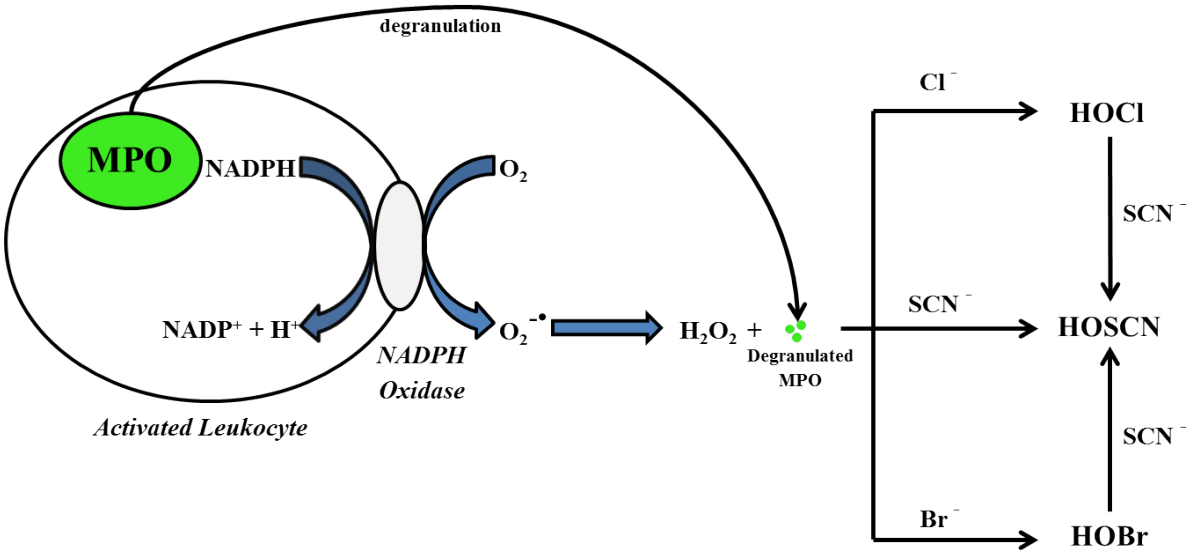

Figure 1.2: **Schematic diagram demonstrating the synthesis of MPO-derived oxidants generated via the two electron oxidation halogenation cycle.** Superoxide is generated from NADPH oxidase, which converts to H_2O_2 spontaneously or enzymatically via superoxide dismutase. H_2O_2 reacts with degranulated MPO in the presence of physiological concentrations of halides to produce HOCl, HOSCN, and HOBr.

Generation of bactericidal oxidants occur in inflammation invoked against foreign pathogens [32]. In cases of chronic inflammation, generation of high concentrations of these reactive oxidants can be damaging to host cells and molecules (lipids, proteins,

peptides, DNA), such as may occur in atherosclerosis [33]. The presence of MPO has been associated with endothelial cell (EC) dimorphism and dysfunction [34]. Moreover, the localisation of MPO and the release of oxidants within the endothelium has been associated with ECM protein fragmentation, cross-linking [35], and modifications to amino acids [33, 36].

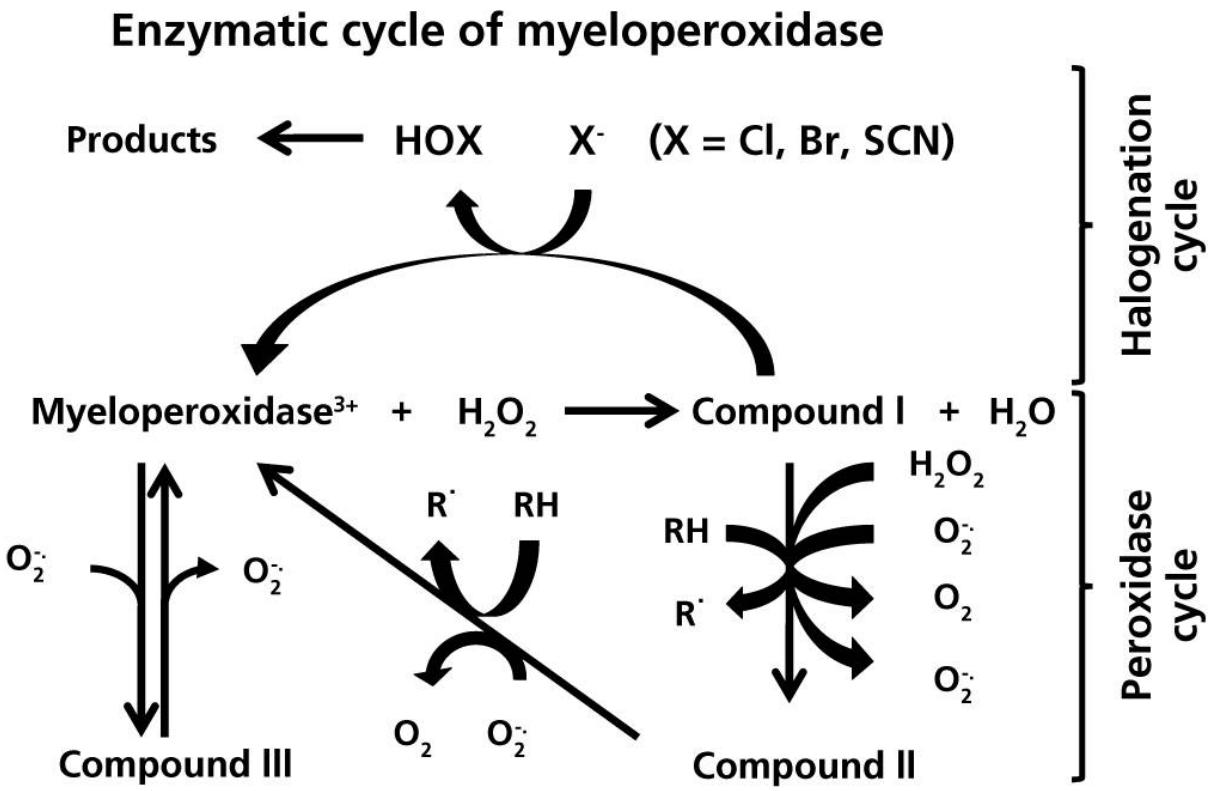

Figure 1.3: **Schematic diagram demonstrating the MPO catalytic cycle.** Image from Davies, 2011 [26]

High levels of plasma MPO have been clinically correlated with a prevalence of coronary artery disease (CAD) [37], with an even greater prevalence in individuals presenting with diabetes [11], and a history of smoking and hypertension [38]. Moreover, deficiency in MPO plasma levels have been correlated with a reduced rate of cardiovascular disease [39]. Previous studies have correlated high systemic levels of MPO with plaque erosion, which is another mechanism that can lead to thrombus occlusion as opposed to the commonly known plaque rupture [40, 41]. Plaques that are susceptible to erosion are associated with

absent or small lipid cores and elevated SMC, whereas plaque ruptures are associated with a lipid rich core, higher levels of migrated inflammatory cells, with greater evidence of matrix degradation and formation of thinner fibrous caps [40, 41]. Plaque erosion have been shown to primarily occur in premenopausal women with coronary thrombosis [42, 43]. MPO, being a cationic compound, has been shown to co-localize in the sub-endothelial matrix with negatively charged proteins such as glucosaminoglycans (GAG) and also FN [21, 22]. Thus, MPO-derived oxidant damage may be one mechanism that modifies the vessel, and is a contributor to unstable plaque formations in atherosclerosis.

1.3.1 Hypochlorous Acid

The physiological concentration of Cl^- is known to be around 100 mM in humans [44]. Due to higher concentrations of Cl^- compared to other halides, cytoxic HOCl is the key component generated in host anti-microbial defense [32]. HOCl is known to be highly reactive and acts on several oxidisable groups including: unsaturated fatty acids, sulfur-ethyl group, sulfhydryl groups, haem groups and iron-sulfur centers [8, 45–48]; by-products generated during oxidation of these groups have been observed in chronic inflammatory diseases. HOCl has been shown to oxidize proteins, peptides, lipid, DNA, RNA, carbohydrate chains and antioxidants [49, 50].

HOCl reacts with amino acid side chains in proteins with a kinetic preference order of: Cysteine (Cys) > Methionine (Met) > Cystine $\sim$ Histidine (His) $\sim$ α-amino $\sim$ > Tryptophan (Trp) > Lysine (Lys) > Tyrosine (Tyr) $\sim$ Arginine (Arg) > Glutamine (Gln) $\sim$ Asparagine (Asn) [49, 51]. The action of HOCl on Cys residues results in the formation of unstable sulfenyl chloride intermediate, which can react with water to yield cysteic acid (RSO_3H) [49]. Furthermore, sulfenyl chloride can also form dilsulfide crosslinks by reacting with other Cys residue or with other thiol groups [49]. Reaction between HOCl and Met has been found to commonly generate methionine sulfoxide (MetSO), a common oxidation species of Met and has been linked to oxidative stress [51, 52]. Depending on the availability of other amino acids, it's likely that HOCl will react with Tyr and Trp residues [26]. This reaction has previously been shown to produce strong di-Tyr and di-Trp crosslinks, which are known to form non-reducible aggregates [53, 54].

HOCl can react with nitrogen containing compounds, such as free α-amino groups or lysine residues found on proteins to form chloramines. In the presence of biological reductants (e.g. Met, ascorbates, and thiols), chloramines can revert back to their parent amines but have also been shown to readily degrade *in vivo* to form aldehydes (Figure 1.4) [55–57]. Decomposition by decarboxylation of chloramines tend to form unstable imines, which can further lose their ammonia group via hydrolysis [49]. The ammonium ion can

cycle back to react with HOCl to form monochloramines and further react with other groups. Furthermore, chloramines can transfer chlorine to Tyr (also His and Lys) residues [58], leading to formation of 3-chloroTyr and subsequently to 3,5-chloroTyr, which are notably long-lived biomarkers of HOCl modifications [48, 59].

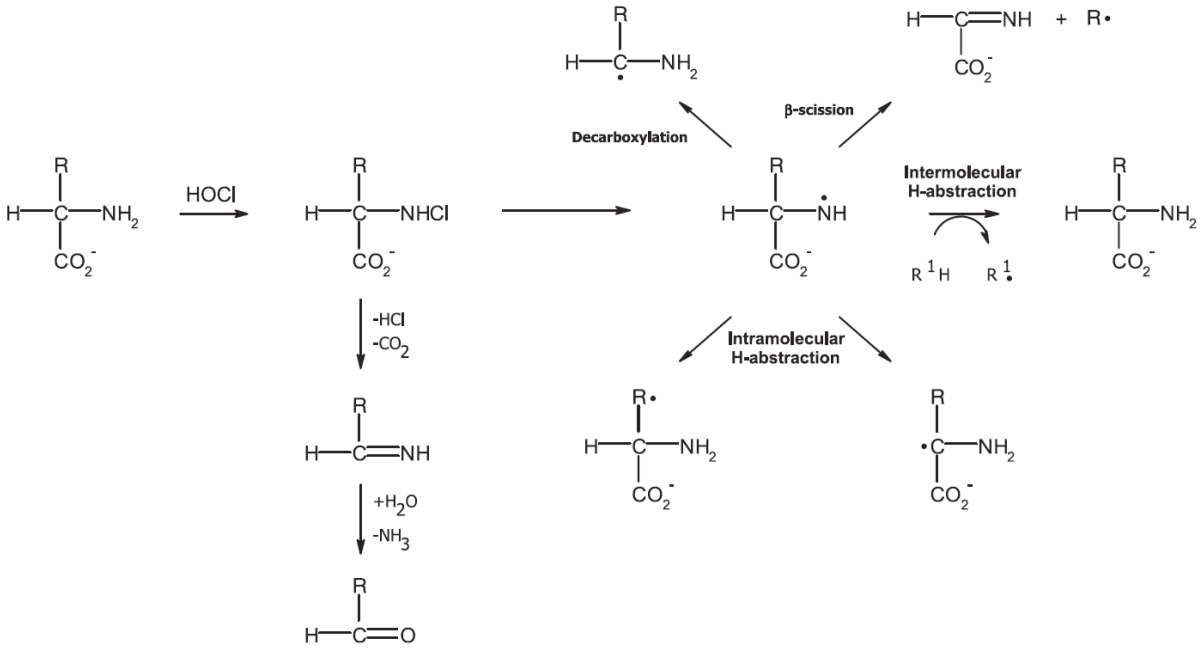

Figure 1.4: **Mechanism of rearrangement in nitrogen-centred radicals.** Image from Hawkins, 2003 [49]

These mechanisms of HOCl oxidation are commonly investigated to elucidate the reaction of HOCl with ECM-derived proteins. Chlorinated Tyr residues, 3-chloroTyr and 3,5-chloroTyr, have been used as biomarkers to indicate MPO activity (Figure 1.5) [48, 60–62]. Chlorinated Tyr are a minor product but are more stable (particularly in acidic conditions) compared to chloramines, and thus can serve as a biomarker for HOCl-mediated modifications [48, 56, 57]. These products can therefore be detected with sensitive and quantitative analytical methods (although they are invasive and destructive to cells and tissues) [57]. However, chlorination can occur in the stomach likely by Cl_2, which is in equilibrium with HOCl, thus chlorinated Tyr can form non-enzymatically in these highly acidic conditions (Figure 1.5) [56]. Other analytical detection methods

that have been used are immunohistochemistry (IHC) or Western blotting utilising an antibody that was originally raised against HOCl-oxidized LDL, known as clone 2D10G9 [63]. This antibody is found to bind to an un-identified HOCl-generated epitope, and has been detected in intermediate and advanced lesions. Localization of 2D10G9 was associated with long thin cells, suggestive of SMC or fibroblasts supported by positive staining of phosphotungstic acid haemotoxylin (PTAH), an SMC marker [8, 63].

In previous studies, it was also found that HOCl targets and modifies ECM proteins as investigated in human atherosclerotic lesions and pig aortae [64]. ECM derived from healthy pig aortae exposed to HOCl resulted in increased levels of oxidized amino acids detected, such as increased formations of di-Tyr, *o*-Tyr, 3-chloroTyr, and L-3,4-dihydroxyphenylalanine (DOPA) [64]. The exposure of SMC-derived ECM to HOCl resulted in the rapid consumption of the oxidant and immediate formation of chloramines and chloramides, which were found to degrade over time [65]. Furthermore, HOCl was found to mediate fragmentation of SMC-derived ECM as seen with increasing detection of radio-labeled amino acids released [65].

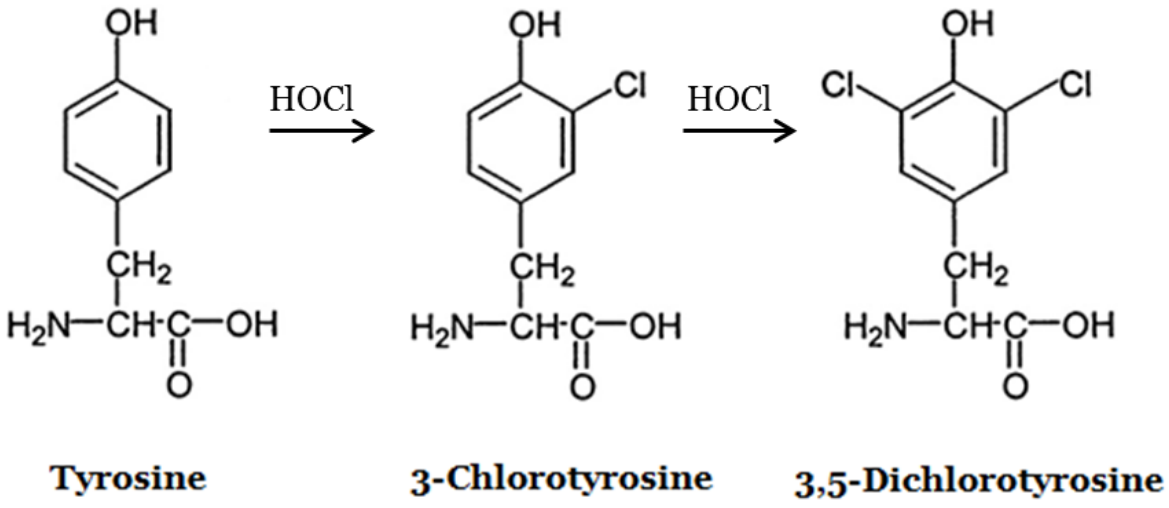

Figure 1.5: **Chlorination of Tyr residues by HOCl to form 3-chloroTyr and 3,5-chloroTyr.** Adapted from Winterbourne and Kettle, 2003 [56].

GAGs, such as heparin/heparan sulfate (HS) and chondroitin sulfate (CS), are polysaccharides that are covalently attached to a core protein to form proteoglycans.

These GAGs have been previously shown to be modified and damaged by HOCl [66]. HS such as found on proteoglycan perlecan, are an important protein ligand (as discussed later in this chapter), and due to being highly anionic has been found to bind to MPO [67]. HOCl was found to not directly modify HS chains despite its highly reactive (N-unsubstituted) glucosamine ($GlcNH_2$) residues. However, it was proposed to mediate MPO-derived HOCl damage on the protein core of perlecan leading to loss of EC adhesion [67]. This damage was found to be attenuated with the addition of heparin, which blocked the binding of MPO [67]. $GlcNH_2$ residues, GlcNAc (N-acetylglucosamine), and $GlcNSO_3$ (glucosamine-N-sulphate) have previously been found to form chloramines/di-chloramines, and N-chlorosulfonamides and chloramides, thus it was interesting to see that this was not the case with whole perlecan protein [68, 69]. Hyaluronic acid and CS exposed to HOCl were also found to form chloramides [70]. These chloramides were found to react with O_2 and mediated fragmentation of the GAGs [71]. Moreover, exposure of SMC-derived whole ECM to HOCl was found to release uronic acid, which is a sugar acid found on GAGs [65]. This suggests that HOCl may react directly with GAGs but in whole protein, it has been found to direct the damage to certain locations on the proteins due to binding and proximity of MPO.

Deposition of fatty acids and cholesterol in the vascular wall is met with oxidation by HOCl leading to formation of chlorohydrins, which has been detected in atherosclerotic plaques [72, 73]. HOCl has a higher reactivity with proteins compared to fatty acids/cholesterols, and therefore resulted in lower levels of chlorohydrins detected [73]. The formation of these species, particularly oxidized LDL, which exhibits proatherogenic properties, can cause downstream effects inducing cellular changes [72], ATP depletion, human myeloid cell toxicity [74], and promotes the development of atherosclerosis [75, 76]. Furthermore, oxidized LDL itself is deleterious within plaques, however it can be taken up by cells, such as migrated leukocytes or EC, leading to damage to perinuclear proteins [76, 77].

HOCl has been found to also oxidize DNA and RNA, in particular guanine, which has the

lowest standard reduction potential compared to the other bases [78]. Oxidation of DNA leads to formation of several products, such as 8-hydroxyguanine and 8-hydroxyadenine, which have been detected in lesions [79]. Moreover, it can also lead to formations of semi-stable chloramines (and subsequent radicals), which have been found to further react with DNA to form crosslinks [49, 80]. Chloramine formation on DNA have been previously shown to occur more rapidly with uridine and thymidine bases (3.0×10^4 M^{-1} s^{-1}) [80]. The mechanism of oxidation are shared between DNA and RNA, whereby exposure of RNA to oxidants commonly formed 8-hydroxyguanosine by-products [81]. The formation of 8-hydroxyguanosine can lead to mutations on the transcription level if they pair with adenine over cytosine in RNA [82]. Exposure of DNA and RNA may lead to defective protein synthesis due to modifications on base pairs that may cause improper pairing and this can be particularly deleterious in EC and SMC in the progression of atherosclerosis [83–85].

Antioxidants generally scavenge or degrade oxidants and prevent further oxidation. Antioxidants, such as glutathione (GSH), are highly reactive with oxidants, and thus react rapidly to scavenge oxidants leading to formation of stable derivatives [86]. In certain situations, antioxidants can be oxidized by HOCl to form chloramines, albeit at a lower kinetic rate compared to Met and GSH residues [87]. GSH is a common agent for preventing intracellular oxidative damage, and exposure of resting neutrophils to HOCl was found to lead to loss a of both protein thiols and GSH levels [88]. Moreover, exposure of human umbilical vein ECs (HUVECs) to low concentrations of HOCl was found to have similar results with loss of protein thiols and GSH levels [89]. Flavonoids are plant-derived polyphenol antioxidants [90], and the flavonol subclass has been found to react with HOCl [91]. Exposure of flavonols to low or moderate concentrations of HOCl was found to slightly increase the antioxidant activity; however exposure to high concentrations of HOCl resulted in the loss of antioxidant activity by the flavonols [91].

As can be seen from these previous studies, HOCl is promiscuous and has been found to react widely with many components of the sub-endothelium and plasma. This leads

to modifications and damage, which can subsequently lead to cellular dysfunction. The vascular environment is highly dependent on the healthy functioning of cells and proteins and thus investigations into the effect of HOCl on ECM proteins would be highly valuable. Current experiments were designed to expand and better shape our understanding of these changes by characterising the mechanism of action of HOCl upon specific and key ECM proteins.

1.3.2 Hypothiocyanous Acid

HOSCN is produced by enzymatic reactions between MPO and SCN^- [26], but can spontaneously occur as a reaction between HOCl and SCN^- [92, 93]. SCN^- is present in varying physiological concentrations within the body with high levels detected within the oral cavity, which is converted to HOSCN by antimicrobial LPO despite substantial excess of chloride [94]. The physiological plasma concentration of SCN^- ranges between 20-40 μM (0.01-3 mM in other areas of the body [95], with elevated plasma concentrations detected in smokers, which can range between 80-400 μM [96–99].

HOSCN has been found to be an effective antimicrobial agent against invading pathogens due to its specificity for sulfhydryl/acidic thiol groups, such as Cys residues [100, 101]. However, in situations where thiol groups are depleted or inaccessible, HOSCN has been found to react with Trp and Lys residues [26, 102]. The reaction between HOSCN and thiol groups have been observed to form unstable thiosulfenyl thiocyanate (RS-SCN), a transitory derivative that can further react with water to generate sulfenic acid intermediates (RS-OH) [94, 103]. These intermediates have been implicated in protein aggregation forming dilsulfide crosslinks and fragmentation [94, 104–107]. As a consequence of the unstable nature of these products, there is a lack of useful biomarkers that can be used to detect HOSCN-derived modifications, limiting investigations with regards to clinical samples. However, fluorometric ThioGlo assay can be used as an alternative *in vivo* method to investigate the loss of thiol groups [57, 108]. This method utilizes a fluorometric compound that binds to free thiol groups that have not been modified/oxidized [57].

The biochemistry of SCN^-/HOSCN is complex, with conflicting studies suggesting that SCN^- can be damaging and others suggesting that it can act as an antioxidant in some inflammatory diseases, such as cystic fibrosis or CVD [93, 99, 109]. MPO has a higher specificity for SCN^- than Cl^- by almost 730 fold (Table 1.1) [98, 110]. Thus, it has been proposed that at elevated levels of SCN^-, up to 50% of H_2O_2 is converted to HOSCN

with the remaining reacting with other halides such as Cl^- [98, 110]. Young individuals with highly elevated levels of plasma SCN^- presented with greater deposition of LDL and increased presence of fatty streaks in the aortae [111]. Furthermore, high plasma levels of SCN^- were associated with increased carbamylation leading to increased formations of homocitrulline, which has been found to have damaging effects in atherosclerosis [112, 113]. However, with regards to CVD, increased plasma SCN^- levels resulted in smaller plaque formations compared to control in mice [114]. Moreover, moderate elevations of SCN^- in combination with low levels of MPO correlated with decreased mortality rate [99].

The effects of HOSCN on ECM proteins are expected to be different to those examined with HOCl due to the oxidants specificity for thiol groups. The mechanism has not been characterized and thus further investigations can assist in elucidating the potential effects of HOSCN on ECM-derived proteins. Furthermore, there is potential in SCN^- acting as an antioxidant and may be able to grant protection from the damaging effects of HOCl.

1.3.3 Other potential oxidants

HOCl and HOSCN are primarily MPO-derived oxidants produced during inflammation. However, other oxidative species exists that elicit their own specific modifications such as seen with hydroxyl radicals ($HO^{\bullet}$), HOBr or HOI, radicals generated in the peroxidase cycle ($NO_2^{\bullet}$ and $TyrO^{\bullet}$), and peroxynitrite ($ONOO^-$/ONOOH) [26, 115, 116].

H_2O_2 is produced by the conversion of O_2^- by superoxide dismutaste [117, 118]. It has previously been implicated as an oxidant and is suggested to interact with proteins as well, and is readily broken down by catalase to oxygen and water [26, 119]. Activity of H_2O_2 is linked with conversion to $HO^{\bullet}$, which is known to be highly reactive and is able to damage proteins, amino acids, and lipids [115, 116, 120]. Generation of $HO^{\bullet}$ occurs either by a catalytic breakdown of H_2O_2, through photolysis or by a Fenton method which uses a $Fe(^{2+})$-EDTA catalysis to simulate reduction by trace iron or copper irons [26, 115, 116, 119, 121, 122]. However, there are low levels of trace ions. Thus, it is likely that modifications are hypohalous acid-derived due to a high reaction rate between MPO, halides, and H_2O_2 [26, 123]. It has been found that at least 40-70% of H_2O_2, in the presence of Cl^-, is converted to HOCl [26, 98, 124]. Furthermore, reactions with H_2O_2 and $O_2^{\bullet-}$ are very slow [116], thus the major contribution of oxidation is likely from hypohalous acids.

Plasma levels of Br^- and I^- have been found to be around 20-100 μM [44] and < 1 μM [27], respectively. Due to the similarities between Cl^- and Br^-, the effects of HOBr has been found to be on par with HOCl [26]. Both of these halides are known to have higher second-order rate constants with MPO and thus have the potential to generate HOBr/HOI over HOCl [27]. HOBr is known to be highly reactive with several oxidisable group analogous to those examined with HOCl but also have been found to react with functional thiol and amine groups [125, 126]. Treatment of GAGs with HOBr was found to yield *N*-Bromo derivatives [127], similar to those found with HOCl treatment [68, 71]. With regards to HOI, there are limited studies investigating the generation and effects

of HOI with early studies observing iodination on extracellular proteins [117]. A more recent study has investigated the effects of I^- as a species to mitigate damage from HOCl [128].

The formation of $ONOO^-$/ONOOH is due to a rapid reaction between $NO^\bullet$ (derived from nitric oxide synthase enzymes; e.g. iNOS/eNOS) and $O_2^{\bullet-}$ [129]. The oxidants ONOOH and $TyrO^\bullet/NO_2^\bullet$ have both been found to mediate Tyr nitration resulting in formation of nitrated Tyr, 3-nitroTyr or 6-nitroTyr [129, 130]. These nitrated Tyr residues have been used as biomarkers to indicate nitration induced damage [129]. In recent studies, these reactive species have been shown to modify key amino acids on ECM proteins leading to cellular dysfunction [130–132].

The generation and modifications by different types of oxidants are broad and certain mechanisms are favoured over others depending on the location and the type of inflammation.

1.3.4 Antioxidants

Oxidative damage can be minimized by various physiological antioxidants, which scavenges oxidants by rapidly reacting with them and preventing damage to host cells [86, 133]. There are many groups of antioxidants, both endogenous and taken up through dietary supplementations [86, 133]. These include: enzyme inhibitors, limiting oxidant production, MPO binding agents, and supplements of vitamins or other compounds.

There are various ways of removing oxidants, particularly H_2O_2, O_2^-, and $ONOO^-$/ONOOH; this is possible due to the endogenous antioxidants available within the body. O_2^- can be consumed by superoxide dismutase and converted to H_2O_2, as seen previously in section 1.3 [19, 20]. H_2O_2 can be scavenge and decomposed by catalase, breaking down the oxidant into water and oxygen [134]. This can subsequently decrease the conversion of H_2O_2 in the presence of physiological halides, to the more damaging hypohalous acids [134].

There are currently no known antioxidant agent that can directly remove HOCl. This poses a problem as HOCl is commonly generated in inflammation and is known to be rather damaging to host cells and proteins [49, 50]. Oxidation by HOSCN has been found to be reversible but can subsequently form non-reversible products [94, 103]. Other than removing the upstream oxidants (H_2O_2 and $O_2^{\bullet-}$), there has been some recent studies examining reduction of HOSCN by thioredoxin reductase [135]. Thioredoxin is a redox protein and in conjunction with thioredoxin reductase may be capable of reducing HOSCN and mitigating subsequent damage [135, 136]. It was proposed that HOSCN acts on the sulfur-thiol group on thioredoxin reductase, thus reducing the oxidant. Furthermore, HOSCN has been observed to be reducible by mammalian thioredoxin reductase but not bacterial thioredoxin reductase; this makes HOSCN less damaging in humans particularly in areas with high concentrations of SCN^- such as in the lungs [135]. There is risk of inactivation of redox enzymes by these oxidants but it was been observed that addition of seleno-compounds (e.g. selenocysteine) resulted in preventing

the inactivation of thioredoxin reductase [137]. These selenocysteine residues are highly advantageous as they are resistant to over-oxidation, whereas their sulphur counterparts are more prone to overoxidation leading to formation of irreversible modifications [137, 138]. This suggests that during inflammation, antioxidants may help to mitigate the oxidative damage induced by HOCl, HOSCN, and other oxidants.

1.4 Extracellular Matrix Overview

The ECM is a complex network of multifunctional proteins with each playing an important role in providing a versatile scaffold, and regulating functions between cell-cells and cells-protein (Figure 1.6) [139, 140]. These vital processes are regulated by interactions of the matrix proteins with cytokines and growth factors, as well as the binding to cell surface integrins and mediating downstream intracellular signalling [141, 142]. The ECM provides a biological scaffold and homeostatic maintenance in a variety of organs within the human body [139, 143]. Furthermore, ECM proteins in both their native and non-native state are vital in instigating inflammation, and subsequent wound healing [144–146].

During the progression of atherosclerosis, extensive vascular remodelling, regeneration, and repair occur in the arterial wall [147, 148]. The ECM can be triggered by nearby cells to initiate extensive turnover, especially when ECM proteins are detected to be damaged by cells [18, 149]. Cells, such as EC and SMC, can up-regulate matrix degrading enzymes such as matrix metalloproteinases (MMPs) and in conjunction with tissue inhibitor of metalloproteinases (TIMPs), works to regulate the degradation of ECM [150]. Moreover, cells can up-regulate gene expressions to activate production of new ECM proteins into the milieu [151]. Modifications to ECM proteins can lead to improper binding to other proteins and/or cells, and can trigger an inflammatory response [131, 152]; these responses have been associated with a variety of inflammatory diseases including those observed in the lungs [153], bones [154], different types of cancers [150], and the cardiovascular system, such as in atherosclerosis [148].

Vascular ECM found in in arterial basement membrane includes: proteoglycans (proteins decorated with GAGs), structural proteins and specialised proteins. The composition is highly dependent on the location within the body, as each protein possess differentiated and specialised structures and properties.

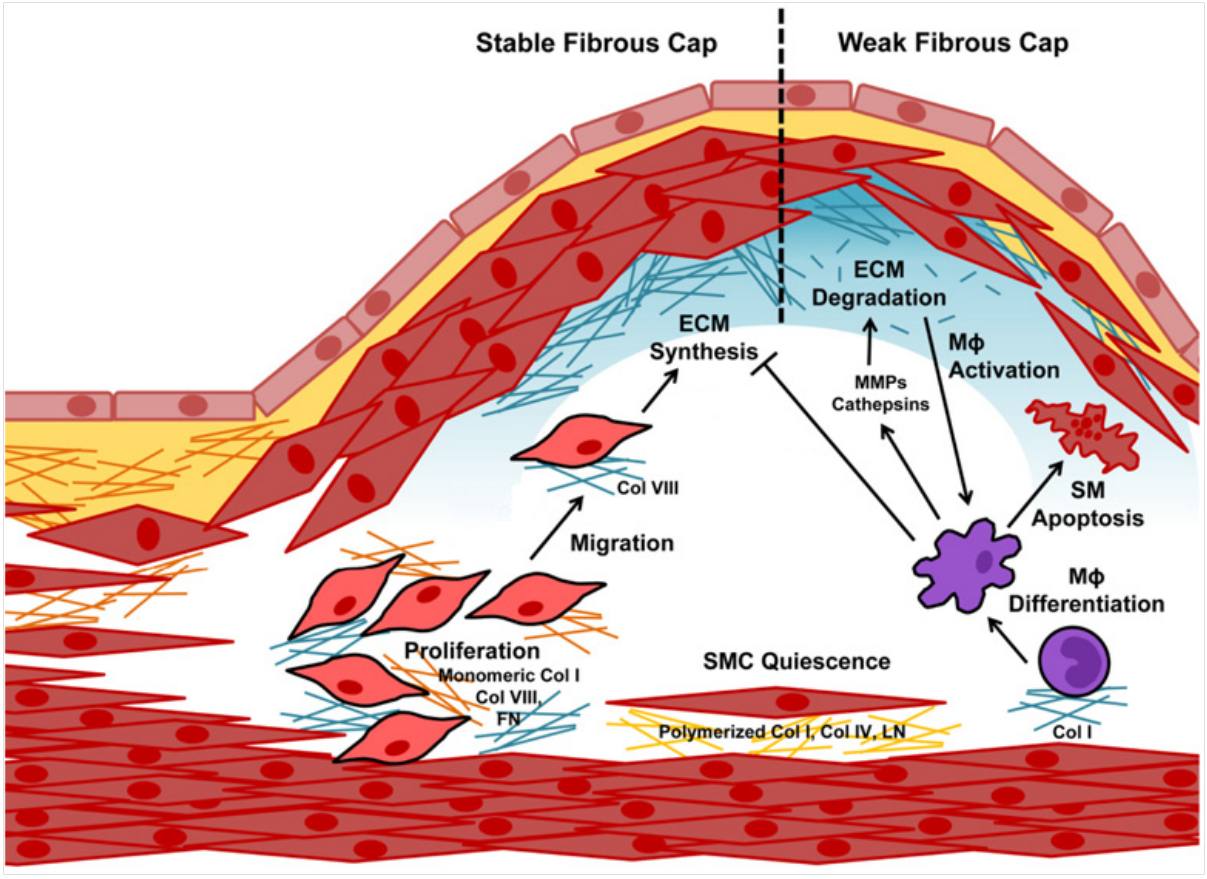

Figure 1.6: **Schematic diagram demonstrating the structure of an artery wall.** This includes the EC layer with the sub-endothelial basement membrane located underneath the EC layer. SMCs are located in the arterial media layer with corresponding basement membrane located beneath the SMC layer. The necrotic core in the arterial wall is characterized by fatty deposits and infiltration of inflammatory cells and develops in the sub-endothelium space. Adapted from Yurdagul *et al*, 2016 [155].

1.4.1 Proteoglycans and Glucosaminoglycans

Proteoglycans are proteins decorated with GAGs, which are long un-branched polysaccharides containing disaccharide repeating regions composed of amino sugar, D-galactosamine or D-glycosamine, and uronic acid, D-glucoronic acid or L-iduronic acid [156, 157]. These GAGs have net negative charges due to the variable sulfated side chains [21]. In addition, the rigidity of proteoglycans provides structural integrity and provides passageways between cells allowing cell migration [158, 159]. GAGs include heparan, chondroitin, dermatan, and keratan sulfates, as well as hyaluronic acid. Proteoglycans are not confined to being decorated with one type of GAG, instead heterogeneity of sugars can exist in the make-up of these proteoglycans. Proteoglycans can be post translationally decorated with HS and CS GAGs within cells at the rough endoplasmic reticulum via O-linked glycosylations by glycosyltransferases [156]. The sulfation of HS has been found to have sites with variable high and low sulfated regions with transitional regions in between [160]. Hyaluronic acid (or hyaluronan) is unique as it is the only GAG that is not sulfated and is not covalently attached to proteins forming a proteoglycan and are the largest polysaccharides produced by vertebrate cells [161].

Proteoglycans can be grouped according to their GAG characteristics, which also defines their function in the ECM (Table 1.2).

Table 1.2: **Types of GAGs present on different proteoglycans and their role in the body.**

Type of GAGs	Proteoglycan	Role	References
Heparan Sulfate	Perlecan	- Pro-angiogenic - Matrix maintenance - Turnover and repair - Cell signaling	[162, 163]
	Syndecan	- Growth factor binding - Matrix adhesion - Cell-cell adhesion	[164, 165]
	Type XVIII Collagen	- Regulator of angiogenesis - Vascular function	[166]
Chondroitin Sulfate	Versican	- Wound healing - Angiogenesis - Vascular disease - Tumour growth	[154, 158]
	Aggrecan	- Osmotic pressure in cartilage - Provides compression resistance	[157, 167]
Dermatan Sulfate		- Interacts extensively with CS - Role in neuronal development - Role in cancer progression	[168–170]
Keratan Sulfate		- Hydration of cornea and cartilage - Structural stability in bone	[171]
Hyaluronan		- Viscosity in cartilage - Lubricates interstitial space - Regulates inflammation - Remodelling of ECM	[161, 172]

1.4.2 Collagen, Elastin, and Laminin

Structural proteins, such as collagen and elastin, are important in providing the integrity and strength to the overall extracellular environment to provide tensile support and to its neighbouring cells [139]. This is particularly important in the basement membrane of the arterial wall as these matrix proteins play a role in maintaining homeostasis and in the progression of atherosclerosis [139, 140, 148].

1.4.2.1 Collagen

Collagen is the most abundant protein in mammals with several extensive studies on its properties, functions and location. It has a large helical structure composed of three left hand helices super coiled into a right hand helix, called collagen microfibrils. In terms of its composition, there are high levels of glycine, proline and two uncommon amino acids, hydroxyproline and hydroxylysine [173]. Furthermore, maturation of collagen fibrils has been observed to be mediated by lysyl oxidase (LOX), which forms cross-links between collagen fibrils [174]. This is vital in forming stable collagen fibrils in the basement membrane [174]. ECs predominantly reside on type IV collagen rich basement membrane in the intimal layer, while smooth muscle cells are surrounded by types I and II collagen in the medial layer [175, 176]. Collagen fibres have been heavily studied with focus on natural remodelling. Further research examines diseases such as atherosclerosis, and collagen's vulnerability to proteolytic degradation by endogenous enzymes (proteases such as MMPs) [173].

1.4.2.2 Elastin

Elastin, another important matrix protein, similarly provides structural integrity, largely in its role to regulate elasticity of the tissue through stress and strain [177]. It is

composed of an assembly of soluble tropoelastin protein and when cross-linked together by desmosine and isodesmosine, it makes a complex insoluble protein molecule [177, 178]. Elastin does not have a high turnover rate like some other matrix proteins [179]. Due to this fact, the degradation of elastin has been suggested to be a contributory factor in aging and many diseases such as atherosclerosis [180, 181].

In the vascular wall, elastin is localised within in the arterial intima, and is important in regulating the mechanical stress and strain due to fluctuations in blood pressure [148]. It is synthesized primarily by elastogenic cells, such as fibroblasts and SMC, and released into the ECM milieu and it self-assembles into the functional monomeric fibrils [182, 183]. Cross-linking of elastin has been observed to be facilitated by LOX, similar to collagen [184]. As atherosclerosis advances, a reduction or fragmentation of elastin was associated with increased risk of plaque rupture [185].

1.4.2.3 Laminin

Laminin plays a key role in cell survivability and maintenance by providing a base for cellular anchorage and mediating cellular proliferation, differentiation, migration and adhesion [186]. It is a heterotrimeric protein composed of alpha (α-), beta (β-), and gamma chains (γ-). Different combinations of $\alpha\beta\gamma$ chains give rise to the sixteen currently identified laminin isoforms found *in vivo* [186]. A murine embryonic epithelium-derive laminin-111 ($\alpha1$, $\beta1$, $\gamma1$) is commonly used in studies and has been found to be present in adult humans, specifically in cranial blood vessels [142]. The sub-endothelium and medial layer of blood vessels in humans have been observed to have a prevalence of laminin $\alpha4$ chain, such as found in laminin 8 ($\alpha4$, $\beta1$, $\gamma1$) and laminin 9 ($\alpha4$, $\beta2$, $\gamma1$) [187, 188]

In atherosclerotic lesions, it has been observed that there is an abundance of different laminin chains detected in both mice and humans [189]. Early studies investigated the attraction between laminin and neutrophils [190], and others emphasised on how laminin/elastin receptors contributed to atherogenesis [191, 192]. Due to the abundance

of laminin endothelial basement membranes, it has been suggested to be a likely target for oxidation during atherosclerosis [131, 132]. However, there are limited studies investigating this reaction between laminin and oxidants, with some recent studies examining the effects of peroxynitrite on basement membrane and laminin [131, 132]. In a few recent studies, investigations observed that oxidised laminin was capable of increasing the attachment of monocytes and ECs [193, 194]. These studies suggests the importance of native and modified laminin in the arterial wall during atherosclerotic lesion development.

1.4.3 Fibronectin

1.4.3.1 Structure and function

FN is a dimeric glycoprotein of approximately 460 kDa in size, is composed of two nearly identical monomer subunits ranging between 220-270 kDa and is bound by disulfide bonds at the carboxy-termini [149, 195, 196]. There are two identified types of FN; soluble plasma FN, produced mainly by hepatocytes and released into plasma, and cellular FN, produced by various cells (such as EC, SMC, and fibroblasts) [149, 195, 196]. Plasma and cellular FN share a number of functional regions, but there are regional differences due to alternative splicing that give rise to their different activities [197].

FN contains three main modules: type $I_{1\text{-}12}$, type $II_{1\text{-}2}$ and type $III_{1\text{-}17}$, and also a non-homologous variable sequence [149, 196]. Specific functional domains are featured on these larger subunits, and when FN is folded, these functional domains are exposed [198, 199]. Cellular FN possesses extra domain A (EDA) and extra domain B (EDB), which are alternatively spliced type III modules that are absent on plasma FN [200]. The EDA and EDB regions are proposed to be important cellular receptors that play a role in matrix assembly, although there are limited studies and research into these domains are ongoing [200].

There are several functional domains on FN including: two heparin binding sites, two fibrin binding sites, collagen binding sites, as well as specific cellular integrin sites [149, 196]. The majority of the type I module is located at the amino-termini with a small section located at the carboxy-termini; the two fibrin binding fragments, and the heparin binding fragment (HBF) I are located in this module [196, 202]. The type II module is the smallest of the three and possesses the collagen binding fragment [202]. The type III module consists of the cell binding fragment (CBF) including the RGD motif (Arg-Gly-Asp), where the $\alpha 5\beta 1$ and $\alpha V\beta 3$ integrin are also located [203]. A complex relationship exists between type III_9 and type III_{10}, which provides a synergistic effect allowing ready

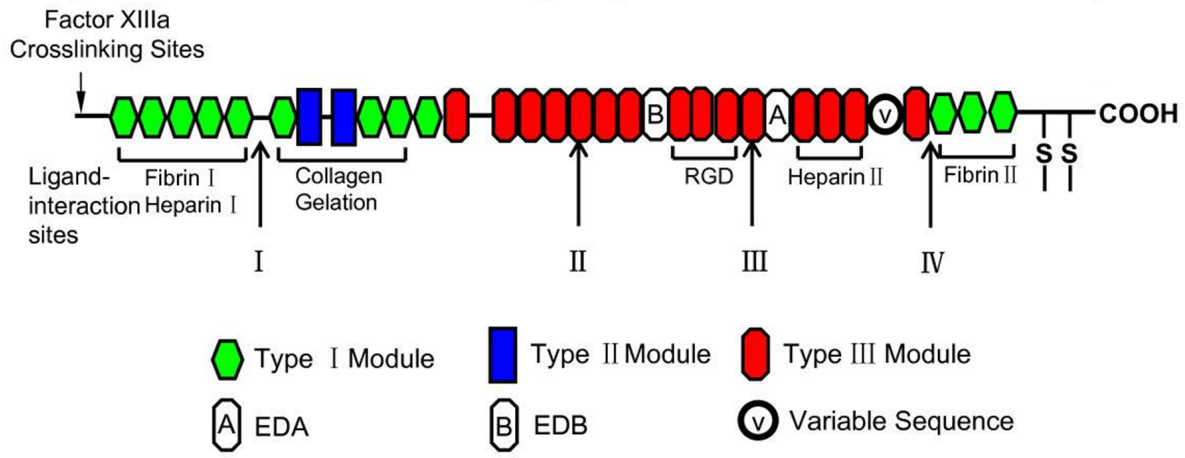

Figure 1.7: **Schematic diagram of a FN monomer chain.** The diagram indicates Type I-III modules, the location of important binding fragments and the alternatively spliced variant domains. Adapted from Wang *et al*, 2008 [201].

access to integrins (e.g. $\alpha 5\beta 1$) [204, 205]. The HBF II on the carboxy-termini has been shown to bind to syndecan-2, and due to the high affinity of this fragment, it has been also found to bind to GAGs on proteoglycan, such as HS and CS [206, 207]. This interaction has been proposed to play a key role in matrix assembly and formation of insoluble fibrils [208]. The alternatively spliced type III_{CS} (also called variable or V) has been found to code for a further two integrin binding sites ($\alpha 4\beta 1$ and $\alpha 9\beta 1$) [200], and has been shown to be involved in heparin binding [209].

The type II module possesses only sixty amino acids in length with several cysteine residues involved in disulfide bonds [202]. This domain is found to play an extensive role in collagen binding and assembly [202, 210]. The type I module at the amino-termini has been observed to play a role in wound healing through fibrin and Factor XIIIa binding. Moreover the absolute or partial deletion of the type $I_{1\text{-}5}$ has been shown to impair FN incorporation into the ECM [211, 212]

As can be derived, FN is a key matrix protein in mediating development and maintenance in the vascular wall.

1.4.3.2 Biological Properties

The complex structure of FN gives rise to its multifunctional properties and allows important interactions with an array of ECM proteins, enzymes, and cells.

Studies have shown extensive interaction between FN and proteoglycans, such as syndecan and versican [164, 213, 214]. Adhesion and spreading of particular cells on syndecan is mediated by the HBF present on FN [206–208]. This process can be seen with vinculin associated focal adhesions of fibroblast cells to FN, which was demonstrated in the presence of heparan sulfated syndecan [164, 165]. This assistance of adhesion and spreading was thought to be due to the active HBF on FN [164, 165]. It was suggested that this particular pathway was due to the recruitment and activation of protein kinase C, a protein that is heavily involved in cell signaling pathways [22]. An interaction with FN, vascular endothelial growth factor (VEGF), and the G3 domain of versican promotes angiogenesis, particularly in brain tumour growth [215, 216].

In addition, ECM assembly and cell adhesion are also regulated and dependent on the important relationships that exists between FN and collagen [217, 218]. Collagen is known to bind to the type II and adjacent type I module of FN, this interaction has been examined extensively in literature. It is suggested that FN assists in mediating binding of collagen to mannose receptors [210]. Mannose receptors are present primarily on macrophages, which acts in both innate and adaptive immune systems, intracellular signaling, and regulating responsive inflammatory molecules [219, 220]. This interaction between FN and collagen also mediates cellular response, whereby studies have shown this interaction can promote cellular migration, improve cell contractibility [221], increase cell proliferation, and healthy cell morphology [222, 223]. The incorporation of collagen into the matrix and proper collagen assembly is dependent on FN binding and assisting in the process [221, 224, 225]. Furthermore, collagen I and FN complexes were also observed to decreases MMP secretion when compared to FN in the absence of collagen, though the mechanism is not completely elucidated [226].

FN also interacts with EC, and SMC via the CBF, which is also known to bind to particular groups of integrins [196, 227], mediating their function and morphology [228–230]. FN in healthy vessels have been shown to assist in regulating vascularization [231], via binding of the integrin to the CBF including the RGD site [232–234]. In vascular tissue, FN anchors EC to the basement membrane providing structural integrity along with also assisting with homeostatic cell functioning in adhesion, proliferation, migration and capillary tube formation [231, 235, 236]; when FN is modified or damaged, such as during inflammation, there is an impairment to FN's ability to support cells [236]. This was seen with the loss of healthy fibril assembly, by inhibition of FN polymerisation, which resulted in inhibition of SMC growth and proliferation [147]. Furthermore, inhibition of type III_1, which is known to mediate FN-FN binding and matrix assembly, resulted in a similar inhibition of vascular SMC growth and proliferation [237]. These studies support the important of health FN in mediating cellular growth and proliferation.

1.4.4 Modulation of ECM, particularly fibronectin, in atherosclerosis

The ECM plays an important role in various areas of the body by providing structural support to overlying tissues and assisting in a multitude of cellular function. If ECM proteins in the arteries are damaged through improper production or modified in diseases, it can lead to detrimental effects causing morbidity or even mortality. Previously, it was observed that perlecan-null mice were found to develop cardiovascular malformations and ruptures of blood vessels [238]. This suggests that perlecan plays an important role in cardiovascular development and likely maintains normal vascular architecture. Perlecan expression was markedly increased in the fibrous caps and in the plaque core of advanced lesion mice models when compared to healthy murine aorta [239]. Furthermore, exposure of perlecan to HOCl and HOBr resulted in extensive modifications to the protein core, which led to a reduction in cell adhesion [67]. Peroxynitrite was observed to alter both the HS chain and protein core of perlecan, which resulted in concentration dependent fragmentation and aggregation of proteoglycan [240].

Collagen has been known to play an important role in fibrous cap formation in atherosclerosis [148]. Fragmentation of fibrillar types I and III collagen resulted in a shift of SMC phenotype from contractile to synthetic [176]. Surrounding ECM was found to be structurally affected in these atherosclerotic lesions and led to changes in fibrous cap organisation, and subsequently plaque stability [176]. MMP-2 and MMP-9 have been detected in atherosclerotic lesions of mice [241], and these proteolytic enzymes have been found to degrade collagen [242, 243]. While there is greater emphasis on the action of MMP [241–244], collagen has been observed to undergo glycation [245, 246] and glycoxidation [247], particularly in regards to complications arising from diabetes. In contrast, there are limited studies examining the effects of MPO-derived oxidants on collagen with one particular studying focusing on modifications to collagen II by hypochlorite [248]. Exposure of collagen to hypochlorite was observed to oxidise and fragment the protein but this was not examined extensively in detail [248].

Laminin is a large basement membrane protein with several functional domains that play a role in cell adhesion, migration, and regulates matrix mediated assembly and signaling [186]. Laminin has been shown to be important in cell-matrix adhesion, via the localisation of the $\alpha 4$ subunit with $\alpha v\beta 3$ integrin-rich focal adhesion [249]. Furthermore, interaction of laminin with collagen, nidogens and HSPGs were found to mediate laminin deposition and matrix assembly [250, 251]. Nidogen is a sulphated glycoprotein and its interaction with laminin is known to stabilise ECM [250, 251]. Nidogen$^{-/-}$ mice were found to have a decreased expression of laminin-411 and abnormal and disorganised basement membrane [252]. In more recent studies, diabetic monocyte-derived oxidant was observed to carbonylate laminin-111, resulting in decreased monocyte attachment and migration [193]. Furthermore, HUVEC exposed to laminin-111 oxidised by ferrous ammonium sulphate resulted in up-regulated expression of ICAM-1 which subsequently increased monocyte adhesion [194]. As can be derived, laminin is important to several ECM functions, and modifications to this protein can further disrupt healthy vascular function particularly in atherosclerosis.

In addition to these previous ECM proteins, FN has also been shown to be highly important in maintaining homeostasis of a healthy vasculature, but in inflammatory diseases, such as atherosclerosis, this property of FN can become impaired due to modifications to the protein.

Early studies on FN have shown that inactivation of FN gene resulted in a cessation of development during embryognesis [253]. These mice models were observed to lack EC that could form healthy blood vessels, suggesting the importance of FN in blood vessel development [253]. Furthermore, defects or deficits in important integrins (e.g. $\alpha 5$ or $\beta 1$) resulted in lethality during embryogenesis [253–256]. Formation of FN during matrix assembly is important in atherosclerosis, whereby the reduction or absence resulted in decreased collagen deposition, thinner arterial layers (intima and media), and increased inflammatory cell infiltration [257]. Inhibition of the collagen/gelatin binding fragment with an anti-60k Fab' antibody (specific for the binding fragment) resulted in a

reduction of both collagen and FN deposition [258]. This suggests the importance of FN-collagen interaction for formation of fibrillar structures in the ECM [258]. Furthermore, interactions between FN, cell surface receptors and integrins are important in initiating matrix assembly [197].

FN plays a large role in matrix assembly by interacting with other ECM proteins, but also interacts with cells (e.g. EC and SMC) to contribute to formation and function of the endothelial intima layer and SMC media layer [14, 259]. Surface coated with FN has been observed to enhance EC adhesion and was able to sustain adhered cells for up to four days [235]. FN exposed to oxidants that are commonly associated with atherosclerosis (such as HOCl and peroxynitrite) were observed to decreased EC adhesion and impaired cell spreading [22, 130, 260, 261]. A certain mechanism of de-adhesion in EC was found to be triggered by an external signal causing intracellular changes to Src and phosphorylaton of Tyr-118 of paxillin [22]. This suggests that mitogenic processes for vascular regeneration are dependent on FN binding growth factors, and the interaction of FN with other ECM proteins. This is demonstrated by consecutively coating the surface with collagen followed by FN and heparin, which resulted in greatly increasing binding of mitogenic glycoprotein and heparin binding growth factor (HBGF) [262].

Collagen and thrombospondin-1 (THBS-1) deposition is highly dependent on the presence of intact FN in the matrix [225]. THBS-1 has been observed to be important in mediating cell-matrix and cell-cell adhesion [263]. Matrix structure and cellular function is highly dependent on the structural integrity of the basement membrane. Deficiency in plasma FN resulted in lower levels of SMC migration into the atherosclerotic plaque, reduction in collagen deposition, and the formation of thinner fibrous caps [264]. Migration of SMC into the atherosclerotic plaques have been reported to be important in generating stable fibrous caps, however FN also promotes lipid retention, and increased inflammatory cell infiltration [265]. Furthermore, it was reported that degraded FN resulted in increased leukocyte migration/chemotaxis across the EC layer [266, 267], and increased neutrophil degranulation [268]. In support of this, inhibition of FN assembly resulted in a reduction

in inflammatory response in atherosclerosis [147, 269]. FN plays an important role in ECM stabilisation and together with other ECM proteins provides strong substrata for EC and SMC. Thus, these studies demonstrate the importance of FN in regulating cell function and ECM assembly within the basement membrane.

During inflammation, the production of MPO has been linked with the co-localisation and binding to ECM proteins [21, 22, 270]. MPO has been shown to bind to GAGs [21, 270], but recently shown to also bind to FN [22]. The co-localisation may suggest ECM FN to be a possible target of MPO-derived oxidant due to their proximity [21, 22]. A number of studies have examined the detrimental effects of hypochlorite on FN such as fragmentation of the protein [22, 260], loss of cell adhesion, loss of specific antibody recognition [22, 261], amino acid changes, and oxidative by-products [46, 64, 271]. Studies have also shown that the reduction of plasma FN levels is associated with lower levels of SMC migrating into atherosclerotic lesions, resulting in plaques that are more prone to rupture as they have decreased collagen and thinner fibrous caps [264]. These studies support a major role for FN in atherosclerotic lesion development [22, 260, 271], and support investigations as to how structural alterations to FN, such as via oxidation, which may alter the function of FN. Furthermore, the deletion of spliced EDA exons of cellular FN showed a reduction in the size of atherosclerotic lesions in mice with atherosclerosis [272, 273]. These studies indicate modifications or absence of either the whole protein or of particular regions can affect the development of an atherosclerotic lesion.

As described, the ECM is important to both the structural integrity of the basement membrane, providing binding sites and harbouring molecules for healthy cell function. Thus, it can be seen how crucial it is to understand how modifications on these particular proteins can have a downstream consequences to the stability of the overlying tissue, particularly in the progression of inflammatory diseases such as atherosclerosis.

1.5 Thesis hypothesis and aims

In light of the current data available, FN is present in vascular walls and mediates remodeling both in healthy matrix turnover but also in inflammatory diseases such as atherosclerosis [18, 148]. It is hypothesised that MPO-derived oxidants (HOCl and HOSCN) will modify ECM-derived proteins particularly FN, which will result in structural and functional changes to the vascular basement membrane. Moreover, modifications induced by HOSCN would be less extensive compared to HOCl due to its specificity. These ECM alterations affect EC behaviour and will result in endothelial dysfunction leading to the subsequent development of atherosclerosis.

This hypothesis will be addressed by the following specific aims:

1. To investigate the structural changes (fragmentation and aggregation) induced by HOCl, on human plasma FN and cellular FN in HCAEC-derived whole ECM extract, and whether it leads to consequential biological dysfunction with regards to cell adhesion, proliferation and gene expression.

2. To investigate the structural changes (fragmentation and aggregation) induced by HOSCN (a more specific oxidant), on human plasma FN and cellular FN in HCAEC-derived whole ECM extract and whether the modifications are as extensive as observed with HOCl.

3. To investigate whether the changes induced by reagent HOCl and HOSCN are observed with treatment utilizing MPO enzyme, H_2O_2, and halides (Cl^- and SCN^-).

4. To determine the extent of modifications on human plasma FN in a mixture of Cl^- and SCN^- utilizing the enzymatic MPO/H_2O_2 system.

5. To determine the occurrence of modified matrix components in human atherosclerotic lesions.

Chapter 2

Materials and Method

2.1 Materials

All products were sourced from Sigma Aldrich (St. Louis, MO, USA) unless otherwise noted. Water used in preparation of solution and use in experiments were filtered through a four-stage Millipore MilliQ system ("MilliQ water"). Chelex was used to remove trace metal ions from buffer solutions and was obtained from Bio-rad (Hercules, California, USA). LPO (from bovine milk; 427489) was purchased from Merck (Darmstadt, Germany). Phosphate buffer saline (20x PBS) was obtained from VWR (Solon, OH, USA). Pierce BCA protein assay solution (23223) was obtained from Life Technologies (Slangerup, Denmark) or Thermo Scientific (Rochford, IL, USA). For SDS-page and Western blot experiments, Xcell Surelock Mini-cell sodium dodecyl sulfate polyacrylamide gel electrophoresis (SDS-PAGE) tank (EI0001), NuPAGE™ 3-8% Tris-Acetate Protein Gels 1.0mm (10 wells, EA0375BOX; 12 wells, EA03952BOX; 15 wells, EA03755BOX), NuPAGE™ Reducing buffer (NP0009), NuPAGE™ LDS sample buffer 4x (NP0007), HiMark™ pre-stained High Molecular Mass standard (LC5699), HiMark™ Unstained Protein standard (LC5688), NuPAGE™ Tris-Acetate SDS Running buffer 20x (LA0041), iBlot 2 Gel Transfer Device (IB21001), and iBlot 2 polyvinylidene fluoride (PVDF) Regular stacks (IB24001) were purchased from Life Technologies (Slangerup, Denmark). Trypsin (R001100), Hoechst 33342 (H1399), ActinRed 555 Ready Probe (R37112) Nuclease-Free water (AM9939) were also purchased from Life Technologies (Slangerup,

Denmark). Western lighting PLUS ECL (NEL104001) solution for developing Western blots was sourced from Perkin Elmier (Waltham, MA, USA). HCAEC, HCAEC Growth Medium (095212), Endothelium Cell Basal media without phenol red (210PR-500; Endo-Basal Media) was obtained from Tebu-bio (Roskilde, Denmark). CellTiter 96® Aqueous One Solution Assay (G3580), was acquired from Promega (Nacka, Sweden). RNAse Zap (79254), RNease Mini Kit (74104), RT2 First Strand Kit (330404), and RT2 SYBR Green ROX qPCR Mastermix were obtained from Qiagen (Copenhagen, Denmark). ThioGlo 1 fluorescence thiol reagent (HC9080) was acquired from Berry and Associate (Michigan, USA).

MPO enzyme was purchased from Planta (Vienna, Austria). Both bovine and human plasma FN was sourced from Sigma Aldrich (St. Louis, MO, USA). Whole human ECM was harvested from HCAEC.

2.1.1 Primary antibodies

Mouse monoclonal antibody probing for FN CBF (clone A17; ab26245) and FN EDB (clone C6; ab154211) were purchased from Abcam® (Cambridge, UK). Mouse monoclonal antibody against FN HBF (clone A32) was obtained from Life Technologies/Thermo Scientific (CSI0053202; Slangerup, Denmark). Mouse monoclonal antibody against FN EDA (close 3E2; F6140) was sourced from Sigma Aldrich (Louise, MO, USA). Mouse monoclonal antibody targeting a HOCl-generated epitope was appreciatively donated by Prof. Ersnt Malle and Prof. Astrid Hammer from Medical University of Graz, Austria [63] (Table Table 2.1).

Table 2.1: **List of primary antibodies and dilutions used in experiments.**

Epitopes	Clone	Dilutions	
		ELISA	WB
FN; Cell Binding Fragment (CBF)	A17	1:50 000	1:10 000
FN; Heparin Binding Fragment (HBF)	A32	1:1000	1:2000
FN; Extra Domain A (EDA)	3E2	1:1000	1:2000
FN; Extra Domain B (EDB)	C6	N/A	1:2000
HOCl-generated epitope	2D10G9	1:50	N/A

2.2 Methods

2.2.1 Reagent and enzymatic oxidant synthesis

2.2.1.1 Hypochlorous Acid

HOCl stock solutions were commercially purchased and regularly checked by diluting in NaOH and using UV-Vis spectrophotometry at 292 nm and a coefficient of 350 M^{-1} cm^{-1} . Stock solutions were generally made to the same molar concentration. HOCl was prepared by diluting stock reagent HOCl in milliQ water to an initial concentration of 50 mM; this solution was then serially diluted accordingly to the required concentrations to form the molar ratio required in each experiments (Table Table 2.2). For 1 μM of FN in Western blotting experiments, a 1:5 dilution was performed to acquire the necessary molar ratio (Table Table 2.2).

Table 2.2: **Diluton of HOCl for required molar ratio in experiments.** This example was prepared for a 1:5 dilution in Western blotting experiments for 1 μM of FN.

Concentration	Total Vol. (μL)	Vol. of higher conc. (μL)	Vol. NaPhosbuffer (μL)	Molar Ratio
50000	100	100	0	10000x
25000	100	50	50	5000x
5000	100	20	80	1000x
2500	100	50	50	500x
1000	100	40	60	200x
500	100	50	50	100x
250	100	50	50	50x
125	100	50	50	25x
50	100	40	60	10x
25	100	50	50	5x

2.2.1.2 Hypothiocyanous acid

Aliquots containing 50 μL of 45 μM LPO were previously prepared. Exactly 850 μL of 10 mM pH 6.6 potassium phosphate buffer was added to dilute the LPO aliquot. To this solution, 200 μL of 150 mM sodium thiocyanate (NaSCN) was utilised to produce

HOSCN. H_2O_2 was added in 10 μL of 75 mM H_2O_2 every minute to a final total of 50 μL while the sample was kept on ice. Samples were quickly inverted to mix the solution, followed by incubation for 15 mins on ice. After incubation, 0.1-0.2 mg of bovine liver catalase was added and incubated for 5 min at 21°C to quench any remaining H_2O_2 in solution. Catalase enzyme was removed by filtering through a 10k cutoff Nanosep Omega filter system followed by centrifuging at 12,000rpm for 5 min 4°C.

To check the concentration of HOSCN, 5-thio-2-nitrobenzoic acid (TNB) assay was utilised to spectrophotometrically determine the optical absorbance at 412 nm using the extinction coefficient, ε_{412} 14150 M^{-1} cm^{-1}. 5,5′-Dithiobis(2-nitrobenzoic acid) (DTNB) stock was prepared by diluting 2 mg of DTNB in 250 μL of 1 M solution of sodium hydroxide (NaOH), and allowed to mix for 5 mins at 21°C. This was then mixed with 4,750 μL of milliQ water in a glass bottle. DTNB reagent was diluted by combining 200 μL of DTNB stock in 9800 μL (9.8 mL) of 0.1 M pH 7.4 sodium phosphate buffer to give diluted DTNB (dilDTNB). The solution was checked using a UV-Vis spectrometer or compatible plate reader against 0.1 M pH 7.4 sodium phosphate buffer as a reference. For most efficient reading, absorbance should be between 0.4-0.6 absorbance.

When determining concentration of HOSCN, 5 μL of HOSCN was diluted in 995 μL dilDTNB (1:200); this was calculated against a control of 5 μL of 10 mM pH 6.6 potassium phosphate buffer also diluted in 995 μL dilDTNB (1:200). Samples were transferred to spectrometric cuvettes (Grenier Bio One; Frickenhausen, Germany) and measured at 412 nm on a Shimadzu UV-vis (Kyoto, Japan), with 0.1 M pH 7.4 sodium phosphate buffer as a reference. Alternatively, measurements can be made using a Greiner UV-Star 96 well plates (M3812) and quantified using a plate reader at 412 nm. Samples were measured in triplicates to obtain an average reading, and the concentration was calculated using the formulae in Figure 2.1.

Once concentration of HOSCN was determined, HOSCN was diluted to an initial concentration of 1 mM in milliQ water. This solution was then serially diluted down

$$[\text{HOSCN}] = \frac{\text{absorbance}}{\text{ex. coefficient}_{(HOSCN)}} - \frac{\text{absorbance}}{\text{ex. coefficient}_{(Blank)}} * 200$$

Figure 2.1: **Formula for calculating the concentration of HOSCN.** The ex. coefficient of TNB (ϵ_{412}) was taken as 14150 M^{-1} cm^{-1},

to the desired concentration and concurrent molar ratio (Table Table 2.3). Below is an example prepared for 1 μM of FN in Western blotting experiments, where a further 1:5 dilution was made to acquire the desired final molar ratio.

Table 2.3: **Diluton of HOSCN for required molar ratio in experiments.** This example was prepared for a 1:5 dilution in Western blotting experiments for 1 μM of FN.

Concentration	Total Vol. (μL)	Vol. of higher conc. (μL)	Vol. milliQ (μL)	Molar Ratio
1000	100	40	60	200x
500	100	50	50	100x
250	100	50	50	50x
125	100	50	50	25x
50	100	40	60	10x
25	100	50	50	5x

2.2.1.3 Enzymatic synthesis of oxidants

To produce HOCl enzymatically, MPO enzyme was used in samples in accordance to the known mechanism of MPO reacting with existing Cl^- and H_2O_2. Samples had sodium chloride (NaCl) added to obtain a final concentration of 100 mM followed by addition of MPO enzyme to acquire the desired concentration (check the concentration used in experiments). H_2O_2 was added in consecutive additions to prevent high concentration of H_2O_2 from inactivating the MPO enzyme. Cl^- can be substituted for SCN^- to generate HOSCN. For more precise concentration and details of MPO in reactions, please refer to corresponding methodology.

2.2.2 ELISA

A stock solution of 1 mg/ml of purified human plasma FN was diluted to a final concentration of 10 μg/mL in 0.5 M pH 7.4 of sodium phosphate buffer, and milliQ water for a final buffer concentration of 0.1 M pH 7.4 sodium phosphate buffer. In a high protein-binding 96-well plates, 50 μL of the 10 μg/mL (concentration rounded to 2 decimal places; 0.02 μM) FN solution was coated onto each well, followed by an overnight incubation at 4°C on a rocker. Maximum FN binding was previously determined using a serial dilution of decreasing FN concentration and a micro-BCA was performed to determine maximum concentrations of bound FN. It was found that there was minimal loss at this concentration and therefore future experiments were based on these results.

On the next day, the 96-well plate was washed twice with 200 μL of 1x PBS. Each well was treated with 50 μL of oxidant by taking the concentration from Table 2.2 or Table 2.3 and diluting to the appropriate molar ratio or concentration in 0.1 M pH 7.4 sodium phosphate buffer (refer to Table 2.4). Plates were then incubated for 2 hr at 37°C before being washed twice again with 1x PBS. Primary antibodies were prepared by diluting the respective antibody (Table 2.1 in 0.1% (w/v) casein 0.1% (w/v) Tween-20 PBST. Human plasma FN treated with HOCl, HOSCN, enzymatic reactions were probed for CBF (1:50000), HBF (1:1000), and HOCl-generated epitope (1:50). Furthermore, whole ECM extract which contains cellular FN was probed for CBF (1:50000), HBF (1:1000), and EDA (1:1000). After an incubation overnight, plates were washed twice with 200 μL of PBST before being incubated with either horse peroxidase (HRP)- or alkaline phosphatase (AP)- linked secondary antibody for 1 hr at 21°C. This was followed by four times washes with PBST, prior to development. Working ABTS solution was prepared fresh by addition of H_2O_2 (1:1000) into pre-made ABTS solution and 100 μL was added into each well. The absorbance was immediately read at 405 nm, followed by another reading at 5 min, 10 min, 30 min, and 60 min.

In the enzymatic experiments, surface-bound human plasma FN (0.02 μM) on 96-well

plates (prepared as above overnight at 4°C on a rocker) was washed twice with TBS and exposed to 50 μL containing: 10 μL of 0.5 M pH 7.4 sodium phosphate buffer, 1 μL of 1 μM of MPO (0.02 μM), 5 μL of 1 M Cl^- (100 mM), and increasing concentrations of H_2O_2 (0, 4, 8, 16, 24, 32 μM) in batch additions (maximum of 0.2 μL of 2 mM H_2O_2 stock solution) (Figure 2.5), and milliQ water for 2 hr at 37°C. Procedure followed as above post treatment substituting the changes as follows: AP-linked antibodies were used in place of HRP-linked antibodies, and 1x Tris-buffered saline (TBS) was used instead of PBS in these experiments. Development of plates was with 100 μL of Alkaline phosphatase Yellow (pNPP) Liquid Substrate (p7998; Sigma), with a stopping solution of 3 N NaOH (25 μL per 100 μL). The absorbance was measured at 405 nm immediately, followed by another measurement at 5 min, and 10 min. Stopping solution was added at 10 min and measured once more immediately after addition.

Table 2.4: **Concentration of oxidants as a molar ratio of human plasma FN for ELISA results.**

FN (μM)	Concentration of (μM)
0.02	0
	5
	10
	25
	50
	100
	200

Table 2.5: **Concentration of H_2O_2 as a molar ratio of human plasma FN for ELISA results.**

FN (μM)	Concentration of H_2O_2 (μM)	Molar Ratio
0.02	0	0x
	4	200x
	8	400x
	16	800x
	24	1200x
	32	1600x

2.2.3 Treatment of purified protein and whole ECM extract for SDS-PAGE

Purified human plasma FN (stock 1 mg/ml) was prepared by diluting it in 0.5 M pH 7.4 sodium phosphate buffer and milliQ water following Table 2.6 to give the desire concentration of human plasma FN in sample. For control samples, oxidants were replaced with milliQ water (FN only control). Prepared samples were then incubated for 2 hr at 37°C, followed by samples being split in half prior to addition of SDS-PAGE reagents so that samples can be ready for loading for protein separation. Samples were split in half as to retain the same treatment conditions when preparing samples for reducing or non-reducing conditions.

Whole ECM extracted from HCAEC was calculated for samples to supposedly contain 1 μM of FN (450 kDa) with the assumption that there's a majority of FN in samples for a final mass of 10 μg. FN concentration was not determined and thus a molar treatment used. Oxidant dilution was appropriately adjusted for 1:10 dilution for sample treatments (Refer to Table 2.2 and 2.3).

The concentrations (and molar ratio) of treatment of human plasma FN with enzymatic MPO/Cl^-/H_2O_2 experiments were based on a previous study by Vissers *et al.* (Table 2.8) [260].

Table 2.6: **Preparation of human plasma FN as 1 μM with treatment with HOCl or HOSCN.**

Solution	Example for six reactions (μL)
1 mg/ml FN	6
0.5 M pH 7.4 Phosphate buffer	2.66
MilliQ water	2
Oxidant (1:5 dilution)	2.66
Total Volume	13.32

Table 2.7: **Preparation of HCAEC-derived whole ECM extract as 1 μM with treatment with HOCl or HOSCN.**

Solution	Example for eight reactions (μL)
Stock HCAEC-derived whole ECM	X
0.5 M pH 7.4 Phosphate buffer	6.67
MilliQ water	Total minus X
Oxidant (1:10 dilution)	3.33
Total Volume	33.33

Table 2.8: **Preparation of human plasma FN as 0.2 μM with enzymatic treatment using MPO, Cl^-, and H_2O_2.**

Solution	Example for eight reactions (μL)	
	0.2 μM MPO	0.8 μM MPO
1 mg/ml FN	5	5
0.5 M pH 7.4 Phosphate buffer	10	10
MilliQ water	Total to 50	Total to 50
MPO (5 μM stock)	1	4
NaCl (1 M stock)	5	5
H_2O_2 (10 mM stock)	0, 0.2, 0.4, 0.6, 0.8	0, 0.2, 0.4, 0.6, 0.8
Total Volume	50	50

Table 2.9: **Preparation of human plasma FN as 0.2 μM with enzymatic treatment using MPO, SCN^-, and H_2O_2.**

Solution	Example for eight reactions (μL)	
	20 μM SCN^-	500 μM SCN^-
1 mg/ml FN	5	5
0.5 M pH 7.4 Phosphate buffer	10	10
MilliQ water	Total to 50	Total to 50
MPO (5 μM stock)	1	1
NaSCN (5 mM stock)	0.2	5
H_2O_2 (10 mM stock)	0, 0.2, 0.4, 0.6, 0.8	0, 0.2, 0.4, 0.6, 0.8
Total Volume	50	50

Table 2.10: **Preparation of human plasma FN as 0.2 μM with competitive enzymatic treatment using MPO, Cl^-, SCN^- and H_2O_2.**

Solution	Example for eight reactions (μL)	
	0.2 μM MPO	0.8 μM MPO
1 mg/ml FN	5	5
0.5 M pH 7.4 Phosphate buffer	10	10
MilliQ water	Total to 50	Total to 50
MPO (5 μM stock)	1	4
NaCl (1 M stock)	5	5
NaSCN (5 mM stock)	0, 0.2, 1, 2, 3, 4, 5	0, 0.2, 1, 2, 3, 4, 5
H_2O_2 (10 mM stock)	0, 0.8	0, 0.8
Total Volume	50	50

2.2.4 SDS-PAGE

Samples were then prepared for separation using 1-dimensional SDS-PAGE under reducing or non-reducing conditions. For reducing samples, 10x NuPAGE reducing solution was added in a 1:10 dilution to the final volume depending on sample prep, and in non-reducing samples, milliQ water was added in place of. All samples had 4x NuPAGE sample buffer added in a 1:4 dilution of the final volume. All samples were then heat denatured for 10 min at 70°C, then the appropriate volume of samples were loaded onto 3-8% (w/v) 1 mm NuPAGE® Tri-acetate gels which were electrophoresed at 160 V for 70 min in 1x Tris-Acetate SDS-Running buffer. HiMark™ Pre-stained high molecular mass protein standard was used as a molecular mass marker with a reference range from 30-460 kDa. Once separation has occurred, gels were visualised using silver staining, or were transferred onto a PVDF membrane by an iBlot 2 system for further Western blot analysis.

Table 2.13 can be used for all enzymatic MPO experiments including the competitive study (Table 2.9 and 2.10).

Table 2.11: **Preparation of treated human plasma FN for SDS-PAGE.**

Solution (μL)	Reducing	
	+	−
Protein sample from Table 2.6	6.67	6.67
10x NuPAGE reducing solution	2.4	0
4x NuPAGE sample buffer	6	6
MilliQ water	12.27	14.67
Total Volume	24	24
Volume loaded	4.8 (0.25 μg of protein per lane)	4.8 (0.25 μg of protein per lane)

Table 2.12: **Preparation of treated HCAEC-derived FN for SDS-PAGE.**

Solution (μL)	Reducing	
	+	−
Protein sample from Table 2.7	16.67	16.67
10x NuPAGE reducing solution	6.4	0
4x NuPAGE sample buffer	16	16
MilliQ water	8.9	15.3
Total Volume	64	64
Volume loaded	16 (1.25 μg of FN per lane)	16 (0.25 μg of FN per lane)

Table 2.13: **Preparation of enzymatically treated human plasma FN for SDS-PAGE which were used with both concentration of MPO experiments.**

Solution (μL)	Reducing	
	+	−
Protein sample from Table 2.8	25	25
10x NuPAGE reducing solution	4	0
4x NuPAGE sample buffer	10	10
MilliQ water	1	1
Total Volume	40	40
Volume loaded	8 (0.5 μg of protein per lane)	8 (0.5 μg of protein per lane)

2.2.4.1 Silver stain

Silver staining was used to visualise structural changes to protein samples such as aggregation or fragmentation. Gels were first removed from casing, and were then fixed in 50% (v/v) ethanol, 10% (v/v) acetic acid for a minimum of 30 min. Once gels were fixed, they were rinsed in 5% (v/v) methanol for 15 min, followed by three 5 min consecutive washes in milliQ water. After the gels were washed, it was submerged in freshly prepared 0.02% (w/v) sodium thiosulfate for 2 min, then washed in milliQ water for 2 min. Gels were incubated in ice cold 0.2% (w/v) silver nitrate for 25 min, then washed in milliQ water for 5 min. Gels were subsequently washed and silver containing liquid discarded according to standard laboratory protocol. Developer solution of 3% (w/v) sodium carbonate, 0.0004% (w/v) sodium thiosulfate (prepared from previously made solution), and 0.05% (v/v) formaldehyde, was poured over the gel until submerged. Developer solution was changed after 2 min, and once bands started appearing, gels were immersed in a stopping solution of 1.4% (w/v) EDTA. Over development of bands were prevented by adding a stop solution before the preferred band density formed.

2.2.4.2 Western blotting

Once separation was performed, gels were transferred onto PVDF membranes using an iBlot 2 gel transfer device (Life Technologies) and ran at 160 V for 70 min. The PVDF membranes were blocked in 1% (w/v) BSA in TBS with 0.1% (w/v) Tween 20 (TBST) for 1 hr on a shaker at 21°C, followed by an incubation with the desired antibody 2.1 at 4°C overnight on a rocker. The next day, membranes were rinsed for 5 min with TBST at 21°C on a shaker, prior to incubating with the respective secondary antibody diluted in 1% (w/v) BSA in TBST for 1 hr at 21°C on a shaker. Membranes were then washed in TBST for 1 hr with a change in washing solution every 15 min, then rinsed in TBS, and left in TBS solution until development.

Membranes were developed using Western lighting PLUS ECL reagents (1:1 ratio of reagent A to reagent B). Membranes were covered in the reagents, and developed on a Bio-rad® Chemidoc™ (California, U.S.A.) system or Syngene G:Box XR5 (Cambridge, UK).

2.2.5 High Performance Liquid Chromatography

Bovine plasma FN samples were treated with HOCl and prepared by following the treatment described in 2.14. Samples were prepared in inscribed hydrolysis vials to a total volume of 200 μL from a stock solution of 90 μL of stock 5 mg/ml bovine plasma FN (final concentration of 5 μM) diluted in 40 μL of 0.5 M pH 7.4 Phosphate buffer, and 30 μL of milliQ water. Each vial was then treated with a 40 μL of oxidant, followed by an incubation for 2 hr at 37°C. Sample vials were delipidated and precipitated by the addition of 25 μL of 0.3% (w/v) deoxycholic acid and 25 μL of 50% (w/v) TCA, which was incubated for 5 min on ice. The samples were spun down at 9000rpm for 2 min at 4°C to form a protein pellet. The protein pellet was washed with ice cold acetone four times with protein pellet being spun down again at 9000rpm for 2 min at 4°C between washes. Remnant acetone was carefully dried off with nitrogen gas. Once samples were dry, the protein pellets were re-suspended in 150 μL of MSA containing 0.2% (w/v) tryptamine, then each samples were transferred to respective pico-tag hydrolysis vials. The pico-tag vials were evacuated three times by alternating 10 secs of nitrogen, followed by 30 secs of evacuation (VWR gas pump), then a final evacuation was performed for 1-2 min, before being incubated overnight (16 hr, keeping each experimental time consistent) at 110°C in an oven. The next day, the vacuum vials were released to check that pico-tag vials were sealed properly before being allowed to cool to 21°C. Samples were neutralized by addition of 150 μL freshly prepared 4 M of NaOH (16% (w/v) NaOH in milliQ water; 1:1 ratio to MSA). Samples were filtered by centrifuging at 10000rpm for 2 min, through 0.2 μm Nanosep filters (Pall). Samples were diluted 10-fold into milliQ water, before 40 μL of the diluted samples were transferred to respective HPLC vials with 200 μL inserts.

Amino acid standard (A9781; Sigma-Aldrich), and 500 μM methionine sulfoxide for analysis was obtained commercially and prepared to 12.5 μM in milliQ water. The standard mixture was diluted further to create a linear standard from 0 to 50 pmol in increments of 10 pmol in milliQ water per 6 μL injection. Standard mix was also

Table 2.14: **Preperation of bovine plasma FN as 5 μM and treated with HOCl for amino acid analysis using HPLC.**

Solution (μL)	Example for one reaction vial
Stock protein (5 mg/ml)	90
0.5 M pH 7.4 Phosphate buffer	40
MilliQ water	30
Oxidant (1:5 dilution)	40
Total Volume	200

filtered through 0.2 μm Nanosep filters (Pall) at 10000 rpm for 2 min, then 40 μL of each standard was transferred to their own HPLC vial with 200 μL inserts in duplicates. Activated fluoraldehyde *o*-Phthaldialdehyde (OPA) reagent solution was prepared with 20:1 dilution to 2-Mercaptanol. The auto-injector was programmed to inject samples with 20 μL of activated OPA.

Table 2.15: **Preperation of amino acid standard derivatisation.**

pmol per 6 μL injection	12.5 μM standard stock (μL)	MilliQ water
0	0	120
10	24	96
20	48	72
30	72	48
40	96	24
50	120	0

The separation of amino acids was completed using a gradient buffer of low to high percentage organic solvent. Buffer A was comprised of 20% (v/v) methanol, 2.5% (v/v) Tetrahydrofuran (THF), 50 mM pH 5.3 sodium Acetate in milliQ water. Buffer B was comprised of 80% (v/v) methanol, 2.5% (v/v) THF, 50 mM pH 5.3 sodium acetate in milliQ water. Both buffers were prepared and filtered through a 0.2 μm Nanosep filters (Pall) using a vacuum apparatus.

Shimadzu HPLC machine was set-up with an auto-sampler programmed to derivatise each sample with 20 μL, followed by samples being mixed 3 times with incubation for 1 min. A Shimadzu Shim-pack xR-ODS, 4.6 mmid x 100 mm column was used, with a gradient elution between buffer A and buffer B (Table 2.17). The flow rate was adjusted

Table 2.16: **Method to prepare HPLC buffer A and buffer B.**

Solution	Buffer A (ml)	Buffer B (ml)
1M sodium acetate pH 5.3	200	200
THF	50	50
Methanol	400	1600
MilliQ water	1350	150

to 1.2 mL/min with the initial buffer A concentration starting at 100% and buffer B at 0%. The percentage of buffer B was increased to 25% slowly over 6 min and maintained at 25% for 1 min, before a steep increase to 62% in 30 sec, and was maintained for 2.5 min. Buffer B was then ramped up to 100% over 2 min, and maintained for 1 min, before buffer A was increased all the way back up to 100% for 3.5 min. The fluorescence of the derivatised amino acid was measured at 340 nm_{ex}, and 440 nm_{em} using a Shimadzu RF-AXS20 fluorescence detector.

A chromatagram of observed amino acid elution was used as seen in figure 2.2.

Table 2.17: **HPLC buffer ratios.**

Time (min)	Flow	Buffer A (%)	Buffer B (%)
0	1.2	100	0
6	1.2	75	25
7	1.2	75	25
7.5	1.2	38	62
10	1.2	38	62
12	1.2	0	100
13	1.2	0	100
13.5	1.2	100	0
17	1.2	100	0

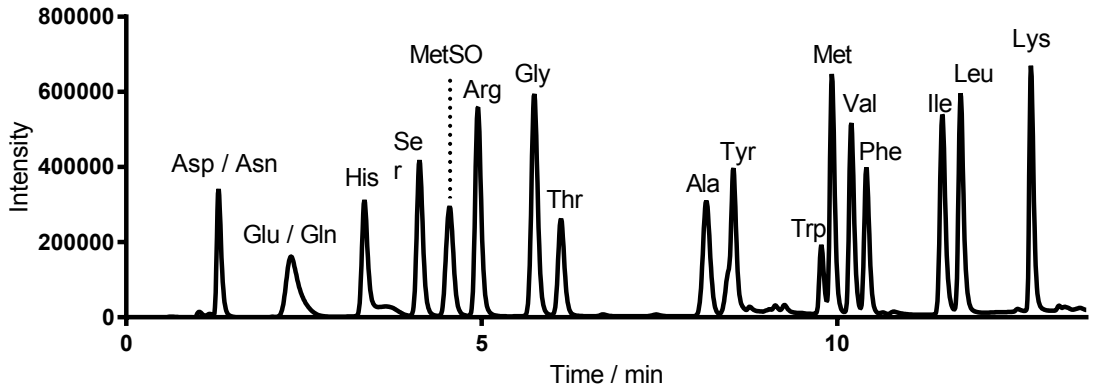

Figure 2.2: **Chromatogram of amino acid elution for HPLC.**

2.2.6 Thiol Assay

Bovine plasma FN sample solution was prepared at 5 μM according to table 2.18. Samples were either untreated or treated with 1x, or 50x molar ratio of HOCl or HOSCN to a final sample volume of 50 μL with a 96-well clear bottom plate. Samples were treated with 0, 5, and 250 μM of HOCl or HOSCN and was incubated for 2 hr at 37°C. An anhydrous 2.6 mM stock solution of ThioGlo (Berry and Associates; HC9080) was prepared following the manufacturer's instructions, which was stored in the dark at 4°C for use.

Table 2.18: **Preperation of bovine plasma FN as 5 μM with treatment with HOCl for Thiol analysis.**

Solution (μL)	Example for one reaction vial
Stock protein (5 mg/ml)	22.50
0.5 M pH 7.4 Phosphate buffer	10
MilliQ water	7.5
Oxidant (1:5 dilution)	10
Total Volume	50

A 5 μM GSH standard stock was prepared in milliQ water by making a 0.5 mM GSH solution in milliQ in a volumetric flask. This 0.5 mM GSH solution was diluted 1:100 to form the final 5 μM GSH solution. A linear standard was made from 0 to 5 μM in an integer of 1 μM according to table 2.19, and then 50 μL was transferred to the 96-well plate in triplicates. Working solution of ThioGlo was prepared by diluting the stock

solution 1:100 in 1x PBS and then 50 μL was transferred into each standard and sample well. The plate was mixed briefly on a plate shaker and incubated for 10 min in the dark at 21°C. The fluorescence was measured at 384 nm_{ex}, and 513 nm_{em}.

Table 2.19: **Method to prepare GSH standard for Thiol Assay.**

Concentration of GSH (μM)	5 μM stock (μL)	MilliQ water
5	400	0
4	320	80
3	240	160
2	160	240
1	80	320
0	0	400

2.2.7 Cell Adhesion

Clear bottom 96-well plates were prepared the same way as an ELISA plate when performing assay using crystal violet and calcein-AM; refer to section 2.2.2. Once plates have been treated they were proceeded under the respective methodology.

2.2.7.1 Cell adhesion – Crystal Violet

Treated plates were rinsed twice with 200 μL of sterile PBS before being blocked with 100 μL of 3% (w/v) BSA in DPBS for 1 hr at 37°C in a cell culture incubator. While plates were being blocked, HCAEC were prepared and re-suspended in 1% (w/v) BSA in Endo-Basal media. Plates were rinsed again twice with 200 μL, followed by being seeded with 50 μL of 2.5 x 10^5 cells/ml per well (12,500 cells), and incubated for 1.5 hr at 37°C in a humidified atmosphere containing 5% carbon dioxide (CO_2) . Any cells that were not adhered were rinsed off twice with 200 μL of sterile DPBS, and remaining adhered cells were fixed with 100 μL of 10% (v/v) formaldehyde in DPBS for 15 min at 21°C. Once cells were fixed, plates were washed four times with 200 μL of deionized water, followed by air drying the plate for 1 hr at 21°C. A 200 μL solution of 0.1% (w/v) crystal violet in 200 mM MES at pH 6.0 was used to stain each well and left for 20 min at 21°C. Excess crystal violet was washed off the plate with four times washes with 200 μL of deionized water before being allowed to air dry for 1 hr at 21°C. The crystal violet taken up by cells were re-solubilised in 200 μL of 10% (v/v) acetic acid, and absorbance was measured at 590 nm.

2.2.7.2 Cell adhesion – Calcein-AM fluorescence

Plates were similarly washed, and blocked with 3% (w/v) BSA in PBS for 1.5 hr at 37°C. HCAEC were trypsinised off the flask and re-suspended back in sterile 1% (w/v) BSA in

Endo-Basal media in a small sterile tube, and incubated with 5 μM per 5 x 10^6 cells/ml for 30 min at 37°C in a humidified atmosphere containing 5% CO_2. Cells were washed once with warm 1% (w/v) Endo-Basal Media, before being seeded onto twice washed with DPBS plates with 50 μL of 2.5 x 10^5 cells/ml per well (12,500 cells), followed by incubation at 1.5 hr at 37 °C in a humidified atmosphere containing 5% CO_2. Plates were carefully washed four times with 200 μL of 1% (w/v) BSA in Endo-Basal media by swirling, and blotting excess media on paper towel. Once relatively blotted dry, add 200 μL of DPBS into each well and the fluorescence was measured at 492nm$_{abs}$, and 517nm$_{ex}$.

2.2.7.3 Cell adhesion – Immunocytochemistry

Cultureslide Lab-Tek II Chamber 8 well (VWR) were coated with 250 μL of 10 μg/ml (0.02 μM) of human plasma FN and BSA used as control at the same concentration, and incubated overnight at 4°C. The next day, chambers were washed twice with 500 μL of sterile PBS before treatment with 250 μL of oxidant (refer to Table 2.4), followed by incubation for 2 hr at 37°C. After incubation, chambers were washed with 500 μL of sterile PBS, then blocked with 500 μL of 3% (w/v) BSA in PBS for 1 hr at 37°C. The chambers were rinsed again with 500 μL of sterile PBS, then HCAEC was seeded with 250 μL of 2*10^5 cells/ml (50,000 cells) into each well, and incubated for 1.5 hr at 37°C in a humidified atmosphere containing 5% CO_2 to allow cells to adhere. Any un-adhered cells were washed off twice with 500 μL of sterile PBS, and fixed with fixing solution of 7.56% (v/v) of 38% formaldehyde, 0.72% (w/v) sucrose in PBS for 15 min at 37°. Chambers were washed twice with PBS to remove excess fixing solution, then cells were permeabilised with permeabilising solution, 10.30% (w/v) sucrose, 0.292% (w/v) NaCl, 0.476% (w/v) HEPES, 0.5% (v/v) Triton X-100 in milliQ water for 5 min at 4°C to allow fluorescence probes to permeate into cells. Each well was rinsed with 500 μL of 0.5% (w/v) Tween-20 PBST before being blocked with 1% (w/v) BSA in PBS for 1 hr at 21°C. Chambers were twice washed with 500 μL PBST, and were incubated overnight at 4°C with 250 μL of 1x rhodamine-phalloidin diluted in 1% (w/v) BSA in PBS to stain

F-actin fibres within cells.

The next day, chambers were washed with 500 μL of PBST, followed by incubation with 250 μL of Hoechst 33342 (H1399; 1:2000 dilution to get a final DMSO concentration of 5 μg/ml) in PBS for 15 min in the dark at 21°C, whereby the stain can permeate into the nuclei. Chambers were washed twice with 500 μL of PBS to remove any excess stain, and left in PBS. When ready to image, remove the plastic chambers, apply one drop of SlowFade Diamond Antifade (S36963; ThermoFisher Scientific) to help mount the slide prolong the fluorescence, then clean the coverslip prior to imaging on a fluorescence microscope.

2.2.8 Cell Metabolic Activity

HCAEC metabolic activity plates were prepared the same way as HCAEC adhesion experiment. After plates have been seeded and incubated with 12,500 HCAEC for 1.5 hr at 37°C in a humidified atmosphere containing 5% CO_2, the plate were twice washed with 200 μL sterile PBS. They were incubated with fresh HCAEC growth medium for 48 hr at 37°C in a humidified atmosphere containing 5% CO_2. This method can also be completed post cell adhesion using Calcein-AM protocol by leaving plates for 48 hr with 200 μL fresh HCAEC growth media. After 48 hr, 20 μL of CellTiter 96® Aqueous One Solution Assay (G3580; Promega) was added into each sample well, and the absorbance was measured at 490 nm, 0 hr, 1hr, 2hr, 3hr, and 4hr. Analysis of data was made on data collected at 2 or 3 hr.

2.2.9 RNA expression

Sterile 6-well culture plates were coated with 2 ml of 20 μg/ml (0.04 μM) of human plasma FN overnight. On the next day, each well was either untreated (0.1 M sodium phosphate pH 7.4 buffer) or treated with 1250x molar ratio (50 μM) of HOCl or HOSCN diluted in 0.1 M sodium phosphate buffer pH 7.4, in triplicates for 2 hr at 37°C. HCAEC were seeded into each well at a density of 5 x 10^6 and incubated for 72 hr at 37°C in a humidified atmosphere containing 5% CO_2. Medium was discarded and each well was rinsed with sterile PBS to wash off any remaining serum and media. Using a Qiagen RNeasy Mini Kit, the HCAEC was harvested by adding 350 μL of RLT buffer and a scraper was used to remove all cells from well surface. The lysates were transferred to sterile eppendorf tubes and the cell pellet was broken up using a 25 gauge syringe and pipetting up and down. To the samples, 350 μL (1:1 ratio to RLT buffer) of 70% ethanol was added to precipitate out DNA and RNA, and the total sample was spun through an Rneasy Mini Spin column for 15 sec at 8000g. The flow-through was discarded before DNA was digested by adding 350 μL of RW1 to the RNeasy column, followed by a centrifuge for 15 sec at 8000g, with the flow-through being discarded. For each sample, DNase 1 working solution was prepared by combining 10 μL of stock solution to 70 μL buffer RDD (1:8 dilution) and gently inverting to mix, followed by a quick centrifuge. To each sample, 80 μL of DNase 1 was added directly to the RNeasy column membrane and incubated for 15 min at 21°C. The RNeasy column was washed with 350 μL of RW1, with the flow-through being discarded, followed by another wash with 700 μL of RW1 with centrifuge for 15 sec at 8000g. Each sample tube was spun down with 500 μL of RPE for 15 sec at 8000g, discarding flow-through, followed by another wash with 500 μL of RPE and centrifuged for 2 min at 8000g. The flow-through was discarded, and the RNeasy spin column was transferred to a new sterile 2 ml collection tube. The column was centrifuged for 1 min at full speed to dry off the membrane. The collection tube was discarded, and the RNeasy column was placed into a new sterile 1.5 ml collection tube. To each sample tube, 30 μL of RNase-free water was directly added to the membrane of the RNeasy spin

column, and centrifuged for 1 min at 8000g to elute out RNA. If concentration of RNA was expected to be greater than 30 μg, another 30-50 μL of RNase-free water can be spun through or the previous eluate can be spun through the column again.

RNA samples were then tested for purity by using a NanoDrop machine or a SpectraDrop micro-volume 24-well microplate, and measuring the spectrum absorbance of samples. When using a SpectraDrop micro-volume 24-well microplate, 2 μL of each sample was pipette into each 0.5-mm spacers sample well, this was measured against RNase-free water. Spectral absorbance measurements were made at 260 nm, 280 nm, 230 nm, and 320 nm. To analyse sample contamination, ratio between 260:230 (organic contamination) and 260:280 (DNA contamination) were calculated 2.20. Nucleic concentration was calculated as the optical density for absorbance at 260 nm (OD260) was 1, which was equivalent to 40 ng/μL of nucleic acid.

Table 2.20: **Absorbance for determining different components in RNA prepped samples.**

Absorbance	**Ratio for high purity RNA**
Abs 260 Nuclein Acid concentration - OD260 = 1 = 40ng/μL	**Abs260/Abs280** 1.8 for DNA purity 1.8 - 2.1 for RNA purity
Abs 230 Detects organic contaminations for example: phenol, trizol	**Abs260/Abs230** <1.8
Abs 280 Protein detection	**Abs260/Abs320** 1.8 - 2.2
Abs 320 Non-nucleic acid or protein contaminant	

Nucleic acid concentration was calculated for each sample for total yield and volume required for 400 ng of nucleic acid for cDNA synthesis using RT2 First Strand Kit (330404: Qiagen). Reagents were thawed out from the kit and briefly centrifuged to settle the solutions. For each sample, genomic DNA elimination (DNA-elim) mix was prepared by combining RNA with Buffer GE, and Nuclease-Free water (Table 2.21). The DNA-elim mix was incubated for 5 min at 42°C, then immediately put onto ice for a minimum of 1 min. The Reverse-Transcriptase (RT) mix was prepared by combining 5x

Buffer BC3 (2:5), Control P2 (1:10), RE3 RT-mix(1:5), and Nuclease-Free water (3:10) to a total volume of 10 μL per reaction (Table 2.22).

Table 2.21: **Preparation for elimination of DNA.**

Component (μL)	Volume (μL)
RNA sample	X (equal to 400ng of RNA)
Buffer GE	2
Nuclease-free water	10 - X
Total Volume	10

Table 2.22: **cDNA synthesis preparation method.**

Component (μL)	Volume (μL) per reaction
5x Buffer BC3	4
Control P2	1
RE3 RT-mix	2
Nuclease-free water	3
Total Volume	10

Into each sample tubes containing 10 μL of DNA-elim mix, 10 μL of RT-mix was added and gently mixed. Samples were incubated in a thermal cycler for 15 min exactly at 42°C, then the RT was inactivated with an immediate incubation for 5 min at 95°C. Samples were centrifuged briefly to spin down any condensation, then 91 μL of RNase-free water was gently mixed in. Samples were placed on ice to continue real-time PCR or stored in -20°C until ready for use.

An RT^2 Profiler PCR Human Extracellular Matrix and Adhesion molecules (330231; QIAGEN) was used for analysing a multi-array of genes associated ECM and adhesion, housekeeping genes, and controls for genomic DNA, RT-transcriptase controls, and positive PCR control. First, RT^2 SYBR Green Mastermix was centrifuged for 10-15 sec to settle the contents. Sample PCR mix was prepared in sterile 2 ml eppendorf tubes by adding in 51 μL of 2x RT^2 SYBR Green Mastermix, and 43 μL of RNase-free water to the 8 μL of cDNA synthesis reaction for a total of 102 μL. This allows for an excess of 6 μL for pipetting errors; samples can be prepared at higher volume for greater error capacity. Pipette tips were changed for each well to avoid cross contamination, and 10 μL

was added to each well. An adhesive plate cover was used to cover each plate, followed by centrifuging for 1 min at 21°C at 1000g to minimise any bubbles present in samples. RT^2 Profiler PCR Array was kept on ice prior to performing PCR. PCR cycling was programmed as per Table 2.23 using ViiA-7 instrument with ViiA-7 Software v1.2 (Life Technologies).

Table 2.23: **Setup for thermocycler for qPCR.**

Stages	Time	Temperature (°C)	Temp Change	Cycles
Hold	10 min	95	1.6	1
PCR	15 sec	95	1.6	40
	1 min	60	1.6	
Melt Curve	15 sec	95	1.6	1
	1 min	60		
	15 sec	95	0.05	

The threshold was defined with the log view of the Y-axis of the amplification plots, and set to 0.02, which should sit above the background signal but should sit in the lower third when examining the amplification plot linear phase. Using the linear plot phase of the Y-axis, the baseline should be set to where the first amplification was visible starting from cycle 2 but no further than cycle 15; amplifications were usually visible around cycles 14 to 18. The threshold should remain the same between all RT^2 Profiler PCR Array to ensure consistent analysis. C_T values were exported to a blank Excel sheet and data analysis can be performed using SABiosciences PCR Array Data Analysis Template and Web-based analysis software (`www.SABiosciences.com/pcrarraydataanalysis.php`).

2.2.10 Immunohistochemistry of Human Atherosclerotic Lesions

Aortae or aortae abdominalis sections were obtained from subjects who have died from cerebral haemorrhage. Lesions obtained this way were classified according to Stary's system to microscopically identify normal to thickened intima (lesion type II-III), to prominent calcified atheroma (lesion type IV). Samples were obtained within 12 hr of post mortem. Tissue were immediately frozen in cryostat (Microm HM500 OM; Microm, Walldorf, Germany) using tissue freezing medium (Tissue Tec OCT-compound; Miles, Elkhard, Ind., USA). Glass slides were used to collect 5 μm of serial cryosections which were air dried for 2 hr at 21°C, followed by fixing with acetone for 5 min at 21°C. Samples were stored at -80°C until required for further analysis.

Acetone fixed tissue sections were thawed for 5 min at 21°C, and PBS was used to rehydrate sections, followed by blocking with Ultra V block for 10 min (Lab Vision, Fremont, CA, USA). Once samples were blocked, they were incubated with primary monoclonal anti-FN or polyclonal anti-FN antibody for 30 min which were diluted with antibody diluent (Dako), followed by a wash with PBS. Sample slides were incubated in appropriate secondary antibodies; Polyclonal anti-FN incubated sections were incubated with HOCl-generated epitope antibody, and monoclonal anti-FN sections were firstly blocked with normal mouse serum (1:25) for 15 min, followed by incubation with Cy-3 labelled anti-HOCl generated epitope antibody in dark moisture chambers at 21 °C.

Sections were mounted with Moviol (Calbiochem-Novabiochem, La Jolla, USA), and analysed with a confocal laser-scanning microscope in sequential mode (Leica SP2, Leica Lasertechnik GmbH, Heidelberg, Germany). Settings used in analysis for Cy-2 (green staining) incubated samples were 488 nm_{ex}, and 500-540 nm_{em}, and for Cy-3 (red staining) were 543 nm_{ex}, and 560-620 nm_{em}

Chapter 3

Modifications to fibronectin by HOCl

3.1 Introduction

FN is a dimeric glycoprotein of approximately 460kDa in size and composed of two monomer subunits (220-270kDa) bound by two disulfide bonds at the carboxyl termini [149, 195, 196]. There are two defined types of FN; soluble plasma FN, which is produced primarily by hepatocytes and released into blood plasma, and insoluble cellular FN, which is produced by various cells, such as fibroblasts and EC, and is present in the basement membrane of tissues [149, 195, 196]. Plasma FN plays a key role in wound healing by interacting with fibrin and causing a coagulation cascade to form blood clots. Cellular FN interacts with the surrounding extracellular matrix (ECM) to create a complex network providing structure and assisting in cellular functions, such as adhesion, proliferation and migration [140, 274]. Furthermore, FN has been found to initiate matrix assembly in response to certain functional sequences (CBF or HBF) by interacting with cell surface receptors and integrins [149, 197].

The integrity of atherosclerotic plaques is highly dependent on vascular remodelling, ECM deposition, and vascular smooth muscle cells (SMC) migration. Changes to a number of these factors can result in smaller, thinner plaque caps, which have been found to be more unstable and have higher risk of rupturing [1]. Plaque ruptures causes a coagulation cascade, forming luminal clots and subsequently myocardial infarction or

strokes [1]. The importance of FN is notable in the development of atherosclerosis and in several other diseases [1, 140, 253, 274]. In the progression of atherosclerosis, increased expression of FN has been found localised within areas of injury and plaque development [275–277]. Patients with coronary artery disease (CAD) were demonstrated to have elevated plasma FN levels [278–280]. However, other studies have shown that circulating plasma FN levels do not correlate with occurrence of CAD [281, 282]. Circulating FN is a potential contributor to CAD development, but it is likely to act in conjunction with other atherosclerosis promoting factors. For example, deficiency of plasma FN in apoE$^{-/-}$ mice was found to result in a smaller number and sizes of atherosclerotic plaques, with reduced levels of monocyte recruitment [264]. However, the plaques that formed were found to have decreased matrix protein deposition, decreased vascular SMC infiltration into injury area, and were thinner and more unstable, which would indicate higher susceptibility to plaque rupture in humans [264]. Furthermore, FN is also known to stimulate EC growth, whereby EC incubated on FN were found to have sustained adherence of up to four days [235]. These important functions are accompanied with increased levels of inflammatory cells, and lipoprotein retention [265]. These findings suggests the importance of FN in plaque development and progression.

Atherosclerotic plaques have been reported to have high levels of inflammatory cells with particularly large numbers of macrophages in the shoulder region of lesions [283]. This means that FN, and other ECM species, are in close proximity with inflammatory oxidants released by activated leukocytes, which suggests that they would be likely targets of these reactive oxygen or nitrogen species [21]. Myeloperoxidase (MPO), is a haem-peroxidase that produces certain reactive oxygen species (ROS) [11]. Hypochlorous acid (HOCl) is one of the major reactive oxygen species to be produced by MPO in response to inflammation, and in high concentrations it has been found to target host proteins, such as ECM molecules, and cells, such as ECs [50, 57, 152, 284]. HOCl is highly reactive and oxidises a range of targets, including: iron-sulfur centres, sulfide (thioether) groups, sulfhydryl groups and unsaturated fatty acids [8, 45–48]. Furthermore, it has

been demonstrated that *in vitro* exposure of FN to HOCl, causes several structural and functional modifications [22, 64, 65, 260, 261]. HOCl has previously been found to fragment FN and cause protein aggregation [65, 260], whereby these structural changes have been proposed to cause loss of FN epitopes important for function and survival [22, 261, 271]. Inhibition of the gelatin binding site with an anti-50k antigen binding fragment (Fab') resulted in a decreased deposition of collagen type I, pro-collagen type III and FN, suggesting that the fibrillar structures formed between the two proteins are important [258].

These data suggest that FN is important in vascular architecture in arterial remodelling and in the initiation and progression of certain diseases. Taking these previous findings into consideration, it was hypothesised that human plasma and cellular FN would be targeted and modified by HOCl. These modifications would cause structural changes to FN, leading to aggregation, fragmentation, and subsequent biological dysfunction of cells incubated on HOCl-modified FN.

3.2 Aims

The experiments carried out during these studies were aimed at elucidating the effects of HOCl on isolated human plasma FN and cellular-derived FN in whole ECM extracts. The structural modifications of FN by HOCl and the subsequent effect on antibody recognition of the FN epitopes important to its function were investigated. Amino acid analysis was performed to examine changes to amino acids using HPLC and ThioGlo. Furthermore, biological changes were examined using HCAEC exposed to HOCl-modified FN, by measuring cellular adhesion, cell metabolism, and gene expression. Lastly, these experiments investigated the occurrence of FN and an HOCl-generated epitope in human atherosclerotic lesions.

3.3 Results

3.3.1 Effect on human plasma fibronectin epitope with HOCl modification

Modifications occur through oxidation by HOCl, leading to structural changes in FN, and the subsequent loss of epitope recognition, and further biological dysfunction. Monoclonal antibodies were utilised to detect sites of functional interests on plasma FN including the CBF, HBF, and the presence of HOCl-generated epitopes. The CBF is very important for cell adherence to the sub-endothelial basement membrane, whereby the loss of this particular interaction could lead to a dysfunctional arterial matrix and wall, while the HBF interacts with heparin and heparan sulfates, which functions to stabilise the matrix and cell adhesion [149, 195, 196]. The 2D10G9 antibody used to detect HOCl-generated damage was originally raised against HOCl-oxidised LDL and binds onto an unidentified HOCl-generated epitope [63]. Measurements were made on plated FN exposed to oxidant, before using an ELISA method to quantify antibody recognition. The types of chemical modification and favoured region cannot be identified using this particular method.

In initial experiments, 50 μL of 10 μg/ml of FN (0.02 μM) in 0.1 M of pH 7.4 phosphate buffer was coated on high-binding protein ELISA plates overnight at 4°C. The sample wells were then washed with 1x PBS to remove any unbound FN, and were treated with 50 μL of corresponding concentrations of reagent HOCl (0, 5, 10, 25, 50, 100, 200 μM) diluted in 0.1 M of pH 7.4 phosphate buffer (refer to Table 2.4). Plates were incubated for 2 hr at 37°C, followed by a wash with 200 μL of 1x PBS to remove any excess HOCl or secondary products to prevent artefacts or other by-products. Plates were then blocked with 100 μL 0.1% (w/v) casein in PBS to prevent any non-specific binding, subsequently washed and incubated with 50 μL primary anti-CBF, anti-HBF, and anti-HOCl epitope antibodies. Sample plates were incubated overnight at 4°C on a rocker to ensure even binding of primary antibody, followed by a wash with 200 μL 0.1% Tween 20

in PBS (PBST) and incubation of respective secondary antibody for 1 hr at 21°C on a rocker. Sample plates were washed four times with 200 μL PBST, and were subsequently quantified with 100 μL of freshly prepared ABTS solution by adding H_2O_2 in a ratio of 1:1000 of stock ABTS. Quantifications were made at 405 nm at 30 min.

Exposure of surface-bound human plasma FN to HOCl was observed to have modifications to the CBF epitope, showing a statistically significant loss of epitope at 500x molar ratio of HOCl (Figure 3.1A). There was approximately 60% loss of recognition at 1250x molar ratio of HOCl and complete loss of the epitope at 2500x molar ratio (Figure 3.1A). FN HBF also showed statistically significant loss at 500x molar ratio with almost complete loss at 2500x molar excess (Figure 3.1B). This loss of recognition was accompanied by the increasing presence of a HOCl-generated epitope detected using the 2D10G9 antibody reaching statistical significance at 2500x molar excess (Figure 3.1C). At higher concentrations, there was a decrease in the presence of HOCl-generated epitopes, likely due to further modifications leading to destruction or aggregation of the protein resulting in regions where the antibodies cannot penetrate.

This result has shown that HOCl modifies FN, particularly at the CBF and HBF functional epitopes, causing loss of antibody recognition. In light of this, further experiments were carried out to investigate potential structural changes to FN using SDS-PAGE, including examination by Western blotting to examine the structural damage of those functional epitopes.

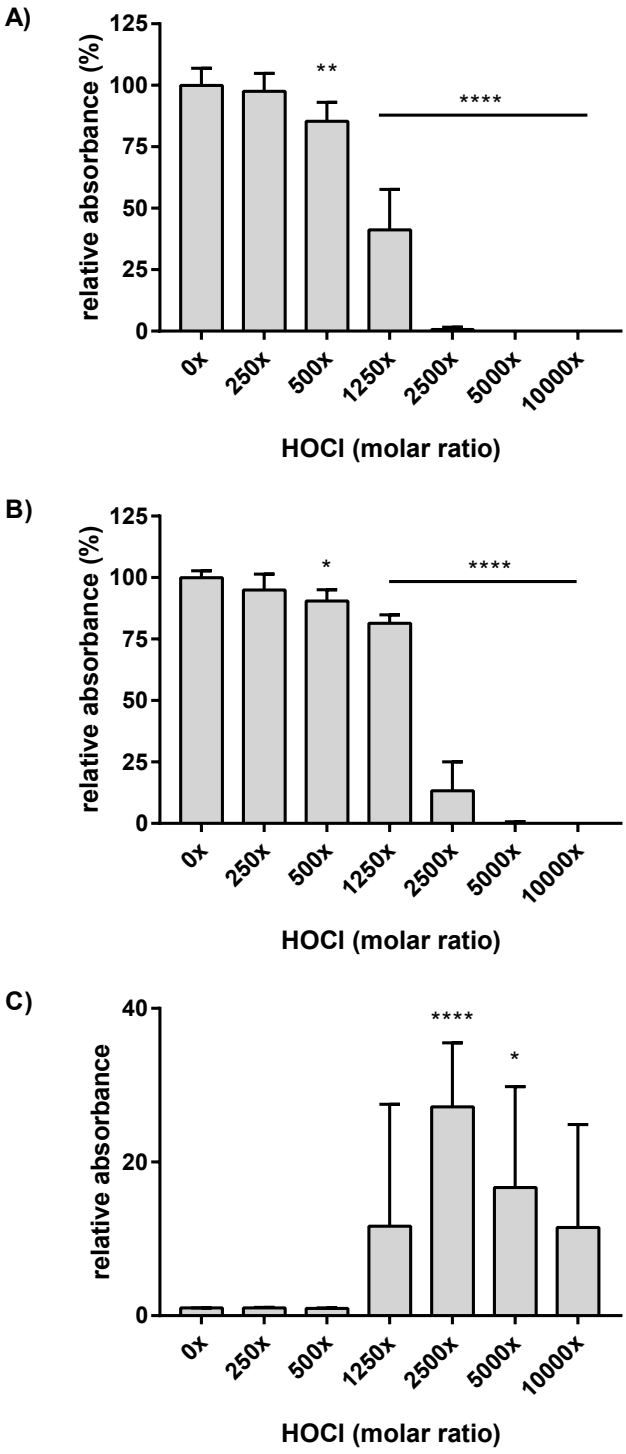

Figure 3.1: **ELISA of human plasma FN treated with increasing concentrations of HOCl.** Each well was coated with 0.5 μg (0.02 μM) of human plasma FN in 0.1 M phosphate buffer and either left untreated (control) or treated with HOCl (0, 5, 10, 25, 50, 100, 200 μM), and incubated for 2 hr at 37°C. FN epitope was detected by using a mouse monoclonal **A)** anti-FN CBF antibody (A17; 1:10000), **B)** anti-FN HBF antibody (A32; 1:1000), **C)** anti-HOCl generated epitope (2D10G9; 1:50), and conjugated with anti-mouse HRP secondary antibody (1:1000). The data are presented as a percentage of the relative absorbance of control (no oxidant; 0 μM treatment). Error bars are ± SD from three technical triplicates obtained from each of three independent experiments. Statistical analysis was performed using one-way ANOVA with Tukey's multiple comparison post hoc tests to determine significance. Statistical significance was identified as follows: * = $p < 0.05$, ** = $p < 0.01$, and **** = $p < 0.0001$.

3.3.2 Effect of HOCl on the structure of human plasma fibronectin

To further investigate HOCl-induced modifications of FN, structural changes were examined using SDS-PAGE separation followed by silver staining and Western blotting of treated proteins to probe for alterations to functional epitopes leading to modifications unrecognised by antibodies. Smaller molar ratios of FN:HOCl were used as to identify minor structural changes of FN (and corresponding functional epitopes) at concentrations lower than the concentration where complete loss of antibody recognition was observed (i.e. $<$ 1250x molar ratio). Silver staining was used to detect protein bands, including the parent dimer band (black arrow) at around 460 kDa (Figure 3.2) and the parent monomer band (white arrow) at 230 kDa (Figure 3.2). SDS-PAGE was used to identify whether there were changes to protein mass arising from HOCl-induced modifications or whether oxidant exposure led to fragmentation or aggregation of FN protein. By having non-reducing and reducing samples, information can be obtained on the possible presence of higher aggregates based on whether they contain new inter-chain (reducible) disulfide bonds or are aggregating by other chemical bonds.

Human plasma FN (2.5 μg at 1 μM) in 0.1 M pH 7.4 phosphate buffer was treated with increasing molar ratios of reagent HOCl (0, 5, 10, 25, 50, 100, 200 μM) diluted in 0.1 M pH 7.4 phosphate buffer, prior to separation on the basis of molecular mass by SDS-PAGE. Gels were subsequently fixed with 10% (v/v) acetic acid and 50% (v/v) methanol solution, and protein bands were detected with silver staining. The data obtained under non-reducing conditions showed increased detection of dimer and decreased detection of monomer bands, with increased presence of both higher aggregates and fragments in a HOCl dose-dependent manner (Figure 3.2A). The samples electrophoresed under reducing conditions showed increasing detection of the monomer band, with dimers/higher aggregates appearing following incubation with high ($>$ 200x) HOCl molar ratios (Figure 3.2B).

After SDS-PAGE separation, protein bands were transferred onto PVDF membranes

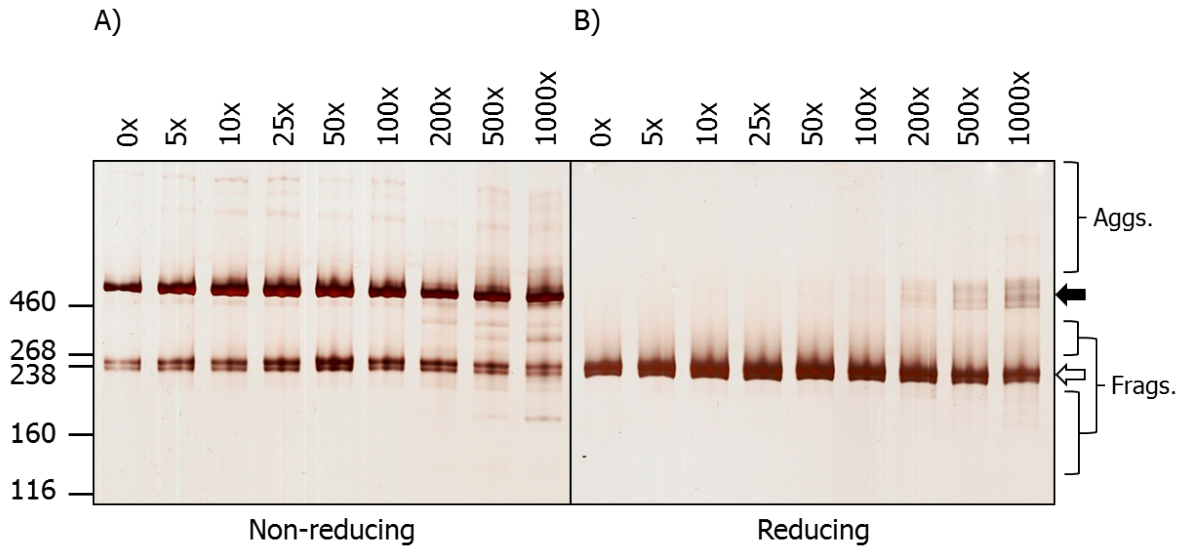

Figure 3.2: **Silver staining of SDS-PAGE gels showing structural changes to human plasma FN treated with increasing molar ratios of HOCl.** Human plasma FN (1 μM) in 0.1 M phosphate buffer was either untreated (control; 0x oxidant treatment) or treated with increasing concentrations of HOCl (0, 5, 10, 25, 50, 100, 200 μM), and incubated for 2 hr at 37°C. Samples were separated using 3-8% Tris-acetate SDS-PAGE gels under **A)** non-reducing or **B)** reducing conditions. Gels were then fixed, and visualised with silver stain and referenced against HiMark™ pre-stained high molecular mass standards. Bands are labelled as follows: black arrow = parent dimer, white arrow = parent monomer band, Aggs. = higher aggregates, and Frags. = fragments.

using an iBlot 2 transfer system and probed for the presence of functional epitopes. PVDF membranes were blocked with 1% (w/v) BSA in 1x TBS and 0.1% (v/v) Tween 20 (TBST), followed by incubation with primary antibody overnight at 4°C. Excess primary antibody was removed by washing with TBST, then the samples were incubated with a HRP-conjugated secondary antibody followed by four washes with TBST before development with ECL reagent and acquisition of blot images with an imaging machine. Western blots were performed and probed for FN CBF under non-reducing and reducing conditions. HOCl-treated FN samples showed an increased detection of both dimer/higher aggregate (black arrow) and monomer (white arrow) bands under non-reducing conditions (Figure 3.3A). Higher mass aggregates and fragments that possessed the CBF were also detected in a dose-dependent manner at higher HOCl molar ratios (Figure 3.3A). Samples electrophoresed under reducing conditions were found to show the presence of dimer/higher aggregate at high HOCl to FN molar ratios (Figure 3.3B). Fragments of FN were also detected with increasing fragmentation occurring at high

molar ratios of HOCl to FN (Figure 3.3B).

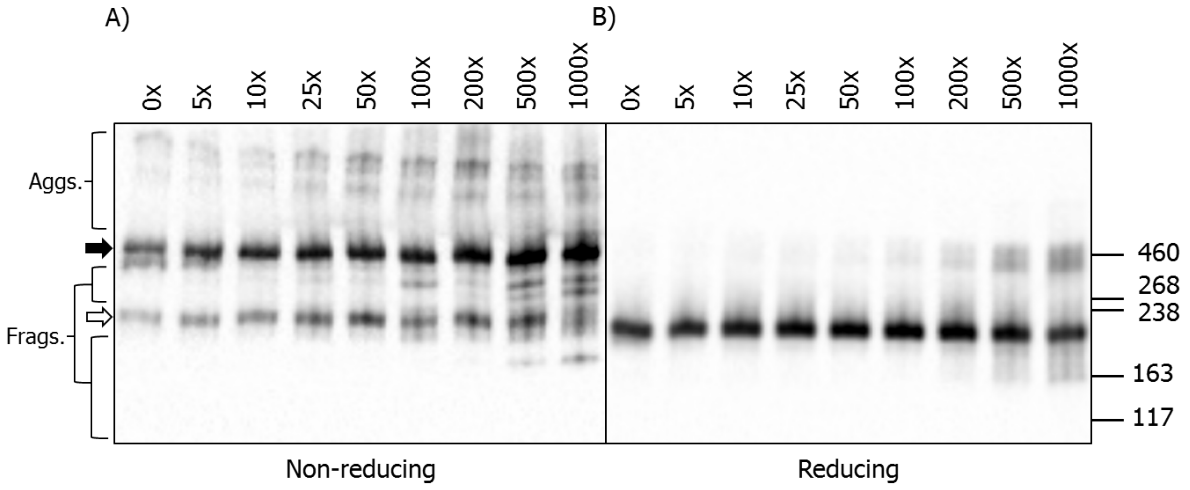

Figure 3.3: **Western blotting showing structural changes to human plasma FN treated with increasing molar ratio of HOCl.** Samples were separated on SDS-PAGE under **A)** non-reducing or **B)** reducing conditions and transferred onto PVDF membranes. PVDF membranes were probed with mouse monoclonal anti-FN CBF antibody (A17; 1:10000), and conjugated with anti-mouse HRP secondary (1:2000). Blots were developed with ECL-plus reagent. Bands are labelled as follows: black arrow = parent dimer, white arrow = parent monomer band, Aggs. = higher aggregates, and Frags. = fragments.

Structural changes on the proteins are usually caused by modifications to the amino acid side chains, leading to changes in interactions between each other, that can cause aggregation, or modifications to the peptide backbone resulting in fragmentations. Thus, amino acid analysis was utilised to assist in identifying what amino acids were targeted on FN during exposure to HOCl.

3.3.3 Amino acid analysis of HOCl treated bovine plasma fibronectin

HOCl is known to target and modify certain amino acids on protein, and by analysing which amino acids are affected, sites of modifications can be identified. Amino acids that are major targets of HOCl in decreasing kinetic order are Cys > Met > His > Cystine > Trp > Lys > Tyr [51]. FN was treated with varying concentrations of HOCl and incubated for 2 hr at 37°C which was then precipitation by adding 0.3% (w/v) deoxycholic acid and 50% (w/v) TCA and incubated for 5 min on ice (Figure 3.4). Samples were spun down to form a protein pellet, which was washed four times with ice cold acetone, with any remaining acetone being removed with N_2 gas. The protein pellet was then hydrolysed with the addition of 0.2% (w/v) tryptamine in MSA in pico-tag hydrolysis vials, under vacuum, and incubated overnight at 110°C to release the free amino acids. Vials were left to cool to 21°C the next day and neutralised with 4 M NaOH, and subsequently filtered through 0.2 μm Nanosep filters (Pall). Quantifications were made with HPLC with fluorescence detection after being tagged with OPA. This particular method is unable to measure changes to Cys/cystine residues and other methods are needed to define these residue modifications. Bovine plasma FN (P07589; Uniprot data), closely related to human FN in structure (90% sequence similarity; Uniprot data), was used for these experiments as this was easier to obtain in the amounts required needed for experiments. Amino acids were separated using a gradient buffer and a Shimadzu Shim-pack xR-ODS column, following method used previously [130].

Amino acid analysis of bovine plasma FN treated with HOCl showed that methionine was heavily modified with a dose-dependent decrease of the parent amino acid. This decrease was statistically significant with a 200x molar ratio and HOCl, and a complete loss of the parent was detected at a 1000x molar ratio (Figure 3.5A). Methionine sulfoxide (MetSO) is commonly regarded as the major product of methionine oxidation [50]. Analysis of FN showed that there was some MetSO present in the untreated samples, and no statistically significant increase was detected with increasing molar ratios of HOCl (Figure 3.5B).

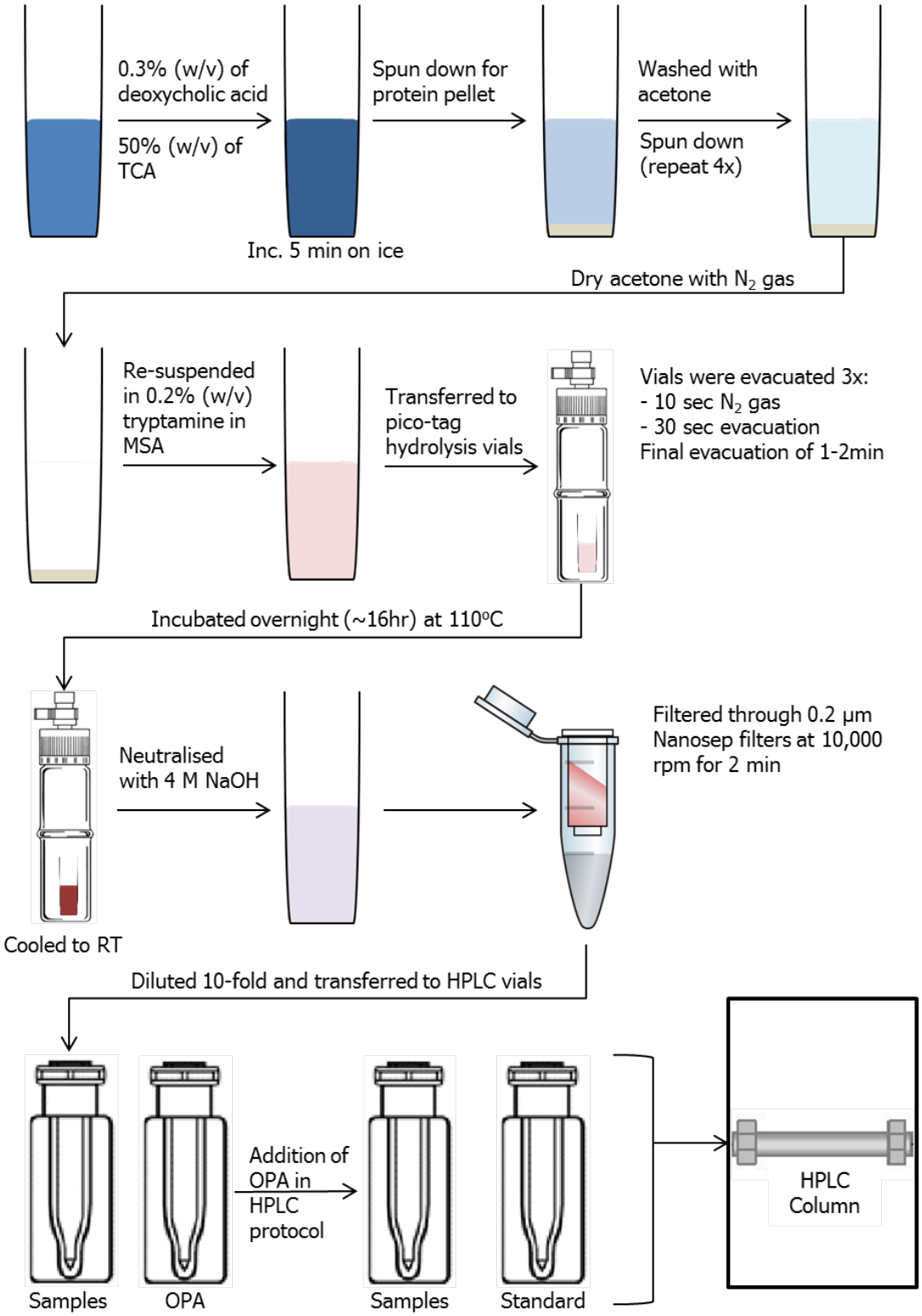

Figure 3.4: **Methodology used to prepare bovine plasma FN for amino acid analysis using HPLC.** Bovine plasma FN was treated with increasing concentration of HOCl, prior to being precipitated and hydrolysed to released free amino acids, which were tagged with OPA, and quantified using HPLC with fluorescence detection.

However, at 1000x molar ratio, there was a statistically significant decrease in MetSO, which was likely due to secondary oxidation of the sulfoxide to the sulfone which cannot be detected in this method.

Trp and Tyr residues are also reactive targets of HOCl [49]. It was demonstrated that when FN was treated with HOCl, there was a decrease in Trp in a dose-dependent manner, with statistically significant loss starting at 200x molar ratio (Figure 3.5C). However, although Tyr is also known to be oxidised by HOCl, there was no changes to the parent Tyr residues of FN when exposed to increasing concentrations of HOCl. This may be due to its low reactivity and the abundance of alternate targets in FN. Other amino acids (Asp, His, Ser, Glu, Arg, Gly, Thr, Ala, Val, Phe, Ile, Leu, Lys) were not found to be targeted by HOCl in these studies and thus were omitted from these results.

Furthermore, a ThiolGlo assay was performed to analyse the modifications to thiol residues on FN treated with HOCl. Treatment with 1x molar ratio of HOCl resulted in no significant changes to the concentrations of thiols (Figure 3.6). Increasing the treatment to HOCl 50x resulted in a loss of thiols of close to 50% (Figure 3.6).

Having identified that FN was structurally modified by exposure to HOCl, likely through changes to certain amino acids or the structural peptide backbone, it was proposed that loss of FN structural integrity would lead to a biological dysfunction. Thus, biological assays were utilised to identify cellular function.

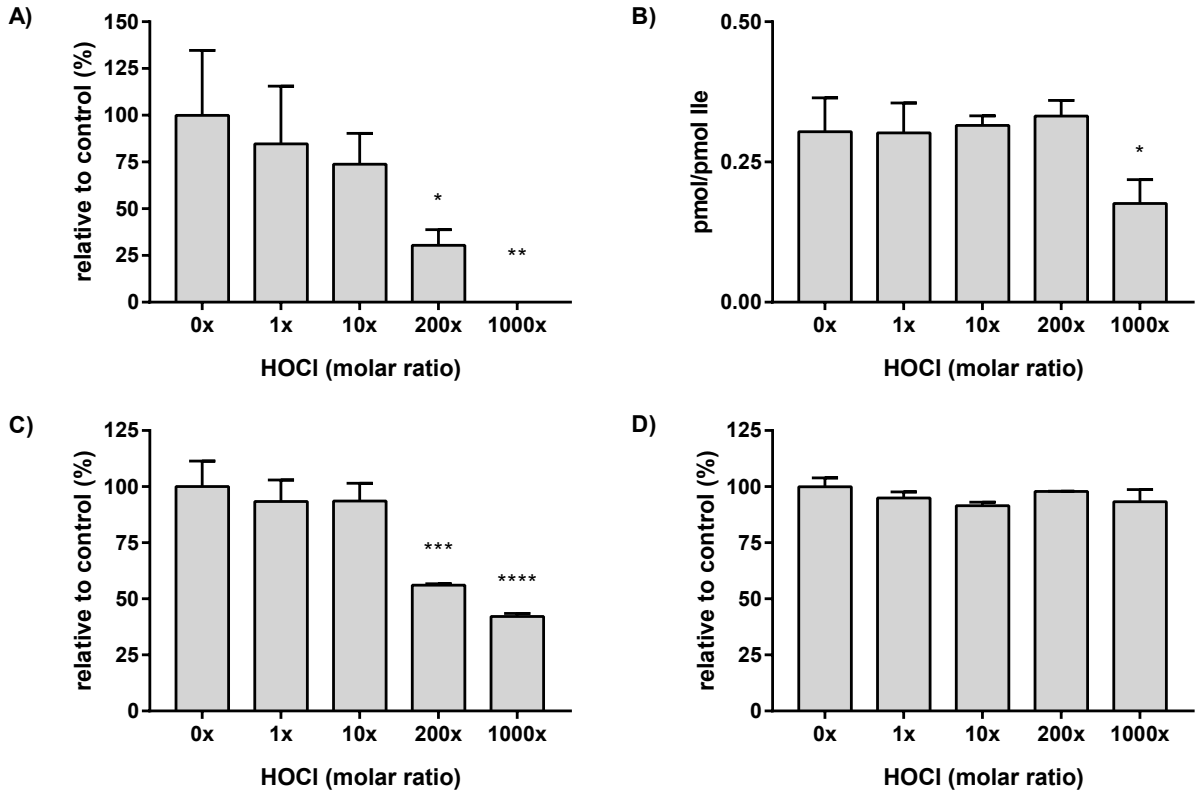

Figure 3.5: **Amino acid analysis of bovine plasma FN treated with increasing molar ratio of HOCl.** Bovine plasma FN (5 μM) was treated with the indicated molar ratio of HOCl (0, 5, 50, 1000, 5000 μM) then hydrolysed and derivatised for detection after separation using HPLC. Data analysis showed changes in **A)** Met, **B)** MetSO, **C)** Try, and **D)** Tyr. The data are presented as a percentage relative to control (no oxidant 0x treatment). Error bars are ± SD obtained from three independent experiments. Statistical analysis was performed using one-way ANOVA with Tukey's multiple comparison post hoc tests to determine significance. Error bars are ± SD from three independent experimental triplicates. Statistical significance is identified as follows: * = $p < 0.05$, ** = $p < 0.01$, *** = $p < 0.001$, and **** = $p < 0.0001$. Other amino acids were not mentioned here as there was an were no changes detected.

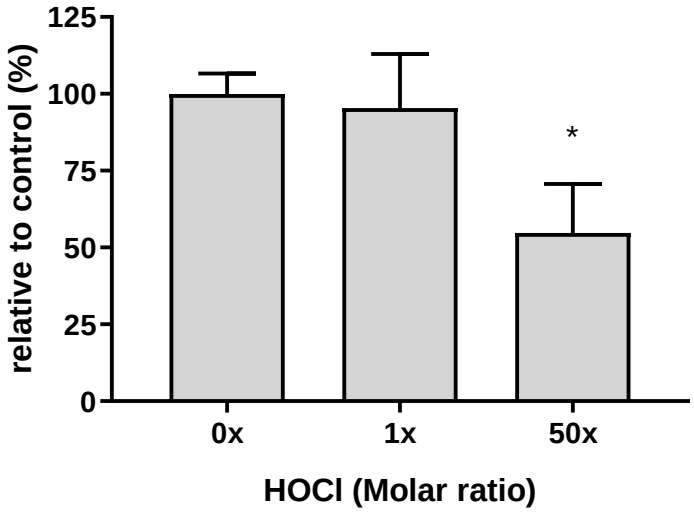

Figure 3.6: **ThioGlo analysis of thiol levels on bovine plasma FN treated with HOCl.** FN (5 μM) was treated with increasing molar ratios of HOCl (0, 5, 250 μM) in a 96-well plate for 2 hr at 37°C then ThioGlo reagent was added to each well. Concentration was measured against a GSH standard to determine absolute concentrations. Statistical analysis was performed using one-way ANOVA with Tukey's multiple comparison post hoc tests to determine significance. Statistical difference is identified as follows: * = $p < 0.05$.

3.3.4 Effect of cell adhesion on HOCl-modified human plasma fibronectin

In light of the structural changes identified above, further investigations into the biological effects that modified FN has on HCAEC activity were undertaken. The CBF is important as it acts as a ligand to integrins on cells to mediate cell adhesion. Experiments were prepared by coating 96-well plates with FN (0.02 μM), and treated with increasing concentration of HOCl for 2 hr at 37°C, followed by a wash with sterile PBS to remove any excess HOCl or by-products to prevent direct interactions with cells. Plates were blocked with 3% (w/v) BSA in PBS, washed with sterile PBS, then HCAEC were incubated onto each plate with 12,500 cells per well, for 1.5 hr at 37°C in a humidified atmosphere containing 5% CO_2. HCAEC were fixed with 10% (v/v) formaldehyde and stained with crystal violet. Plates were then washed with subsequent air drying four times, and cell stained with crystal violet were re-solubilised with acetic acid for the absorbance to be read at 590 nm.

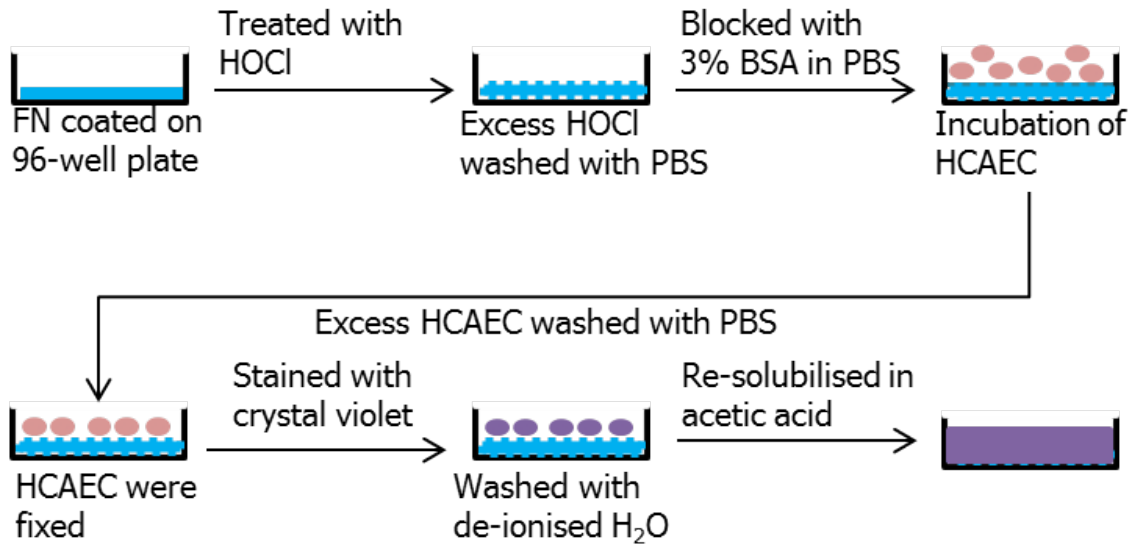

Figure 3.7: **Methodology used to prepare HCAECs incubated on HOCl-modified FN for quantification with crystal violet.** Human plasma FN was coated on a 96-well and exposed to increasing concentration of HOCl. It was then blocked and incubated with HCAEC, which were fixed and stained with crystal violet. Acetic acid was used to re-constitute crystal violet to measure absorbance at 590nm.

The experiment demonstrated a loss of cell adhesion, which was seen by a dose-dependent decrease in cell adhesion with increasing concentrations of initial HOCl, with statistical significance detected with a 500x or greater molar excess of HOCl (Figure 3.8). This loss of cell adhesion corresponded with loss of recognition to the CBF of FN as demonstrated by the ELISA experiment examining epitope antibody recognition (Figure 3.1A).

In light of these promising data indicating a loss of cell adhesion when HCAEC are left to adhere to HOCl-modified FN, further experiments were carried out in which HCAEC morphology were examined using immunocytochemistry (ICC) to identify cell integrity. An 8-well glass chamber slide was coated with FN (0.02 μM) overnight in 0.1 M pH 7.4 phosphate buffer, then the slides were washed with PBS, treated with HOCl, prior to blocking with sterile 3% BSA in PBS to reduce non-specific binding. The wells were seeded with 50,000 cells and incubated for 1.5 hr at 37°C in a humidified atmosphere containing 5% CO_2, and any un-adhered cells were washed off with sterile PBS. Cells were fixed (7.56% (v/v) of 38% formaldehyde, 0.72% (w/v) sucrose in PBS) for 15 min at 37°, then permeabilised by adding permeabilising solution (10.30% (w/v) sucrose, 0.292% (w/v) NaCl, 0.476% (w/v) HEPES, 0.5% (v/v) Triton X-100 in milliQ water) for 5 min

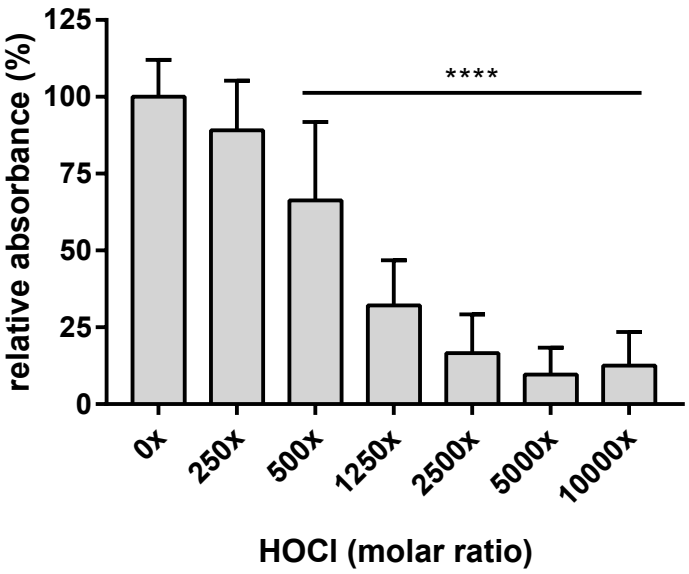

Figure 3.8: **Crystal violet staining of HCAEC adhesion on HOCl-modified human plasma FN.** Human plasma FN (0.02 μM) was treated with increasing concentrations of HOCl (0, 5, 10, 25, 50, 100, 200 μM) and incubated for 2 hr at 37°C before being fixed, stained with crystal violet, and re-solubilised with acetic acid. The data are presented as a percentage relative to control (no oxidant; 0x treatment). Error bars are ± SD from three technical replicates obtained from each of three independent experiments. Statistical analysis was performed using one-way ANOVA with Tukey's multiple comparison post hoc tests to determine significance. Statistical significance was identified as follows: **** = $p < 0.0001$.

on ice to allow fluorescent dye to penetrate cells, washed with PBST, then blocked with 1% BSA in PBS for 1 hr at 21°C. Each well was incubated with rhodamine-phalloidin diluted in 1% BSA in PBS overnight at 4°C, which stains F-actin fibres red. Plates were washed with PBST, then subsequently incubated with Hoechst 33342 for 15 min at 21°C, which stained cell nuclei blue. Slides were mounted using SlowFade Diamond antifade, and imaged using a fluorescence microscope.

The chosen concentrations for ICC were based on the concentration/molar ratio where significant loss of recognition of the antibody or decrease in cell adhesion were observed on ELISA and crystal violet results. FN treated with 500x, 1250x, 2500x molar ratio of HOCl demonstrated decreased number of HCAEC attached onto the treated FN with less nuclei (DAPI blue fluorescence) stained, when compared to untreated control (0x oxidant treatment) (Figure 3.10). Loss in cell numbers were also accompanied by impaired cellular spreading as seen with the reduction in F-actin filaments spreading (red fluorescence),

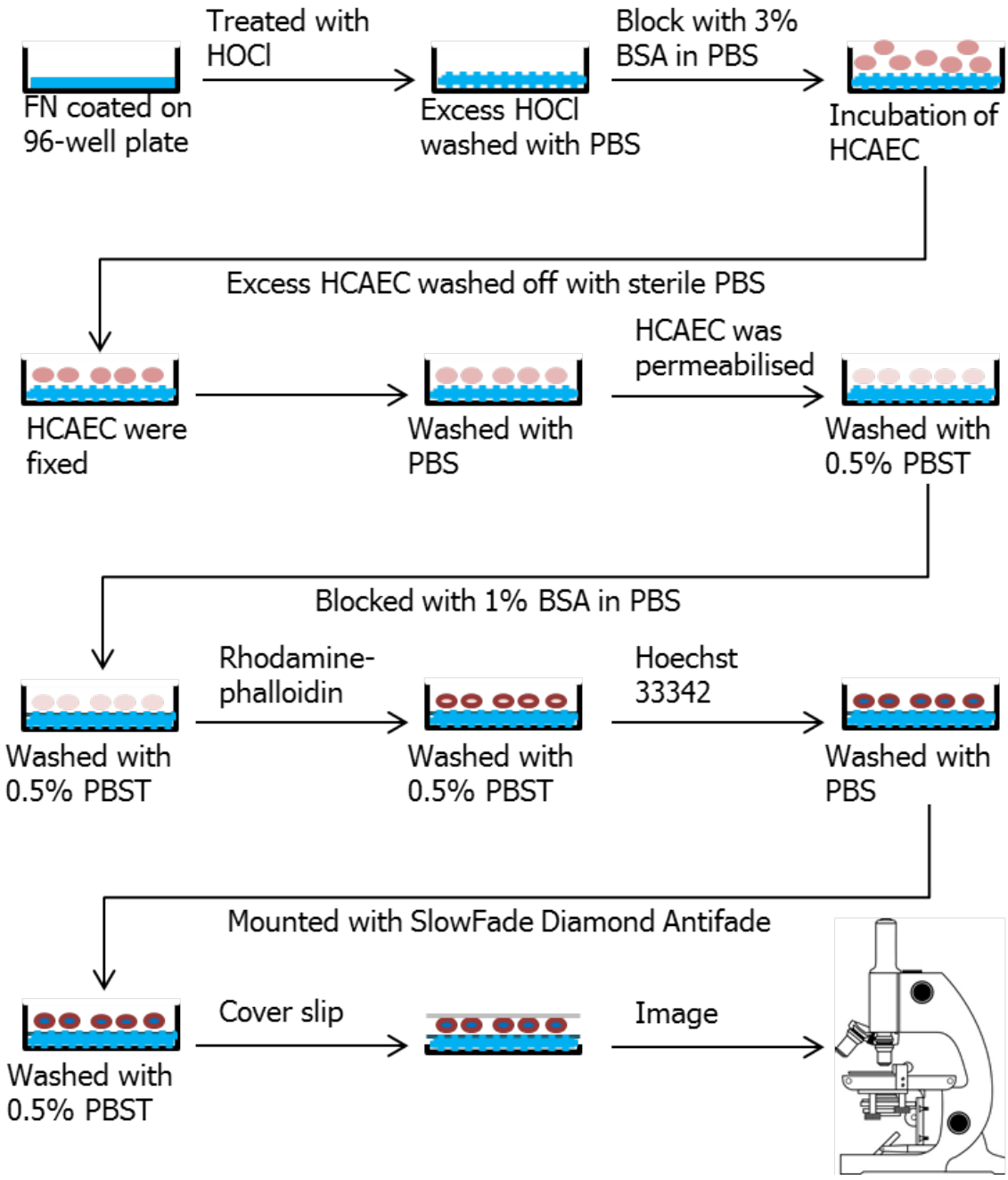

Figure 3.9: **Methodology used to prepare HCAECs incubated on HOCl-modified FN for quantification with immunocytochemistry.** FN was coated on at 8-well slide and exposed to HOCl. Each sample wells were blocked, and incubated with HCAEC. Bound HCAEC were permeabilised and stained with rhodamine-phalloidin, followed by staining with Hoechst. Slide was mounted with SlowFade Diamond Antifade prior to imaging with fluorescence microscope.

whereby cells incubated on FN treated with higher concentrations of HOCl were unable to spread into contact with adjacent HCAEC (Figure 3.10).

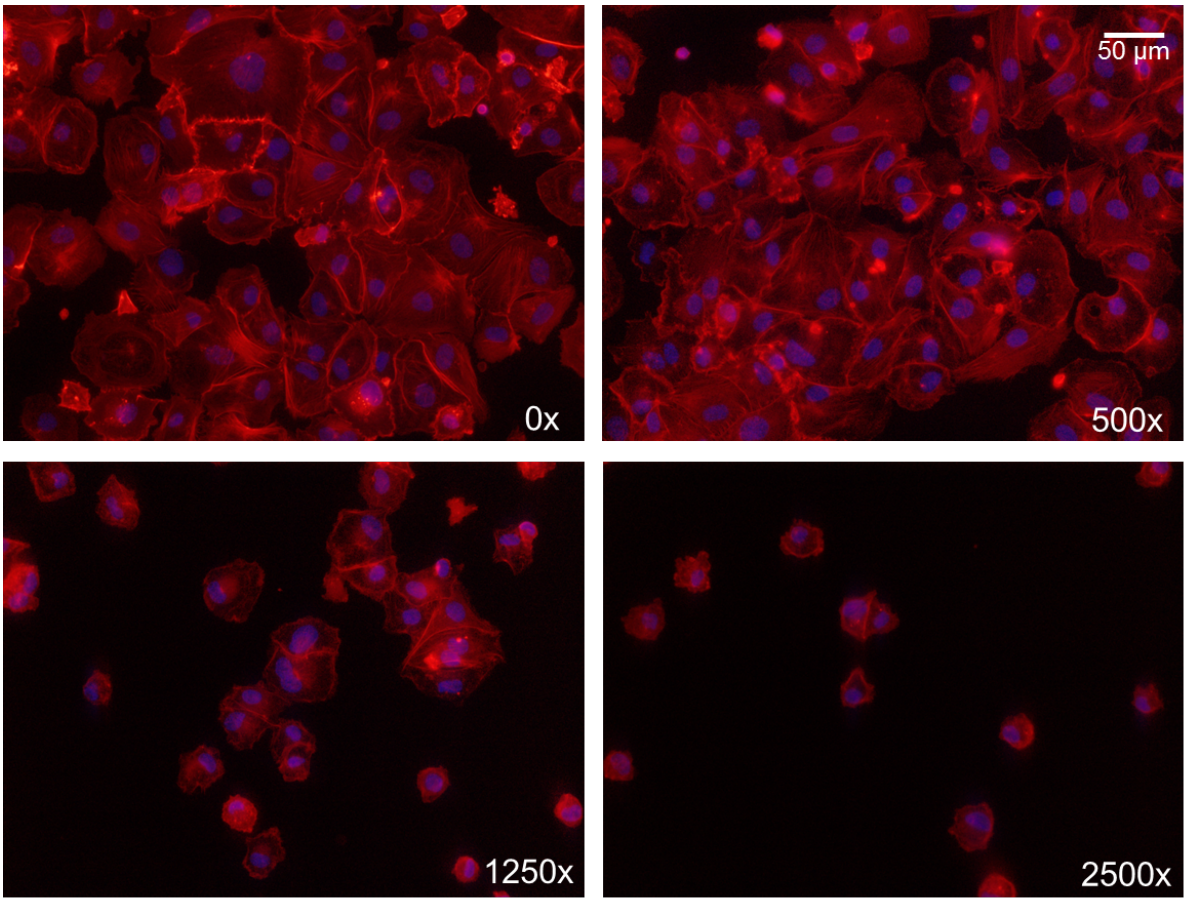

Figure 3.10: **Immunocytochemistry of HCAEC adhesion on HOCl-modified human plasma FN.** Human plasma FN (0.02 μM) was coated on an 8-well glass chamber slide treated with increasing concentrations of HOCl (0, 10, 25, 50 μM) for 2 hr at 37°C before being fixed then stained with rhodamine-phalloidin for F-actin (red) and Hoechst 33342 for nuclei (blue) for fluorescence microscopic imaging.

Although cells may retain their ability to adhere to HOCl-treated FN, not all adhered cells are metabolically active. Cell metabolism was therefore investigated to determine whether these adhered cells are still metabolically active.

3.3.5 Effect of cell metabolic activity on HOCl-modified human plasma fibronectin

To further examine the biological effects that HOCl-modified FN has on ECs; cell metabolism was measured using a live cell MTS assay which involves the reduction of MTS tetrazolium to a coloured formazan. This reduction is thought to occur intracellularly of metabolically active cells through the NAD(P)H-dependent dehydrogenase enzymes [285]. Experiments were performed following the same method used for cell adhesion (Figure 3.7). Instead of fixing cells, endothelial growth media was re-introduced into the wells to allow the HCAEC to recover over 48 hr before cell metabolic activity was quantified by addition of MTS reagent to each sample well. The absorbance of each sample well was measured at 490 nm at 3 hr.

When compared to untreated control (0x), HOCl-modified FN showed a decrease in cell metabolic activity in a dose-dependent manner. There was a statistically significant decrease of almost 50% cellmetabolic activity at 2500x molar excess, with an even greater decrease observed at 5000x and 10000x molar excess of HOCl compared to untreated controls (0x) (Figure 3.11). This greatly reflects that a decreased in cells attached would also caused a decrease in cell metabolic activity.

Both cell adhesion and metabolic activity were observed to be affected when HCAEC were incubated on HOCl-treated FN. In light of this, real time qPCR was performed to further investigate cellular responses to HOCl-treated FN by examining gene expression in HCAEC.

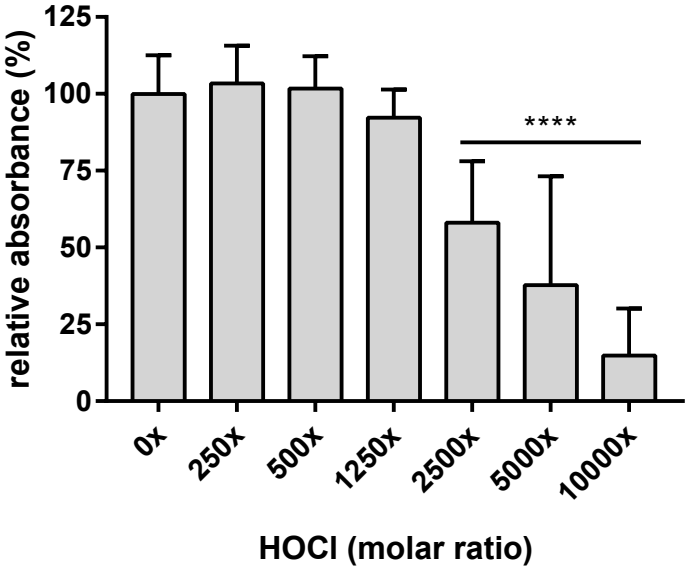

Figure 3.11: **MTS assay of HCAEC metabolic activity on HOCl-modified human plasma FN.** Human plasma FN (0.02 μM) was treated with increasing concentrations of HOCl (0, 5, 10, 25, 50, 100, 200 μM) and incubated for 2 hr at 37°C before adding MTS reagent to each well. The data are presented as a percentage relative to control (no oxidant; 0x treatment). Error bars are ± SD from three technical replicates obtained from each of three independent experiments. Statistical analysis was performed using one-way ANOVA with Tukey's multiple comparison post hoc tests to determine significance. Statistical significance was identified as follows: **** = $p < 0.0001$.

3.3.6 Effects of HOCl modified human plasma fibronectin on HCAEC gene expression

Quantitative real-time PCR (qPCR) was performed to measure changes to gene expression in HCAEC adherent on HOCl-treated human plasma FN. Surface bound FN on 6-well plates were either left untreated (control; 0x oxidant treatment) or treated with a 1250x molar ratio (50 μM) of HOCl, for 2 hr at 37°C. The wells were then washed with sterile PBS to remove any excess HOCl or by-products to prevent their interactions directly with HCAEC. HCAEC (500,000 cells) were seeded into each well and incubated for 72 hr, prior to collection and extraction using a Qiagen RNeasy Mini Kit. A Qiagen RT^2 Profiler PCR Human Extracellular Matrix and Adhesion molecules Array (330231; QIAGEN) was used to analyse a multi-array of genes associated with ECM and adhesion, housekeeping genes, and controls for genomic DNA, RT-transcriptase controls, and positive PCR control. Data analysis was performed using SABiosciences PCR Array

Data Analysis Template and Web-based analysis software (`www.SABiosciences.com/pcrarraydataanalysis.php`). Fold regulations were calculated using data compared to control with normalisation within each sample set; significance was taken at p-value $<$ 0.05. A table consisting of all genes examined are listed below (Table 3.1) with a following table showing genes that showed significant changes in gene expression when compared to untreated (0x oxidant treatment) control (Table 3.2).

Certain types of genes that were found to be up- or down-regulated were ADAMTS, growth factors, integrin chains, adhesion molecules (CTNN and selectins), matrix metalloproteinases (MMP), thrombospondin (THBS), ECM proteins such as collagen chains, FN, laminin chain, versican, and ECM promoter. ADAMTS13, collagen chains (5A1, 6A1), CTGF, CTNN (A1, B1, D1), integrin chains (A2, A7, B3, B4), MMP (11, 2), SELL, SELP, SPG7, THBS (2, 3), TIMP (1, 2), ECM1, FN1, LAMA2 chain, and VCAN genes were observed to be down-regulated with statistical significance ($p < 0.05$), when HCAEC was incubated on HOCl-treated FN (Table 3.2). Certain genes were observed to be significantly up-regulated under the same condition, such as integrin alpha 4 (ITGα4), MMP1, and SELE (Table 3.2). The changes to integrin chains α4, β3 are important to FN as they form the basis for cell binding.

The effects of HOCl on both the structure of plasma FN and the biological effects of HOCl-modified FN on HCAEC were established, however cellular FN produced in the subendothelial matrix may interact differently with HOCl. Cellular FN possesses variant splice sequences on each chain, which are pertinent to matrix assembly and function. The next experiments were designed to investigate the changes on the structure of cellular FN exposed to HOCl in a whole ECM mixture harvested from HCAEC.

Table 3.1: **Gene expression investigated for ECM and adhesion molecules.**

Genes	Description
ADAMTS Type I, Type 13, Type 8	von Willebrand factor-cleaving protease
CD44	CD44 antigen; cell-cell interaction
CDH1	E-cadherin
CLEC3B	Tetranectin
CNTN1	Contactin 1
[COL]1A1, 5-8A1, 11-12A1, 14-16A, 4A2, 6A2	Collagen chains
CTGF	Connective Tissue Growth factor
[CTNN]A1, B1, D1, D2	Catenin α1, β1, δ1-2
ECM1	Extracellular matrix 1
FN1	Fibronectin
HAS1	Hyaluronan Synthase 1
ICAM1	Intercellular Adhesion Molecule 1
[ITG]A1-8, B1-5, AL, AM, AV	Integrin chains
KAL1	Anosmin 1
[LAMA] A1-3, B1, B3, C1	Laminin Chains
[MMP]1-3, 7-16	Matrix Metalloproteinases 1-3, 7-16
NCAM1	Neural cell adhesion molecule 1
PECAM1	Platelet EC cell adhesion
SELE, SELL, SELP	E-selectin, L-selectin, P-selectin
SGCE	Sarcoglycan ϵ
SPARC	Secreted protein acidic and cysteine rich
SPP1	Secreted phosphoprotein 1
TGFB1	Transforming growth factor beta induced
[THBS]1-3	Thrombospondin 1-3
[TIMP]1-2	TIMP metallopeptidase inhibitor 1-2
TNC	Tumor Necrosis Factor
VCAM1	Vascular cell adhesion protein 1
VCAN	Versican
VTN	Vitronectin
ACTB, B2M, GAPDH, HPRT1, RPLP0	House keeping genes

Table 3.2: **Gene expressions of HCAEC incubated on human plasma FN (0.04 μM) pre-treated with a 1250x molar ratio (50 μM) of HOCl.**

Genes	Function	Fold Regulation	*P*-Value
ADAMTS13	von Willebrand factor-cleaving protease	-2.00	0.008
COL12A1	Interaction between collagen I fibrils and matrix	-5.09	0.011
COL5A1	Type V collagen pro-α1(V) chain chain	-1.30	0.005
COL6A1	Type VI α1(VI) chain	-1.86	0.022
CTGF	Connective Tissue Growth Factor	-1.12	0.009
CTNNA1	Plays a role in cell adhesion	-1.24	0.020
CTNNB1	Adherens conunctions protein	-1.39	0.018
CTNND1	Armadillo protein for signal transduction adhesion	-1.21	0.048
ITGA2	Integrin α2 partial chain receptor to ECM proteins	-1.24	0.026
ITGA4	Integrin α4 partial chain receptor for FN	1.69	0.008
ITGA7	Integrin α7 partial chain laminin	-3.90	0.046
ITGB3	Integrin β3 partial chain for ECM & cell adhesion	-1.81	0.003
ITGB4	Integrin β4 partial chain for laminin	-3.10	<0.001
MMP1	Cleaves collagen	1.33	0.021
MMP11	Weakly degrades ECM; control of cell proliferation	-1.89	<0.001
MMP2	Degrades ECM and signal transduction molecules	-1.35	0.002
SELE	CAM important in inflammation	1.91	0.004
SELL	CAM between ECs and lymphocytes	-5.39	<0.001
SELP	CAM on ECs	-5.37	<0.001
SPG7	Paraplegin; regulator of cell and proteins	-1.17	0.002
THBS2	cell-cell & cell-matrix interactions	-1.86	0.023
THBS3	cell-cell & cell-matrix interactions	-1.76	0.016
TIMP1	MMP inhibitor	-1.58	0.002
TIMP2	MMP & EC proliferation	-1.52	0.004
ECM1	ECM formation & angiogenesis	-1.88	0.026
FN1	Formation of plasma & cellular FN	-1.26	0.007
LAMA2	Laminin α2 chain	-1.56	0.045
VCAN	Versican protein	-1.47	0.021

3.3.7 Effect of HOCl on cellular-derived fibronectin epitopes

Plasma and cellular FN are both shown to be present in atherosclerotic plaques [18, 148]. Cellular FN possesses spliced variants which gives rise to their specific vessel and matrix assembly functions such as the detectable EDA and EDB. However, the EDA and EDB region is proposed to be important in wound healing, thrombosis, and maintaining vascular wall integrity [286–288]. Whole ECM consists of a mixture of proteins, which are bound to each other by specific functional epitopes. By using whole ECM extract in samples, we can examine whether FN is a target when present amongst a mixture of proteins.

HCAECs were cultured over a week in 96-well plates to establish an ECM into each well. HCAECs were removed with ammonium hydroxide and washed with PBS. The sample wells now containing HCAEC-derived ECM was then treated with varying concentration of HOCl (0, 5, 10, 25, 50, 100, 200 μM) diluted in 0.1 M pH 7.4 phosphate buffer for 2 hr at 37°C. Excess HOCl was washed off with PBS and blocked with 0.1% (w/v) casein in PBS to prevent non-specific binding, before being incubated with primary antibody overnight at 4°C. Unbound antibody was then washed off with PBST, and the sample wells were subsequently incubated with secondary antibody, and developed using ABTS solution. The absorbance was measured at 405nm.

It was observed that FN CBF epitope was targeted, which resulted in a statistically significant loss of epitope recognition at 5 μM excess (Figure 3.12A). A greater loss of epitope recognition was detected in a dose-dependent manner of increasing HOCl concentrations to FN (Figure 3.12A). The HBF epitope was also detected to be modified by HOCl, with a statistically significant loss of epitope recognition detected at 5 μM excess of HOCl (Figure 3.12B). Increasing the concentration of HOCl resulted in a proportionate loss of antibody recognition to HBF epitope (Figure 3.12B). The loss of recognition to the CBF and HBF epitope, which are shared between cellular and plasma FN, were found to be similarly modified by HOCl as observed on plasma FN (Figure 3.1). The EDA epitope

found on cellular-derived FN was found to significantly lose antibody recognition upon exposure to 10 μM excess of HOCl (Figure 3.12C). No further loss in epitope recognition was observed when increasing concentration of HOCl.

Investigating the structural changes on cellular FN followed this experiment as modifications to the functional epitope would suggest modification to the structural integrity of the protein.

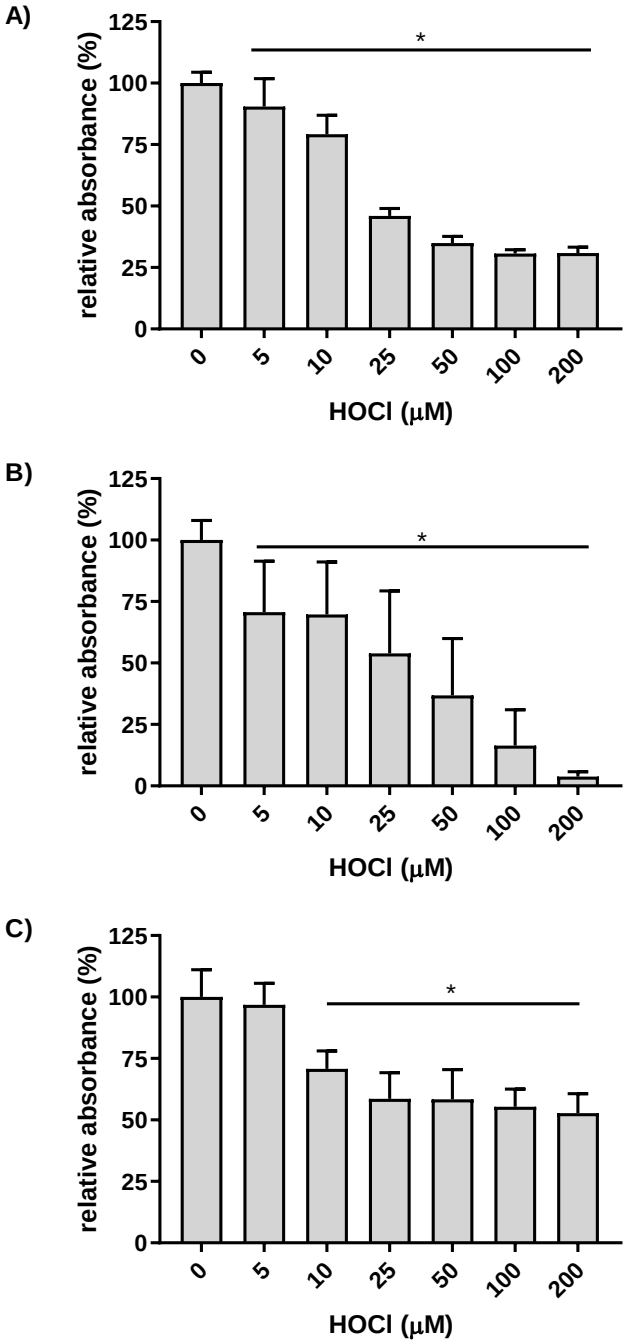

Figure 3.12: **ELISA of HOCl-modification of whole ECM-derived from HCAEC.** HCAEC-derived whole ECM on 96-well plates were treated with increasing concentrations of HOCl (0, 5, 10, 25, 50, 100, 200 μM). FN epitope was detected by using a mouse monoclonal **A)** anti-FN CBF antibody (A17; 1:10000), **B)** anti-FN HBF antibody (A32; 1:1000), **C)** anti-FN EDA antibody (3E2; 1:1000), and conjugated with anti-mouse HRP secondary (1:1000). The data are presented as a percentage relative to control (no oxidant; 0 μM treatment). Error bars are $\pm$ SD from three technical replicates obtained from each of three independent experiments. Statistical analysis was performed using one-way ANOVA with Tukey's multiple comparison post hoc tests to determine significance. Statistical significance was identified as follows: * = $p < 0.05$, and **** = $p < 0.0001$.

3.3.8 Effect of HOCl modification on cellular-derived fibronectin

To investigate changes to the structure of cellular FN by HOCl, Western blotting was performed and probed for the important CBF, HBF and EDA functional epitopes. Whole ECM was extracted from HCAEC, and diluted to "1 μM" (not actual concentration) FN which was then treated with increasing concentration of HOCl. Samples were run on SDS-PAGE under reducing conditions, and then was transferred onto a PVDF membrane prior to Western blotting.

A loss of epitope recognition was detected on the CBF of FN when treated with increasing concentration of HOCl. There was a notable loss of antibody recognition of the monomer band (white arrow) beginning at 25x molar ratio excess of HOCl, and greater loss detected at higher concentrations of HOCl (Figure 3.13A). Formation of aggregates or altered species (black arrow) were detected at 100 μM and 200 μM excess of HOCl (Figure 3.13A). The changes to HBF were found to be similar with loss of antibody recognition of the monomer band (white arrow) detected at 50 μM of HOCl, and aggregates (black arrow) appearing at 100 μM and 200 μM excess of HOCl (Figure 3.13B).

The cellular-derived FN EDA region loss epitope recognition of the monomer band (white arrow) with increasing molar excess of HOCl. This loss was detected upon exposure to 25x molar ratio or greater of HOCl (Figure 3.13C). When incubated with a 100 μM or 200 μM excess of HOCl, aggregates were detected with smearing of bands noted from the monomer band (white band) up to 460 kDa (Figure 3.13C). Binding at 190 kDa was also detected, which loss recognition when treated with higher concentration of HOCl, and was not detectable at 200 μM excess of HOCl (Figure 3.13C).

Due to the effects of HOCl-induced modifications on both plasma and cellular FN, investigations into the presence of FN within atherosclerotic lesions were investigated. IHC analysis was performed to identify the presence and location of FN and HOCl-generated damage.

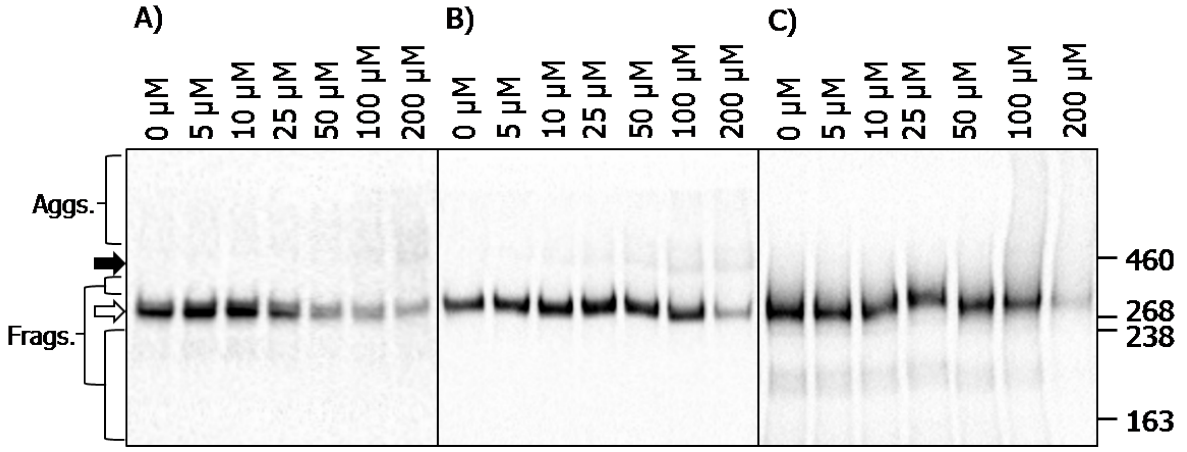

Figure 3.13: **Western blot showing structural changes to whole ECM-derived from HCAEC treated with increasing molar ratio of HOCl.** Samples that were separated on SDS-PAGE under reducing conditions and transferred onto PVDF blots and probed with mouse monoclonal **A)** anti-FN CBF antibody (A17; 1:10000), **B)** anti-FN HBF antibody (A32; 1:2000), **C)** anti-FN EDA antibody (3E2; 1:2000) and conjugated with anti-mouse HRP secondary (1:2000). Blots were developed with ECL-plus reagent and data is labelled as follows: black arrow = dimer/higher aggregates, and white arrow = monomer band.

3.3.9 Presence of native and modified fibronectin in human atherosclerotic lesions

IHC analysis was performed to elucidate whether FN exists in advanced atherosclerotic lesions, whilst simultaneously examining the presence of a HOCl-generated epitope. By identifying and examining where they are situated and whether they are co-localised, it would further support the finding that FN is targeted by HOCl. FN plays several keys roles in the healthy functioning of the arterial wall in blood vessels and has been previously detected in atherosclerotic lesions. Human atherosclerotic lesions (Type II-III), identified using the Stary's system of classification, were cryosectioned onto glass slides at 5 μm. Sections were incubated with either polyclonal anti-FN, or monoclonal anti-FN CBF antibody with Cy-3 labelled anti-HOCl generated epitope. Sections were mounted with Movial (Calbiochem-Novabiochem, La Jolla, USA), before analysis using a confocal laser-scanning microscope in sequential mode (Leica SP2, Leica Lasertechnik GmbH, Heidelberg, Germany). Data in this section include sample processing and imaging was obtained in collaboration with Professor Ernst Malle from Institute of Molecular Biology

and Biochemistry, Centre of Molecular Medicine, at Medical University of Graz, Austria, and Professor Astrid Hammer of the Institute of Cell Biology, Histology, and Embryology, Centre of Molecular Medicine, at Medical University of Graz.

Examination using polyclonal anti-FN antibody provides an overall distribution of FN located within lesion tissues, whereas FN CBF monoclonal antibody binds specifically to the CBF of FN assists in identifying specific areas where FN-CBF may be critically targeted, which may be modulated and damaged during the progression of atheroslcerosis.

Advanced type II-III atherosclerotic lesions were shown to contain high abundance of FN, which was this found to be localised particularly in the basement membrane of ECs, with some detected in the deep media layer of the arterial sections (green fluorescence, Figure 3.14A and 3.14D). Polyclonal anti-FN antibody detected a large distribution of FN throughout the arterial wall, with greater abundance at the intima layer, and in certain areas in the medial layer (green fluorescence, Figure 3.14A). In polyclonal anti-FN antibody lesion samples, Cy-3 labelled 2D10G9 antibody (which binds to HOCl-generated epitopes) was found to be highly abundant within the intima layer of the arterial wall, with lower abundance detected throughout the medial layer (red fluorescence, Figure 3.14B). Merging of polyclonal anti-FN antibody and HOCl-generated epitope showed co-localisation of these two species localised at the intimal layer, but was also present within the medial layer (yellow fluorescence, Figure 3.14C).

Detection of FN using anti-FN monoclonal antibody showed a high abundance of FN in the intima, with some presence in the medial layer (green fluorescence, Figure 3.14C), but at lower intensity of fluorescence compared to polyclonal anti-FN antibody samples (green fluorescence, Figure 3.14A). HOCl-generated epitope was detected throughout the whole lesion sample with higher abundance on the intimal layer, and with lighter presence also detected through the medial layer similar to the polyclonal anti-FN antibody sample (red fluorescence, Figure 3.14A and 3.14E). Merging monoclonal anti-FN and HOCl-generated epitope showed co-localisation of these two epitopes with localised distribution

within the intima, with some distinct areas of co-localisation in the medial layer (yellow fluorescence, Figure 3.14F). Co-localisation in the medial layer was much less intense in fluorescence signal in comparison to the samples which were incubated with polyclonal anti-FN antibody (yellow fluorescence, Figure 3.14C).

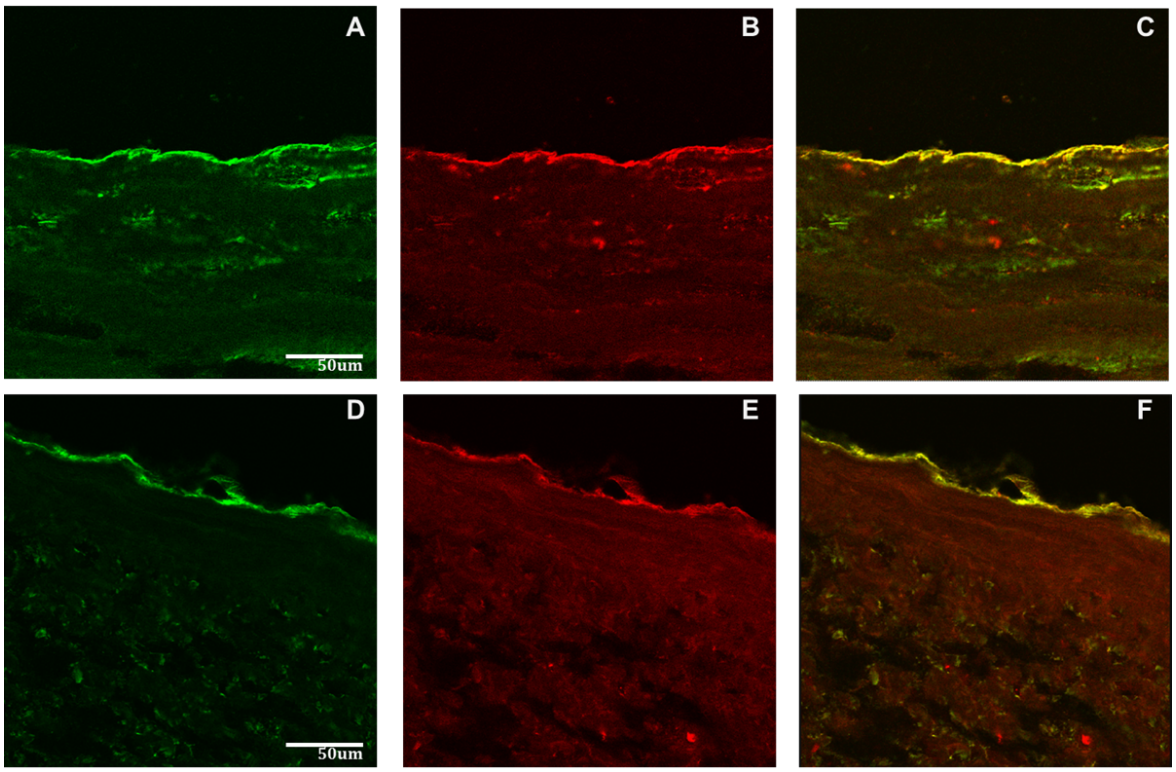

Figure 3.14: **IHC of advanced human atherosclerotic plaque showing localisation of FN and HOCl-generated epitope.** Advanced human atherosclerosis lesions sections were incubated with either **A)** polyclonal anti-FN or **D)** monoclonal anti-CBF of FN (green), while a HOCl-generated epitope was detected with **B, E)** 2D10G9 antibody (red). Images were merged to identify areas of **C, F)** colocalisation (yellow).

Furthermore, protein extracted from human atherosclerotic lesions were investigated by separation on SDS-PAGE under reducing conditions and transferred on PVDF membranes by Western blotting. Membranes were probed for using anti-FN EDA and anti-FN EDB antibodies to look for epitopes specific to cellular FN. Both epitopes were found to be present with FN bands detected at around 460 kDa and around 230-240 kDa (Figure 3.15) similar to what has been found previously with HCAEC-derived ECM (Figure 3.13). Moreover, fragments of FN were found to be present at lower molecular mass with greater intensity particularly at 140 kDa (Figure 3.15).

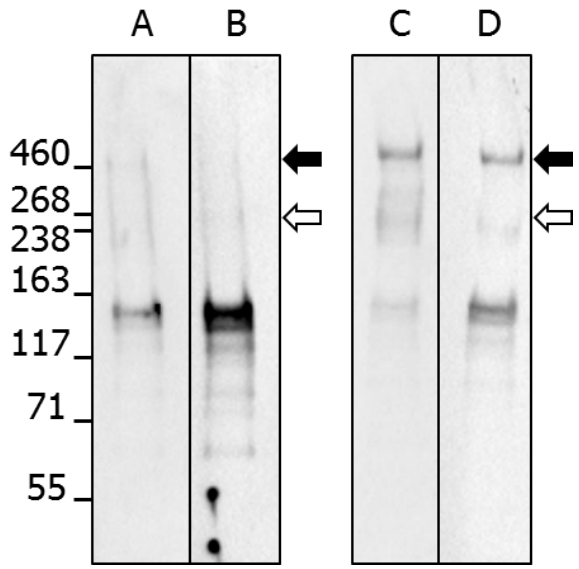

Figure 3.15: **Western blots of advanced human atherosclerotic lesions from two donors.** Advanced human atherosclerosis lesions from two different donors were electrophoresed on SDS-PAGE under reducing conditions and transferred onto PVDF membranes. Membranes were probed for **A, C)** anti-FN EDA antibody (3E2; 1:2000) or **B, D)** anti-FN EDB antibody (C6; 1:2000) found on cellular FN, which were conjugated with anti-mouse HRP secondary (1:2000). Blots were developed with ECL-plus reagent and data is labelled as follows: black arrow = dimer/higher aggregates, and white arrow = monomer band.

These results evidentially support the presence of FN and HOCl-generated epitope in advanced human atherosclerotic lesions and that they are a likely target for modifications by HOCl.

3.4 Discussion

FN plays a pivotal role as an ECM protein in maintaining the integrity of the basement membrane to provide a stable environment for cells, such as arterial ECs. FN possesses a variety of functional sites, equivalent to those of other ECM proteins, such as the collagen and heparin binding epitopes. More importantly, FN contains a CBF, which contains a well known RGD cell binding site via $\alpha 5\beta 1$ and $\alpha \mathrm{B}\beta 3$ integrin [196]. Changes to ECM proteins can lead to a disruption in cellular activity and cause downstream negative effects. HOCl is a known oxidant to be produced during inflammation, and high concentrations in a localised area has been known to cause damage to host cells and proteins. The proximity of FN in the arterial wall to areas of plaque formation make it important for investigating the changes that can occur during the progression of atherosclerosis. In the studies reported here, it was found that plasma and cellular-derived FN were both targeted and modified by HOCl leading to structural changes and loss of antibody recognition to biologically critical epitopes. These modifications were also found to cause biological effects leading to loss of cell adhesion and metabolic activity, and causing changes to gene expression of HCAEC.

The structure of FN was shown to be susceptible to oxidation and modification by HOCl. These modifications result in the fragmentation and formation of larger aggregates on FN, causing subsequent changes to functional epitopes. It was observed that structural changes to FN occur at as low as 5x molar ratio as observed on silver staining (Figure 3.2), whereby both aggregation and fragmentation were observed with increasing molar ratio of HOCl. Protein aggregation (or an altered species) (black arrow) were formed and observed under non-reducing SDS-PAGE (Figure 3.2A), which are likely formed by the oxidation of sulfhydryl groups, producing di-sulfide crosslinks or shuffling of existing disulfide bonds leading to formation of tetramers. It may also be possible that changes to protein charge due to oxidation may also lead to altered electrophoresis through the gels. HOCl had been shown previously to target these reactive sulfhydryl groups, oxidising

them to sulfenic acids (R-SOH), which readily react with other free sulfhydryl group to form disulfide crosslinks causing protein aggregation [49, 289, 290]. When samples were processed under reducing conditions (Figure 3.2B), a majority of these dimers/higher aggregates were reduced, supporting the fact that those examined under non-reducing conditions were formed by disulfide crosslinks. Although some crosslinks were reduced to their disulfide forms to recover the native monomer, some dimers/higher aggregates were still present, which could be formed by other stronger intermolecular covalent bonds, such as di-Tyr and di-Trp [53, 54]. These non-reducible aggregates are likely produced by the formation of di-Tyr crosslinks, a secondary species resulting from the dimerisation of two Tyr phenoxyl radicals [64, 291]. These protein aggregation have been observed previously with FN treated with HOCl [260], which coincided with the formation of di-Tyr [64]. Thiol oxidation and consequential formation di-Tyr formation has been found to be associated with inflammatory oxidation, and are co-localised in atherosclerotic plaques [130, 292, 293], along with the increasing presence of chlorinated Tyr residues (3-chloroTyr), di-Tyr, *o*-Tyr, and DOPA [64]. Aggregation of FN can lead to certain functional epitopes becoming buried and undetectable due to the nature of protein folding, and fragmentation of FN, particularly within functional sequences, which can lead to a decreased or total loss of recognition by cells or other ECM proteins.

Reducing samples were shown to present with decreased protein fragment intensity. The reduction of samples were previously performed as to reduce the occurrence of re-oxidation by alkylating the proteins [294]. Furthermore, the decreased in fragment intensity could be explained by the alteration of Cys/Cystine residues in samples by the reducing agent, such as DTT [295]. This alteration would change the way FN electrophoreses through the gel leading to a decrease in the fragment bands observed under non-reducing conditions. This would be the case for the silver stains and the Western blots in each of the following chapters.

FN possesses 27 Met and 63 Cys residues, with only 3 of of the Cys residues not present in the form of disulfides [296]. These amino acids are known to be targeted by HOCl, and

have been found to be highly reactive and readily oxidised by this oxidant [50, 51]. FN possesses only 2 free thiols (Cys residues), which have been found to be buried within the protein [297]. Due to this knowledge, it was thought that HOCl would not be targeting these free Cys residues prior to the other more readily available amino acids. Met on FN were found to be oxidised by HOCl with increasing loss detected by amino acid analysis with increasing HOCl treatment concentration (Figure 3.5A). MetSO is readily formed by Met oxidation [50], which was shown to be present in non-treated samples of FN, and increased a small amount with increasing molar ratios of HOCl (Figure 3.5B). MetSO is a common oxidation product associated with inflammatory processes and is believed to contribute to biological aging [298, 299]. Available Met on protein have been proposed to be targeted by oxidants as an antioxidative mechanism to prevent modifications on other species [300, 301]; although the slow reduction rate of MetSO to the native Met may make it an ineffective antioxidant [302]. It was previously shown that the addition of Met to samples treated with HOCl correlated with an inhibition of crosslinks [260].

The data obtained in the current study showed a decrease in MetSO concentration at the highest molar ratio of HOCl (Figure 3.5B), which can be explained by further oxidation of MetSO to the corresponding sulfone $MetSO_2$ which was not analysed/quantified here. MetSO formation has been suggested to precede the formation of carbonyls [303]; protein carbonyls are common biomarkers for oxidative stress. *In vivo*, the body contains a family of MetSO reductase enzymes which helps in reducing the MetSO formed; these reductase enzymes have been reported to be at low levels in certain pathologies and thus enable the accumulation of MetSO [304]. In certain cases, instead of the two-electron oxidation which produces MetSO, a one-electron oxidation is also a possible mechanism that leads to the formation of methionine radial cations [304]. Each species is produced by different mechanisms and each induces specific secondary effects. The formation of MetSO at certain active sites on protein can lead to an inactivation and a loss of functional binding epitope; an example of enzyme inactivation due to MetSO formation is α1-proteinase [305].

Other amino acids that are also susceptible to HOCl are Tyr residues leading to formation of chlorinated Tyr, and free amine groups or lysine residues leading to formation of chloramines and secondary products [64, 65, 306]. Tyrosyl residues readily react with HOCl forming 3-chloroTyr, and 3,5-chloroTyr, which are long-lived products and common biomarkers of HOCl modification [48, 59]. These have been shown to be present in atherosclerotic lesions, though only in small quantities but significantly elevated over control samples [64]. Chloramine formation is also highly likely in these experiments, and further modifications may be induced by chloramines over longer periods of incubation. A common mechanism of chlorinated Tyr formation is the transfer of chlorine from chloramines to Tyr residues [49], which have been shown to cause further reactions on the parent, and the decay of chloramines has been correlated with increased levels of carbonyls [49, 59].

Protein carbonyls are a non-specific biomarker associated with protein oxidation and oxidative stress. Previous experiments with bovine FN treated with HOCl in the same manner, have shown that carbonyl formation occurs readily with this oxidant as detected with a protein carbonyl Western blotting technique (Siriluck Vanichkitrungruang, Honours thesis, 2013). The overall increased levels of carbonyl content in HOCl-treated ECM correlated with an increased occurrence of aggregation and fragmentation [260]. These results are consistent with previous studies which examined hypochlorite treatment of P388D1 cells, which showed increased levels of carbonyls and a corresponding drop in cell viability, thiol levels, and protein Met and Trp residues [46]. Amino acid analysis of Tyr residues in bovine FN were found to be unchanged upon exposure to increasing molar ratios of HOCl (Figure 3.5D); suggested that this detection method was not sensitive enough to pick up small changes. Further experiments need to be performed to investigate the formation of chlorinated Tyr in samples as possible by-products of FN oxidation by HOCl.

Chloramines have been found to have a varible stability with this dependent on time and temperature as shown in *in vitro* experiments [260, 307]. Chloramine decomposition

has been shown to induce chlorination of Tyr [308, 309], and these species are also known to be a major driver for protein fragmentation [310]. Chloramine decomposition produces nitrogen-centred radicals, which along with hydrolytic reactions have been found to lead to fragmentation of proteins [307, 311]. The actions of chloramines have been previously observed by detection with EPR and SDS-PAGE, to cause fragmentation of plasma proteins [307]. Furthermore, this was observed on ECM proteins using radio-labelled amino acids [65]. *In vivo*, chloramines are susceptible to reduction by biologically occurring reductants, particularly Met, ascorbate, and thiols such as glutathione [310]. Formation of chloramines may be reduced by Met residues on FN, supporting the loss of Met in HOCl-treated plasma FN samples (Figure 3.5A). Elevated levels of chlorinated Tyr, in particular 3-chloroTyr have been found to be present in LDL isolated from human atherosclerotic lesions [312, 313]. Furthermore, modified Tyr residues were found in atherosclerotic ECM samples derived from human atherosclerotic plaques, which was not the case in healthy human and pig aorta [64], as well as in other inflammatory diseases [314, 315]. High concentrations of 3-chloroTyr can be subsequently converted to 3,5-chloroTyr, which has also been found to be a biomarker for atherosclerosis [48, 59]. Lastly, Trp residues which were found to be targeted by HOCl (Figure 3.5C), have previously been found to be modified in FN during treatment with HOCl [260]. Trp have also been found to form crosslinks as a by-product of oxidation, but there are limited studies on the nature of such crosslinks and the relevance of specific species - this area is worthy of further investigation [316]. The mechanism of fragmentation and amino acid modifications on FN should be further investigated, along with elucidating the location of these modifications. This would assist in defining areas of susceptibility and what functional epitopes are targeted that lead to a loss of functionality with other ECM proteins or cells.

FN possesses 100 Tyr and 39 Trp residues (Uniprot data; P02751); 56 of these Tyr residues and all of the Trp residues are located in functional sites [130]. The CBF, which contains the RGD site, is situated in the region 1267-1540 of the amino acid sequence and

possesses 1 Met, 3 Trp, and 10 Tyr. The HBF II is situated between residues 1721-1991 of the amino acid sequence and possesses 3 Met, 3 Trp, and 11 Tyr residues (Uniprot data; P02751). Two neighbouring Cys residues are positioned on 1232 and 2136, which present as disulfide bonds (Uniport data; P02751). Based on the amino acid analysis of FN, it was found that Met and Trp parent amino acids were modified by treatment with HOCl (Figure 3.5). This suggests that the modifications on these residues may impact on the integrity of these functional sites, and subsequently cause a loss of the antibody recognition and changes to biological activity of HCAEC on HOCl-modified FN.

It was found that FN CBF was susceptible to modifications by HOCl, leading to loss of epitope recognition (Figure 3.1A and 3.3) and loss in cell adhesion (Figure 3.8). These results corresponded with previous findings that showed that the CBF and collagen binding fragments were susceptible to modifications upon exposure of the sub-endothelial matrix to HOCl [261]. Furthermore, it was shown that ECs derived from umbilical cord vein were lower in number as viewed under contrast microscopy, and cell spreading was impaired as noted by the rounding of cells, which indicated that these cells adhered less well on matrix that was exposed to HOCl [261]. This was similarly observed in HCAECs incubated on HOCl-modified FN (Figure 3.10).

The collagen-binding domain was also found to be modified by HOCl, which led to a decrease in epitope recognition, albeit to a lesser extent compared to the CBF [261]. The HBF II that is recognised by the antibody used (clone A32) is positioned in the third domain of FN; HBF interacts with heparin/heparan sulfate, and it has been found that modifications to amino acids within this domain led to decreased heparin binding to FN [317]. This supports the current data where it was found with that the HBF was modified by HOCl which led to loss of epitope recognition (Figure 3.1B). Matrix assembly is highly dependent on the interactions between ECM proteins; the loss of integrity of this complex mixture can affect the production of ECM by cells, and lead to an unstable plaque formation during the progression of atherosclerosis.

These structural modifications causing aggregation and fragmentation have been demonstrated to also cause HCAEC to behave differently. HCAEC incubated on FN exposed to HOCl were shown to have decreased binding capacity to FN and an inability to spread their F-actin to adjacent cells (Figure 3.10). This inability for cells to adhere onto oxidatively modified FN is consistent with previous studies [22, 130, 261], which supports the notion that changes to FN structure leads to decreased cell adhesion. It has also been previously shown that low concentrations of HOCl can cause small changes to protein folding leading to an increase affinity to certain antibodies, while higher concentrations of HOCl caused a decrease in recognition [271]. Furthermore, knock-out of the EDA exon of FN has been implicated in a reduction of atherosclerotic lesion size in apoE$^{-/-}$ mice [272, 273]. EDA in conjunction with the Toll-Like Receptor 4 (TLR-4), which is a signalling molecule for an inflammatory cytokine pathway, have been shown to promote dose-dependent NFκB-mediated inflammation [318]. Therefore, these modified FN in lesion sites may not only cause biological function changes, but also activate an inflammatory response [225]. It has been observed previously that degraded FN promotes leukocyte migration and chemotaxis to the injury site [266, 267], and increases neutrophil degranulation [268]. Additionally, the inflammatory response was observed to be lower when FN assembly was inhibited [147, 269], supporting the importance of FN in mediating inflammation-induced leukocyte recruitment. This may suggest that FN is modified by HOCl-mediated damage, causing vascular remodelling, cellular dysfunction and promotion of leukocyte recruitment to the injury site. This positive feedback loop may lead to further damage, and subsequently a detrimental cycle in the development of atherosclerotic plaque.

HCAECs incubated on HOCl-modified FN were found to cause changes to HCAEC gene expressions (Table 3.2). The genes examined were specific for ECM and adhesion molecules, some of which are expressed exclusively by EC, while others are also expressed by other cells, such as leukocytes. A complex and balanced homeostatic relationship is required between MMP, ADAMTs, and TIMPs in normal turnover of basement membrane

ECM. It was found that MMP-2, MMP-11, and MMP-14 had decreased gene expression when HCAEC were incubated on HOCl-modified FN (Table 3.2). MMP-2 is normally expressed during vascular formation and remodelling, and has been found to promote the formation of atherosclerotic lesions, with MMP-2 deficient apoE$^{-/-}$ mice found to have reduced atherogenesis [319]. Furthermore, up-regulation of MMP-2 has been associated with aortic atherosclerotic lesion development [320], accompanied by a thin fibrous cap which increases risk of plaque rupture and intra-plaque haemorrhage [321]. Down-regulation of MMP-2 gene expression in HCAEC exposed to HOCl-modified FN could suggest that in an acute injury, there are attempts at preservation of remaining intact ECM and vasculature (Table 3.2).

Both MMP-11 and MMP-14 have been found to be elevated in atherosclerotic plaque; particularly in areas with increased risk of rupture [322, 323]. MMP-11 weakly degrades matrix protein, and preferentially targets serum proteinase inhibitors [324] and signal transduction molecules [325]. The degradation of serum proteinase inhibitors have been correlated with increased neointima formation, and fibrotic scarring on blood vessels [324]. Furthermore, MMP-11$^{-/-}$ mice models showed extensive degradation of the internal elastic lamina accompanied by abundant levels of intimal cells [324]. In addition, MMP-14 cDNA, expressed from adenovirus vector, is linked to focal adhesion kinase degradation, and was examined to cause rounding of cells along with decreased cell adhesion of Baboon aortic VSMC, which was not dependent on integrin levels [326]. In contradiction, there have been mixed findings where previously MMP-14 expression has been suggested to increase thickness of fibrous cap to promote plaque stability by its promotion of VSMC migration and proliferation into the area [327].

It has been found that MMP-2 expression is due to presence of membrane type MMP (such as MMP-14); the activation of MMP-2 is correlated to an up-regulation of MMP-14 [328, 329]. Down-regulation of MMP-14 could suggest the subsequent down-reglation of MMP-2 in HCAECs incubated on HOCl-modified FN (Table 3.2. It was shown that FN-derived synthetic peptides up-regulate the expression of MMP-9, MMP-2, and MMP-14 in

human T lymphocyte cell lines [330]. This suggest that response of HCAECs incubated on HOCl-modified FN are down-regulating MMP-2 and MMP-14 (Table 3.2). Down regulation of MMP-14 was found to occur in HCAEC when they were incubated on HOCl-modified FN, suggesting that loss of FN integrity was unable to upregulate MMP-14 expression and subsequently activate MMP-2 (Table 3.2). In previous studies, it has been shown that HOCl activates pro-MMP-7 due to oxidation of Cys residues [331]. In atherosclerotic plaques, there was an up-regulated expression of MMP-7, MMP-13, and MMP-3 genes [332]. These gene expressions were not observed to be upregulated in HCAEC incubated on HOCl-modified FN, which is likely because the activators for these genes are different or different cells are producing these MMPs in lesions.

TIMPs are inhibitors for MMP, and hence inhibit remodelling of the vasculature; each TIMP possesses specificity for their respective MMP with possible weaker activity on others. TIMP-1 effectively inhibits MMP-7, MMP-9, and MMP-14 and MMP-3, whereas TIMP-2 is more effective at inhibiting and cleaving membrane type MMP-2 [333, 334]. Elevated expression of MMPs are observed in atherosclerotic plaques with corresponding elevation of both TIMP-1 and TIMP-2 expressions, which is required to compensate for the increased activity of MMPs [335]. Low to moderate levels of TIMP-2 are important for the activation of MMP-2 [336], with TIMP-$2^{-/-}$ mice showing heavily impaired MMP-2 activation [336]. HOCl-modified FN was shown to cause a down-regulation of TIMP-2 in HCAEC (Table 3.2); decreases in TIMP-2 have been observed in atherosclerotic lesions when compared to healthy samples [337]. The presence of TIMP-2 has also been observed to inhibit VSMC migration and proliferation [338]. Furthermore, over-expression of TIMP-2 resulted in decreased migration of macrophages into the area, and reduced atherosclerotic plaque size [339]. TIMP-1 has been observed to either be unchanged [337], or elevated in atherosclerotic plaques [340]. TIMP-$1^{-/-}$ mice were observed to have increased matrix accumulation in the neointimal area compared to mice that expressed TIMP-1 [341]. TIMP-1 and TIMP-2 gene expression were both observed to be down-regulated when HCAEC was incubated on HOCl-modified FN (Table 3.2), which is likely

a response to the down-regulation of MMPs.

ADAMTS13 are primarily produced in the liver but vascular EC are found to have small quantities of the mRNA for this enzyme which regulates thrombosis, angiogenesis, and down regulates inflammation [342]. Past studies have identified von Willebrand factor (vWF) as the only known substrate for ADAMTS13, which functions in both thrombosis and inflammation [343–345]. It has been previously shown that ADAMTS13$^{-/-}$ and vWF$^{+/+}$ mice resulted in increased leukocyte rolling on unstimulated mesenteric veins [346]. Furthermore, these knockout mice were also found to have increased leukocyte adhesion with additional knockout of vWF showing markedly less changes compared to WT [346]. A later study supported these findings and further showed that mice with both apoE$^{-/-}$ and ADAMTS13$^{-/-}$ were more prone to developing early atherosclerotic lesions in the aorta [347]. Moreover, lesions from apoE$^{-/-}$/ADAMTS13$^{-/-}$ knockout mice were found to have increased macrophage numbers, and were also found to have a lower content of collagen [347]. Low levels of ADAMTS13 have been associated with increased risk of CVD, particularly with increased risk of myocardial infarction in younger patients that presented with high levels of vWF levels [348, 349]. Although the risk of CVD are dependent on both ADAMTS13 and vWF levels in individuals, it has also been reported that there is no direct correlation between ADAMTS13 and vWF levels [349]. The down-regulation of ADAMTS13 expression in HCAEC incubated on HOCl-modified FN may suggest an inflammatory response by HCAEC to increase recruitment of both leukocyte and macrophages to the area of injury.

Cell surface integrins are important in cellular interactions with the surrounding ECM, and thus modifications to ECM proteins can lead to consequential effects on cell activity. A wide variety of cells express integrins and within the qPCR array performed, some were either not expressed by EC or were not identified to adhere to FN [350] and hence will not be discussed here. The RGD sequence in the CBF of FN is the site of cell adhesion via integrins $\alpha5\beta1$ and $\alpha V\beta3$; the variable region on FN also possesses a site for binding to $\alpha4\beta1$ integrin presented by cells [149, 196, 351, 352]. The down-regulation of

ITGB3 is likely a response to HOCl-modified FN presenting without an adhesion ligand for β3 integrin to bind to (Table 3.2). The αVβ3 region plays a role in cell survival, proliferation and migration [353]. In the early stages of atherosclerosis, elevated levels of αVβ3 adhesion molecules were found, and might be a response by the EC attempting to promote cell proliferation and migration [350, 354]. The αVβ3 integrin is found to be present in arteries, regardless of the presence of an atherosclerotic plaque, colocalised to both ECs and SMCs within tissues [355]. The α4 integrin chain is expressed on EC for FN, for initiation of ECM remodelling [356], and is a mechanism for recruiting macrophages to atherosclerotic plaques [357]. There were no statistically significant changes to αV, α5, and β1 expression from HCAEC incubated on HOCl-modified FN (Table 3.2). Down-regulation of β3 was likely a response to the modified CBF on FN, as cells detected loss of the ligand, thus in response up-regulated α4 attempting to increase HCAEC binding capabilities to the variable region on FN, and recruit more macrophages to the site of injury.

Selectins are part of a family of cell adhesion molecules (CAM), and are located as transmembrane single chain glycoproteins. E-selectin and P-selectin are expressed by ECs, whereas L-selectin is solely expressed by leukocytes and will not be discussed here [350]. E-selectin on inactive resting EC is expressed at very low levels, with an up-regulation occurring in response to inflammatory cytokines/stimuli [358, 359]. It has been shown that up-regulation of E-selectin occurs in EC from atherosclerotic intima, but not in non-atherosclerotic control samples [360]. Furthermore, it was also found that the expression of E-selectin in individuals was exclusively on ECs, and expressed along with ICAM-1 and VCAM-1 in the neovasculature of atherosclerotic plaques [360]. As inflammation occurs, inflammatory cytokines IL-1 and TNF-α are released and have been shown to up-regulate E-selectin expression [361, 362]. The up-regulation of the SELE gene by HCAEC incubated on HOCl-modified FN is likely an inflammatory response to promote the migration of leukocytes to the area of injury.

P-selectins (SELP) are expressed on ECs but predominantly on platelets, and plays an

important role in leukocyte adhesion and recruitment in apoE$^{-/-}$ mice; this functions to promote inflammation and consequentially atherosclerosis [363]. In the presence of P-selectin in apoE$^{-/-}$ mice, plaques were found to be bigger with more calcification and fibrosis [363]. Elevated levels of P-selectin were also found to be correlated with coronary heart disease risk factors [364], and are found to be associated with thickening of the intima-media layer, supporting its role in preclinical atherosclerosis [365]. The expression of P-selectin is associated with an acute inflammatory response, as they are stored internally in ECs and are able to be released immediately [358, 364, 366]. Down-regulation of the SELP gene in HCAEC incubated on HOCl-modified FN may be due to a chronic response to recruit leukocytes to the area by up-regulating SELE instead. Furthermore, due to the action of P-selectin in recruiting platelets to sites of injury, the down-regulation of SELP may be a response to decrease platelet binding thus preventing clotting at the site of injury.

This was a preliminary study looking at gene expression, and further investigations clearly need to be undertaken to further elucidate these changes, particularly in correlation with protein expression and whether this reflects their respective gene expression. The changes of gene expression in HCAEC as a result of acute or chronic injury might be a mechanism that prevents instability of the ECM of which cells are bound to.

The importance of FN in maintaining vascular integrity is believed to be due to its interactions with other ECM proteins, and cells, such as ECs, to provide a strong and tensile ECM. The modifications and degradation of FN can lead to a reduction in ECM integrity, negatively impacting cellular activity, preventing proper cell adhesion or proliferation. The loss in healthy cell function and an intact ECM can increase the likelihood of a thinner and more unstable fibrous cap. These unstable caps are more susceptible to rupture, consequentially causing thrombosis in the affected area, which can lead to myocardial infarction or stroke in individuals. These experiments have shown that FN is susceptible to HOCl modifications, but there are other oxidants known to be formed by the MPO system, such as HOSCN. HOSCN is highly specific and their effects

on FN will be explored in the next chapter.

Chapter 4

Modifications to fibronectin by HOSCN

4.1 Introduction

FN is an ECM protein that exists in the basement membrane of arterial EC. In combination with other proteins, FN provides a healthy environment and network for cells [149, 195, 196]. It is important for vascular remodelling during inflammation amongst other important functions as discussed in Section 1.4.3 and Section 3.1.

Leukocyte migration into the arterial wall occurs as part of an inflammatory response to the deposition of LDL [5]. MPO is released from leukocytes, which are known to generate HOCl from H_2O_2 and physiological concentrations of Cl^- [50, 51, 57]. However, it is known that MPO has a higher specificity for SCN^- when compared to Cl^- (by almost 730 fold), and elevated levels of this pseudohalide is found to produce elevated concentrations of HOSCN [94, 99, 110, 367]. MPO compound I has a rate constant for SCN^- of $9.6 \pm 0.5 \times 10^6$ M^{-1}, with a lower rate constant for Cl^-, which is $2.5 \pm 0.3 \times 10^4$ M^{-1} s^{-1} [27]. Elevated plasma levels of SCN^- (80-400 μM [96–99]) have been found to occur in smokers, where CN^- is detoxified to SCN^- [98], as a result of ingestion of certain plants, fruits, and nuts [368], and exposure to drugs such as nitroprusside [369].

HOCl is less specific and has been seen to react widely with several oxidisable groups [49, 50]. However, HOSCN has previously been shown to specifically target thiols and cysteine residues leading to reversible products such as RS-SCN adducts, sulfenic acids,

and disulfides [106, 370]. These products can be reversed via GSH or by enzymes such as glutaredoxin or thioredoxin reductase [106, 370]. Further oxidation of reversible products can generate irreversible products such as cysteic acid [106]. The presence of HOSCN is dependent on MPO and SCN^- concentrations, and has been reported to have either a detrimental or a protective effect [99, 106, 367, 371].

FN has been shown previously to be modified by HOCl (see Chapter 3 and references therein) leading to structural changes and causing biological dysfunction, however there is very limited information of the effects of HOSCN on ECM proteins with most studies on this oxidant having investigated the cellular effects of this species. In light of the current studies available about HOSCN, it was hypothesised that human plasma and cellular FN might be targeted and modified by HOSCN but to a lesser extent in comparison to HOCl.

4.2 Aim

The experiments performed in this chapter aimed to elucidate the effects HOSCN has on human plasma FN and cellular-derived FN in whole ECM extracts. Protein structural changes and antibody recognition to specific functional epitopes were examined using SDS-PAGE, Western blotting and ELISA assays. To determine thiol oxidation on FN by HOSCN, ThioGlo assay was utilised against a GSH standard. Lastly, investigations were carried out on the biological effects that HOSCN-treated FN has on HCAEC by utilising cell adhesion and cell metabolic activity assays, and real time qPCR to determine changes in gene expression.

4.3 Results

4.3.1 Potential effects of HOSCN on human plasma fibronectin epitopes

The concentration of SCN^- in plasma is generally lower than Cl^- but elevated levels of plasma SCN^- have been detected in smokers [99]. By identifying the changes made by HOSCN on FN, we can elucidate how extensive these modifications are and detect changes that may occur in these individuals that have elevated SCN^- (80-400 μM) levels. Preparation and treatment of FN using HOSCN followed the method used in Section 3.3.1. HOSCN was prepared by incubation of LPO in the presence of SCN^- and H_2O_2, prior to being diluted in 0.1 M pH 7.4 phosphate buffer and added to FN samples.

Human plasma FN (0.02 μM) was treated with HOSCN (0, 5, 10, 25, 50, 100, 200 μM) (Table 2.4), and changes to the CBF epitope were measured using ELISA. Human plasma FN treated with HOSCN showed only minor changes to the recognition of the CBF epitope with increasing HOSCN concentration (Figure 4.1). Treatment with HOSCN led to a small loss of CBF epitope recognition with no marked loss with increasing molar excess (Figure 4.1A). However, a statistically significant loss of epitope recognition was detected at 2500x and 10000x molar excess (Figure 4.1A).

As these data suggests, there are some modifications caused by HOSCN to the FN CBF, further investigations were conducted to examine the structural integrity of FN when treated with HOSCN.

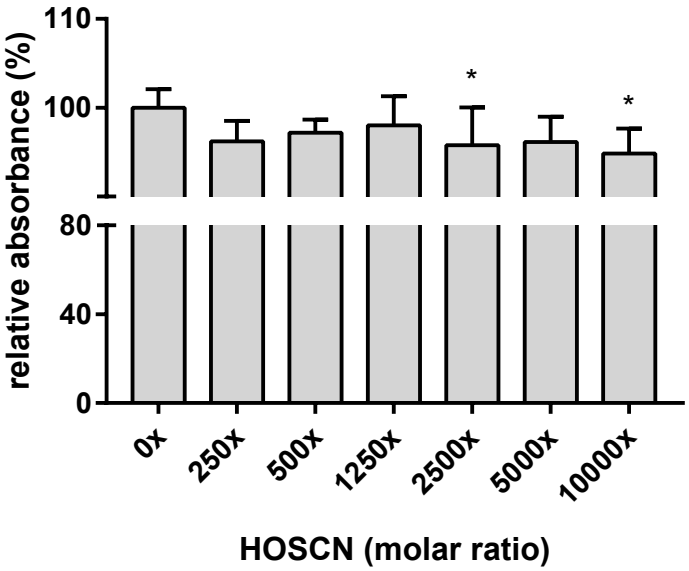

Figure 4.1: **ELISA of human plasma FN treated with increasing concentrations of HOSCN.** Each well was coated with 0.5 μg FN (0.02 μM) in 0.1 M phosphate buffer and either left untreated (control; 0x oxidant treatment) or treated with HOSCN (0, 5, 10, 25, 50, 100, 200 μM), and incubated for 2 hr at 37°C. FN epitope was detected by using a mouse monoclonal anti-FN CBF antibody (A17; 1:10000), and conjugated with anti-mouse HRP secondary (1:1000). The data are presented as a percentage relative to control (no oxidant; 0x oxidant treatment). Error bars are ± SD from three technical replicates obtained from each of three independent experiments. Statistical analysis was performed using one-way ANOVA with Tukey's multiple comparison post hoc tests to determine significance. Statistical significance is identified as follows: * = $p < 0.05$.

4.3.2 Effect of HOSCN on the structure of human plasma fibronectin

FN possesses two disulfide bonds at the carboxyl termini with 2-3 free thiols present on the protein (Uniprot data; P02751) [296]. Due to the specificity of HOSCN for thiol residues, it was therefore of interest to investigate whether this oxidant modifies FN protein structure by using SDS-PAGE. Purified human plasma FN was left untreated (0x oxidant control) or treated with increasing concentrations (0, 5, 10, 25, 50, 100, 200 μM) of HOSCN. A lower molar ratio was used to examine the minor structural changes induced by HOSCN on FN. Samples were then separated by SDS-PAGE under non-reducing or reducing conditions with added high molecular mass marker, and then silver staining was performed. Experiments were carried out as described in Section 3.3.2, to examine potential changes such as aggregation or fragmentation.

Silver staining of human plasma FN samples exposed to HOSCN separated under non-reducing conditions showed fragmentation of the protein with increasing molar excess of HOSCN (Figure 4.2A). These fragments can be seen just below the dimer/higher aggregate band (black arrow), and with the darker silver staining intensity just above and below the monomer band (white arrow) (Figure 4.2A). Aggregation or formation of an altered species are particularly evident at higher concentrations of HOSCN just above the dimer band (black arrow), and evident by the smearing of the samples (Figure 4.2A). Samples electrophoresed under reducing conditions did not show these fragments or higher aggregates (or altered species) to such a notable extent (Figure 4.2B). No changes were detected in the monomer band (white arrow), but there was a slight increase in the dimer parent band (black arrow) with this being dependent on the molar ratio of HOSCN to FN (Figure 4.2B).

To further investigate possible damage to FN, Western blotting was performed to detect structural changes to the CBF epitope (clone A17). Treated samples were separated on SDS-PAGE and transferred to PVDF membranes using an iBlot2 machine following the method outlined in Section 3.3.2. Under non-reducing conditions, treatment of FN with

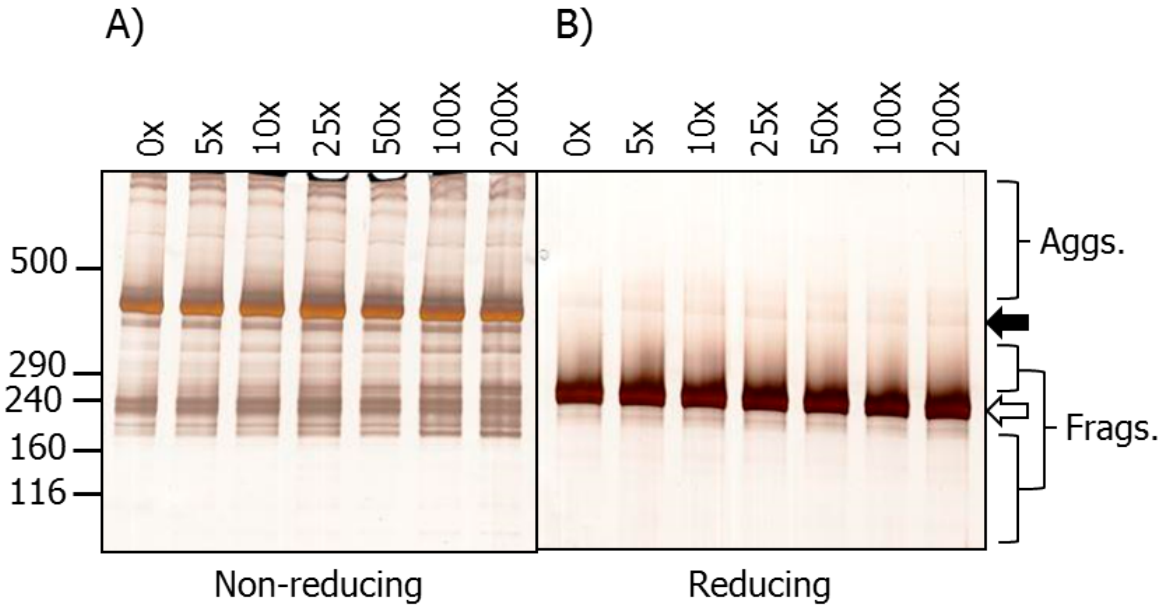

Figure 4.2: **SDS-PAGE with silver staining shows structural changes to human plasma FN treated with increasing molar ratios of HOSCN.** Purified human pFN (in 0.1 M pH 7.4 phosphate buffer) was either left untreated (control) or treated with increasing concentrations of HOSCN (0, 5, 10, 25, 50, 100, 200 μM), and incubated for 2 hr at 37°C. Samples were separated using 3-8% Tris-acetate SDS-PAGE gels under **A)** non-reducing or **B)** reducing conditions. Gels were then fixed, and visualised with silver stain and referenced against HiMark™ pre-stained High Molecular Mass standard. Data are labelled as follows: black arrow = dimer/higher aggregates, and white arrow = monomer band.

increasing molar excesses of HOSCN resulted in a small loss of epitope recognition of the monomer band (white arrow) (Figure 4.3A). HOSCN treated FN also showed increasing evidence of fragmentation, as observed both above and below the monomer bands (white arrow) (Figure 4.3A). Samples electrophoresed under reducing conditions showed that the monomer parent band (white arrow) decreased in intensity with increasing molar excesses of HOSCN compared to control (0x oxidant treatment). Furthermore, there seems to be a very slight decrease in the intensity level of dimer bands (black arrow) with increasing concentrations of HOSCN (Figure 4.3B).

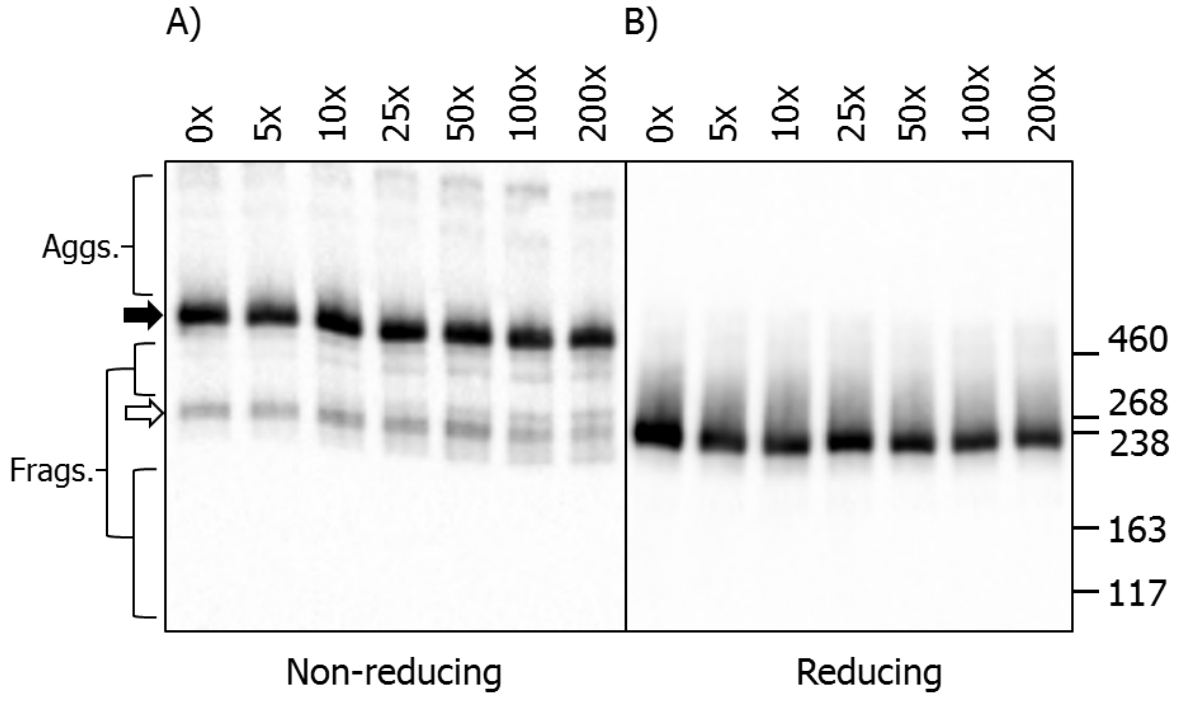

Figure 4.3: **SDS-PAGE followed by Western blotting shows structural changes to human plasma FN treated with increasing molar ratios of HOSCN.** Samples that were separated on SDS-PAGE under **A)** non-reducing or **B)** reducing conditions and transferred onto PVDF blots and probed with a mouse monoclonal anti-FN CBF antibody (A17; 1:10000), and conjugated with anti-mouse HRP secondary (1:2000). Blots were developed with ECL-plus reagent and data is labelled as follows: black arrow = dimer/higher aggregates, and white arrow = monomer band.

In light of the data found and knowledge known about HOSCN, changes to thiol residues were next investigated to determine whether these are targeted by HOSCN.

4.3.3 Thiol assay analysis of HOSCN treated bovine plasma fibronectin

FN possesses a low number of free thiol groups with 2-3 free thiols on the protein, which may be targeted by HOSCN during oxidation [296]. Modifications to free thiols can lead to protein structural changes (possibly via formation of intra-protein disulfide bonds) and affect biological function. By examining whether free thiols are targeted by HOSCN, a picture can be formed about HOSCN and its interaction with FN. Bovine plasma FN was used for these experiments as it was easier to obtain the amounts required, however the structure of human and bovine FN are closely related (90% sequence similarity; Uniprot data). Bovine plasma FN (5 μM) bound on 96-well plates in 0.1 M pH 7.4 phosphate buffer was exposed to increasing concentrations of HOSCN for 2 hr at 37°C. ThiolGlo solution was prepared as a working solution following manufacturers instructions, and transferred in a 1:1 ratio to samples and GSH standard. Samples were incubated for 10 min at 21°C on a shaker in the dark. Fluorescence was measured at 384nm_{ex} and 513nm_{em}.

Non-treated (control) samples were found to have approximately 80 nM of detectable thiol concentration. With FN samples exposed to 1x molar of HOSCN, thiol levels were found to have decreased to 50% of control samples (Figure 4.4). Increasing the HOSCN concentration to a 50x molar ratio relative to FN, it was observed the thiol concentration was eventually zero with a statistically-significant loss compared to the control samples (Figure 4.4).

These data suggests that HOSCN targets thiol residues on FN and causes small structural changes leading to epitope modifications. As a consequence, further studies were carried out to examine the biological effects of modifications induced by HOSCN on FN.

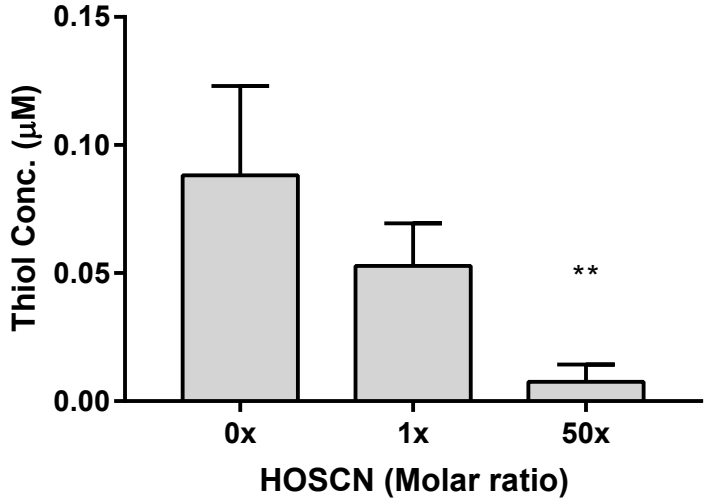

Figure 4.4: **ThioGlo analysis of thiol levels on bovine plasma FN treated with HOSCN.** FN (5 μM) was treated with increasing molar ratios of HOSCN (0, 5, 250 μM) in a 96-well plate for 2 hr at 37°C then ThioGlo reagent was added to each well. Concentration was measured against a GSH standard to determine absolute concentration. Statistical analysis was performed using one-way ANOVA with Tukey's multiple comparison post hoc tests to determine significance. Statistical difference is identified as follows: ** = $p < 0.01$.

4.3.4 Effect of cell adhesion HOSCN-modified human plasma fibronectin

The biological effects of HOSCN-treated FN on HCAEC was further elucidated by performing a cell adhesion assay. These experiments were performed as described in Section 3.3.4. Surface-bound FN (0.02 μM) was treated with increasing concentrations of HOSCN (0, 5, 10, 25, 50, 100, 200 μM) diluted in 0.1 M pH 7.4 phosphate buffer, followed by washing with PBS to remove excess oxidant to prevent direct interaction of the oxidant with HCAEC. HCAEC were added to each sample well at a density of 12,500 cells per well, followed by rinsing with 1% casein in PBS to remove any unadhered HCAEC. Adhered HCAEC were fixed then stained with crystal violet, which was resolubilised in acetic acid and absorbance was measured at 590 nm.

Exposure of human plasma FN to HOSCN resulted in minor changes in the ability of cells to bind when compared to untreated (0x oxidant treatment) FN. However, increasing HOSCN concentrations showed variable results, with no statistical significance detected

with increasing concentrations of HOSCN (Figure 4.5).

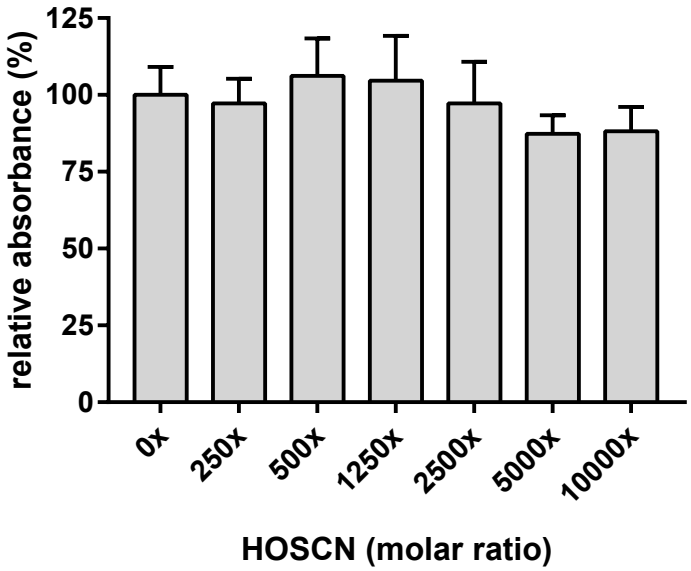

Figure 4.5: **Cell adhesion of HCAEC on HOSCN-modified human plasma FN.** Surface-bound human plasma FN (0.02 μM) was treated with HOSCN (0, 5, 10, 25, 50, 100, 200 μM) and incubated for 2 hr at 37°C before being fixed, stained with crystal violet and absorbance was measured. The data are presented as a percentage relative to control (no oxidant; 0x oxidant treatment). Error bars are ± SD from three technical replicates obtained from each of three independent experiments. Statistical analysis was performed using one-way ANOVA with Tukey's multiple comparison post hoc tests to determine significance. Statistical significance was not found.

To examine changes to the cellular structure, ICC was performed using a Hoechst nuclei blue fluorescence stain and a rhodamine-phalloidin F-actin red fluorescence stain. Experiments were carried out as described in Section 3.3.4 (Figure 3.9). Both cell number and cell spreading can be examined with this method. Surface-bound human plasma FN on an 8-well slide was treated with HOSCN, washed with PBS, and incubated with 50,000 cells for 1.5 hr at 37°C in a humidified atmosphere containing 5% CO_2 before being stained with Hoechst and rhodamine-phalloidin. The samples were imaged using fluorescence microscopy.

The changes to the extent and nature of HCAEC adhesion and spreading on HOSCN-treated FN (compared to controls) were less extensive compared to that induced by HOCl (Figure 3.8). The number of cells did not fluctuate but appeared to be constant with increasing concentrations of HOSCN (Hoechst blue fluorescence) (Figure 4.5B).

The ability of cells to spread and interact with other ECs was observed to be similar to untreated control (0x oxidant treatment) samples (Phalloidin red fluorescence) (Figure 4.5B).

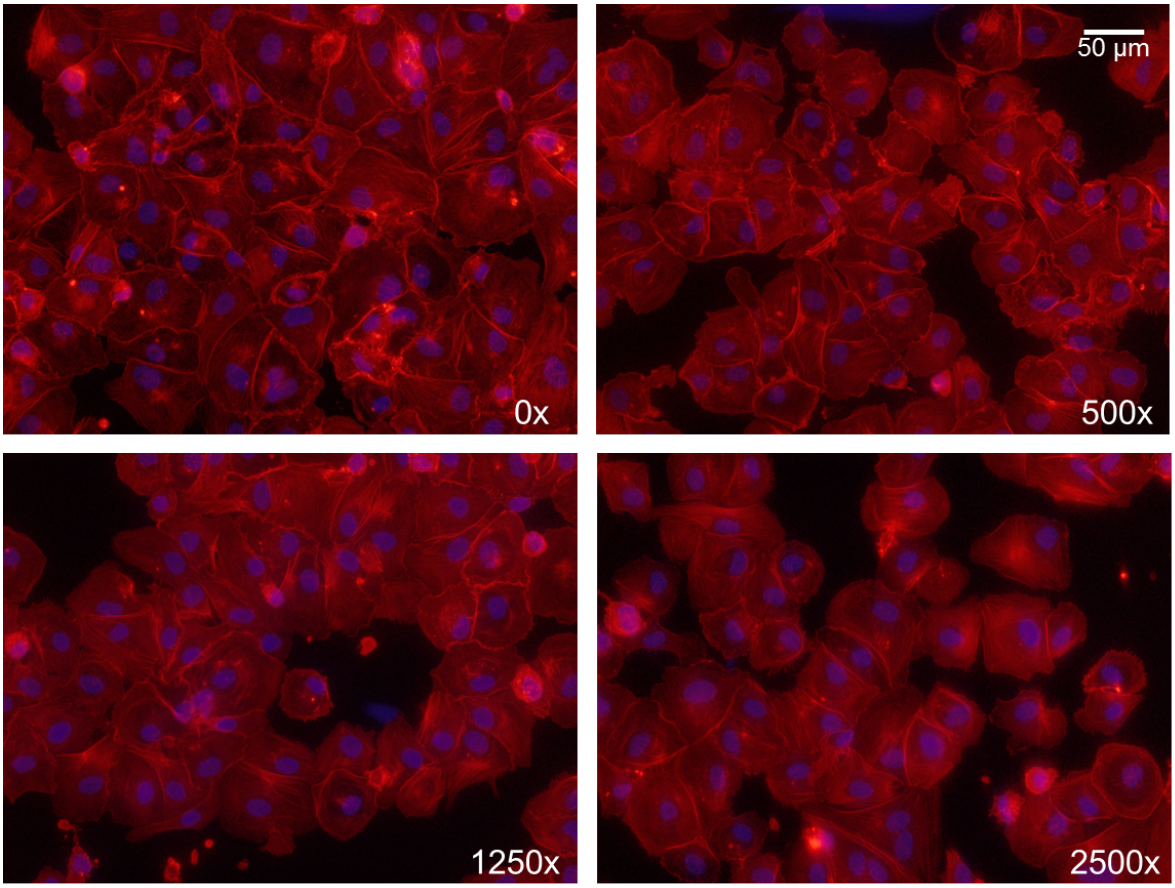

Figure 4.6: **Immunocytochemistry of HCAEC adhesion on HOSCN-modified human plasma FN.** Human plasma FN (0.02 μM) was coated on an 8-well plate treated with increasing concentrations of HOSCN (0, 10, 25, 50 μM) for 2 hr at 37°C before being exposed to HCAEC, which were subsequently fixed and stained with rhodamine-phalloidin (red) and Hoechst 33342 (blue) for fluorescence microscopic imaging.

These data suggests that HOSCN-modified FN may not alter the adhesion of HCAEC, however the oxidant treatment may still generate other long term changes, which were subsequently investigated by investigating cellular metabolic activity.

4.3.5 Effect of cell metabolic activity HOSCN-modified human plasma fibronectin

Cellular metabolic activity can be affected independently of cell adhesion, and impairment of this process can be identified using an assay to examine whether cells maintain their activity. Surface-bound FN was either untreated (0x oxidant control) or treated with increasing concentrations of HOSCN, then washed to remove excess oxidant following methods describe in Section 3.3.5. Each well was incubated with 12,500 cells per well, and any unbound cells were washed away with 1% casein in PBS. Fresh growth media was then added to each well, and HCAEC were incubated under normal tissue culture conditions for 48 hr to recover, prior to addition of MTS reagent to measure absorbance at 490 nm at 3 hr.

HCAEC adhesion on HOSCN-modified FN showed variable changes (Figure 4.5). However, HCAEC incubated on HOSCN-modified FN showed a constant level of cell metabolic activity with increasing concentration of HOSCN treatment of the FN (Figure 4.7). No statistically-significant changes were detected and HOSCN-modified FN, therefore did not significantly affect the ability of the HCAEC to proliferate (Figure 4.7). Decreased cell metabolic activity would be heavily influenced by a decreased in cells attached to the plate.

Due to the specificity of HOSCN oxidation, certain biological effects may not be severely effected, but HCAEC may react by expressing different genes to deal with environmental changes. Real time qPCR therefore was performed in light of the previous data to identify possible changes in HCAEC gene expression when incubated on HOSCN-treated FN.

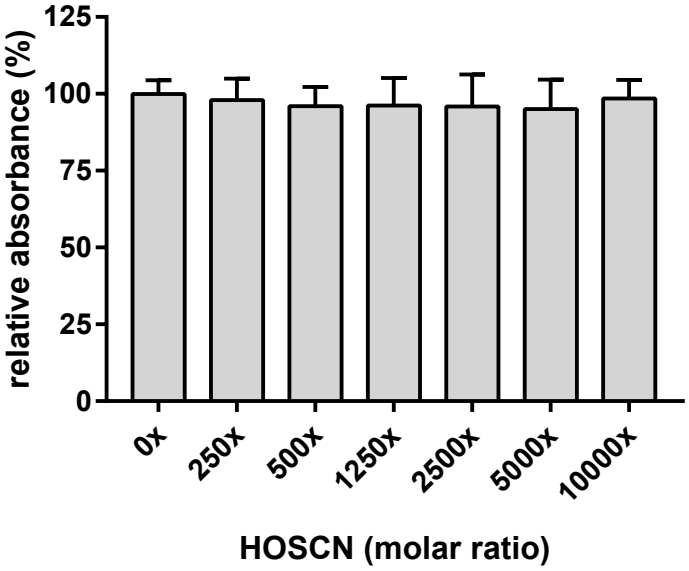

Figure 4.7: **MTS assay of HCAEC metabolic activity on HOSCN-modified human plasma FN.** Human plasma FN (0.02 μM) was treated with increasing concentrations of HOSCN (0, 5, 10, 25, 50, 100, 200 μM) and incubated for 2 hr at 37°C before adding MTS reagent to each well. The data are presented as a percentage relative to control (no oxidant; 0 μM treatment). Error bars are ± SD from three technical replicates obtained from each of three independent experiments. Statistical analysis was performed using one-way ANOVA with Tukey's multiple comparison post hoc tests to determine significance. Statistical significance was not found.

4.3.6 Effects of HOSCN modified fibronectin on HCAEC gene expression

Gene expression can be up- or down-regulated as a cellular response to change. Experiments were carried out as described in Section 3.3.6. Surface-bound FN on 6 well plates were treated with 1250x molar excess (50 μM) of HOSCN for 2 hr at 37°C, prior to incubation with 500,000 HCAEC for 72 hr, followed by sample extraction using a Qiagen RNeasy Mini Kit. A Qiagen RT^2 Profiler PCR Human Extracellular Matrix and Adhesion molecules (330231; QIAGEN) kit was utilised to investigate multiple gene expression including ECM and adhesion molecules, housekeeping genes, and experimental controls (Table 4.1). Data were analysed using SABiosciences PCR Array Data Analysis Template in conjunction with a Web-based analysis software from SABiosciences (`www.SABiosciences.com/pcrarraydataanalysis.php`). Treated samples were compared against untreated (0x oxidant control) samples (Table 4.2).

Table 4.1: **Gene expression investigated for ECM and adhesion molecules.**

Gene	Description
ADAMTS Type I, Type 13, Type 8	von Willebrand factor-cleaving protease
CD44	CD44 antigen; cell-cell interaction
CDH1	E-cadherin
CLEC3B	Tetranectin
CNTN1	Contactin 1
[COL]1A1, 5-8A1, 11-12A1, 14-16A, 4A2, 6A2	Collagen chains
CTGF	Connective Tissue Growth factor
[CTNN]A1, B1, D1, D2	Catenin α1, β1, δ1-2
ECM1	Extracellular matrix 1
FN1	Fibronectin
HAS1	Hyaluronan Synthase 1
ICAM1	Intercellular Adhesion Molecule 1
[ITG]A1-8, B1-5, AL, AM, AV	Integrin chains
KAL1	Anosmin 1
[LAMA] A1-3, B1, B3, C1	Laminin Chains
[MMP]1-3, 7-16	Matrix Metalloproteinases 1-3, 7-16
NCAM1	Neural cell adhesion molecule 1
PECAM1	Platelet EC cell adhesion
SELE, SELL, SELP	E-selectin, L-selectin, P-selectin
SGCE	Sarcoglycan ϵ
SPARC	Secreted protein acidic and cysteine rich
SPP1	Secreted phosphoprotein 1
TGFB1	Transforming growth factor beta induced
[THBS]1-3	Thrombospondin 1-3
[TIMP]1-2	TIMP metallopeptidase inhibitor 1-2
TNC	Tumor Necrosis Factor
VCAM1	Vascular cell adhesion protein 1
VCAN	Versican
VTN	Vitronectin
ACTB, B2M, GAPDH, HPRT1, RPLP0	House keeping genes

A down-regulation of ADAMTS13, COL5A1, CTNNA1, FN1, MMP8, SELL, SELP was shown to occur when HCAEC were incubated on FN treated with HOSCN (Table 4.2). SPARC was shown to be up-regulated in HCAEC incubated on HOSCN-treated FN (Table 4.2) when compared to native FN.

Table 4.2: **Gene analysis of HCAECs incubated on human plasma FN treated with 1250x (50 μM) of HOSCN.**

Gene	Fold Regulation	*P*-Value
ADAMTS13	-1.52	0.009
COL5A1	-1.23	0.009
CTNNA1	-1.17	0.019
FN1	-1.25	0.002
MMP8	-9.58	0.050
SELL	-1.56	0.009
SELP	-1.44	0.039
SPARC	+1.18	0.045

In light of these data showing modifications on plasma FN, cellular FN was next examined as it is a significant component of the basement membrane of the arterial wall. Furthermore, studies on a mixture of ECM extracted from HCAEC culture was also examined to assist in establishing whether cellular FN reacts in the same way when it is present amongst the complex mixture of other proteins similar to what would be found *in vivo*.

4.3.7 Effect of HOSCN on cellular-derived fibronectin epitopes

Cellular FN possesses extra protein domains arising from splice variants with these extra domain being important in vascular maintenance and matrix assembly; these extra domain are known as EDA and EDB. Examining the effects HOSCN has on cellular FN in a mixed ECM sample can give information on whether HOSCN targets FN amongst other matrix proteins, and whether the important functional sites CBF, HBF and the cellular EDA are modified. HCAEC were cultured over a week in 96 well plates, before bound cells were removed and ECM in each well was exposed to HOSCN as described in Section 3.3.7. Samples were probed for functional CBF, HBF and EDA epitopes using specific antibodies, with absorbance measured using ELISA.

Whole HCAEC-derived ECM treated with HOSCN samples probed for the CBF (clone A17) were found to not be targeted by HOSCN and showed no changes with increasing treatment concentration of HOSCN (Figure 4.8A). Examination of the HBF on FN showed no statistically significant changes with increasing concentrations of HOSCN (Figure 4.8B). Probing for FN EDA when treated with increasing concentrations of HOSCN showed that epitope recognition did not change with increasing concentrations of the oxidant (Figure 4.8C).

These data establish that there were no changes to these specific FN epitopes when exposed to HOSCN. However, as changes may also occur at other sites on FN, further investigations were made to examine changes to FN protein structure within the complex HCAEC-derived ECM.

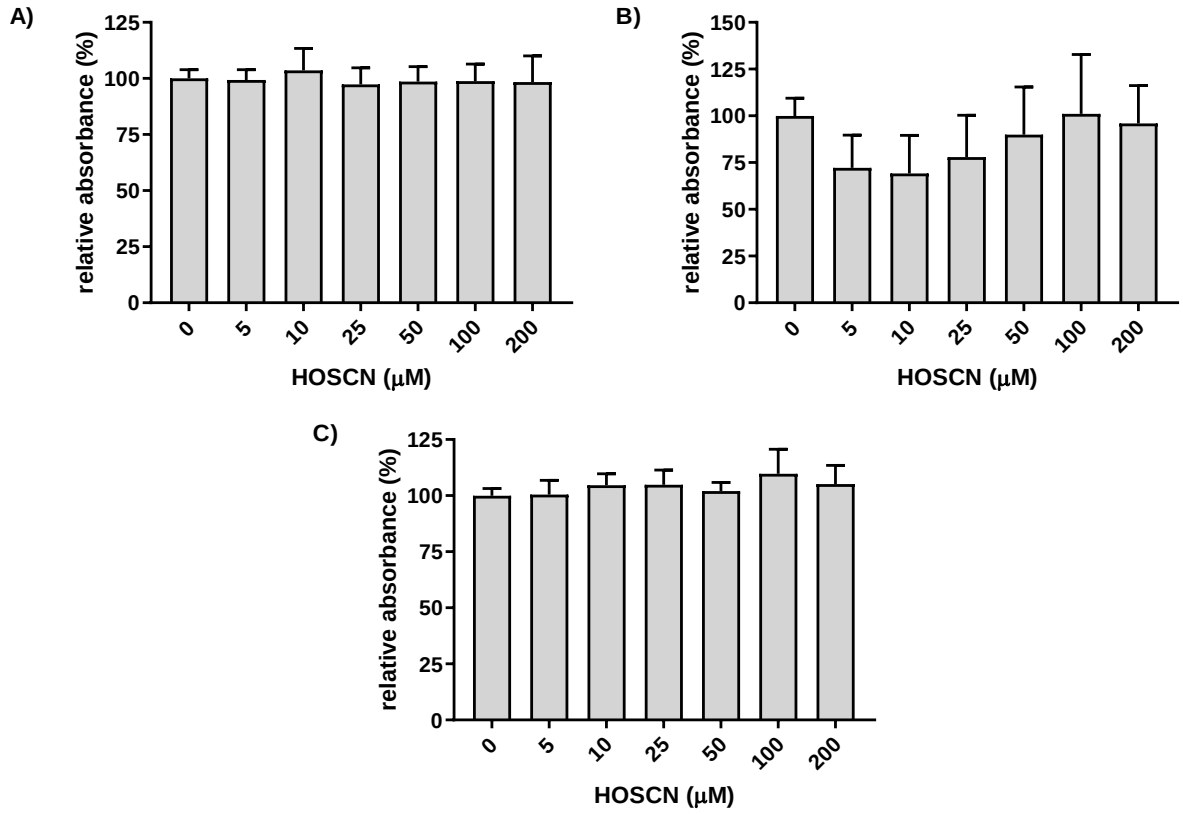

Figure 4.8: **ELISA of whole ECM-derived from HCAEC exposed to HOSCN.** HCAEC produced ECM on 96-well plates were treated with increasing concentrations of HOSCN (0, 5, 10, 25, 50, 100, 200 μM). Specific FN epitopes were detected by using a mouse monoclonal **A)** anti-FN CBF antibody (A17; 1:10000), **B)** anti-FN HBF antibody (A32; 1:1000), **C)** anti-FN EDA antibody (3E2; 1:1000), and conjugated with anti-mouse HRP secondary (1:1000 dilution). The data are presented as a percentage relative to control (no oxidant; 0 μM oxidant treatment). Error bars are $\pm$ SD from three technical replicates obtained from each of three independent experiments. Statistical analysis was performed using one-way ANOVA with Tukey's multiple comparison post hoc tests to determine significance. No statistical significance was detected.

4.3.8 Effect of HOSCN modification on cell-derived fibronectin

The CBF, HBF, and EDA sites on FN are important in maintaining cell and vascular health and integrity. Whole ECM extracted from HCAEC cultures were treated with increasing molar excesses of HOSCN, and separated under reducing conditions on SDS-PAGE. Proteins were then transferred onto PVDF membranes and probed for these three functional epitopes.

Whole ECM-extracts exposed to HOSCN showed changes to ECM structure with increasing molar excess of oxidant. The CBF of FN was shown to have slightly decreased antibody recognition particularly of the monomer band (white arrow) at the higher molar ratios of HOSCN, such as at 150 μM (Figure 4.8A). This loss of epitope recognition correlated closely with what was measured in the ELISA examining loss of CBF epitope recognition of human plasma FN treated with HOSCN (Figure 4.1A), although this loss was not detected with whole ECM ELISA samples (Figure 4.9A). Examining the HBF of FN, it was shown that HOSCN induced loss of epitope recognition to the monomer band (white arrow) with 10 μM to 50 μM of HOSCN with the recognition returning at higher molar excesses of HOSCN (Figure 4.9B).

The EDA, which is specific to cellular-derived FN, did not seem to be modified by HOSCN; epitope recognition of the monomer band (white arrow) was not observed to change with increasing doses of HOSCN (Figure 4.9C). A similar result was found when an ELISA was performed on whole ECM exposed to HOSCN (Figure 4.9C). Thus, there does not seem to be any major fragmentation or aggregation changes occurring for these domains, which could be determined under these reducing gel conditions (Figure 4.9). However structural changes may have occurred which may not be detected under reducing gel conditions.

These data suggests that HOSCN acts on FN in lieu of other proteins present, but with the severity of modifications being less extensive compared to FN exposed to HOCl. The

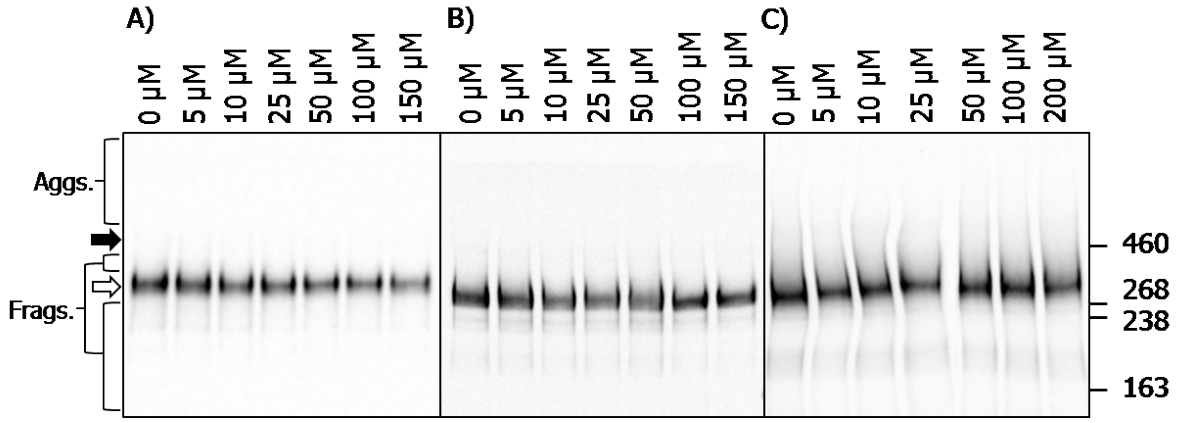

Figure 4.9: **Western blots showing structural changes to whole ECM-derived from HCAEC treated with increasing molar ratios of HOSCN.** Samples were separated by SDS-PAGE under reducing conditions and transferred onto PVDF blots and probed with mouse monoclonal **A)** anti-FN CBF antibody (A17; 1:10000 dilution), **B)** anti-FN HBF antibody (A32; 1:2000), **C)** anti-FN EDA antibody (3E2; 1:2000), and conjugated with anti-mouse HRP secondary (1:2000 dilution). Blots were developed with ECL-plus reagent and data is labelled as follows: black arrow = dimer/higher aggregates, and white arrow = monomer band.

effects that HOSCN has on FN are discussed further below.

4.4 Discussion

FN is known to play an important role in maintaining vascular integrity and health. It exists in the basement membrane of ECs and acts as a scaffold by binding to other ECM proteins and cells [148, 196]. During the development of atherosclerosis, inflammation takes place and releases oxidants, such as HOCl and HOSCN [33]. The reaction of HOCl have been extensively studied in previous research [49, 50]. In contrast, the chemistry and biology of HOSCN, a much more specific oxidant that produces reversible oxidative products by targeting thiols (RSH, Cysteine), has been studied to a much more limited extent [94]. This study aimed to examine the effects that HOSCN has on FN, and how these modifications might affect the biological functions of this protein.

FN exposed to HOSCN was observed to have distinctively less modifications under non-reducing conditions when compared at the same molar ratio of HOCl. Starting at 5x molar ratio, FN was found to form specific fragments, which can be seen above 290 kDa, and above and below the monomer band (white arrow) (Figure 4.3). These fragments are observed to increase with increasing molar ratios of HOSCN. Furthermore, treatment of FN with HOSCN was observed to form aggregates under both non-reducing and reducing conditions (Figure 4.3). This phenomenon is consistent with previous studies that showed treatment of LDL with HOSCN, which led to a loss of parent protein with subsequent formation of aggregates and fragments [371]. In previous studies, protein unfolding and aggregation has been linked to HOSCN treatment, particularly under non-reducing conditions via formation of disulfide bonds but there are limited studies investigating protein fragmentation with this oxidant [102, 103].

HOSCN is known to reversibly oxidise Cys residues and GSH, although with a lower kinetic rate constant compared to HOCl [50, 51]. Reduced:oxidised thiol ratios have been used as an oxidative stress indicator, whereby changes to this ratio can indicate high oxidative stress [372]; this particular ratio has been used as a predictor of early atherosclerosis [373]. As previously stated, HOSCN has been found to react more

specifically with thiol-containing protein in cells than HOCl using the thiol-specfic fluorescent probe IAF [374]. High concentrations of HOSCN has been correlated with depletion of thiol levels, as observed in the plasma of smokers [99]. In support of this, a decrease in plasma thiol levels were shown to be correlated with increased risk of the early stages of atherosclerosis [372, 373].

HOSCN treatment of protein thiols are found to form unstable transitory RS-SCN derivatives, which are found to further react with water to generate sulfenic acid intermediates (RS-OH) [94, 103]. Further reactions of this species with another thiol can lead to the formation of disulfide bonds [94, 104–107]. FN possesses 2-3 free thiols, which are likely to be the first targets for HOSCN depending on their accessibility (Uniprot data; P02751). The oxidation of these free thiols would be expected to lead to the formation of new disulfides between protein chains. This would explain the occurrences of higher aggregates detected as seen a smear above the dimer band (black arrow) (Figure 4.3). Another potential mechanism for the formation of such species is that thiol oxidation can lead to thiol-disulfide exchange, whereby disulfide links are broken and reformed with another Cys residue [105, 107, 375, 376]. Thiol-disulfide exchange can cause conformational changes to FN which may lead to a shift in the observed molecular mass on SDS-PAGE due to alterations in the rate of which the protein runs through the gel. The mechanism leading to fragmentation is not fully understood and requires further investigation to elucidate this process.

Although Cys residues are likely to be the first targets of HOSCN, this oxidant has also been found to target Trp and Lys residues, especially if there is a lack of Cys residues [26, 102]. Treatment of LDL with HOSCN has shown that Cys and Lys residues are modified [371]. Degradation of HOSCN leads to formation of cyanate (OCN^-) which has been found to act on Lys residues (as well as other residues) to generate homocitrulline [112, 113]. This process is called carbamylation and has been found to be correlated with increased risk of CAD, with higher levels of homocitrulline found to be present in human lesions [112, 113]. Protein carbamylation has been shown to cause HDL dysfunction,

which would lead to a reduction in efficacy of lipid and partially reverse cholesterol transport [113]. Furthermore, lipoprotein carbamylation was found to transform LDL into a macrophage-targeted ligand which is taken up via scavenger receptors, and leads to increased accumulation of cholesterol and foam-cell formation [112].

The FN CBF domain which involves residues 1267-1540 of the protein sequence possesses 5 Lys and 3 Trp residues, and the HBF domain (residues 1727-1991) possesses 15 Lys and 3 Trp residues (Uniprot data; P02751). There are also two free Cys residues located at positions 1232 and 2136 (Uniprot data). In light of HOSCN reactivity with these amino acids, the low levels of free thiols that can be targeted by HOSCN means these Lys or Trp residues could be modified. The ThioGlo assay identified that free thiols were targeted by HOSCN leading to a decrease in the levels of thiols detected (Figure 4.4). As certain thiols may not be accessible to the oxidant and may not be detected, there are limitations to the current experimental data with regards to the detection of total concentration of Cys residues. However, it can be seen that there are likely minor modifications induced by HOSCN to these domains, causing loss of antibody recognition (Figure 4.2, 4.8, and 4.9), with structural changes seen as the formation of aggregates and fragments (Figure 4.3). These effects may also be limited by the conformation of FN where certain areas are inaccessible to the effects of HOSCN.

Gene expressions in HCAEC incubated on HOSCN-treated FN (Table 4.2) differed to HOCl-treated FN (Table 3.2) with fewer number of genes altered in their level of expression compared to control (0x treatment). Unlike the down-regulation of multiple MMPs in HCAECs exposed to HOCl-treated FN, HCAEC incubated on HOSCN-treated FN were found to only down-regulate MMP-8 by almost 10 fold (Table 4.2). MMP-8 is an important collagenase alongside MMP-13, which functions to breakdown type I-III collagens [377, 378]. It has been shown previously that EC treated with condensate from cigarette smoke had increased expression of MMP-1, MMP-9, and MMP-8 [379]. Furthermore, elevated levels of MMP-8 and MMP-13 have been associated with formation of unstable plaques due to effects of these enzymes and macrophages on collagen within

plaque [380–382]. MMP-8$^{-/-}$ and MMP-13$^{-/-}$ in apoE$^{-/-}$ mice were found to have decreased lesion sizes, with lower macrophage population, and increased collagen content giving rise to a more stable plaque phenotype [380–382]. MMP-8 has been linked to not only increase in VCAM-1 expression in EC, but also decreased Ang II levels associated with high blood pressure, a risk factor for atherosclerosis [380]. The reason that HCAEC exposed to HOSCN-treated FN down-regulates MMP-8 may be to retain collagen binding and prevent further collagen degradation along with decreased leukocyte migration to the site of injury. This may help maintain arterial wall integrity, by forming a more stable fibrotic plaque with a reduced risk of plaque rupture.

FN with HOSCN-induced modifications have also shown to modulate HCAEC selectin gene expression (Table 4.2) but less so in comparison to HOCl-modified FN (Table 3.2). SELE was found not to be changed in response to HOSCN treated FN unlike HOCl-treated FN; however SELP was down-regulated by both treatment. Both of these selectins are expressed on EC, whereas SELL is solely expressed on leukocytes and hence will not be discussed further here [350]. Elevated levels of SCN^{-} (80-400 μM), such as in smokers, have been found to elevate both SELE and SELP, with a corresponding increased expression of other inflammatory markers such as interleukin-6 (IL-6), and C-reactive protein [383–385]. Furthermore, HOSCN has been shown to induce up-regulation of SELE and ICAM-1 expression in HUVECs via the NFκB pathway; this led to an increased neutrophil adhesion on EC and recruitment of leukocytes [385]. This altered regulation of SELE shown by HCAEC incubated on HOSCN-treated FN may be a primary reaction to HOSCN-treated FN, with later responses occurring downstream.

SELP is expressed on both EC and (to a greater extent) on platelets and is found to assist in leukocyte adhesion and recruitment as seen in apoE$^{-/-}$ mice [363]. As discussed in Section 3.1, elevated levels of SELP were associated with CVD risk fators [364], development of fibrotic atherosclerotic plaques [363], and intima-media thickening of the arterial wall [365]. It may be that HCAEC down-regulates SELP expression in an attempt to decrease leukocyte migration and reduce inflammation within the affected

area. Furthermore, it may be an attempt to also reduce platelet binding, which would lead to clot formation and possible downstream blockage of the artery.

One gene that was found to up-regulated by HCAEC incubated on HOSCN-treated FN and not HOCl-treated FN was Secreted Protein Acidic And Cysteine Rich (SPARC). SPARC has been shown to play a role in ECM synthesis during remodelling, in wound healing, and functions in cell repair by promoting changes to cell shape [386, 387]. SPARC interacts with ECM and cytokines, and regulates growth factors to affect cell growth; cell proliferation can be regulated by SPARC through the G1 phase of the cell cycle [386, 387]. Furthermore, SPARC has been found to cause bovine aortic EC (BAEC) to secrete less FN, but increase type-1 plasminogen activator inhibitor levels, which is important for matrix remodelling [388]. High concentrations of SPARC have also been shown to cause rounding of BAEC [388]. Knockout of SPARC ($SPARC^{-/-}$) in mice was found to reduce concanavalin A (Con A)-induced necroinflammation coinciding with a reduction in TNF-α and IL-6 levels [389]. $SPARC^{-/-}$ mice were also found to have a reduction in collagen fibers, and necroinflammation with decreased infiltration and proliferation of CD4+ T cells and subsequently decreased fibrosis in liver [390]. The effects of SPARC is further supported in previous studies where inhibition of SPARC through knockout using lentivirus was found to reduce numbers of apoptic cells and increased binding capacity of human microvascular EC to FN [389]. Inhibition of SPARC also led to decreased adhesion and migration of lymphocytes across the EC monolayer [389].

This up-regulation in SPARC appears to be linked with the other alterations in gene expression in HCAEC incubated on HOSCN-treated FN, whereby the cells appear to be attempting to create collagen fibers within the injury area. Although SPARC has been found to promote inflammation and migration of leukocytes, its extent of promotion compared with other inflammatory-based genes may be less and thus minimize the final total amount of inflammation. Some of the other down-regulated genes are involved in the prevention of collagen degradation and with the up-regulation of SPARC, these data could be interpreted as HCAEC are attempting to remodel the basement membrane to

form a more fibrotic environment.

Curiously, the sequence on FN involved collagen binding which lies between amino acids 308-608, with the critical binding site being residues 464-477, possesses 23 Cys residues (Uniprot. data; P02751). These Cys are all involved in disulfide bonds (Uniprot. data; P02751). This region is the foundation for the binding between FN and collagen, giving structural integrity to the basement membrane and is vital to the linkage between collagen and cells [202, 222, 391]. Further investigation is needed to elucidate the modifications induced by HOSCN in the collagen binding epitope on FN. It may be that HOSCN is modifying this collagen binding fragment, decreasing overall efficacy of collagen binding between cells and FN. Although, cells were able to maintain binding to FN via the CBF and corresponding RGD site, it has been found that collagen and FN in combination helps to in initiate and enhance cell spreading and migration [222]. The importance of collagen extends to the formation of stable fibrous caps in atherosclerotic lesions, and reduced plaque rupture.

The differences in expression and regulation fold between HOCl-treated FN (Table 3.2) and HOSCN-treated FN (Table 4.2) appears to be associated with the severity of the modifications induced to FN by each oxidant. The extensive modifications caused by HOCl appears to lead to a greater response, which may be involved with the possible recruitment of leukocytes and ECM remodelling, and attempts to lay down healthy ECM and generate new binding ligands for HCAEC. However, the HCAEC plated on HOSCN-treated FN seem to retain their binding capacity, and appear to induce gene changes that may be designed to maintain collagen integrity and a ”healthy” basement membrane.

This chapter examined modifications induced by HOSCN on FN in terms of protein structure and functional epitopes, and how this might affect cellular function. Further investigations would help to elucidate in greater detail the effects that HOSCN has on FN, for example through amino acid analysis to identify changes to specific functional side chains, and examination of other functional epitopes which may harbour more cysteine

residues that could be targeted, such as the collagen binding fragment. Furthermore, *in vivo* conditions may result in less extensive modifications due to the presence of antioxidants in cells and surrounding ECM [392, 393], such as vitamins C and E, and GSH, which helps to convert vitamin C and E back into their active form [393, 394]. Further research into the reaction between HOSCN and antioxidants may be of use.

The complex interrelationships between MPO, HOCl, and HOSCN can be seen over these two chapters. Exposure to HOCl resulted in heavily modified peptides and subsequently biological dysfunction. HOSCN has been shown to be a much milder oxidant causing reversible oxidation at lower concentrations, giving rise to lower levels of oxidation than that found with HOCl, but has been shown to also be somewhat damaging to both proteins and cells at higher concentrations. The extent of HOCl and HOSCN generation at sites of inflammation in the body has been shown to be closely correlated with MPO levels, and thus the experiments reported in the next chapter used the enzymatic MPO system to examine FN modifications and its downstream biological effects.

Chapter 5

Effects of modifications to fibronectin by Myeloperoxidase, Chloride or Thiocyanate, and Hydrogen Peroxide

5.1 Introduction

MPO generates HOCl and HOSCN during inflammation in atherosclerosis, which are known to react with lipids, DNA, peptides, and proteins [49, 50]. MPO has been found to co-localise with ECM proteins mediating MPO-derived damage [21, 22, 395]. Replication of this mechanism was performed with MPO, in the presence of Cl^- or SCN^-, and H_2O_2 to better understand the relationship between FN and MPO-derived oxidants. Exposure of sub-endothelial matrix or FN to reagent HOCl or MPO/Cl^-/H_2O_2 has previously been shown to result in structural changes to the protein, chloramine formation, and a reduction in cell adhesion to these modified matrix proteins [22, 260, 261]. The studies in this chapter were based on these previous results.

5.2 Aim

This Chapter aims to elucidate the effects of MPO, in the presence of Cl^- or SCN^-), and H_2O_2, on human plasma FN. Two concentrations of MPO were used to reflect a normal and diseased state. The modifications were examined with treatments using a lower (0.02 μM) and a higher (0.1 μM) concentration of MPO, physiological concentrations of Cl^-, and a lower (20 μM) or higher (500 μM) concentration of SCN^-. Structural modifications were examined using silver staining and Western blotting, whereby modification to epitopes were examined using Western blotting and ELISA. Biological functions were investigated using Calcein-AM assay for HCAEC adhesion and MTS assay for HCAEC metabolic activity.

5.3 Results

5.3.1 Effects of myeloperoxidase, chloride, and hydrogen peroxide on human plasma fibronectin epitopes detected by ELISA

HOCl is enzymatically formed by MPO, Cl^-, and H_2O_2. In these studies the overall extent of HOCl formation was varied by increasing the H_2O_2 concentrations. As previously mentioned, the CBF and HBF epitopes of FN play a key role in maintaining matrix integrity and cell adhesion. ELISA experiments were carried out following the methods outlined in Section 3.3.1 while replacing reagent HOCl with MPO enzyme, Cl^-, and batch additions of H_2O_2. An AP antibody was used instead of HRP secondary to prevent non-specific interactions between HRP and samples. Samples were developed using a pNPP solution (p7998; Sigma) and absorbance was measured at 405 nm at 10 min.

Incubation of human plasma FN by the MPO/Cl^-/H_2O_2 system resulted in a statistically significant loss of recognition of the CBF epitope starting at 800x molar excess of H_2O_2 in a dose-dependent manner (Figure 5.1A). There was approximately 35% loss of epitope recognition at 1600x molar excess of H_2O_2 (Figure 5.1A). Investigation of the FN HBF showed similar dose-dependent loss of epitope recognition with a statistically significant loss observed at 800x molar excess of H_2O_2 and even greater loss of recognition of almost 50% compared to CBF at 1600x molar excess of H_2O_2 (Figure 5.1B). Modifications to these functional epitopes were accompanied by a dose-dependent increase in a HOCl-generated epitope as detected by the monoclonal 2D10G9 antibody (Figure 5.1C). Statistically significant detection of the HOCl-generated epitope was detected with 800x molar excess of H_2O_2 and increasing levels were detected with increasing concentrations of H_2O_2 (Figure 5.1C).

Establishing that physiological levels of Cl^- (100 mM) along with MPO and H_2O_2 generates damage to the functional epitopes on FN as well as a HOCl-generated epitope

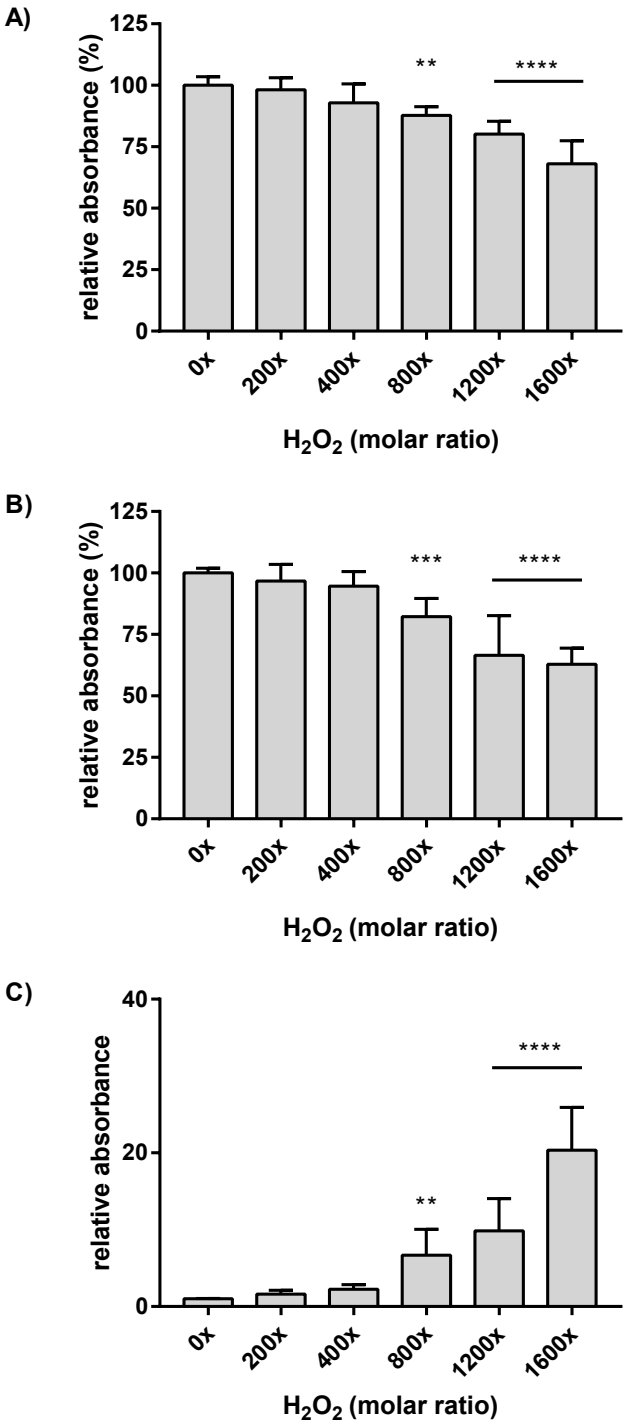

Figure 5.1: **ELISA of human plasma FN modified using enzymatic treatment with MPO/Cl^-/H_2O_2.** Each well was coated with 0.5 μg (0.02 μM of FN in 0.1 M phosphate buffer) and either left untreated (0 μM H_2O_2) or treated with MPO/Cl^- and increasing concentrations of H_2O_2 (0, 4, 8, 16, 24, 32 μM), and incubated for 2 hr at 37°C. FN epitopes were detected using a mouse monoclonal **A)** anti-FN CBF antibody (A17; 1:10000), **B)** anti-FN HBF antibody (A32; 1:1000), **C)** anti-HOCl generated epitope (2D10G9; 1:50), and conjugated with anti-mouse AP secondary (1:1000). The data are presented as a percentage relative to control (0 μM H_2O_2). Error bars are ± SD from three technical replicates obtained from each of three independent experiments. Statistical analysis was performed using one-way ANOVA with Tukey's multiple comparison post hoc tests to determine significance. Statistical significance is identified as follows: ** = $p < 0.01$, *** = $p < 0.001$, and **** = $p < 0.0001$.

indicates a similar mechanism observed with reagent HOCl (Figure 3.1). Experiments were subsequently carried out to investigate the structural changes on FN under these treatment conditions.

5.3.2 Effects of myeloperoxidase, chloride, and hydrogen peroxide on the structure of human plasma fibronectin

Structural modifications were investigated using SDS-PAGE with silver staining (Figure 5.2), and epitope structure was examined using Western blotting (Figure 5.3 and 5.4). Samples were treated with MPO enzymatic system with either 0.02 μM or 0.1 μM of MPO (Figure 5.2), 100 mM of Cl^-, and increasing concentrations of H_2O_2 (0, 20, 40, 80, 120, 160 μM), prior to performing separation by mass using gel electrophoresis and silver staining following the methods previously described in Section 3.3.2.

Silver staining of FN treated with MPO/Cl^-/H_2O_2 showed a range of modifications. Under non-reducing conditions, at 100x molar excess of H_2O_2, formation of dimers/higher aggregates (black arrow) were observed when treated with both 0.02 μM and 0.1 μM of MPO (Figure 5.2A and 5.2B). Increasing presence of higher aggregates were detected as smearing on the gels with increasing concentrations of H_2O_2. Samples treated with 0.1 μM of MPO showed similar increasing presence of higher aggregates but also a detectable loss in both dimers (black arrow) and monomer bands (white arrow) (Figure 5.2A). Formations of species with higher aggregates or altered structures were also detected with both 0.02 μM and 0.1 μM of MPO both above and below the monomer bands (white arrow) (Figure 5.2A and 5.2B). Furthermore, a shift in protein molecular mass was observed of the dimer bands (black arrow) with the addition of H_2O_2 compared to control (no H_2O_2 treatment) (Figure 5.2A).

SDS-PAGE under reducing condition showed an increasing presence of aggregates with higher concentrations of H_2O_2 in a dose-dependent manner (Figure 5.2B). Greater detection of aggregates were detected when FN was treated with 0.02 μM of MPO and 20 μM of H_2O_2, which increased with higher intensity of aggregates detected at 600-800x molar excess of H_2O_2 (Figure 5.2B). Protein smearing was detected at high concentrations of H_2O_2 (600-800x molar ratio) (Figure 5.2B). This formation of aggregates seemed to

be less with 0.1 μM of MPO treatment but higher aggregate smearing was observed at 400-800x molar excess of H_2O_2 (Figure 5.2B). An increasing amount of species with altered structure was detected with greater intensity at 0.02 μM treatment of MPO just above the monomer bands (white arrow) (Figure 5.2B). No changes were detected on the monomer bands when compared to their untreated counterparts.

Western blots of treated samples were used to examine the functional CBF and HBF epitopes on FN, to obtain complementary data to that found in the silver staining experiments. Probing for the CBF (clone A17), showed loss of antibody recognition in a dose dependent manner, with greater loss observed to occur with 0.1 μM treatment of MPO and 100-800x molar excess of H_2O_2 where there is a detectable loss in intensity of both the monomer (white arrow) and dimer (black arrow) bands (Figure 5.3A). Furthermore, formation of higher aggregates was observed with 0.02 μM of MPO treatment, and there appeared to be lower levels of aggregates detected with 0.1 μM of MPO treatment at the same H_2O_2 concentrations (Figure 5.3A). Under reducing conditions, there were notable formation of aggregates and smearing of bands with masses greater than 460 kDa, which can be seen with both 0.02 μM and 0.1 μM MPO treatment, particularly at 800x molar excess of H_2O_2 (Figure 5.3B). This was more marked with 0.02 μM of MPO compared to 0.1 μM of MPO.

Repeating this method and examining the FN HBF showed similar modifications as seen with the CBF antibody (Figure 5.4). Under non-reducing conditions, a loss of antibody recognition was detected for the dimer bands (black arrow) with increasing concentrations of H_2O_2, where greater loss was detected with 0.1 μM of MPO and 800x molar excess of H_2O_2 (Figure 5.4A). There were modifications leading to a molecular mass shift of the dimer/higher aggregates (black arrow) of FN when treated with MPO/Cl^-/H_2O_2. Under reducing conditions, there was more notable loss of HBF-antibody recognition of the monomer bands (white arrow) with a greater extent of loss observed with 0.1 μM of MPO (Figure 5.4B). As seen with the CBF results (Figure 5.3B), dimers/higher aggregates were also detected particularly with 0.02 μM of MPO treatment and at high

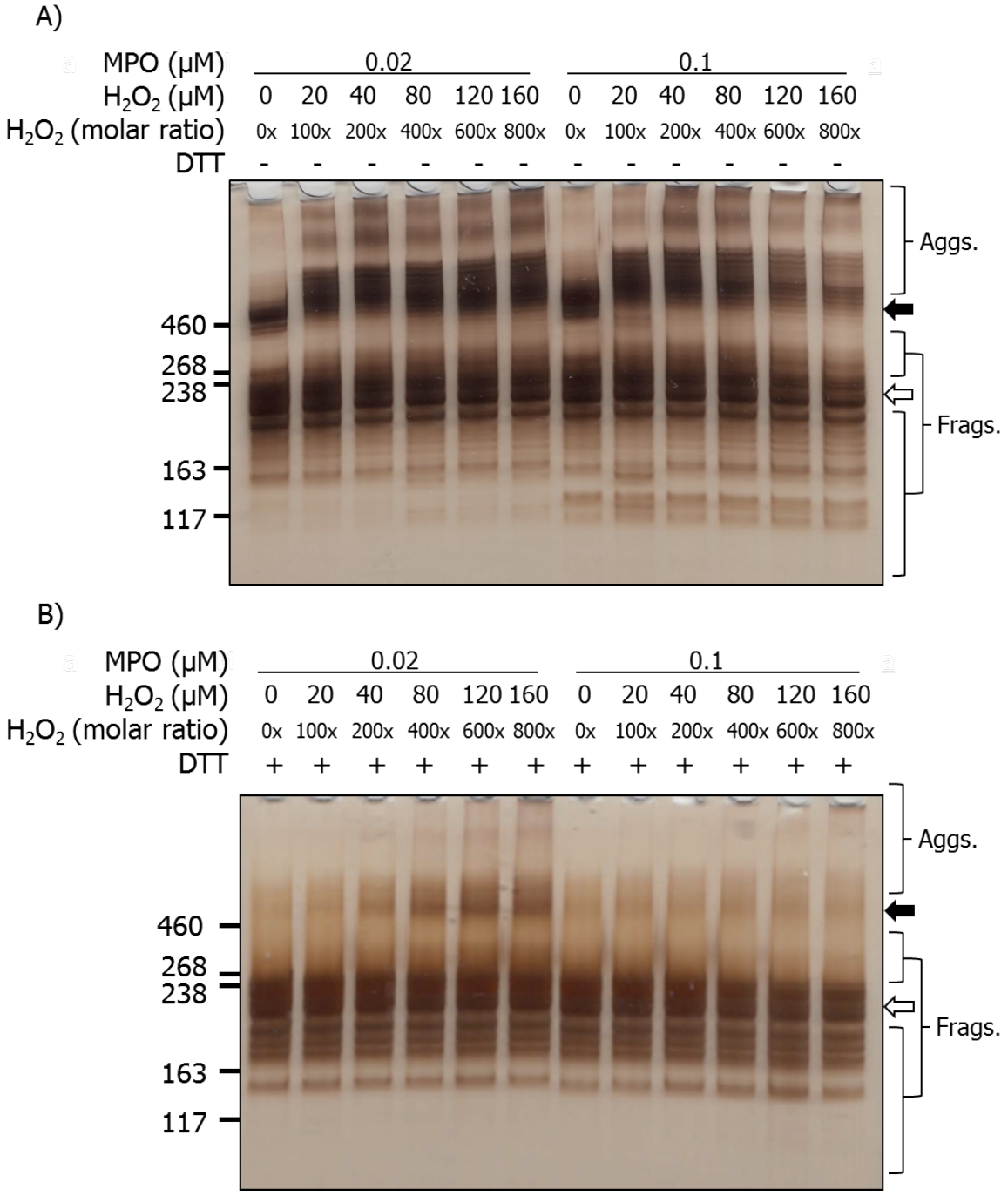

Figure 5.2: **Silver staining showing structural changes to human plasma FN treated with MPO/Cl^-/H_2O_2.** Purified human plasma FN (0.2 μM in 0.1 M phosphate buffer) was either left untreated (control 0x H_2O_2) or treated with MPO/Cl^- and increasing concentrations of H_2O_2 (0, 20, 40, 80, 120, 160 μM), and incubated for 2 hr at 37°C. Samples were electrophoresed on 3-8% Tris-acetate SDS-PAGE gels under **A)** non-reducing or **B)** reducing conditions. Gels were then fixed, and visualised with silver staining and referenced against HiMark™ pre-stained High Molecular Mass standards. Data is labelled as follows: black arrow = dimer/higher aggregates, and white arrow = monomer bands.

concentrations of H_2O_2 (black arrow) (Figure 5.4B).

In light of these data showing modifications to FN epitopes, particularly to the biologically important CBF, further assays were performed to investigate the effects of this oxidant system on HCAEC adhesion and HCAEC metabolic activity.

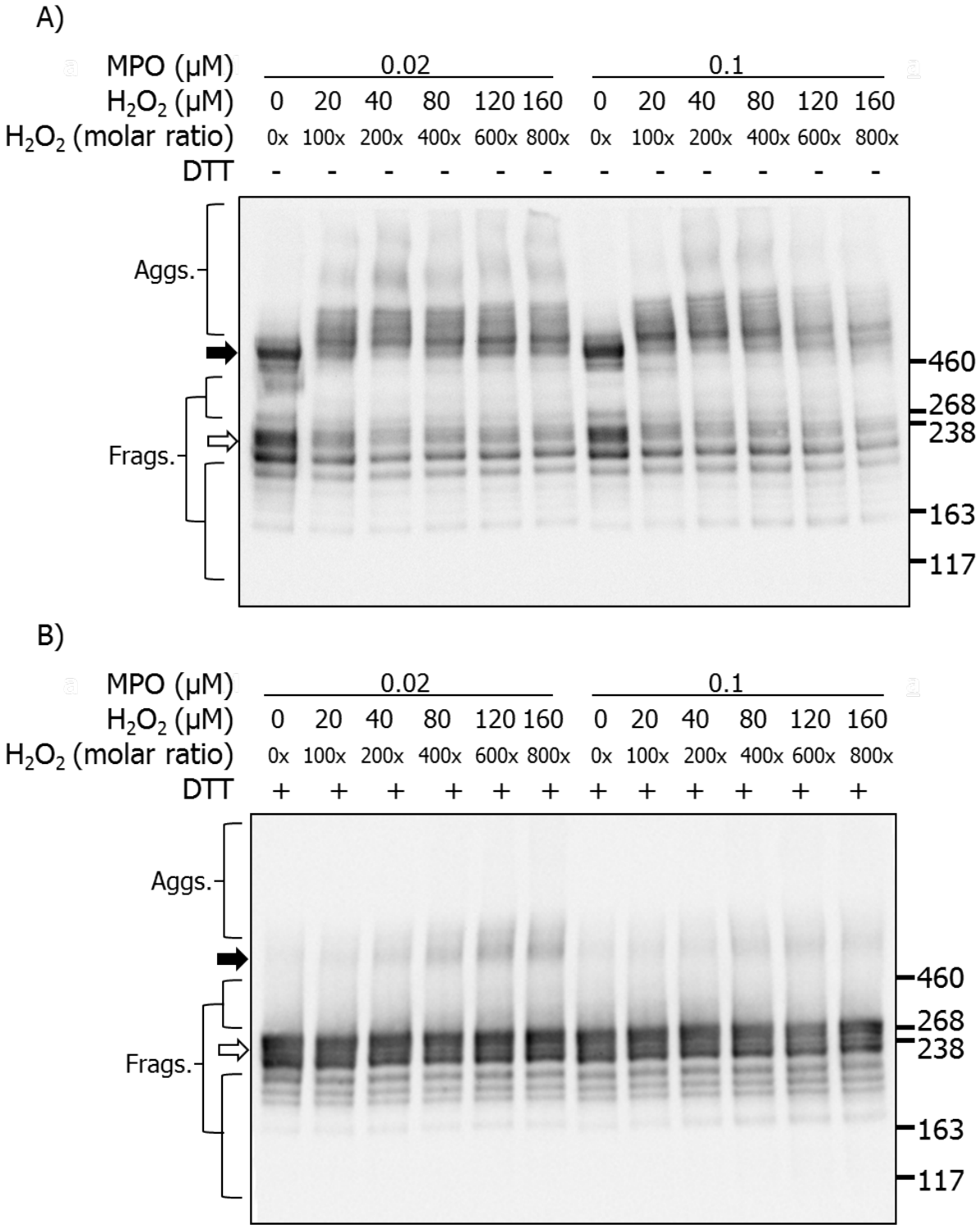

Figure 5.3: **Western blotting of structural changes to human plasma FN treated with MPO/Cl^-/H_2O_2.** Samples were separated on SDS-PAGE under **A)** non-reducing or **B)** reducing conditions and transferred onto PVDF membranes and probed with mouse monoclonal anti-FN CBF antibody (A17; 1:10000), followed by anti-mouse HRP-conjugated secondary antibody (1:2000). Blots were developed with ECL-plus reagent and data were labelled as follows: black arrow = dimer/higher aggregates, and white arrow = monomer bands.

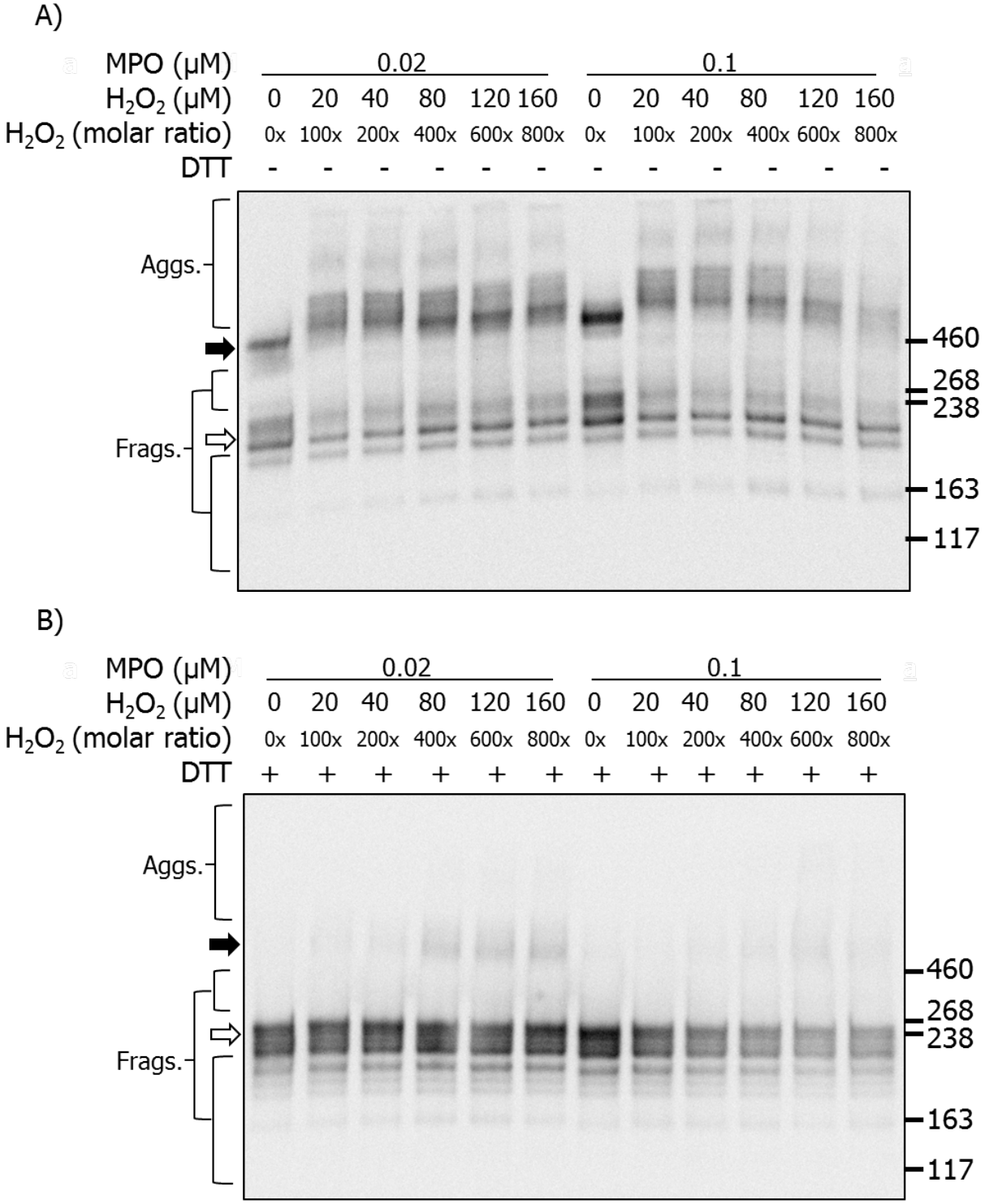

Figure 5.4: **Western blotting of structural changes to human plasma FN treated with MPO/Cl^-/H_2O_2.** Samples were electrophoresed on SDS-PAGE under **A)** non-reducing or **B)** reducing conditions and transferred onto PVDF membranes and probed with mouse monoclonal anti-FN HBF antibody (A32; 1:2000), followed by anti-mouse HRP-conjugated secondary antibody (1:2000). Blots were developed with ECL-plus reagent and data were labelled as follows: black arrow = dimer/higher aggregates, and white arrow = monomer bands.

5.3.3 Effects of myeloperoxidase, chloride, and hydrogen peroxide on human plasma fibronectin cell adhesion

Modifications on human plasma FN with MPO-derived HOCl also led to biological dysfunction leading to decreased cell adhesion. Surface-bound human plasma FN (0.02 μM) was left untreated (control) or treated with MPO enzyme, Cl^- and increasing concentration of H_2O_2, followed by two washes with sterile PBS to remove excess MPO enzyme and H_2O_2. This prevents any direct interaction of the oxidant system with HCAEC. HCAEC were pre-incubated with Calcein-AM live cell stain, prior to seeding 12,500 cells into each well. HCAEC were to adhere for 1.5 hr at 37°C in a humidified atmosphere containing 5% CO_2. Calcein-AM becomes fluorescent after hydrolysis by intracellular esterases and is used as a live cell assay. Fluorescence was measured at λ_{ex} 492nm, and λ_{em} 517nm to determine the number of adherent cells.

Exposure of human plasma FN to 0.02 μM MPO, 100 mM of Cl^- and increasing concentrations of H_2O_2 resulted in a dose-dependent decrease in HCAEC adhesion (Figure 5.5). A statistically significant loss of cell adherence was detected at 1600x molar excess of H_2O_2 with approximately 30% loss in cell numbers when compared to untreated control samples (0x H_2O_2 molar excess) (Figure 5.5).

Having established that HCAEC adherence to FN are affected when incubated with an enzymatic MPO system, further investigations were conducted to examine cell metabolic activity under the same conditions.

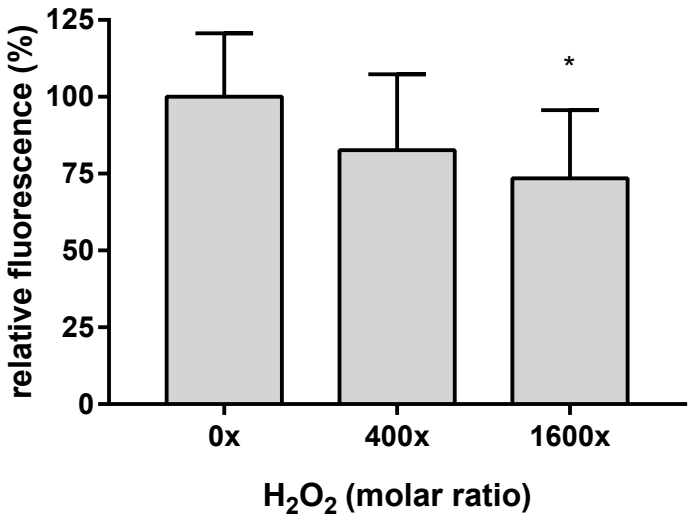

Figure 5.5: **Calcein-AM fluorescence of HCAEC incubated on human plasma FN treated with MPO/Cl^-/H_2O_2.** Surface-bound human plasma FN (0.02 μM) was left untreated (0x H_2O_2) or treated with MPO/Cl^- and increasing concentration of H_2O_2 (0, 8, 32 μM) and incubated for 2 hr at 37°C before incubation with HCAEC pre-stained with Calcein-AM and subsequent detection of fluorescence. The data are presented as a percentage relative to control (no oxidant 0 μM treatment). Error bars are ± SD from three technical replicates obtained from each of three independent experiments. Statistical analysis was performed using one-way ANOVA with Tukey's multiple comparison post hoc tests to determine significance. Statistical significance is identified as follow: * = $p < 0.05$.

5.3.4 Effects of myeloperoxidase, chloride, and hydrogen peroxide on human plasma fibronectin on cell metabolic activity

It has been shown that human plasma FN exposed to MPO enzyme and H_2O_2 leads to a reduction in HCAEC adhesion (Figure 5.5). Certain HCAEC may retain their adhesive ability but unable to proliferate. By measuring HCAEC metabolic activity, it is possible to examine whether modified FN further impairs HCAEC functions leading to a reduction in growth rate of HCAEC. FN was exposed to MPO, Cl^-, and increasing concentrations of H_2O_2 (0, 8, 32 μM). Excess treatment was washed off with sterile PBS to prevent interaction of the oxidant system directly with HCAEC. HCAEC were seeded at 12,500 cells per well and left to adhere for 1.5 hr at 37°C in a humidified atmosphere containing 5% CO_2, before being washed with sterile PBS to remove any unadhered HCAEC. Growth media was added back to each samples and these were left to recover for a further 48 hr period, prior to addition of MTS reagent, and quantification of absorbance at 490 nm

after a 3 hr incubation.

HCAEC that were incubated on human plasma FN treated with MPO/Cl^-/H_2O_2 resulted in a decrease in cell metabolic activity with significance detected at 400x and 1600x molar excess of H_2O_2 compared to no treatment (0x molar ratio) control (Figure 5.6). A greater loss of cell metabolic activity was not observed at higher concentrations of H_2O_2 (Figure 5.6).

Treatment of FN with MPO/Cl^-/H_2O_2 resulted in structural modifications including a loss of antibody recognition to functional epitopes. This loss of functional epitopes was found to be reflected in a decrease in HCAEC adhesion and metabolic activity. Further investigations were therefore conducted with the SCN^- system to determine whether similar modifications and changes would be detected as seen with the MPO/Cl^-/H_2O_2 systems.

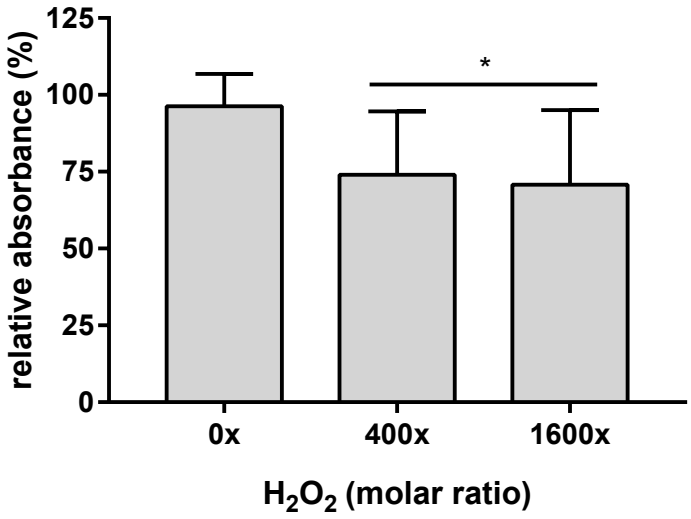

Figure 5.6: **MTS assay of HCAEC metabolic activity on human plasma FN treated with MPO/Cl^-/H_2O_2.** Surface-bound human plasma FN (0.02 μM) was treated with MPO/Cl^- and increasing concentrations of H_2O_2 (0, 8, 32 μM), which was incubated for 2 hr at 37°C. Plates were washed prior to addition of growth media and HCAEC were left to recover over 48 hr. MTS reagent was added into each well and absorbance was measured at 490 nm after 3 hr. The data are presented as a percentage relative to control (0x H_2O_2). Error bars are ± SD from three technical replicates obtained from each of three independent experiments. Statistical analysis was performed using one-way ANOVA with Tukey's multiple comparison post hoc tests to determine significance. Statistical significance is identified as follows: * = $p < 0.05$.

5.3.5 Effects of myeloperoxidase, thiocyanate, and hydrogen peroxide on human plasma fibronectin epitopes detected by ELISA

To further elucidate the effects that oxidants have on FN, an MPO enzymatic system was used to generate HOSCN, using MPO, a low and a high concentration of SCN^-, and increasing concentrations of H_2O_2 (0, 4, 8, 16, 24, 32 μM). ELISA experiments were carried out following Section 3.3.1 and Section 5.3.1, with either 20 μM or 500 μM of SCN^-. Samples were then probed for functional CBF, and HBF epitopes, which are important in cellular functions, matrix assembly, and vascular integrity.

Human plasma FN exposed to 0.02 μM of MPO with 20 μM of SCN^-, and 1600x molar excess of H_2O_2 showed no changes to the CBF epitope (Figure 5.7A). When SCN^- was increased to 500 μM and exposed to increasing concentrations of H_2O_2, it was shown that at 400x molar excess of H_2O_2 there was a statistically significant increase in epitope recognition which remained with increasing H_2O_2 concentrations (Figure 5.7B). Examination of the FN HBF epitope at 20 μM of SCN^- with increasing concentrations of H_2O_2, showed no modifications to this functional epitope (Figure 5.7C). At 500 μM of SCN^-, with increasing molar excess of H_2O_2, it was shown that there was an increased recognition of HBF epitope at 400x molar excess of H_2O_2 (Figure 5.7D). Increasing the H_2O_2 concentration to 800x molar excess showed a statistically significant loss of recognition to the HBF epitope which remained constant up to 1600x molar ratio (Figure 5.7D).

Further investigations were then made to examine possible structural changes to these functional epitopes using SDS-PAGE, silver staining and Western blotting.

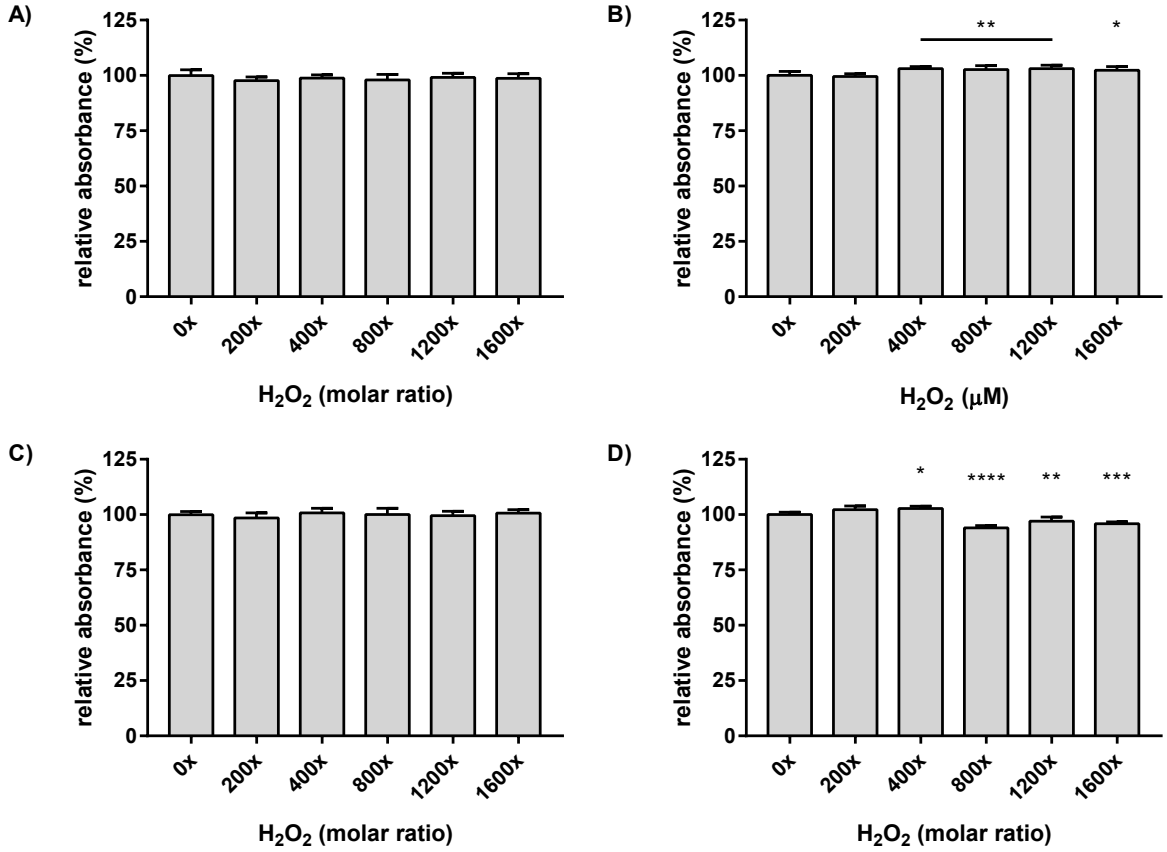

Figure 5.7: **ELISA of human plasma FN modified using enzymatic treatment with MPO/SCN^-/H_2O_2.** Each well was coated with human plasma FN (0.02 μM in 0.1 M pH 7.4 phosphate buffer) and was either left untreated (control) or treated with 0.02 μM of MPO, **A, C)** 20 μM or **B, D)** 500 μM of SCN^-, with increasing concentrations of H_2O_2 (0, 4, 8, 16, 24, 32 μM) and incubated for 2 hr at 37°C. FN epitopes were detected using mouse monoclonal **A-B)** anti-FN CBF antibody (A17; 1:10000), **C-D)** anti-FN HBF antibody (A32; 1:1000), and AP conjugated secondary antibody (1:1000). The data are presented as a percentage relative to control (0x H_2O_2 control). Error bars are ± SD from three technical replicates obtained from each of three independent experiments. Statistical analysis was performed using one-way ANOVA with Tukey's multiple comparison post hoc tests to determine significance. Statistical significance was identified as follows: * = $p < 0.05$, ** = $p < 0.01$, *** = $p < 0.001$, and **** = $p < 0.0001$.

5.3.6 Effects of myeloperoxidase, thiocyanate, and hydrogen peroxide on the structure of human plasma fibronectin

SDS-PAGE protein separation was performed to further investigate the changes that MPO-derived HOSCN has on the structure of FN. Human plasma FN (0.02 μM) was incubated with 0.02 μM of MPO, either 20 μM or 500 μM of SCN^-, and increasing concentrations of H_2O_2. Samples were separated on SDS-PAGE under non-reducing or reducing conditions followed by silver staining following the methodology described in Section 3.3.2.

Exposure of FN to 0.02 μM of MPO, 20 μM of SCN^-, and increasing concentrations of H_2O_2 resulted in changes to the protein structure (Figure 5.8). At 200x molar excess of H_2O_2, there were species of altered structures detected below the dimer band (black arrow) (Figure 5.8A). Higher mass aggregates or another altered species (> 460 kDa) was detected above the dimer parent bands (black arrow) and a fragment band was detected at around 130 kDa (Figure 5.8A). These structural changes became more marked with increasing concentrations of H_2O_2. In the presence of 500 μM of SCN^-, these species of altered structure of FN was observed with a smearing of protein bands below the dimer bands (black arrow) (Figure 5.8A). Increasing intensity of higher mass protein aggregates or altered species were also formed when treated with 500 μM of SCN^-, and were detected above the dimer bands (black arrow) as well as at the top of the gels in each wells at 200-800x molar excess of H_2O_2 (Figure 5.8A).

Under reducing conditions, exposure of human plasma FN to 20 μM of SCN^- and increasing concentration of H_2O_2 did not result in fragments and aggregates that were previously noted under non-reducing conditions (Figure 5.8B). At 400x molar excess of H_2O_2, it was observed that there were dimer/higher aggregates present (black arrow) (Figure 5.8B). In the system with 500 μM SCN^- and 400x molar excess of H_2O_2, there was an increasing presence of dimers/higher aggregates (black arrow) compared to the 20

μM of SCN^- condition (Figure 5.8A). At higher concentrations of H_2O_2, a greater intensity of aggregates or altered species were detected above the dimer band (black arrow) and at the top of each well (Figure 5.8B).

SDS-PAGE gels were transferred onto PVDF membranes to be probed for FN CBF and HBF functional epitopes, to further elucidate the effects of MPO/SCN^-/H_2O_2 on the FN structure. Examining the changes to FN CBF under non-reducing conditions showed similar structural changes to these seen with silver staining (Figure 5.9A). Treatments with 20 μM of SCN^-, and starting at 200x molar excess of H_2O_2 resulted in loss of antibody recognition to both the parent dimer (black arrow) and the parent monomer band (white arrow) with a dose-dependent manner with H_2O_2 concentrations (Figure 5.9A). Exposure with 20 μM of SCN^- resulted in fragments possessing the CBF site below the parent dimer bands (black arrow), and above and below the parent monomer bands (Figure 5.9A).

Increasing the SCN^- concentration to 500 μM, showed loss of recognition to the parent dimer (black arrow) and the parent monomer bands (white arrow) (Figure 5.9A), but to a lesser extent compared to 20 μM of SCN^- (Figure 5.9A). Fragmentation of FN was also observed, but more smearing (as opposed to defined bands) was detected with 500 μM of SCN^- compared to 20 μM of SCN^- (Figure 5.9A). Under reducing conditions, a minor loss of antibody recognition to the CBF was detected with both concentrations of SCN^- for the parent monomer band (white arrow) (Figure 5.9B). Fragmentation was not observed, but a decreased recognition of both dimers around 460 kDa and higher mass aggregates (black arrow and above) were detected with increasing H_2O_2 concentrations (Figure 5.9B).

Probing for the FN HBF gave similar results to those seen for the FN CBF. Under non-reducing conditions, with both 20 μM and 500 μM of SCN^-, it was found that there was a dose dependent loss of recognition to both the parent dimer (black arrow) and the parent monomer bands (white arrow) at 200-800x molar excess of H_2O_2 (Figure 5.10A). Starting at 200x molar excess of H_2O_2 for both concentration of SCN^-, species of altered

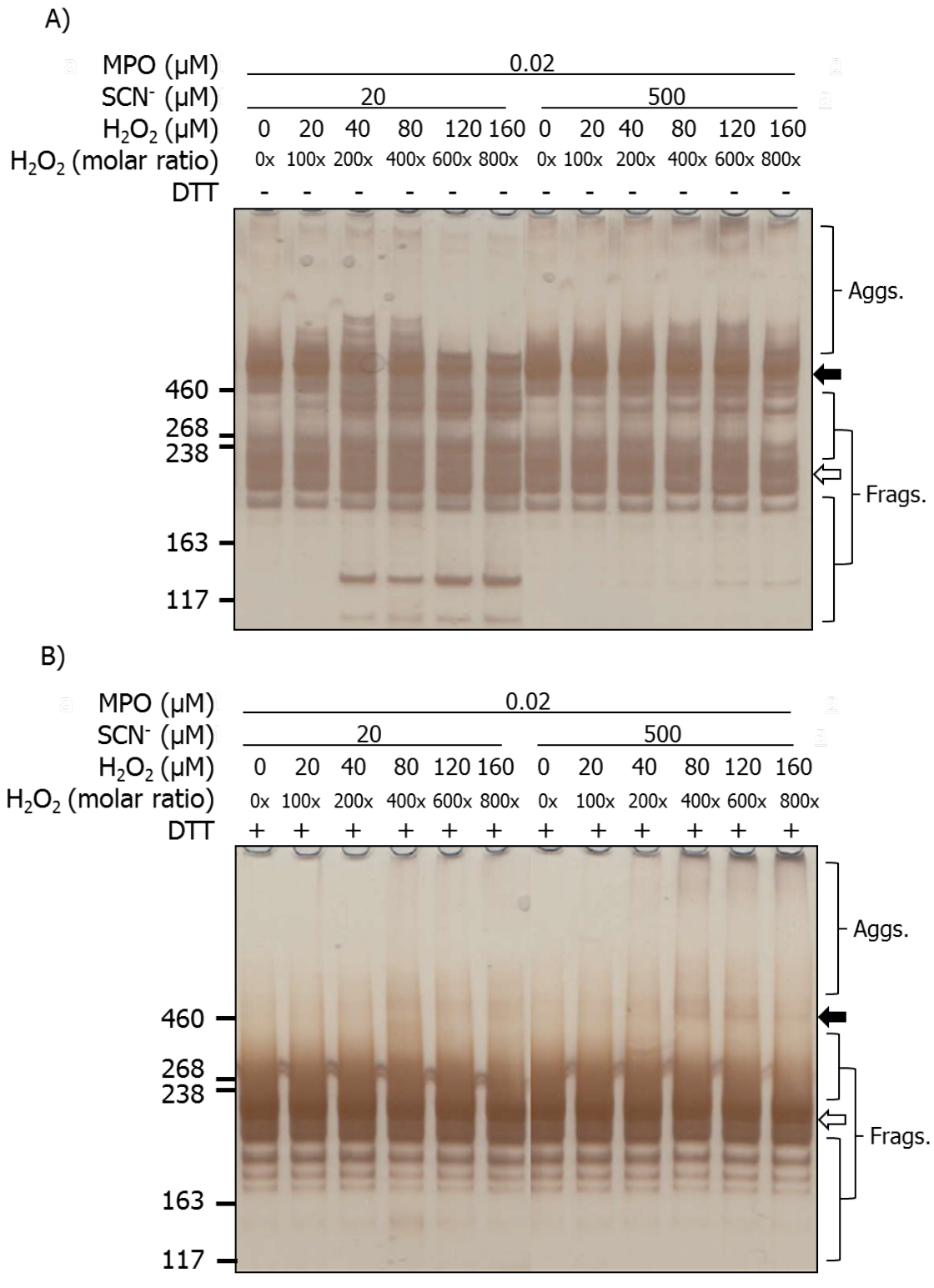

Figure 5.8: **Silver staining showing structural changes to human plasma FN treated with MPO/SCN$^-$/H_2O_2.** Purified human plasma FN (0.2 μM in 0.1 M phosphate buffer) was either left untreated (0x H_2O_2) or treated with MPO/SCN$^-$ and increasing concentrations of H_2O_2 (0, 20, 40, 80, 120, 160 μM), and incubated for 2 hr at 37°C. Samples were separated using 3-8% Tris-acetate SDS-PAGE gels under **A)** non-reducing or **B)** reducing conditions. Gels were then fixed, and visualised with silver staining and referenced against HiMark™ pre-stained High Molecular Mass standard. Data is labelled as follows: black arrow = dimer/higher aggregates, and white arrow = monomer band.

structures were observed under the parent dimer bands (black arrow) (Figure 5.10A); these bands were more notable with 20 μM of SCN^-. Samples electrophoresed under reducing conditions showed variable antibody recognition with increasing concentrations of H_2O_2; it appeared that at 20 μM of SCN^-, HBF epitope recognition increased with increasing concentrations of H_2O_2 (Figure 5.10B). At 500 μM of SCN^-, the intensity of the monomer band (white arrow) did not change with increasing concentrations of H_2O_2 (Figure 5.10B). Neither fragmentations nor crosslinks were observed for either low or high concentrations of SCN^- under reducing conditions (Figure 5.10B).

These data showed that the overall FN structure is modified by treatment with MPO/SCN^-/H_2O_2. This result was similarly reflected in the Western blots, though no distinguishable differences could be determined. Cellular function was further investigated to determine whether HCAEC incubated on MPO/SCN^-/H_2O_2 treated FN would modulate HCAEC adhesion and metabolic activity.

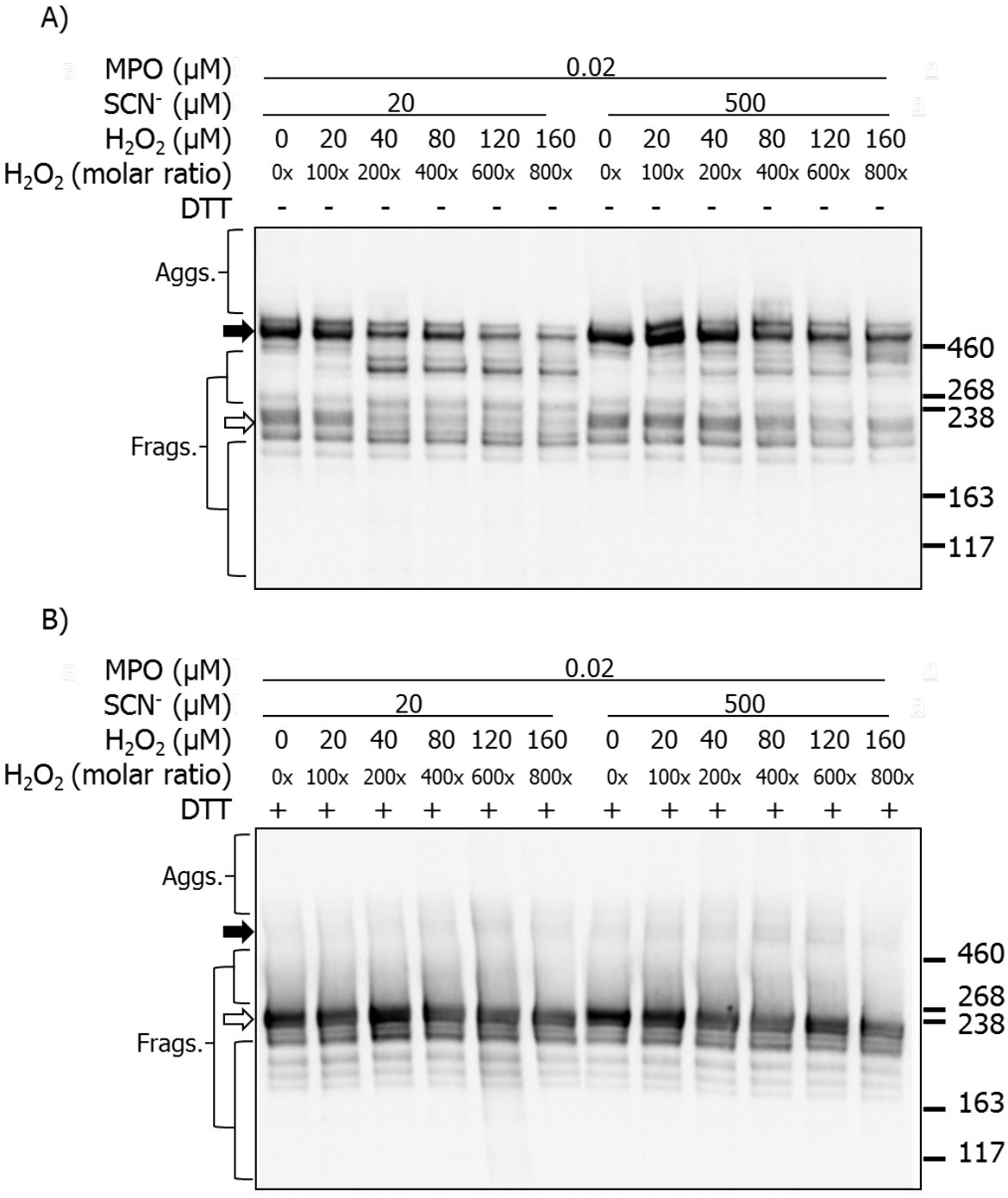

Figure 5.9: **Western blotting of structural changes to human plasma FN treated with MPO/SCN^-/H_2O_2.** Human plasma FN was separated using SDS-PAGE under **A)** non-reducing or **B)** reducing conditions and transferred onto PVDF membranes and probed with mouse monoclonal anti-FN CBF antibody (A17; 1:10000), followed by HRP conjugated anti-mouse HRP secondary antibody (1:2000). Blots were developed with ECL-plus reagent and data is labelled as follows: black arrow = dimer/higher aggregates, and white arrow = monomer band.

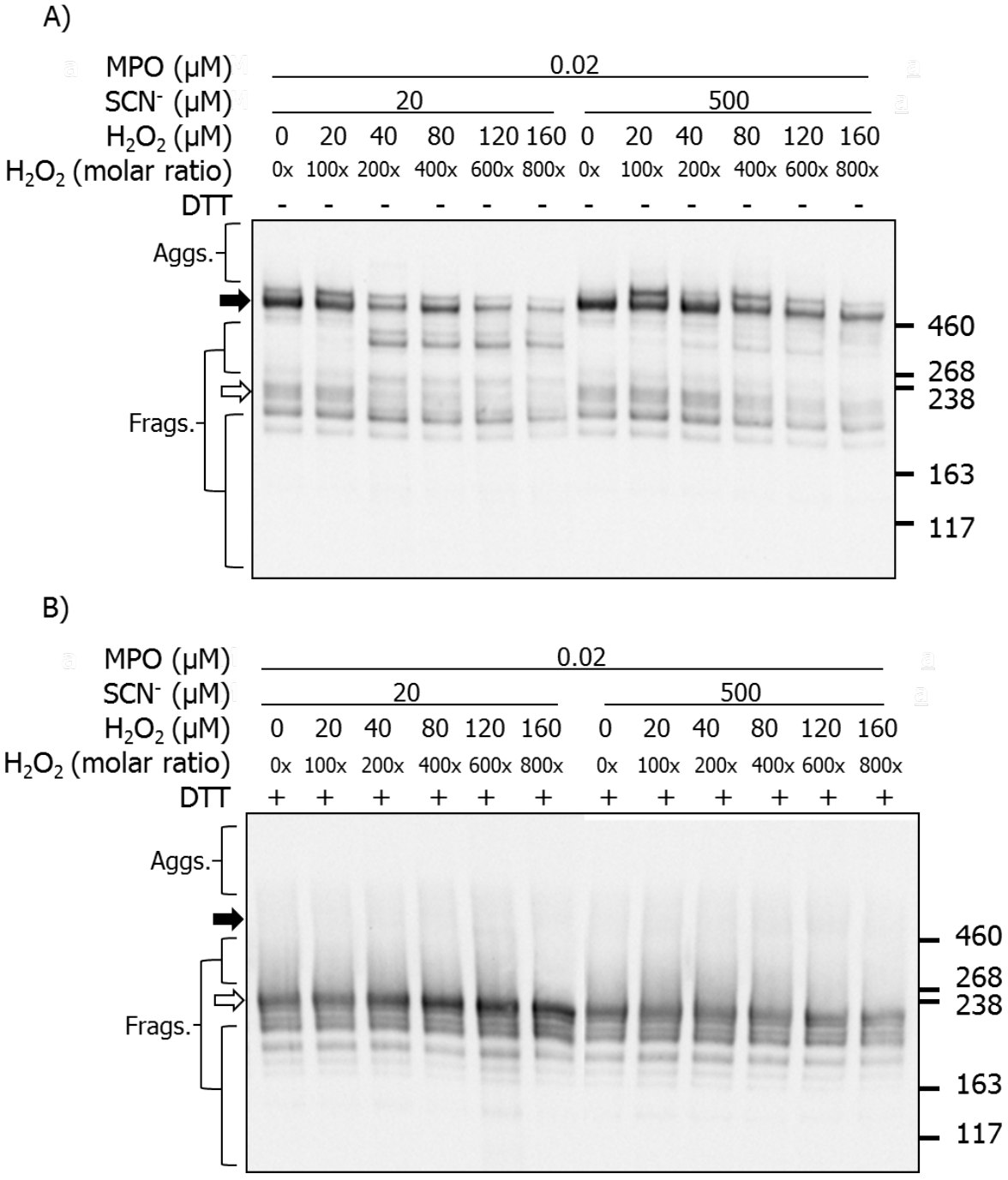

Figure 5.10: **Western blotting of structural changes to human plasma FN treated with MPO/SCN$^-$/H_2O_2.** Human plasma FN was separated using SDS-PAGE under **A)** non-reducing or **B)** reducing conditions and transferred onto PVDF membranes and probed with mouse monoclonal anti-FN HBF antibody (A32; 1:2000), followed by HRP conjugated anti-mouse HRP secondary antibody (1:2000). Blots were developed with ECL-plus reagent and data is labelled as follows: black arrow = dimer/higher aggregates, and white arrow = monomer band.

5.3.7 Effects of myeloperoxidase, thiocyanate, and hydrogen peroxide on human plasma fibronectin on cell adhesion

As reported in the previous Sections, HOSCN generated by the MPO system can modify FN structure. It was therefore important to identify whether modifications to FN CBF and HBF epitopes would affect HCAEC functions. Surface-bound FN (0.02 μM) was incubated with MPO, SCN^-, and increasing concentrations of H_2O_2 (0, 8, 32 μM), as described in Section 5.3.3. After treatment, the wells were washed with sterile PBS to remove any excess oxidant and prevent direct interaction with HCAEC. HCAEC were pre-stained with Calcein-AM live cell stain prior to seeding into each sample well at a density of 12,500 cells per well, and left to adhere for 1.5 hr at 37°C in a humidified atmosphere containing 5% CO_2. Fluorescence was subsequently measured using λ_{ex} 492nm and λ_{em} 517nm to quantify the number of cells adhered to the control and modified FN.

Human plasma FN treated with 20 μM of SCN^-, and either 400x or 800x molar excess of H_2O_2 showed no statistically significant changes in HCAEC adhesion when compared to the no oxidant (0x H_2O_2) treatment control (Figure 5.11A). Experiments using 500 μM SCN^-, and either 400x or 800x molar excess of H_2O_2 also showed no statistically significant changes in cell adhesion (Figure 5.11B). In light of this data, cell metabolic activity was further investigated to complement these findings.

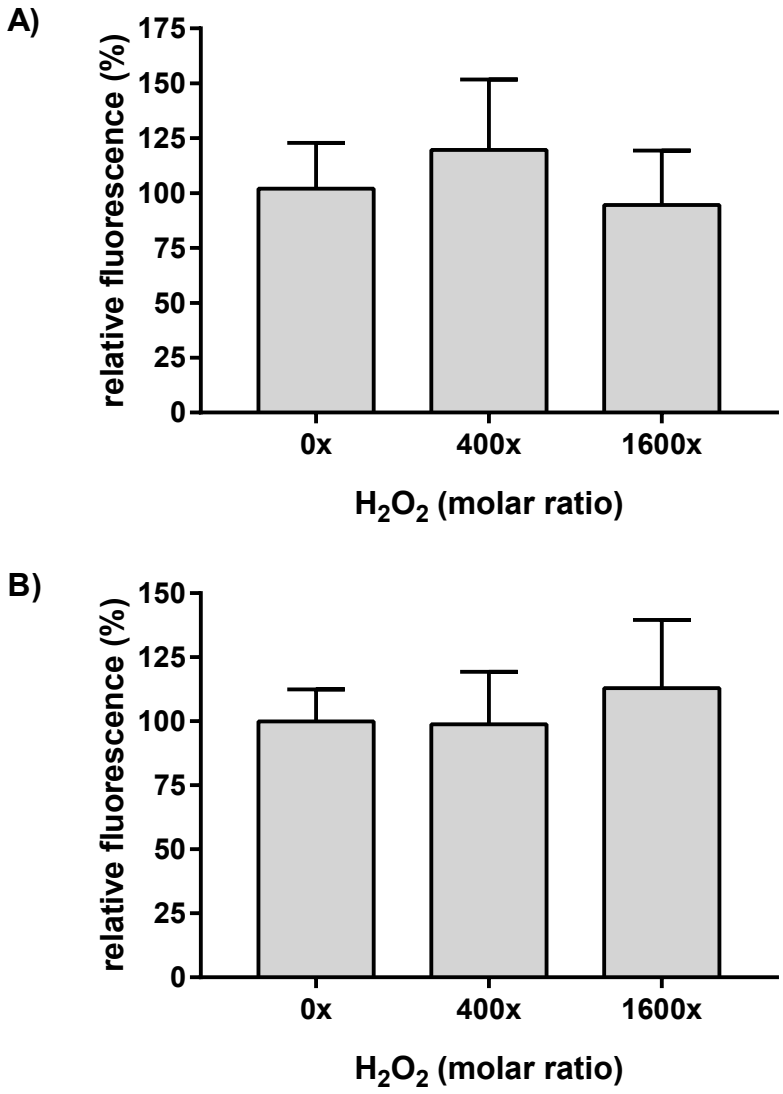

Figure 5.11: **Calcein-AM fluorescence was employed to determine the extent of HCAEC adhesion to control human plasma FN, or FN exposed to MPO/SCN^-/H_2O_2.** Surface-bound human plasma FN (0.02 μM) was treated with 0.02 μM of MPO, **A)** 20 μM or **B)** 500 μM of SCN^-, and increasing concentrations of H_2O_2 (0, 8, 32 μM), which was incubated for 2 hr at 37°C. HCAEC were pre-stained with Calcein-AM and fluorescence was subsequently quantified. The data are presented as a percentage relative to control (0x H_2O_2 treatment). Error bars are ± SD from three technical replicates obtained from each of three independent experiments. Statistical analysis was performed using one-way ANOVA with Tukey's multiple comparison post hoc tests to determine significance. No statistical significance was observed.

5.3.8 Effects of myeloperoxidase, thiocyanate, and hydrogen peroxide on human plasma fibronectin on cell metabolic activity

HCAEC may adhere to modified FN but nay not retain healthy metabolic activity levels. To test this hypothesis, surface-bound FN was left untreated or was exposed to 0.02 μM of MPO, 20 μM or 500 μM of SCN^-, and increasing concentrations of H_2O_2 (0, 8, 32 μM) for 2 hr at 37°C. The treatment was washed off with sterile PBS to prevent direct interactions with HCAEC, followed by seeding 12,500 cells into each well, which were left to adhere for 1.5 hr at 37°C in a humidified atmosphere containing 5% CO_2. Fresh endothelial growth media was added back to each sample well, and HCAEC were allowed to recover over a 48 hr period prior to quantification of MTS absorbance at 490 nm after a 3 hr incubation.

Treatment with 20 μM of SCN^-, and both 400x and 800x molar excess of H_2O_2 showed no statistically significant changes to cell metabolic activity compared to untreated (0x H_2O_2) controls (Figure 5.12A). Treatment with 500 μM of SCN^-, and either 400x or 800x molar excess of H_2O_2 also showed no statistical significance in HCAEC metabolic activity compared to controls (Figure 5.12B).

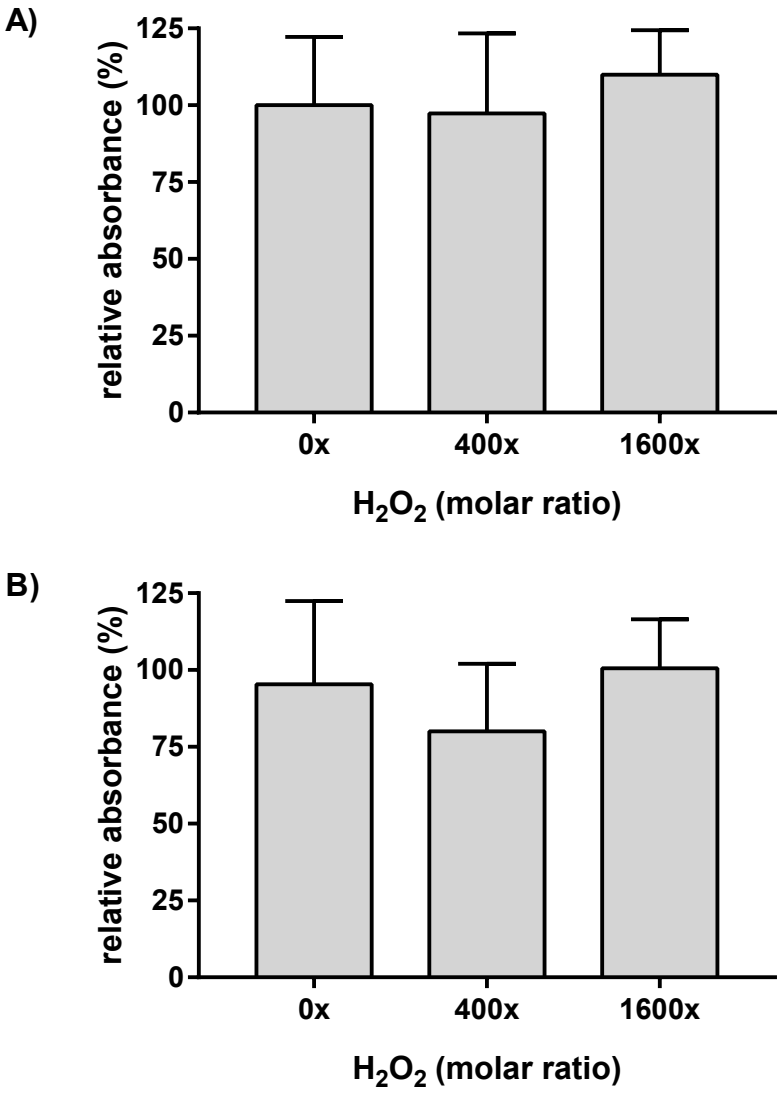

Figure 5.12: **MTS assay for cell metabolic activity of HCAEC incubated on native human plasma FN, or FN treated with MPO/SCN^-/H_2O_2.** Surface-bound human plasma FN (0.02 μM) was treated with 0.02 μM of MPO, **A)** 20 μM or **B)** 500 μM of SCN^-, and increasing concentrations of H_2O_2 (0, 8, 32 μM), which was incubated for 2 hr at 37°C. MTS reagent was added to each sample, and absorbance was measured after a 3 hr incubation. The data are presented as a percentage relative to control (0x H_2O_2). Error bars are ± SD from three technical replicates obtained from each of three independent experiments. Statistical analysis was performed using one-way ANOVA with Tukey's multiple comparison post hoc tests to determine significance. No statistical significance was observed.

5.4 Discussion

MPO released into the ECM milieu has been known to interact with certain proteins and proceeds to generate reactive oxidant, which can be damaging to the surrounding ECM proteins. This chapter aims to elucidate the interaction between MPO and FN, and simulate the *in vivo* enzymatic reaction (MPO system) to examine the modifications on human plasma FN.

High levels of plasma MPO has previously been associated with prevalence of CAD [11, 396], and found to to bind to the sub-endothelial matrix [21, 22, 395]. MPO can be released into the matrix from leukocytes present in the sub-endothelium, but has also been found to transcytose through EC from plasma [21, 270, 397]. MPO, as a highly cationic enzyme, interacts strongly with negatively charged GAGs via electrostatic interactions [270]. Moreover, MPO has previously been found to co-localise with sub-endothelial FN, which has been suggested to potentiate MPO activity [21, 22]. This localisation of MPO to vascular ECM proteins has been linked to increased modifications induced by reactive species produced by MPO including radicals, chlorinating and nitrating species [21, 22, 395]. Early studies have linked the transcytosis of MPO into the sub-endothelium with increased levels of nitration on ECM proteins, as indicated by the presence of NO_2-Tyr formation in wild type mice models (vs $MPO^{-/-}$) and human atherosclerotic lesions [21, 395]. Moreover, co-localisation of MPO- and HOCl-modified proteins with macrophages has been observed in lesions associated with intracoronary thrombi [398]. The co-localistion of MPO with sub-endothelial FN has been found to potentiate formation of di-Tyr [35, 399] and carbonyl compounds [260], damage to FN and subsequent biological dysfunction [22, 261]. Higher concentrations of FN were found to increase the extent of MPO binding, with binding of MPO to FN resulting in a reduction in MPO mobility on gel electrophoresis [270]. The reported close proximity of MPO and FN suggests that oxidative species produced by MPO are likely targeting FN at specific sequences, however there are limited studies investigating the binding relationship between MPO and FN.

Analysis of the effects of MPO/Cl^-/H_2O_2 human plasma FN using SDS-PAGE and silver staining have shown that formation of aggregates occurs with low (100x molar ratio) concentrations of H_2O_2 (Figure 5.2). Aggregates were observed under both reducing and non-reducing conditions with higher levels detected in the latter case, consistent with the formation of both reducible and non-reducible crosslinks. This pattern of aggregate formation is similar to that which was observed previously when FN was treated with reagent HOCl (Refer to Section 3). These aggregates are therefore likely to be formed as a result of the generation of HOCl by the MPO system, with this causing structural modifications on human plasma FN. MPO-derived HOCl is known to react with the sulfhydryl groups of Cys, leading to the generation of R-SOH, which can subsequently react with another free sulfhydryl group to form disulfide crosslinks [49, 289, 290]. This can either be within a single protein structure (intramolecular cross-links) or between different proteins (intermolecular cross-links); the latter may be the cause of (some of) observed reducible aggregates [49, 289, 290]. When samples were electrophoresed under reducing conditions, a considerable proportion of the dimers/aggregates were reduced to monomers but a certain amount of aggregates were found to be non-reducible (Figure 5.2). These aggregates may arise from the generation of intermolecular di-Tyr or di-Trp linkages, which contain stronger (non-reducible) intermolecular covalent bonds [53, 54]. As previously discussed in Section 3, di-Tyr crosslinks result from the dimerisation of two Tyr phenoxyl radicals [64, 291]. These di-Tyr have been shown to form in FN on treatment with an MPO system, and at greater quantities compared to treatment with reagent HOCl [260]. Moreover, di-Trp may result from similar reactions of two Trp indolyl radicals [316].

Fragmentation of FN was found to be similar when treated using the MPO/Cl^-/H_2O_2 system (Figure 5.2) and with reagent HOCl (Figure 3.2). Fragments were more notable at higher concentrations of reagent HOCl, and it is probably that increased concentrations of H_2O_2 would also result in greater fragmentations. Protein fragmentation can arise as a result of both carbonyl and chloramine/chloramide formation [260, 310]. Nitrogen-

centred radicals are formed by decomposition of chloramines and chloramides, which are known mediators of protein fragmentation as is the hydrolysis of the backbone carbonyl [307, 311] (c.f. discussion on structural modifications induced by HOCl in Section 3.4).

An interesting structural modification of FN that was observed upon treatment with the MPO/Cl^-/H_2O_2 system was the apparent shift in the molecular mass of FN (Figure 5.2). This was observed only after addition of H_2O_2 (i.e. not a result of binding of MPO to FN above), thus it may arise from the interaction of MPO-oxidant and FN, in combination with a structural change caused by MPO-derived HOCl [22]. MPO-derived HOCl is known to oxidise certain side chains causing an unfolding of FN protein, which may result in greater access for MPO or its oxidants to certain sequences on FN, thus increasing the molecular mass of FN [270, 271]. The shift in molecular mass may also be due to binding of FN fragments through disulfide bonds or di-Tyr/di-Trp formations, or increased binding of SDS to the protein as a result of the charge alteration or protein unfolding [400–402]. Further investigation is needed to define the exact mechanism of this molecular mass shift.

HOSCN is assumed to be the major oxidative species generated by the MPO system when SCN^- is substituted for Cl^-. Treatment of human plasma FN with MPO/SCN^- and increasing amounts of H_2O_2 (Figure 5.8) resulted in structural modifications that reflect those observed when FN was treated with LPO-derived reagent HOSCN (see Figure 4.2 and Section 4). As discussed in Section 4.4, HOSCN has a marked specificity for thiol residues, thus aggregates are likely formed from thiol oxidation leading to formation of new disulfides [94, 104–107] or as a result of oxidant catalysed thiol-disulfide exchange [105, 107, 375, 376]. The observed alterations in FN mass on the gels could be a result of conformational changes or protein fragmentation although there are limited studies investigating HOSCN-induced mechanisms of protein fragmentation [102, 103].

These structural modifications may explain the epitope changes on FN protein observed when the protein was treated with the MPO/H_2O_2 system using either Cl^- or SCN^-. If

MPO is binding to FN at a particular location, this may result in a localised damage, and identification of these sites could assist in identifying the sequence at which FN binding occurs. Previous studies have shown that treatment of FN with MPO/Cl^-/H_2O_2 system was associated with decreased adhesion of ECs, along with ECs retracting and rounding up [22, 261]. This was suggested to occur due to the inability of cells to bind to modified ECM via an F-actin mediated adhesion pathway [22]. Cell adhesion was similarly found to be impaired when FN was first treated with MPO/Cl^-/H_2O_2 system prior to the addition of HCAEC. Treatment of FN using this MPO system has been shown to cause a reduction in antibody recognition to the CBF, which is important in mediating cell binding (Figure 5.1), and this is consistent with the observed decrease in cell adhesion (Figure 5.5). Thus MPO appears to be converting H_2O_2 and Cl^- to HOCl, which subsequently modifies FN at the CBF epitope in a similar manner to what was found with reagent HOCl treatment (Figure 3.1, 3.8, and 3.10). Treatment of FN with MPO/SCN^-/H_2O_2 system also showed some limited modifications on the CBF epitope but this was much less than detected with LPO-derived reagent HOSCN and MPO-derived HOCl. Both LPO-derived and MPO-derived HOSCN were found to have little effects on FN HBF epitope (Figure 5.7). Consistent with these data, the results of experiments carried out to examine HCAEC cell adhesion and proliferation on MPO/SCN^-/H_2O_2-treated FN showed no significant changes.

The ability for HCAEC to proliferate was also decreased when incubated on FN treated with the MPO/Cl^-/H_2O_2 system, but not with the MPO/SCN^-/H_2O_2 system. FN has been found to be a promoter of cell proliferation with cells other than ECs [403–405], and this reduction is therefore likely to be due to modifications induced on FN by the oxidants. However, there is little data on the mechanism by which this may occur, but it may be contributed to by the role that FN plays in cell growth through cell shape modulation [406], and interaction with certain cell-surface integrins [259, 404].

In addition to the evidence for alterations to the CBF and HBF functional epitopes induced by MPO/Cl^-/H_2O_2 system, evidence has also been obtained for the formation

of a HOCl-generated epitope. This epitope was found to be present on HOCl-modified LDL, which this antibody (clone 2D10G9) was originally raised against [63, 407]. The presence of this epitope supports the conclusion that HOCl is being produced by this MPO/Cl^-/H_2O_2 system and is modifying FN. Other HOCl-induced modifications are also highly likely to be present in these samples (e.g. 3-chloroTyr and di-Tyr), thus it would be sensible to further investigate and quantify the formation of chlorinated species and crosslinks [50, 57].

This chapter has provided preliminary evidence to support that MPO, in the presence of Cl^- or SCN^- and H_2O_2, generates the oxidative species, HOCl and HOSCN, respectively, and that these oxidants modify FN. These enzymatic systems may simulate more closely to situations that is occurring *in vivo* than with the reagent oxidant, as there may be interactions between MPO enzyme and FN protein which could dictate the severity and location of modifications. The MPO/Cl^-/H_2O_2 system has been found to modify FN structure, causing alterations to the CBF and HBF epitopes, with subsequent formation of a HOCl-derived epitope. A loss of cellular adhesion and proliferation were found to occur with HCAEC when they were incubated on FN pre-treated with MPO/Cl^-/H_2O_2. Treating FN with MPO/SCN^-/H_2O_2 caused minor structural changes similar to those observed with HOSCN, but these effects were more limited and this system did not appear to target the CBF or HBF epitopes, causing no significant changes to cell adhesion or proliferation.

In light of these interesting findings, further investigations were conducted whereby Cl^- and SCN^- were present simultaneously in the reaction system, to determine whether there is competitive formation of the two oxidants, HOCl and HOSCN, and hence whether certain oxidative modifications preside over the other. The next Chapter therefore reports on investigations into the competition between Cl^- and SCN^- as the substrate for MPO, to further elucidate the effects of the MPO/Cl^-/SCN^-/H_2O_2 system on FN.

Chapter 6

Analysis of competitive oxidation of chloride and thiocyanate by myeloperoxidase

6.1 Introduction

As described in the earlier chapter of this thesis, MPO plays a key role in the generation of oxidants, such as HOCl and HOSCN, from physiological concentrations of halides (Cl^-) and pseudohalides (SCN^-) in the presence of H_2O_2 [50, 396]. Higher concentrations of SCN^- can divert MPO to produce more HOSCN, and mitigate HOCl-induced damage to proteins, cells, and other targets.

Past studies have reported that the presence of SCN^- have both a detrimental and protective effect when investigated in *in vitro* and *in vivo* experiments [50, 94]. It has been found that addition of SCN^- to MPO/Cl^-/H_2O_2 system attenuated HOCl-induced damage on LDL [371] and FN [22, 408]. Moreover, SCN^- has been found to protect against cellular injury mediated by MPO, reducing apoptosis in HL-60 cells [409]. The damaging effects versus the protective nature of SCN^- is an important aspect in the development of atherosclerosis, whereby smokers for example are usually found to have elevated plasma SCN^- levels [98, 99, 410]. This particular dichotomy will be explored more thoroughly.

6.2 Aim

The studies in this Chapter investigated the effects of adding increasing concentrations of SCN^- to MPO/Cl^-/H_2O_2 treatment of human plasma FN in order to determine whether this modulates the extent of damage to FN. Epitope recognition was examined using ELISA which probed for the FN CBF and HBF epitopes as well as a HOCl-generated epitope. Structural modifications were investigated using both silver staining and Western blotting for FN CBF and HBF epitopes.

6.3 Results

6.3.1 Effects of enzymatic treatment with myeloperoxidase, hydrogen peroxide, chloride, and increasing concentrations of thiocyanate on functional epitopes of human plasma fibronectin

SCN^- has a higher kinetic rate than Cl^- for reaction with Compound I of MPO with these reactions resulting in the formation of the hypohalous acids, HOSCN and HOCl, respectively [51]. Oxidation caused by HOSCN is highly specific to thiols but is also more readily reversible than the modifications caused by HOCl. The presence of SCN^- in samples causes the reaction to produce HOSCN over HOCl until either the SCN^- or H_2O_2 is depleted.

Surface-bound human plasma FN (0.02 μM) on 96-well plates were incubated with 0.02 μM of MPO, 100 mM of Cl^-, increasing concentrations of SCN^- from 0 μM to 500 μM, and 32 μM of H_2O_2 for 2 hr at 37°C. Sample were washed twice with PBS to remove any excess oxidants or enzymes prior to probing for the FN functional CBF, HBF epitopes, and a HOCl-generated epitope. An AP bound secondary antibody was used to detect the epitopes using pNPP solution as described in Section 5.3.1.

The CBF epitope plays an important role in cell binding, and when modified, can lead to cellular dysfunction and a decrease in cell adhesion (see Section 3). Human plasma FN (0.02 μM) treated with 0.02 μM of MPO, 100 mM of Cl^-, and 1600x molar excess of H_2O_2 reduced antibody recognition to FN CBF epitope (Figure 6.1A), replicating what was found previously (see Figure 5.1A). When 20 μM of SCN^- was added into samples prior to addition of H_2O_2, this led to a retrieval of epitope recognition of the FN CBF epitope back to almost the same level as control (Figure 6.1A). Furthermore, an increase in the concentration of SCN^- resulted in no further changes to the CBF epitope recognition (Figure 6.1A).

In further experiments, exposure of human plasma FN to 0.02 μM of MPO, 100 mM of Cl^-, and 1600x molar excess of H_2O_2, resulted in a statistically significant loss of HBF antibody recognition (Figure 6.1B), similar to what was observed previous (Figure 5.1B). With the addition of 20 μM of SCN^- to similar reaction systems, antibody recognition of the HBF site returned approximately to the same level as controls (Figure 6.1B). With further increases in SCN^- concentration, no increase or decrease of HBF epitope recognition was observed (Figure 6.1B).

The HOCl-generated epitope recognised by the antibody 2D10G9 was found to be present in samples treated with MPO, 100 mM of Cl^-, and 1600x molar excess of H_2O_2, at levels almost 18-fold higher than present in controls (Figure 6.1C); this is similar to what was observed previously (Figure 5.1C). With the addition of 20 μM of SCN^- to the treatment system, the HOCl-generated epitope was not detected, with the absorbance values decreased to control levels (Figure 6.1C). No further changes were seen with increased SCN^- concentrations in the samples. These studies also showed that HOSCN does not produce any epitope recognised by this antibody clone (Figure 6.1C). Furthermore, maximal inhibition was found to occur at 20 μM of SCN^- as reported for all epitopes examined.

These data together show that treatment of human plasma FN with MPO/Cl^-/H_2O_2 can lead to modifications that can be reversed with the addition of relatively modest concentrations of SCN^-. Further investigations were therefore conducted to examine structural changes to FN and the CBF and HBF epitopes using silver staining and Western blotting.

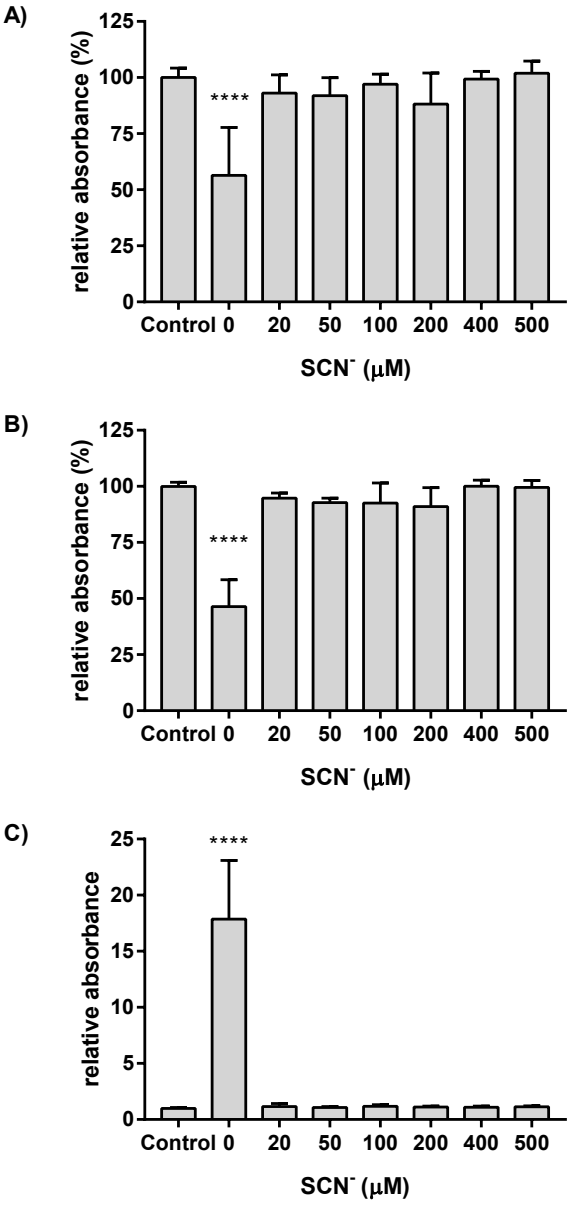

Figure 6.1: **ELISA of human plasma FN modified following enzymatic treatment with MPO/Cl^-/H_2O_2 and increasing concentrations of SCN^-.** Each well was coated with 0.25 μg FN (0.02 μM in 0.1 M phosphate buffer) was either left untreated (control) or treated with 0.02 μM MPO, 100 mM of Cl^-, increasing concentrations of SCN^- and 32 μM of H_2O_2. Samples were incubated for 2 hr at 37°C. FN epitopes were detected using a mouse monoclonal **A)** anti-FN CBF antibody (A17; 1:10000), **B)** anti-FN HBF antibody (A32; 1:1000), **C)** anti-HOCl generated epitope (2D10G9; 1:50), and conjugated with anti-mouse AP secondary antibody (1:1000). The data are presented as a percentage relative to control (no oxidant treatment). Error bars are ± SD from three technical replicates obtained from each of three independent experiments. Statistical analysis was performed using one-way ANOVA with Tukey's multiple comparison post hoc tests to determine significance. Statistical significance is identified as follows: **** = $p < 0.0001$.

6.3.2 Effects of enzymatic treatment with myeloperoxidase, hydrogen peroxide, chloride and increasing concentrations of thiocyanate on the structure of human plasma fibronectin

Having shown that SCN^- can retrieve epitope recognition for these particular functional sites and also decrease the presence of a HOCl-generated epitope, the effects of increasing SCN^- on the structural changes induced by HOCl on FN was examined. Purified human plasma FN (0.02 μM) was either left unoxidised (MPO only control) or treated with either 0.02 μM or 0.1 μM of MPO, 100 mM of Cl^-, with 160 μM of H_2O_2, and increasing concentrations of SCN^- from 0 to 500 μM. Samples were then separated on SDS-PAGE under non-reducing or reducing conditions prior to silver staining to examine possible structural changes.

Human plasma FN (0.02 μM) was treated with 0.02 μM of MPO, 100 mM of Cl^-, with 800x molar excess (160 μM) of H_2O_2 and in the absence of SCN^-, reflects the modifications previously found (Figure 5.2A). Under non-reducing conditions, FN parent monomer bands (white arrow) were found to have decreased in staining intensity when treated with MPO/Cl^-/H_2O_2 in the absence of SCN^- (Figure 6.2A). This treatment was also found to cause fragmentation of the protein with the formation of additional bands, particularly those below the monomer bands (white arrow) (Figure 6.2A). Aggregates or other higher molecular mass species were also detected. With the addition of 20 μM of SCN^-, there are less higher aggregate bands formed but more protein bands were found to be present with masses between 268-460 kDa (Figure 6.2A). Furthermore, fragments with a mass of approximately 190 kDa appeared to be more prominent with increasing concentrations of SCN^- (Figure 6.2A). At 400 and 500 μM of SCN^-, which is greater than the concentration of H_2O_2 added (160 μM), fewer protein bands between 268-460 kDa were observed (Figure 6.2A).

Treatment with 0.1 μM of MPO under non-reducing conditions, gave similar modifications

to those seen with the lower concentration of MPO, together with greater loss of the parent dimer (black arrow) and monomer bands (white arrow) (Figure 6.2A). At 100 and 400 μM of SCN^-, aggregates caused by the treatment can be seen as a smear of the protein bands and at the top of each well (Figure 6.2A). At 500 μM of SCN^-, the modifications detected were found to be similar to those generated by pre-formed HOSCN, particularly the bands that are found to form above and below both the parent dimer and monomer (Figure 4.2A).

FN samples treated with 0.02 μM of MPO, 100 mM of Cl^-, with 800x molar excess (160 μM) of H_2O_2 in the absence of SCN^- and electrophoresed under reducing conditions, resulted in fragmentation of FN with a band detected at approximately 180 kDa. This FN fragment was observed with concentrations of SCN^- between 0 to 100 μM (Figure 6.2B). However, when the concentration of SCN^- was in excess over the H_2O_2 concentration (i.e 400 to 500 μM of SCN^-), the fragment around 180 kDa was not detected (Figure 6.2B). At 400 μM of SCN^-, formation of dimers/higher aggregates were detected (black arrow) (Figure 6.2B).

Under reducing conditions, treatment with the 0.1 μM MPO system showed modifications to the monomer bands (white arrow), which were more extensive in the absence of or at low concentrations of SCN^-, and particularly at 20 to 50 μM of SCN^- (Figure 6.2B). At 100 μM of SCN^-, the modification seems to be minimised, and increasing SCN^- concentration to 400 μM (i.e greater than the concentration of H_2O_2) did not result in the fragment at around 180 kDa (Figure 6.2B). Furthermore, there was also an increased presence of dimers/larger aggregates caused by this treatment, which was observed at 400 μM and 500 μM SCN^- (Figure 6.2B).

To further elucidate the structural changes on FN, Western blotting for the FN CBF and HBF epitopes was utilised. Proteins separated by SDS-PAGE were transferred to PVDF membranes and were probed for either the CBF (clone A17) or HBF (close A32) of FN. Under non-reducing conditions, examination of the CBF epitope showed that incubation

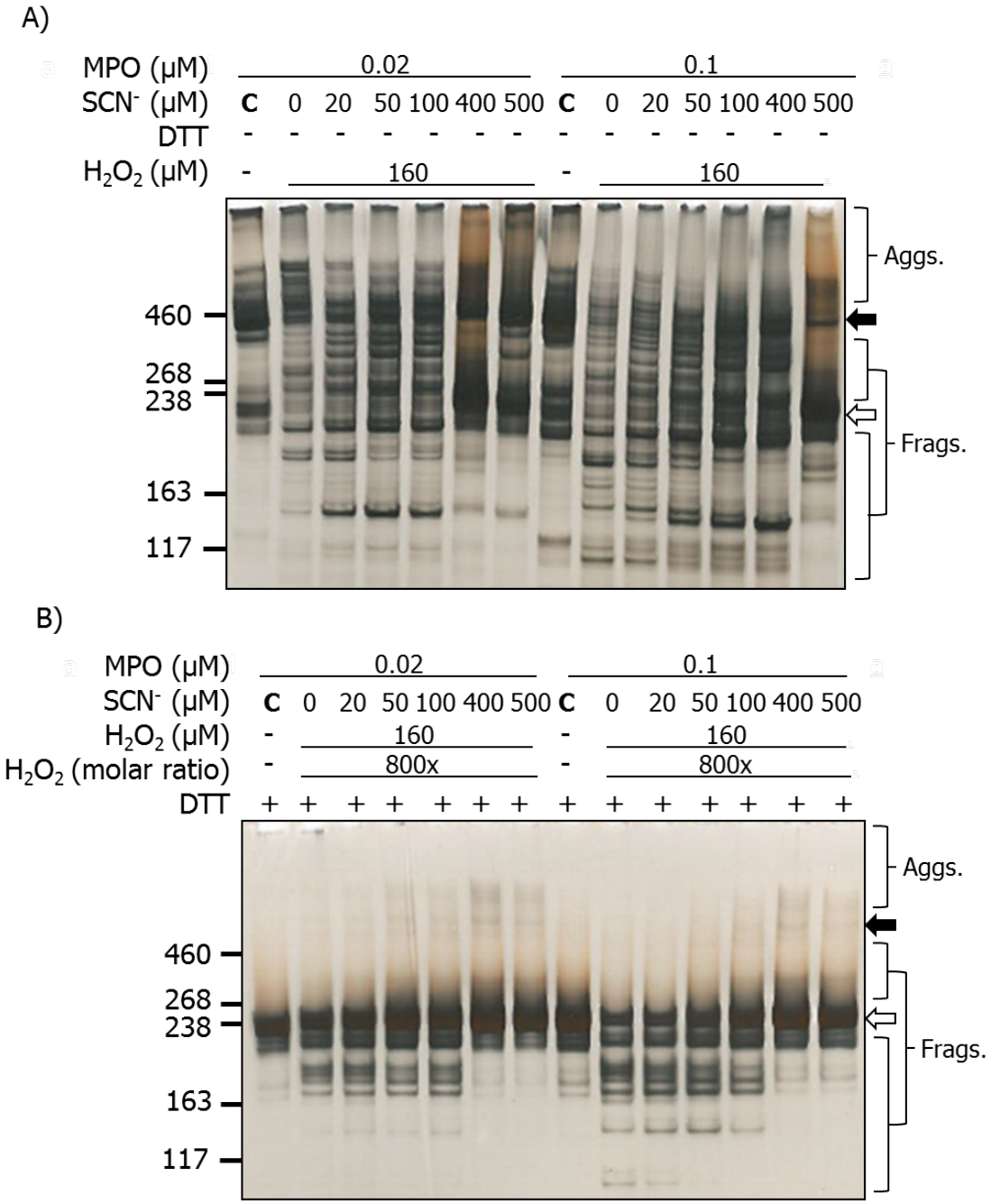

Figure 6.2: **Silver staining showing structural changes to human plasma FN treated with MPO/Cl^-/H_2O_2 and increasing concentrations of SCN^-.** Purified human plasma FN (0.2 μM in 0.1 M phosphate buffer) was either left untreated (MPO only control) or treated with MPO/Cl^-/H_2O_2 and increasing concentrations of SCN^- and incubated for 2 hr at 37°C. Samples were electrophoresed using 3-8% Tris-acetate SDS-PAGE gels under **A)** non-reducing or **B)** reducing conditions. Gels were then fixed, and visualised with silver stain and referenced against HiMark™ pre-stained High Molecular Mass standard. Data are labelled as follows: black arrow = dimer/higher aggregates, and white arrow = monomer bands.

of FN with only 0.02 μM of MPO (in the absence of SCN^- and H_2O_2) did not show any changes to the CBF epitope (Figure 6.3A). In the presence of 100 mM of Cl and 800x molar excess (160 μM) of H_2O_2 (absence of SCN^-) resulted in extensive aggregate and fragment formation (Figure 6.3A), which were similar to those observed in the previous Chapter (Figure 5.2A). Moreover, it can be seen that treatment with Cl^- and H_2O_2 caused a loss of antibody recognition of the monomer (white arrow) and dimer bands (black arrow) (Figure 6.3A). Addition of 20 μM of SCN^- resulted in several notable fragments, particularly those between the dimer (black arrow) and monomer bands (white arrow) (Figure 6.3A). Increasing the concentration of SCN^- led to a decrease in HOCl-induced modifications, and were found to produce fragments and aggregates similar to those seen with HOSCN (compared to figure 4.2 and 4.3) (Figure 6.3A). A notable modification was observed when FN was treated with only 0.1 μM of MPO (in the absence of SCN^- and H_2O_2), with additional bands detected above and below the monomer bands (white arrow); these were not detected with the lower concentration of MPO (Figure 6.3A).

Exposure of human plasma FN to only 0.1 μM of MPO caused a small increase in intensity of the fragment band below the monomer bands (white arrow) (Figure 6.3B). The addition of 0.02 μM of MPO and 800x molar excess (160 μM) of H_2O_2 to human plasma FN were found to cause non-reducible aggregates and fragments at approximately 170-180 kDa (Figure 6.3B). Low concentrations of SCN^- of 20-50 μM resulted in a decrease in aggregate formation (black arrow and above), and also decreased in intensity of the 170-180 kDa fragment band (Figure 6.3B). Higher concentrations of SCN^- (100 to 500 μM) resulted in the detection of lower intensity of aggregates compared to controls, but also prevented the formation of the HOCl-specific fragments observed at approximately 170-180 kDa (Figure 6.3B). With 0.1 μM of MPO, under the same treatment conditions, the addition of 800x molar excess (160 μM) of H_2O_2 led to a greater smearing of FN and greater intensity of fragments formed below the monomer bands (white arrow) at 170-180 kDa (Figure 6.3B). Moreover, it required > 100 μM of SCN^- before these aggregates and fragments were prevented from forming (Figure 6.3B).

Examination of blots that were probed for the HBF epitope of FN showed similar modifications under both non-reducing and reducing conditions (Figure 6.4). Fragments and aggregates occurred upon exposure to MPO, 100 mM of Cl^- and 800x molar excess (160 μM) of H_2O_2 (Figure 6.4). Addition of SCN^- was found to reverse the formation of certain aggregates or fragments, however at higher concentrations of SCN^-, the fragments or aggregates that were detected were similar to those observed with MPO-derived HOSCN (compare Figure 6.4 with 4.3).

Overall, these data indicate that there are interactions between MPO, H_2O_2, Cl^-, and SCN^-, which may determine the relative yields of HOCl and HOSCN formed by MPO have on the specific modifications that occur on FN. The following (discussion) section describes the nature of these interactions between the enzyme and its mixture of substrates in greater detail.

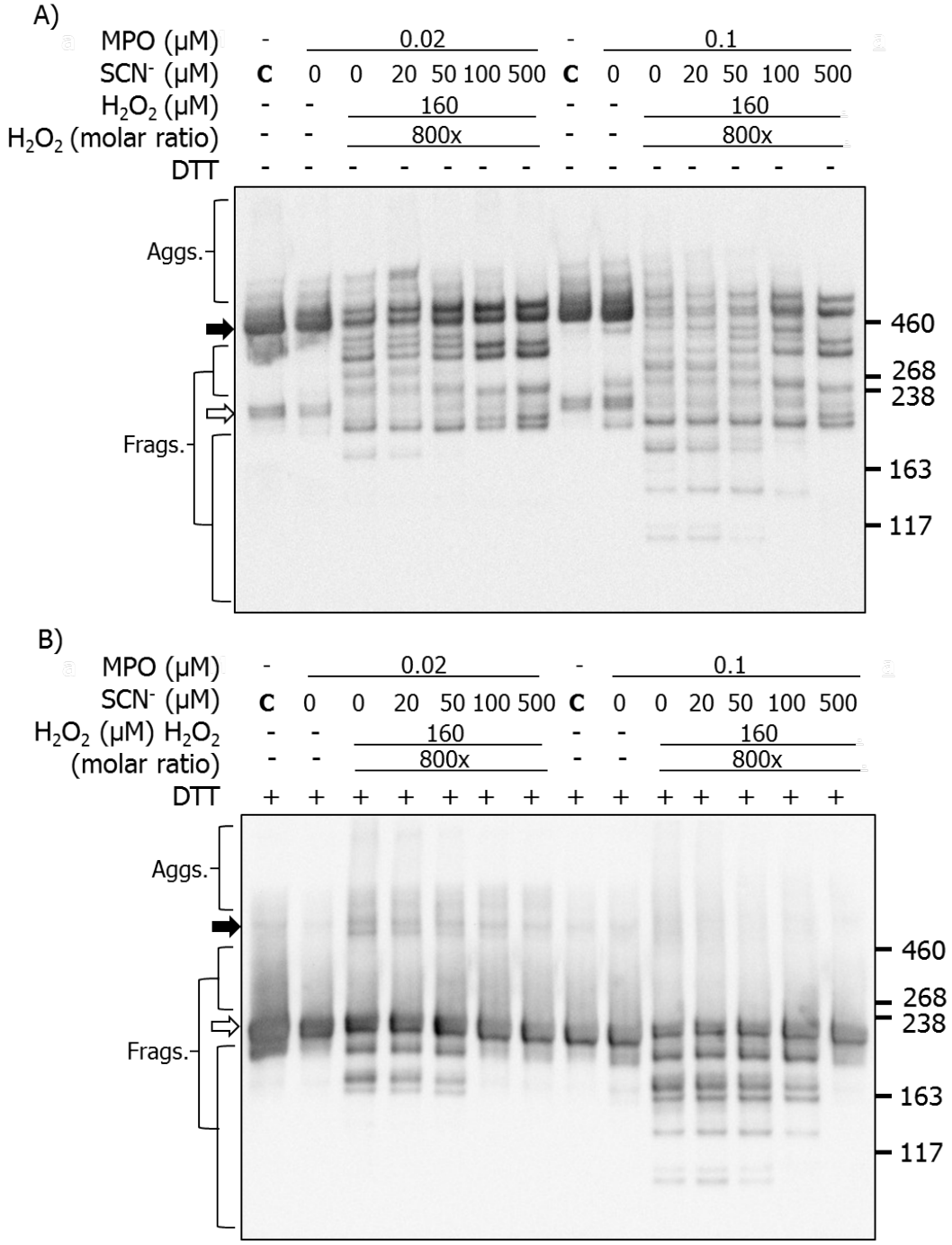

Figure 6.3: **Western blotting for CBF showing structural changes to human plasma FN treated with the stated concentrations of MPO/Cl^-/H_2O_2 and increasing concentrations of SCN^-.** Purified human plasma FN (0.2 μM in 0.1 M phosphate buffer) was either left untreated (MPO only control) or treated with MPO (0.02 or 0.1 μM), Cl^- (100 mM), H_2O_2 (160 μM) and increasing concentration of SCN^-, and incubated for 2 hr at 37°C. Samples were electrophoresed on SDS-PAGE under **A)** non-reducing or **B)** reducing conditions, transferred onto PVDF membranes and probed with a mouse monoclonal anti-FN CBF antibody (A17; 1:10000), and conjugated with anti-mouse HRP secondary antibody (1:2000). Blots were developed with ECL-plus reagent and data is labelled as follows: black arrow = dimer/higher aggregates, and white arrow = monomer bands.

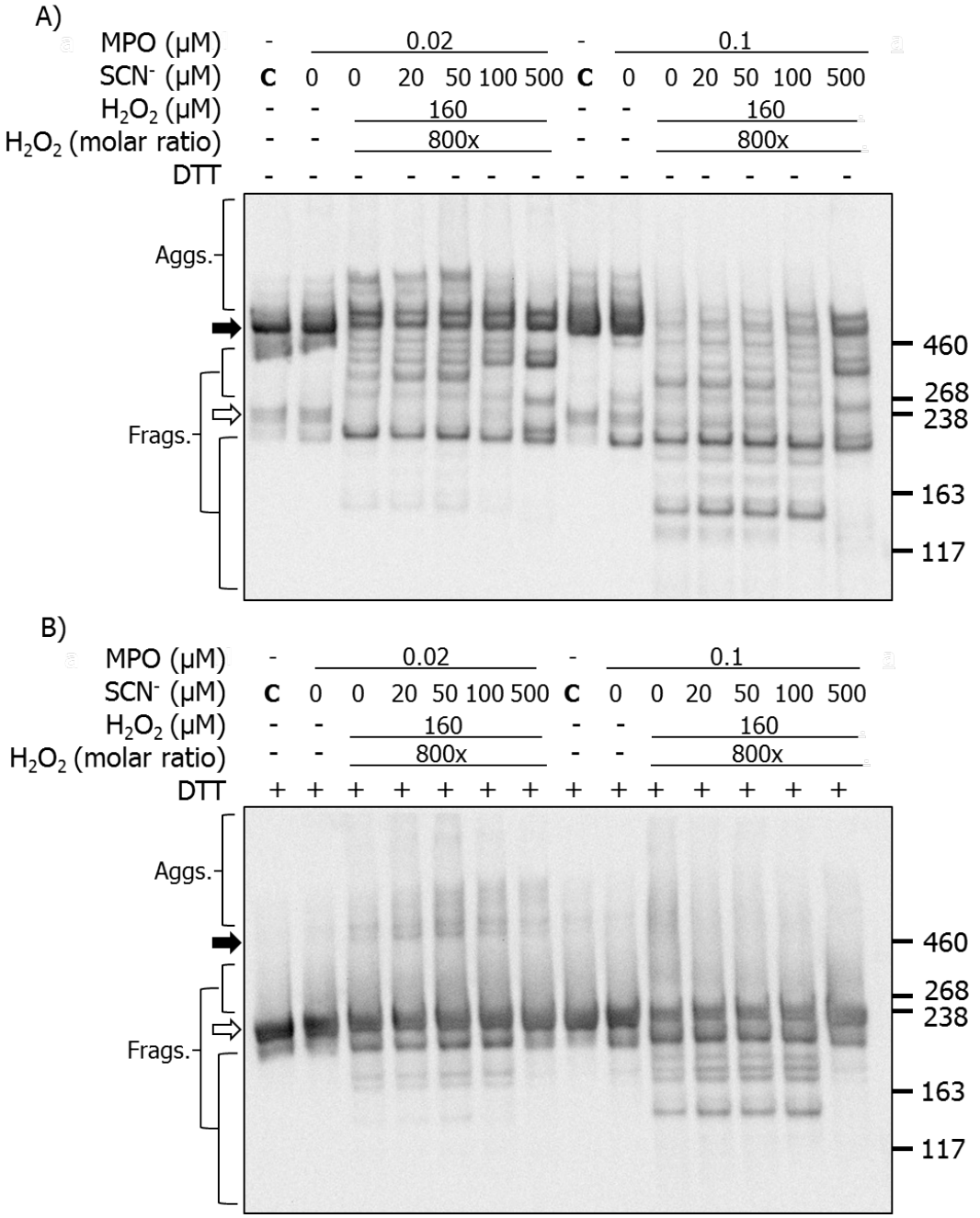

Figure 6.4: **Western blotting for HBF showing structural changes to human plasma FN treated with MPO/Cl^-/H_2O_2 and different concentrations of SCN^-.** Purified human plasma FN (0.2 μM in 0.1 M phosphate buffer) was either left untreated (MPO only control) or treated with MPO (0.02 or 0.1 μM), Cl^- (100 mM), H_2O_2 (160 μM) and increasing concentration of SCN^-, and incubated for 2 hr at 37°C. Samples were electrophoresed on SDS-PAGE under **A)** non-reducing or **B)** reducing conditions, transferred onto PVDF membranes and probed with a mouse monoclonal anti-FN HBF antibody (A32; 1:5000), and conjugated with anti-mouse HRP secondary antibody (1:2000). Blots were developed with ECL-plus reagent and data is labelled as follows: black arrow = dimer/higher aggregates, and white arrow = monomer band.

6.4 Discussion

MPO is important in the inflammatory response against invading pathogens and its potential role is to generate reactive bactericidal species to kill pathogens. However, excessive or inappropriate formation and amounts of oxidants can also be damaging to host cells and their surrounding ECM. Within the body, Cl^- concentrations are typically in the range of 100-150 mM whereas SCN^- fluctuates, with concentrations of 20-250 μM reported for different individuals [95]. Hence, the relative concentrations of Cl^- and SCN^- determine the amount of the two hypohalous acids, HOCl and HOSCN, generated by MPO at a site of inflammation. With Cl^- being more abundant than SCN^-, it would be expected that HOCl is the major species produced although SCN^- is the more favoured substrate for the enzyme [51]. Another known mechanism of HOSCN production is through a non-enzymatic interaction between HOCl directly with SCN^- [92, 93]. This reaction occurs rapidly ($k = 2.34 \times 10^7$ M^{-1} s^{-1}) and spontaneously reducing highly reactive HOCl concentrations and generating more specific, yet less reactive oxidant HOSCN with the latter species being specific for thiols [26, 50, 92, 94]. By determining the nature of interaction between MPO, Cl^- and SCN^-, in the presence of H_2O_2 to a biologically important protein target FN, it was hoped that the extent and specificity of protein modifications induced by HOCl vs HOSCN could be identified, and the nature of the modifications induced by these species can be further elucidated.

In the previous Chapter, the modifications of FN induced by MPO/Cl^-/H_2O_2 were explored. The addition of SCN^- at increasing concentrations resulted in the detection of a greater number of apparent fragments or altered species together with a decreased intensity of the aggregate bands (Figure 6.2). Previous studies have shown that MPO has a greater specificity constant for SCN^- over Cl^- by 730 fold [26, 110]. Furthermore, it has been reported that at least 40% of H_2O_2 consumed by MPO under some conditions reacts with SCN^- to generate HOSCN, with a small percentage being used to oxidise other halides (Br^- or I^-), with the remaining H_2O_2 being converted to HOCl [26, 98]. Therefore,

the presence of lower concentrations of SCN^- in the samples is likely to produce small amounts of HOSCN, which are likely to target Cys residues on FN. However, it is highly likely that significant amounts of HOCl are still being generated.

In previous studies, MPO in the presence of physiological concentrations of Cl^- and SCN^- combined, was found to have a synergistic effect leading to greater oxidation of TNB than the sum of each separate species [110]. This suggestion was supported by data indicating that the consumption of H_2O_2 was greater in the mixed Cl^- and SCN^- system, with the rate of consumption proportionate to the concentration of SCN^- [110]. The synergistic generation of oxidant could suggest that *in vivo*, the mixture of halides is important in generating a greater inflammatory response, which in turn could modify host proteins more extensively. This hypothesis may potentially explain why there appears to be a greater, or altered pattern of modifications on FN with the addition of SCN^- to the MPO/Cl^-/H_2O_2 system.

Increasing the concentrations of SCN^- (> 100 μM or approaching 1:1 ratio with 160 μM of H_2O_2) resulted in less formation of fragments and aggregates. Furthermore, the loss of antibody recognition also appears to be mitigated. There appears to be a shift in what is assumed to be MPO/Cl^-/H_2O_2-derived modifications to MPO/SCN^-/H_2O_2-derived modifications. The MPO/SCN^-/H_2O_2 system does not seem to modify significantly the functional CBF or HBF epitopes with no changes in antibody recognition seen in ELISA or Western blots (Figure 6.1), nor affect the biological functions dependent on these epitopes as found in previous chapters (Section 4 and 5). This suggests that although MPO-derived HOSCN is modifying FN in a specific way, it is not targeting CBF or HBF functional epitopes. HOSCN may target FN at different sequences or epitopes that are rich in Cys residues which have not been investigated in this study; further investigations are required to confirm this.

Exposure of FN to MPO, Cl^-, and 1600x molar excess (32 μM) of H_2O_2 was observed to decrease recognition to both the functional CBF and HBF epitopes, with a corresponding

increase in presence of a HOCl-generated epitope (Figure 6.1). The addition of 20 μM of SCN^-, which is similar in concentration to the amount of H_2O_2 present, resulted in a complete return of recognition to the CBF and HBF epitopes. Moreover, addition of SCN^- led to the disappearance of the HOCl-generated epitope recognised by 2D10G9 with the absorbance levels returning to those found in the controls (Figure 6.1). It may be likely that MPO in the presence of 20 μM of SCN^- and 1600x molar excess (32 μM) of H_2O_2 is producing more HOSCN than HOCl, mitigating the damage to the functional CBF and HBF epitopes, and reducing the formation of the HOCl-generated epitope.

The ELISA results repeated in this chapter in the presence of SCN^- did not show a greater modifications to these FN functional sites (as seen on the gels and by Western blotting) but rather a return of epitope recognition with the addition of increasing concentrations of SCN^- (Figure 6.1), unlike what was observed earlier in the silver staining and Western blotting results. There are several reasons why this may not be detected with the ELISA treatment. Firstly, 1600x (32 μM) of H_2O_2 was used instead of 800x molar excess (160 μM) of H_2O_2. Higher concentration of H_2O_2 will inevitably lead to a greater formation of oxidant, and oxidation observed in the silver stain and Western blot experiments, and less in the ELISA experiments despite the lower molar ratio. Moreover the ratio of H_2O_2:SCN^- was different between the two sets of experiments thus the ratio of oxidants (HOCl:HOSCN) is likely to be different between the two sets of experiments. Interestingly, a ratio of 5:8 (SCN^-:H_2O_2) which was common for both ELISA and silver staining/Western blotting experiments, a decreased MPO/Cl^-/H_2O_2-derived modifications, and a shift to what appears to be MPO/SCN^-/H_2O_2-derived modifications was observed. What may be happening in this case is that the presence of SCN^- at a concentration close to H_2O_2 is either diverting MPO production to HOSCN instead of HOCl or SCN^- is scavenging HOCl [26, 110]. This suggestion is supported by the presence of a HOCl-generated epitope when FN was treated with MPO/Cl^-/H_2O_2 in the absence of SCN^-, but the addition of 20 μM of SCN^- led to a reduction in the levels of the HOCl-generated epitope back to levels close to those levels observed in controls (Figure 6.1).

This would suggest that at 0.02 μM of MPO, 100 mM Cl^-, 20 μM of SCN^-, 32 μM of H_2O_2 the major oxidising agent that gives rise to the detectable modifications on FN using the approaches examined here is HOSCN.

One limiting factor in these experiments was that it could not determine whether HOSCN was produced or whether SCN^- was scavenging HOCl. Due to time constraints, it was difficult to create a larger set of experiments. In future experiments, the use of monochlorodimedon would help to determine whether HOCl was generated in this process [411]. The use of monochlorodimedon would decrease the reaction between MPO and Cl^-, and thus determine whether HOSCN was produced or whether HOCl was scavenged by SCN^-.

This chapter has shown that the modifications induced on FN by treatment with a MPO/Cl^-/H_2O_2 system can somewhat be attenuated by the addition of SCN^-. The addition of low concentrations of SCN^- was found to potentially increase structural damage on FN, possibly as a result of damage to a limited number of critical Cys residues, whereas higher concentrations of SCN^- resulted in the change from HOCl-derived modifications to less damaging HOSCN-derived modifications. By elucidating the relationship between MPO, Cl^-, SCN^-, and H_2O_2, a greater understanding can be obtained as to the role of SCN^- in the progression or prevention of atherosclerosis.

Chapter 7

Discussion and future directions

7.1 Overview and Summary

FN is a key ECM protein in maintaining basement membrane homeostasis through protein-protein and protein-cell interactions. FN dimeric protein consists of two nearly identical monomers bound by two disulfide bonds present near the carboxy-termini [149, 195, 196]. There are two types of FN: soluble plasma FN and insoluble cellular FN, which are both reported to be found within the arterial wall sub-endothelial matrix [149, 195, 196]. The two types of FN are similar, with the exception that cellular FN possesses additional EDA and EDB domains, which have been proposed to play a role in matrix assembly and atherogenesis [140, 273, 274]. FN possesses several functional domains that interact with other ECM proteins and integrin binding sites on cells [149, 197].

Deposition of LDL in the sub-endothelial matrix is believed to initiate an inflammatory response leading to the migration of leukocytes and a release of inflammatory species [1]. MPO, a heme-peroxidase that can be detected in plasma, has been shown to transcytosed into the sub-endothelial matrix, or are released at this location by activated leukocytes that have migrated into the site of inflammation [21, 270, 397]. High levels of circulating MPO have been linked to an increased prevalence of CAD in the population [11, 396], and a deficit was previously linked with a reduced rate of CVD [39]. MPO converts H_2O_2 in the presence of physiological concentrations of Cl^- and SCN^- to generate HOCl

and HOSCN, respectively [26]. High concentrations of these reactive oxidants have been shown to modify and damage host lipids, DNA, peptides, and proteins [49, 50].

In Chapter 3, it was shown that exposure of human plasma FN to reagent HOCl caused fragmentation and aggregation of FN, leading to a loss of antibody recognition of the functional CBF and HBF epitopes, and increased detection of a HOCl-generated epitope. HOCl was found to target Met, Trp, and free thiol residues with further oxidation of MetSO occurring leading to subsequent by-products. Exposure of HCAEC to HOCl-modified FN resulted in a loss of HCAEC adhesion and metabolic activity. Furthermore, HCAEC incubated on HOCl-modified FN were found to modulate the expression of several ECM and adhesion genes in response. Reagent HOCl was also found to damage HCAEC-derived *cellular* FN CBF, HBF, and EDA epitopes leading to a loss of antibody recognition to these functional sites. Furthermore, FN was shown to be present in advanced Type II-III human atherosclerotic lesions, and were found to co-localise with a HOCl-generated epitope as seen with IHC.

In Chapter 4, the results of analogous experiments reported in which human plasma FN was exposed to reagent HOSCN (generated using an LPO/SCN^-/H_2O_2 system). This treatment resulted in minor modifications (when compared to those observed with HOCl exposure) with limited fragmentation, aggregation or changes in gel mobility due to protein unfolding. FN thiols were found to be modified upon exposure to HOSCN, which is consistent with the known specificity for thiol residues by this oxidant. There were limited modifications induced on the FN CBF epitope by HOSCN, and this treatment did not cause any changes to HCAEC adhesion nor metabolic activity. However, HCAEC incubated on HOSCN-modified FN were found to show altered expression of certain genes which were different to those induced by HOCl-modified FN. Exposing HCAEC-derived *cellular* FN to HOSCN did however induce small changes to the functional CBF, HBF, and EDA epitopes. This may have arisen from HOSCN targetting key Cys residues in other domains with this resulting in subsequent changes to these functional epitopes, which are known to be lacking in these residues.

In Chapter 5, human MPO/H_2O_2 with either 100 mM of Cl^- or 20 or 500 μM of SCN^- was used to treat human plasma FN. This enzymatic reaction system should more closely replicate the reaction that is occurring *in vivo*. Exposure of human plasma FN to MPO/Cl^-/H_2O_2 system was found to induce structural changes with formation of fragments, aggregates, and altered mass species possibly arising from protein unfolding. Moreover, exposure of FN to MPO/Cl^-/H_2O_2 resulted in modifications to the functional CBF and HBF epitopes causing a loss of antibody recognition, and subsequent exposure of HCAEC to modified FN was found to decrease HCAEC adhesion and metabolic activity. Exposure to MPO/SCN^-/H_2O_2 was found to induce minor structural changes to human plasma FN when compared to MPO/Cl^-/H_2O_2. MPO/SCN^-/H_2O_2 treatment of FN resulted in minor modifications to the CBF and HBF epitopes, and when HCAEC were incubated with this modified FN, HCAEC adhesion and metabolic activity was not affected.

In Chapter 6, human plasma FN was exposed to MPO/Cl^-/SCN^-/H_2O_2 to investigate the competitive generation of HOCl and HOSCN. As expected on the basis of the above data, exposure to MPO/Cl^-/H_2O_2 system resulted in extensive modifications to FN. The addition of SCN^- mitigated HOCl-derived modifications and at higher concentrations of SCN^-, modifications consistent with the MPO/SCN^-/H_2O_2 system were detected. Furthermore, the addition of SCN^- was found to retrieve antibody recognition of the functional CBF and HBF epitopes, with a corresponding decrease of the HOCl-generated epitope recognised by 2D10G9, which was generated in samples where SCN^- was absent.

These results are consistent with previous studies examining changes to ECM proteins by reactive oxidants [22, 64, 65, 130, 260, 261]. The proximity of FN to the arterial wall cells and the importance of FN for vascular ECM integrity makes it an interesting target to investigate with respects to whether it is targeted and modified by HOCl and HOSCN. Modifications to FN can lead to subsequent loss of biological function, and particularly its ability to interact with other ECM proteins, and cells (ECs and SCMs) [22, 130, 131, 261]. It would therefore be insightful to investigate changes to other ECM

proteins, other functional epitopes on FN, the possible protective mechanism of SCN^- or other antioxidant species that may protect against modifications to FN.

7.2 The implication of modifications to FN by HOCl or HOSCN, and their interactions with other ECM proteins and cells

FN possesses functional epitopes including those that are important in interacting with cells (e.g. via the CBF), collagen/gelatin, fibrin and heparin (the latter two have two domains on FN) [196]. Modifications to the CBF on FN are known to have a drastic effect on cellular adhesion [22, 130, 261], thus modifications to other functional epitopes may identify what effect modified FN may have *in vivo* [130, 258, 318, 412].

The FN collagen binding fragment is known to bind to collagen [217, 218], with a greater specificity to the denatured form (gelatin) than the native form [258]. This suggest that FN may be binding with gelatin to initiate degradation of collagen peptides through activation of collagenases [413]. Some studies have found that collagen triple helices unfolds at physiological temperatures, which may increase the interaction between native FN and collagen *in vivo* [414, 415]. The importance of collagen to FN assembly has previously been shown in Mov13 mice, whereby inactivation of COL1A1 gene resulted in sparse assembly of shorter FN fibrils [416]. Furthermore, FN and collagen have been observed to co-localise, and when FN assembly in SMC culture was inhibited using an anti-$\alpha 5\beta 1$ integrin antibody, this subsequently inhibited collagen assembly [417]. Blocking the gelatin binding site on FN was also found to prevent deposition of both collagen and FN fibrils in fibroblast cell culture [258]. These studies support the important nature of the interactions between FN and collagen, and support the hypothesis that modifications to the collagen/gelatin binding fragment by oxidants can have a profound effect on collagen deposition and ECM assembly [418].

In previous studies, it has been proposed that procollagen, which can be cleaved intracellularly to collagen may interact with FN prior to excretion into the ECM [419, 420]. If this were the case, the collagen/gelatin binding fragment may be occupied, and FN may be in an altered or unfolded state, thus it may change what sequence is

susceptible to HOCl or HOSCN modifications. In recent studies, investigations have examined the mechanical forces between ECM proteins and cells; it has been shown that FN-collagen interactions were important in reducing load-bearing on FN and decreased cell mediated stretching of FN (compared to FN-only) [391]. The interaction between FN and collagen would mean that FN would be less strained, which may modulate some of the modifications generated by HOCl and HOSCN, which are dependent on protein conformation and accessibility to epitopes. The amino acid sequence of the collagen binding fragment is located between 308-608, which posses 23 Cys residues (Uniprot. data; P02751). The reaction of oxidants in this region may be important due to the high reactivity of HOCl and the specificity of HOSCN to thiol residues [50]. If this region were to be modified by either HOCl or HOSCN, this may affect the interactions between FN and collagen, resulting in improper FN-collagen (and subsequently matrix) assembly [418].

The fibrin binding fragment in the Type I module of plasma FN plays an important role in wound healing by binding to fibrin and platelets, providing a strong clot scaffold [197]. Formation of the fibrin-FN clot is mediated by coagulation factor XIII binding to the N-terminus on FN [421]. Furthermore, the incorporation of FN into clots has been found to be important in cellular function of platelets [422, 423], and activation of fibroblasts [424]. Fibroblast binding and activation is mediated by the FN cell binding domain (type $III_{9\text{-}10}$), a variably spliced domain (type III_{CS}), in combination with HBF (which alone does not result in cell adherence) [424]. Cellular FN is then deposited by cells, and both plasma and cellular FN stimulate the deposition of collagen leading to granulation of injured tissue and fibrosis [197, 425]. Plasma FN deficiency and $FN^{+/-}$ (expression of half the amount of FN) in mice were observed to have delayed thrombus formation and slower rate of arterial occlusion [426, 427]. Infusion of rat plasma FN in $FN^{+/-}$ mice was found to retrieve the thrombotic defect [427]. The fibrin binding fragment is important in initiating wound healing, and this may be important in the case of a plaque rupture [428, 429]. Furthermore, if this fragment were to be modified, it may affect the interaction

between FN and fibrin and subsequent collagen formation for fibrosis (particularly in plaque cap development).

The FN HBF plays in a myriad of roles, one of which is binding to cell-surface heparan sulphate proteoglycans (HSPG) [164, 430]. There are two HBF domains in both forms of FN, HBF I is located at the N-termini and has a weaker binding affinity than HBF II which is located near the carboxy-termini on the type $III_{12\text{-}14}$ module [196, 431]. This type III_{13} domain is known to play a pivotal role in binding Syndecan-2 [207, 432]. Due to its high binding affinity, it has been found to also bind to GAGs and particularly CS, although perhaps not as strongly as to heparin [206]. Furthermore, it has been previously found that the variable region can be alternatively spliced in the type III_{CS} region in cellular FN [209]. The HBF in FN is important in matrix assembly and has been found to increase the distribution of FN in Chinese Hamster Ovary cells (CHO) [208]. Furthermore, binding of heparin to FN also increased the binding of collagen [433]. Modifications on the FN HBF, as seen with exposure to HOCl (Section 3) or MPO enzymatic system (Section 5), may lead to an inability of binding between FN to heparin or GAG. This may cause impairment in collagen binding and subsequent loss of integrity in matrix assembly.

Anastellin is a fragment located on the carboxy-termini of the type III_1 domain (amino acid sequence 627-702) and has been shown to regulate polymerization/fibril formation of FN [434]. The binding of anastellin to FN is dependent on the protein unfolding to give access to the binding site [435]. It acts on FN to initiate the formation of superfibronectin (super-FN), which has increased cell adhesion properties, and suppresses cell migration [436], and proliferation [434]. Moreover, anastellin has been found to elicit an anti-angiogenic effect [437], although this mechanism is not fully elucidated. It has been proposed that perhaps the conformational change may cover up certain domains such as the EDA domain on cellular FN [438]. This suggest that there may be a relationship between anastellin and the association between EDA and $\alpha 4\beta 1$ integrin [439]. Modifications to this domain (which possesses 3 Trp, 4 Tyr, and no Met or Cys residues)

by oxidants (HOCl) may have an implication on FN matrix assembly *in vivo*. The Tyr-666 residue is known to be critical in binding for ananstellin and the deletion of Type $III_{1\text{-}3}$ (amino acid 614-901) was shown to have barely detectable levels of matrix fibrils [440, 441]. Recent study by another member of the group, has identified that anastellin Tyr-666 (and Tyr-687) residues were targets for chlorination upon exposure to HOCl and MPO/Cl^-/H_2O_2 system (Tina Nybo, 2018, Unpublished data). This may suggest that modifications to this Tyr-666 residue would have an implication in the assembly of FN and super-FN, and may play a minor role in disturbing cellular adhesion between FN and HCAEC (as seen in Section 3 and 5).

Cellular FN is alternatively spliced during production and thus possesses the additional EDA and EDB domains which are absent in plasma FN [196]. The EDA region, which is the more extensively researched of these two domains, has been found to mediate binding to $\alpha 4\beta 1$ and $\alpha 9\beta 1$ [439, 442]. EDA is particularly important during early vascular development [443–445], and knock-out of both the EDA and EDB domains ($EDA^{-/-}$/$EDB^{-/-}$) was found to be lethal to mice embryos with these observed to have defects in embryonic cardiovascular development [446]. $EDB^{-/-}$ mice were observed to develop normally, but fibroblasts derived from these animals were slow growing and deposited lower levels of FN [447]. Atherosclerotic plaques have been observed to have elevated levels of EDA containing FN, and these plaques were observed to be more stable in $apoE^{-/-}$ mice [412]. Furthermore, $apoE^{-/-}$/$EDA^{-/-}$ mice developed smaller plaques but had higher levels of macrophage infiltration, lower levels of collagen deposits, and higher levels of MMP expression and activity [412]. This suggests that EDA is required to form thicker fibrous plaques that are likely to be more stable and less likely to rupture. However, there are relatively few studies on the roles of the EDA and EDB domains, and the extent of their function is not full understood. From the data available, it appears that these extra domains are important in matrix assembly and mediating cellular functions. Oxidation and modifications to these domains such as seen as part of these studies may lead to the formation of more unstable plaques [318], which are commonly associated

with decreased levels of collagen deposition, and high macrophage numbers.

The importance of FN in maintaining a healthy vasculature can be seen by how it interacts with other proteins to form matrix and assist in cellular function. Certain functional epitopes may be reactive with oxidants (HOCl or HOSCN), and can lead to cellular dysfunction and also improper matrix assembly. There is current ongoing research investigating which amino acids are targets for HOCl on FN and what peptides/domains are subjected to significant oxidation and chlorination (Tina Nybo, 2018, Unpublished data) [448]. This method is likely to be replicable in examining the oxidative effects of HOSCN on FN. Further investigations of protein-protein interaction can complement these findings by identifying whether particular modifications effect the ability for FN to interact to other ECM proteins [449, 450]. Immunoprecipitation or co-immunoprecipitation (Co-IP), which are used for strong or stable protein-protein interactions may be favoured for well-known and categorised interactions [449]. Quartz Crystal Microbalance (QCM) is a method that utilises a quartz crystal resonator to measure changes in frequency; it has been used in determining protein-protein interactions and also provides data on the affinity between two molecules [451]. Biacore is another detection method that could be utilised to examine native and oxidant-induced modifications of protein-protein interactions [452]. This method is based on surface plasmon resonance (SPR), to measure affinity, kinetic rate constants and thermodynamics of the interactions between proteins [452]. There are several other methods that can be utilised, some of which are more preliminary (e.g. protein affinity chromatography or affinity blotting) and others being more specific [449, 450].

Many of the FN domains have been implicated in playing a role in cellular function, and these functions should be further examined using cells incubated on modified FN [453]. A common technique employed for examining cell migration is a scratch test, where a surface area is scratched free of cells and the migration of cells back into this area is monitored [454]. A Boyden Chamber assay can also be employ to test cell migration, which is a technique that utilises a porous membrane sitting within medium containing the species

of interest such as modified FN [455]. Cells will migrate through the semi-permeable membrane and are subsequently quantified.

As there are current research identifying sites of modifications induced by HOCl and MPO/Cl^-/H_2O_2 system (Tina Nybo, 2018, Unpublished data), it would be interesting to expand this further and investigate the effects SCN^-. MS analysis of sites of modifications can be utilised to identify whether SCN^- is able to be reduce or prevent the modifications induced by HOCl and the MPO/Cl^-/H_2O_2 system. Furthermore, it would be important to elucidate whether HOSCN and MPO/SCN^-/H_2O_2 targets and modifies specific residues on FN. If HOSCN does target specific residues, then it can be identified whether these modifications would lead to dysfunction or whether it may reducible by physiological reductants such as GSH, or ascorbate [392, 393].

Protein-protein interaction is important in identifying whether particular FN functional domains are more likely targeted than others. However, a mixture of proteins exist *in vivo* with FN bound to other ECM proteins and cells (such as EC and SMC) [18, 196, 456]. This suggests that certain targets may be inaccessible to oxidative modifications due to being bound to cells or other ECM proteins. In these studies, it was shown that whole HCAEC-derived ECM exposed to HOCl resulted in cellular FN functional epitopes (CBF, HBF, and EDA) were modified and less extensively by HOSCN. Examination of other functional sites that are important in binding to other ECM proteins may elucidate whether those sites are blocked or whether it is still targeted by these oxidants. Moreover, examination of other ECM proteins, such as laminin, collagen and perlecan, in whole HCAEC-derived ECM extract are also targeted by these oxidants and modified.

These future studies can further help to determine the role FN has during development of atherosclerosis, and whether changes to FN can mediate certain responses. By elucidating these effects, it would assist in identifying whether FN is a suitable target for developing treatments or prevention of atherosclerosis.

7.3 Interaction between fibronectin and cells in healthy and atherosclerotic blood vessels

Cellular FN, which contains alternatively spliced EDA, EDB, and type III_{CS} domains are known to express different types of integrins that can interact with receptors from different types of cells [196]. In this study, it was observed that the CBF and EDA domain on FN was modified by MPO-derived oxidants, subsequently leading to loss of adhesion by HCAEC. Other cells also play a role in the progression of atherosclerosis including SMC, fibroblasts, and a number of leukocytes. The interactions between FN and cells may change depending on the structural integrity of FN and their corresponding binding sites and should be further investigated.

Vascular SMC have been known to play an important role in plaque stability and subsequent prevention of plaque rupture [14]. It is also known that vascular SMC both interact and produce FN within the vascular wall [14]. During the development of blood vessels, SMC has been observed to co-localise with $\alpha4\beta1$ receptors on cellular FN, located on one of the alternatively spliced domains [227]. Mechanical stress and elasticity within the vascular wall are known to be modified by FN [457], and activate arteriole SMC response via surface integrins to initiate vasodilation or vasoconstriction [458]. Interactions with FN integrin sites have been shown to mediate SMC migration [459, 460], and proliferation [461, 462]. SMC has been found to interact with $\beta1$-containing integrins (e.g. $\alpha5\beta1$), which mediate migration and mobility [459, 460]. Furthermore, the migration of SMC was observed to occur with $\alpha V\beta3$, both in vivo and in vitro [463–465]. Migration of vascular SMC into the injury site is important in synthesising matrix to form a strong structural fibrous cap [14]. Inhibition of $\alpha5\beta1$ by blocking with an RGD peptide or mimetic has been shown to cause a reduction in vessel wall thickening in mice models [466, 467], which may indicate a decrease in fibrotic fibres.

Mechanical stress and stiffness of FN was found to also mediate SMC migration, but not

so in a FN and laminin mixture [468]. It is known that FN is important in regulating matrix stiffness by interacting with other ECM proteins and cells [457, 469]. FN has been observed to regulate SMC cell cycle, whereby SMC incubated on FN remained in the G0/G1 phase for 6 days with increased cycle D1 expression [470]. The addition of serum activated the S phase in the cell cycle and these processes were found to be absent in SMC incubated on laminin [470]. These past studies support the interactions between native FN and the cellular functions of SMC in blood vessels. Modified FN may lead to changes in this relationship affecting the ability for SMC to migrate, initiate cell cycle and respond to new stimulus within the blood vessels.

Another cell type that has been observed to interact with FN are fibroblasts, which resides in the adventitia of arteries and known to function in angiogenesis [471, 472]. Migration of REF52 fibroblasts has been previously observed to be dependent on the CBF, HBF, EDA domains, and in particular the $\alpha 5\beta 1$ and $\alpha v\beta 3$ integrin on FN [473]. Inter- and intramolceular cross-linked FN (by glutaraldehyde) resulted in decreased directional persistence in REF52 fibroblast migration, lower spread area, and an inability to form polarized protrusions [473], indicating that the access to epitopes was important for fibroblast migration and cell shape. FN mechanical gradient was observed to mediate durotaxis of NIH 3T3 fibroblasts, which was found to be absent with laminin or mix FN-laminin experiments [474]. This indicates that FN plays a role in migration of fibroblasts but *in vivo*, this may differ depending on the interaction of ECM proteins between each other and the availability of epitopes to attract fibroblasts.

Previous studies have observed that interactions between $\alpha 4\beta 1$ and EDA domain on FN promote stress fibre formation and initiation of fibrosis through FN synthesis, deposition of matrix, and actin assembly [473, 475]. This suggests that fibroblasts play a role in the generation of fibrotic fibres at injury sites. This may be important when fibroblasts differentiate into myofibroblasts in response to injury to initiate fibrosis. The phenotype of myofibroblast differentiation was found to be determined by the EDA and EDB FN domains, whereby EDA deposition mediated increased α-SM actin and myofibroblasts

formation via Transforming Growth Factor β1 (TGF-β1) conversion [476, 477]. This may indicate that fibroblast migration and differentiation is dependent on FN functional domains, especially in terms of formation of fibrotic tissue at an area of injury such as the necrotic core of an atherosclerotic plaque. In this study, it was observed that the EDA domain was modified by reagent HOCl, thus the dependence of fibroblasts on the cellular-derived EDA domain and the integrins present on the CBF may suggest improper migration and differentiation of fibroblasts [473, 476, 477]. This may subsequently lead to reduced fibrosis and smaller plaque cap formation [473, 475].

Inflammatory cells (such as leukocytes, monocytes, and macrophages) have also previously found to bind to certain ECM proteins during their adhesion and subsequent transmigration through the EC layer. The type III_{CS} domain of FN has been found to bind monocytes via an α4 integrin in a similar fashion to VCAM-1 [478]. Deamidation of NGR motifs in FN, was observed to increase U937 monocyte adhesion, and binding of primary human monocytes mediated by the $\alpha v\beta$3 integrin [479]. Blocking of the type III_{CS} domain was found to reduce monocyte adhesion by approximately 20%, suggesting it may be a minor regulator of monocyte recruitment compared to blocking of VCAM-1 which reduced monocyte adhesion by approximately 80% [480]. Furthermore, inhibition of $\alpha 4\beta 1$ attenuated recruitment of leukocytes (neutrophils and macrophages) and reduced neointimal formation in $apoE^{-/-}$ mice [481]. Inhibition of β1 integrin with an antibody decreased $\alpha D\beta 2$ integrin (CD11d/CD18) mediated monocyte adhesion by approximately 50% on FN [482]. EDA deficiency in $apoE^{-/-}$ mice was observed to result in lower levels of lipid accumulation in macrophages suggesting that the FN EDA domain may also play a role in foam cell formation [272]. Neutrophils incubated on stiff FN fibres showed stronger adherence and greater cell spreading than those incubated on looser fibres [483, 484]. Stiffness of FN fibres was determined with different concentrations of FN. Therefore, FN appears to be important in the binding of inflammatory leukocytes to integrins, but also in determining different macrophage responses via the EDA domain. These studies suggest that FN may play a role in the recruitment of inflammatory cells into the injury

area by providing integrin binding sites. Modifications to the EDA (and possibly other functional sites), as seen in these studies, may suggests changes to foam cell formation and recruitment of inflammatory cells [272].

Interactions between cells and ECM proteins are complex, and the interactions between a mixture of proteins *in vivo* and purified proteins can differ greatly. Further investigations are clearly needed to examine the relationships between different cell types and native and modified FN. Cell adhesion, cell metabolic activity, and migration can be tested utilising the methods described in Sections 2 and 7.2. Since there are limited studies examining gene expressions, such investigations may contribute greatly to the understanding of cellular response to blood vessel changes such as modifications to FN or other ECM proteins. Gene expression by HCAEC adhered on modified FN generated by MPO/Cl^-/H_2O_2 or MPO/SCN^-/H_2O_2 systems would contribute to our understanding of possible changes and comparison of the data obtained to what has shown in the studies reported here with reagent HOCl and HOSCN could be very informative. The competitive system using MPO/Cl^-/H_2O_2 with the addition of SCN^- may expose different gene regulations, perhaps to a lesser degree than in the absence of SCN^-, and this should be examined further. Gene expression, such as conducted in this study (Section 3.3.6), could be complemented by investigating protein expression. Gene expression and protein expression are not always proportionately up- or down-regulated and thus should be examined. Protein expression can be examined by probing for specific proteins with specific antibodies using Western blotting or ELISA. This will assist in visualising the relationship and pathways between gene expression and protein expression, as inhibition or stimulation may occur upstream of protein expression.

7.4 Protective and damaging effects of thiocyanate and other therepeutics

Lifestyle changes have been used as the first stage of treatment for early and advanced atherosclerosis. This includes healthier eating habits, increased physical activity, control of body weight, cessation of smoking, and dealing with any underlying mental health problems, such as chronic stress. A healthy lifestyle in young adults has been found to significantly decrease the risk of developing atherosclerosis during middle age [485]. Dietary changes are a factor in implementing these changes. This includes reducing consumption of fatty foods, and shift to a low-fat vegetarian diet, which can reduce LDL and cholesterol content and results in regression of atherosclerosis [486]. Previous studies have reported that antioxidant supplementation does not give rise to any changes in the risk of CVD in patients [133, 487]. It has been then proposed that diverting conversion of a highly reactive oxidant such as HOCl, to a more specific and often reversible oxidant such as HOSCN may help in the treatment of atherosclerosis [99, 114, 410]. The studies reported previously have shown conflicting results, where a small elevation in plasma levels of SCN^- showed a protective effect, decreasing HOCl-induced modifications [99, 114, 410]. However other studies have reported that highly elevated plasma levels of SCN^- led to irreversible modifications induced by HOSCN [99, 114, 410].

The levels of HOSCN in an individual have been proposed to be highly dependent on the presence of SCN^- substrate. Non-smoking individuals have plasma SCN^- levels of 20-40 μM, whereas plasma concentration of SCN^- in smokers have been reported to be up to 80-400 μM [96–99]. This is a result of smokers having elevated levels of cyanide (CN^-), which the body detoxifies to form SCN^- [98, 488, 489]. Smokers have been shown to have a higher deposition of apoE and an earlier development of atherosclerosis when compared to non-smokers [490]. These depositions were accompanied by an increased population of foam cells (lipid-laden macrophages) in the area of injury compared to non-smoking counterparts [490]. These effects have been linked to elevated levels of plasma SCN^-

[94]. Aside from smoking, elevated plasma levels of SCN^- can also occur as a result of consumption of food products such as cassava, stone fruits, lima beans, and flaxseed [368]. Certain cyanogenic plants, such as broccoli, cabbage, and sprouts can also give rise to elevated levels of CN^- which is detoxified to SCN^- in the body [368].

MPO has a higher specificity for SCN^- when compared to Cl^- by almost 730 fold, with studies proposing that up to 50% of H_2O_2 is converted to HOSCN [98, 110]. However, smokers also have high levels of H_2O_2 [491], therefore higher SCN^- may not be protective as a higher conversion of H_2O_2 to HOSCN would be expected compared to HOCl [98, 110]. Elevated plasma SCN^- have been linked to accelerated development of atherosclerosis in younger people, with these individuals presenting with greater deposition of oxidised LDL and increased formation of fatty streaks in the aortae [111]. As previously discussed, individuals with higher concentrations of plasma SCN^- have been suggested to enzymatically convert this to HOSCN, which targets thiols and cysteine residues, and results in MPO-induced depletion of thiols [99]. Reaction of HOSCN with certain key Cys residues can lead to enzyme inhibition e.g. of protein Tyr phosphatase enzymes, and modulate cell signalling [108, 410]. In a previous study, high SCN^- levels were not shown to be correlated with atherosclerosis but rather showed correlation with increased carbamylation [112]. This process is linked to increased levels of OCN^-, which is formed by decomposition of HOSCN [112, 492]. Carbamylation has been found to target lysine residues leading to formations of homocitrulline, and found to have several detrimental effects during the development of atherosclerosis (e.g. dysfunction of HDL) [112, 113].

Reaction of high levels of HOSCN with thiols has been reported to cause high levels of irreversible products, such as cysteic acid, via over-oxidation of thiols [106]. High levels of HOSCN has also been shown to be particularly detrimental by inducing protein thiol depletion and promoting apoptosis in murine macrophage cells with corresponding increased levels of cytochrome c being released into the cytosol [374]. Furthermore, treatment with HOSCN led to a higher number of necrotic cells in comparison to controls

and treatment with the same concentration of HOCl or HOBr [374]. Plasma SCN^- levels have been reported to be inversely proportionate to 3-chloroTyr concentrations on plasma proteins, which is a common biomarker for HOCl oxidation [367]. This coincided with a reduction in di-Tyr levels, and this was found to be significant in both smokers and non-smokers [367]. It is known that HOCl is converted to HOSCN when there is a high concentration of SCN^- [92], this may lead to a skewing of oxidative biomarker levels such as 3-chloroTyr, where humans or animals with elevated levels of SCN^- would have lower plasma levels of 3-chloroTyr biomarker [367].

Although SCN^- has been found to detrimentally impact certain proteins and enzymatic processes [94, 371], there have been studies showing that certain concentrations of SCN^- can have a somewhat protective mechanism [22, 98, 367]. This protective mechanism of SCN^- has been linked to low levels of MPO, and results in a decreased mortality rate [99]. Low levels of MPO were found to produce lower levels of oxidation overall with high levels of SCN^- favouring the generation of HOSCN, a less reactive oxidant, over the more reactive HOCl [99]. Low levels of HOSCN has been found to cause readily reversible Cys-derived species, such as RS-SCN adducts, sulfenic acids, and disulfides [106, 370]. These species are repairable by GSH and redox enzymes including glutaredoxins and thioredoxin reductase [106, 370]. Reversible thiols were more readily formed at low levels of HOSCN in cells as they possess high levels of protein thiols and GSH [493]. However, low levels of free thiols are present in the extracellular fluids with less than 10 μM of low molecular mass, and as low as 600-700 μM on proteins [99, 367]. This may mean that with higher concentrations of HOSCN, there is a greater likelihood that oxidation of extracellular thiols may lead to irreversible products by over oxidation and also damage to other amino acid side chains.

HOCl, a more reactive oxidant is known to target several amino acid chains leading to highly modified peptides [50, 51]. Increased levels of SCN^- and hence HOSCN have been found to reduce damage on non-thiol targets on BSA, in comparison to HOCl at physiological concentrations [367]. Met, Trp and Tyr residues, which are targets of HOCl,

were found to be protected, along with Lys and His residues [367]. Increased HOSCN formation has also been suggested to be biologically relevant, leading to reduced cell cytoxicity (e.g. to EC, pancreatic cells, and a neuronal cell line) caused by HOCl, and to protect against inflammatory diseases, such as cystic fibrosis [93]. Inhibition of apoptosis and caspase 3 has been reported in human EC at low HOSCN doses, further supporting the proposed protective mechanism afforded by this oxidant [494]. The protective capability of HOSCN is highly reliant on the levels of MPO, SCN^-, and redox enzymes that are able to repair the reversible damage, such as glutaredoxin, thioredoxin reductase, and protein disulfide isomerases [495]. SCN^- supplementation may therefore help in decreasing the necessity for invasive treatments such as percutaneous coronary intervention (PCI) [496], or coronary artery bypass grafting (CABG) [497], and subsequently reduce the risk of advanced atherosclerosis. However, these studies are preliminary and only show this protective mechanism to be present at lower concentrations of SCN^-. Elevated levels of SCN^- and long exposure to HOSCN were found to be detrimental rather than protective. Therefore, further investigations are needed to define the appropriate range of SCN^- that is protective rather than damaging in humans.

There are also other possible therapeutics that are currently being studied such as I^- [128], which is another MPO substrate found at very low concentrations in the body [27], and seleno-compounds [498]. The second-order rate constant of the reduction of MPO compound I by I^- is $7.2 \pm 0.7 \times 10^6$ M^{-1} s^{-1}, which is close to that of SCN^- of $9.6 \pm 0.5 \times 10^6$ M^{-1} s^{-1} [27]. These rates are much higher than for Cl^-, which is $2.5 \pm 0.3 \times 10^4$ M^{-1} s^{-1} [27]. There are few studies examining oxidation of I^- to HOI by MPO and the subsequent effects of HOI. One study examining the effects of HOCl and halides showed that the MPO/Cl^-/H_2O_2 system oxidised 2'-deoxyguanosine (dG) [128]. Addition of increasing concentrations of I^- (> 1 μM) attenuated this consumption of dG by MPO/Cl^-/H_2O_2 [128]. However, the typical physiological concentration of I^- within the body is < 1 μM, so the relevance of these higher levels of I^- is not known [27]. Ischemic reperfusion (IR) injury occurs after a heart attack and is known to produce an inflammatory response and

recruitment of MPO releasing leukocytes [499, 500]. A recent study has reported that I^- supplementation can significantly reduce heart damage, characterised by a reduction in infarct volume and decreased myocardial infarct protein troponin-1 [501]. Elevated levels of I^- may therefore be a possible treatment that can modulate the development of severity of atherosclerosis, but clearly further investigations are needed due to limited studies thus far.

Another therapeutic approach that has been studied recently is seleno-containing compounds [498]. Sulfur-containing side chains, such as thiols and thioethers residues, are readily targeted by MPO-derived oxidants and downstream materials such as *N*-chloramines [50]. It is known that HOCl and HOSCN have a greater reactivity with selenium species compared to their sulfur analogues [138, 502], and the oxidation products from these selenium species are more readily reversible than their sulphur counterparts [137, 138, 503, 504]. It has been reported that seleno-methionine (SeMet) was effective at scavenging HOCl, and was also reactive with *N*-chloramine species [498]. Furthermore, the product from SeMet - the corresponding selenoxide (SeMetO) has been reported to be readily reduced by endogenous thiols such as GSH [503, 505]. Selenocysteine containing thioredoxin has been observed to be resistant to over-oxidation and are readily reversible unlike their sulfur counterparts [137, 138]. This suggests that selenium-containing compounds may play a role in scavenging biologically relevant HOCl and *N*-chloramines and reduce cellular damage during inflammation in inflammatory diseases, such as atherosclerosis.

High levels of MPO plays a major role in the progression of atherosclerosis [37], therefore there has been recent studies investigating inhibition of MPO as possible therapeutics [506, 507]. There are several types of MPO inhibitors but most aim to inhibit the active sites and prevent the generation of more damaging oxidants [508, 509]. Hydroxamates have been previously studied as a potential inhibitor of MPO activity but were found to poorly inhibit MPO activity [510]. Recent studies investigated the effects of substituted aromatic hydroxamates to examine their inhibitory performance on MPO [506]. It

was observed that higher binding affinity between MPO and substituted aromatic hydroxamates resulted in inhibition of the MPO halogenation cycle, thus inhibiting generation of oxidants [506]. An irreversible target inhibitor currently being investigated is PF-1355 (Pfizer), which has been found to decrease plasma MPO activity in peritonitis and vasculitis [507]. These studies have primarily been conducted *in vitro* or in mice models, thus further investigations are needed before human application.

There is on-going research investigating these possible therapeutics amongst others. Perhaps a combination of life style changes based on these recent findings may help to decrease the severity of CVD and subsequently reduce the risk of heart attacks and strokes as a consequence of atherosclerosis.

7.5 Concluding remarks

The studies in this Thesis provides an insight into the reaction between MPO-derived oxidants, HOCl and HOSCN, on ECM protein, FN. It has been shown that human plasma FN and HCAEC-derived whole ECM were structurally modified by what is believed to be physiologically relevant concentrations of HOCl and HOSCN (reagent and within an MPO/halide/H_2O_2 system) resulting in important functional domains becoming modified and unrecognisable by specific antibodies. Moreover, exposure of human plasma FN to reagent HOCl and MPO/Cl^-/H_2O_2 system was observed to form a HOCl-generated epitope recognised by antibody clone 2D10G9.

Structural modifications to human plasma FN exposed to MPO-derived oxidants were observed to impair biological function. Reagent HOCl and MPO/Cl^-/H_2O_2 were both observed to modify the human plasma FN leading to a reduction in HCAEC adhesion and HCAEC metabolic activity, likely due to changes to the functional CBF. Furthermore, exposure of HCAEC to HOCl- and HOSCN-modified FN resulted in different gene expressions compared to HCAEC exposed to non-treated (native) human plasma FN. However, exposure of human plasma FN to HOSCN or enzymatic MPO/SCN^-/H_2O_2 system also resulted in minor structural modifications but to a lesser extent compared to the more reactive HOCl. In the competitive study, the addition of SCN^- to MPO/Cl^-/H_2O_2 system was observed to attenuate some modifications and damage occurring from exposure to HOCl likely generated from the MPO/Cl^-/H_2O_2. This suggests that FN is targeted and modified by MPO-derived oxidants with low to moderate levels of SCN^- possibly being capable of reducing the severity of modifications. It is clear that further investigations are needed to fully elucidate the mechanism of damage and the relationship between FN, HOCl, and HOSCN.

These studies contribute greatly to the current knowledge of oxidative damage to ECM proteins by MPO-derived oxidants, HOCl and HOSCN. Developing an understanding of the role of native and modified FN in mediating endothelial dysfunction, and the factors

that modulate vascular remodelling could greatly expand the current knowledge about the progression of atherosclerosis. Furthermore, by elucidating the role and relationship between FN and MPO-derived oxidants, perhaps a novel therapeutic target could be identified. This could subsequently lead to a decreased risk of vulnerable plaque rupture or erosion by formation of more stable plaques, and thus reduction in the occurrences of myocardial infarction and strokes.

7.6 Appendix

Table 7.1: **All gene expressions of HCAEC incubated on human plasma FN (0.04 μM) pre-treated with a 1250x molar ratio (50 μM) of HOCl or HOSCN.**

Genes	Fold Regulation	*P*-Value	Fold Regulation	*P*-Value
ADAMTS1	1.20	0.062	-1.24	0.138
ADAMTS13	-2.00	0.008*	-1.52	0.009*
ADAMTS8	1.55	0.404	1.59	0.196
CD44	1.04	0.718	-1.01	0.861
CDH1	-3.06	0.263	1.04	0.781
CLEC3B	1.12	3.81	2.82	0.961
CNTN1	-2.47	0.353	-1.86	0.413
COL11A1	-1.29	0.913	1.79	0.345
COL12A1	-5.09	0.011*		
COL14A1	1.89	0.320	-1.16	0.848
COL15A1	-1.07	0.526	1.37	0.26
COL16A1	-1.91	0.124	1.13	0.376
COL1A1	-1.07	0.526	1.37	0.426
COL4A2	1.08	0.912	1.25	0.539
COL5A1	-1.30	0.005*	-1.23	0.009*
COL6A1	-1.86	0.022*	1.25	0.176
COL6A2	-1.10	0.588	1.42	0.634
COL7A1	1.02	0.960	1.60	0.652
COL8A1	-1.12	1.79	-1.12	0.147
CTGF	-1.12	0.009*	-1.12	0.147
CTNNA1	-1.24	0.020*	-1.17	0.019*
CTNNB1	-1.39	0.018*	-1.15	0.66
CTNND1	-1.21	0.048*	-1.13	0.119
CTNND2	-1.07	0.526	-1.07	0.517
ECM1	-1.88	0.026*	-1.08	0.560
FN1	-1.26	0.007*	-1.25	0.002*
HAS1	-3.69	0.076	-1.44	0.295
ICAM1	-1.01	0.989	1.03	0.691
ITGA1	-1.26	0.162	-1.10	0.422
ITGA2	-1.24	0.026*	-1.42	0.110
ITGA3	-1.09	0.084	-1.18	0.271
ITGA4	1.69	0.008*	-1.17	0.549
ITGA5	-1.29	0.202	1.07	0.276
ITGA6	1.09	0.127	1.01	0.799
ITGA7	-3.90	0.046*	-1.92	0.211
ITGA8	1.98	0.404	-1.22	0.389
ITGAL	-2.01	0.388	1.62	0.814
ITGAM	-3.71	0.126	-1.25	0.616
ITGAV	-1.11	0.309	-1.25	0.127
ITGB1	-1.15	0.174	1.05	0.350
ITGB2	-1.34	0.583	-6.79	0.536
ITGB3	-1.81	0.003*	-1.00	0.981
ITGB4	-3.10	<0.001*	-1.05	0.703
ITGB5	-1.06	0.376	-1.06	0.481
ANOS1	7.86	0.0.333	-1.07	0.517

Genes	Fold Regulation	*P*-Value	Fold Regulation	*P*-Value
LAMA1	-1.07	0.526	-1.07	0.517
LAMA2	-1.56	0.045*	-1.47	0.451
LAMA3	-1.01	0.911	-1.19	0.407
LAMB1	-1.24	0.055	-1.19	0.064
LAMB3	-1.12	0.115	-1.17	0.192
LAMC1	-1.30	0.113	-1.13	0.435
MMP1	1.33	0.021*	1.02	0.583
MMP10	-1.05	0.454	1.07	0506.
MMP11	-1.89	<0.001*	-1.20	0.212
MMP12	3.11	0.512	-1.07	0.392
MMP13	-10.12	0.150	-9.02	0.152
MMP14	-1.46	0.061	-1.35	0.226
MMP15	-1.51	0.259	-1.03	0.876
MMP16	-1.26	0.104	-1.19	0.159
MMP2	-1.35	0.002*	1.00	0.945
MMP3	-2.13	0.245	-3.60	0.112
MMP7	-1.58	0.771	-2.03	0.683
MMP8	-3.14	0.129	-9.58	0.050*
MMP9	-2.58	0.239	-2.27	0.316
NCAM1	2.36	0.553	-2.56	0.397
PECAM1	-1.08	0.393	1.16	0.280
SELE	1.91	0.004*	-1.06	0.615
SELL	-5.39	<0.001*	-1.56	0.009*
SELP	-5.37	<0.001	-1.44	0.039*
SGCE	-1.03	0.693	1.17	0.069
SPARC	-1.00	0.943	+1.18	0.045*
SPG7	-1.17	0.002*	-1.06	0.479
SPP1	1.05	0.526	-1.07	0.517
TGFBI	1.05	0.781	1.02	0.972
THBS1	-1.03	0.834	-1.10	0.413
THBS2	-1.86	0.023*	-1.11	0.679
THBS3	-1.76	0.016*	-1.31	0.145
TIMP1	-1.58	0.002*	-1.07	0.456
TIMP2	-1.52	0.004*	-1.10	0.247
TIMP3	1.46	0.499	1.92	0.285
TNC	1.18	0.500	1.06	0.706
VCAM1	-1.22	0.348	-1.07	0.512
VCAN	-1.47	0.021*	-1.03	0.702
VTN	-1.08	0.811	-2.79	0.171

Table 7.2: **Gene expressions that were up- or down-regulated of HCAEC incubated on human plasma FN (0.04 μM) pre-treated with a 1250x molar ratio (50 μM) of HOCl or HOSCN.**

Genes	Function	Fold Regulation	*P*-Value	Fold Regulation	*P*-Value
ADAMTS13	von Willebrand factor-cleaving protease	-2.00	0.008*	-1.52	0.009*
COL12A1	Interaction between collagen I fibrils and matrix	-5.09	0.011*		
COL5A1	Type V collagen pro-α1(V) chain chain	-1.30	0.005*	-1.23	0.009*
COL6A1	Type VI α1(VI) chain	-1.86	0.022*		
CTGF	Connective Tissue Growth Factor	-1.12	0.009*		
CTNNA1	Plays a role in cell adhesion	-1.24	0.020*	-1.17	0.019*
CTNNB1	Adherens conunctions protein	-1.39	0.018*		
CTNND1	Armadillo protein for signal transduction adhesion	-1.21	0.048*		
ITGA2	Integrin α2 partial chain receptor to ECM proteins	-1.24	0.026*		
ITGA4	Integrin α4 partial chain receptor for FN	1.69	0.008*		
ITGA7	Integrin α7 partial chain laminin	-3.90	0.046*		
ITGB3	Integrin β3 partial chain for ECM & cell adhesion	-1.81	0.003*		
ITGB4	Integrin β4 partial chain for laminin	-3.10	<0.001*		
MMP1	Cleaves collagen	1.33	0.021*		
MMP8	Degrades fibrillar type I, II, and III collagens.			-9.58	0.050*
MMP11	Weakly degrades ECM; control of cell proliferation	-1.89	<0.001*		
MMP2	Degrades ECM and signal transduction molecules	-1.35	0.002*		
SELE	CAM important in inflammation	1.91	0.004*		
SELL	CAM between ECs and lymphocytes	-5.39	<0.001*	-1.56	0.009*
SELP	CAM on ECs	-5.37	<0.001	-1.44	0.039*
SPG7	Paraplegin; regulator of cell and proteins	-1.17	0.002*		
THBS2	cell-cell & cell-matrix interactions	-1.86	0.023*		
THBS3	cell-cell & cell-matrix interactions	-1.76	0.016*		
TIMP1	MMP inhibitor	-1.58	0.002*		
TIMP2	MMP & EC proliferation	-1.52	0.004*		
ECM1	ECM formation & angiogenesis	-1.88	0.026*		
FN1	Formation of plasma & cellular FN	-1.26	0.007*	-1.25	0.002*
LAMA2	Laminin α2 chain	-1.56	0.045*		
VCAN	Versican protein	-1.47	0.021*		
SPARC	Regulates cell growth via interaction with ECM and cytokines			+1.18	0.045*

Bibliography

1. Lusis, A. J. Atherosclerosis. *Nature* **407,** 233–241 (2000).
2. Lawrence, G. D. Dietary Fats and Health : Dietary Recommendations in the Context of Scientific Evidence. *Advances in Nutrition* **4,** 294–302 (2013).
3. Parthasarathy, S., Raghavamenon, A., Garelnabi, M. O. & Santanam, N. Oxidized Low-Density Lipoprotein. *Methods in Molecular Biology* **610,** 403–417 (2010).
4. Yoshida, H. & Kisugi, R. Mechanisms of LDL oxidation. *Clinica Chimica Acta* **411,** 1875–1882 (2010).
5. Mitra, S., Goyal, T. & Mehta, J. L. Oxidized LDL, LOX-1 and atherosclerosis. *Cardiovascular Drugs and Therapy* **25,** 419–429 (2011).
6. Upston, J. M. *et al.* Disease Stage-Dependent Accumulation of Lipid and Protein Oxidation Products in Human Atherosclerosis. *The American Journal of Pathology* **160,** 701–710 (2002).
7. Goldstein, J. L., Ho, Y. K., Basu, S. K. & Brown, M. S. Binding site on macrophages that mediates uptake and degradation of acetylated low density lipoprotein, producing massive cholesterol deposition. *Proceedings of the National Academy of Sciences of the United States of America* **76,** 333–337 (1979).
8. Hazell, L. J. *et al.* Presence of hypochlorite-modified proteins in human atherosclerotic lesions. *Journal of Clinical Investigation* **97,** 1535–1544 (1996).
9. Miller, Y. I., Choi, S. H., Fang, L. & Tsimikas, S. Lipoprotein modification and macrophage uptake: role of pathologic cholesterol transport in atherogenesis. *Subcellular biochemistry* **51,** 229–251 (2010).
10. Virmani, R., Kolodgie, F. D., Burke, A. P., Farb, A. & Schwartz, S. M. Lessons From Sudden Coronary Death. *Arteriosclerosis, Thrombosis, and Vascular Biology* **20,** 1262–1275 (2000).
11. Kataoka, Y. *et al.* Myeloperoxidase levels predict accelerated progression of coronary atherosclerosis in diabetic patients: Insights from intravascular ultrasound. *Atherosclerosis* **232,** 377–383 (2014).
12. Taniyama, Y. & Griendling, K. K. Reactive oxygen species in the vasculature: molecular and cellular mechanisms. *Hypertension* **42,** 1075–1081 (2003).
13. Nicholls, S. J. & Hazen, S. L. Myeloperoxidase and cardiovascular disease. *Arteriosclerosis, Thrombosis, and Vascular Biology* **25,** 1102–1111 (2005).
14. Bennett, M. R., Sinha, S. & Owens, G. K. Vascular Smooth Muscle Cells in Atherosclerosis. *Circulation Research* **118,** 692–702 (2016).
15. Hansson, G. K. & Hermansson, A. The immune system in atherosclerosis. *Nature Immunology* **12,** 204–212 (2011).

16. Gimbrone, M. A. & García-Cardeña, G. Endothelial Cell Dysfunction and the Pathobiology of Atherosclerosis. *Circulation Research* **118,** 620–636 (2016).

17. Tarnawski, R., Tarnawski, R. & Grobelny, J. Changes in elastin in human atherosclerotic aorta: Carbon-13 magic angle sample-spinning NMR studies. *Atherosclerosis* **115,** 27–33 (1995).

18. Chistiakov, D. A., Sobenin, I. A. & Orekhov, A. N. Vascular Extracellular Matrix in Atherosclerosis. *Cardiology in Review* **21,** 270–288 (2013).

19. Thomas, E. L. Myeloperoxidase, hydrogen peroxide, chloride antimicrobial system: Nitrogen-chlorine derivatives of bacterial components in bactericidal action against Escherichia coli. *Infection and Immunity* **23,** 522–531 (1979).

20. McKenna, S. M. & Davies, K. J. The inhibition of bacterial growth by hypochlorous acid. Possible role in the bactericidal activity of phagocytes. *Biochemical Journal* **254,** 685–692 (1988).

21. Baldus, S. *et al.* Endothelial transcytosis of myeloperoxidase confers specificity to vascular ECM proteins as targets of tyrosine nitration. *Journal of Clinical Investigation* **108,** 1759–1770 (2001).

22. Rees, M. D. *et al.* Targeted subendothelial matrix oxidation by myeloperoxidase triggers myosin II-dependent de-adhesion and alters signaling in endothelial cells. *Free Radical Biology and Medicine* **53,** 2344–2356 (2012).

23. Fiedler, T. J., Davey, C. A. & Fenna, R. E. X-ray crystal structure and characterization of halide-binding sites of human myeloperoxidase at 1.8 A resolution. *Journal of Biological Chemistry* **275,** 11964–11971 (2000).

24. Bolscher, B. G. & Wever, R. A kinetic study of the reaction between human myeloperoxidase, hydroperoxides and cyanide. Inhibition by chloride and thiocyanate. *Biochimica et Biophysica Acta* **788,** 1–10 (1984).

25. Furtmuller, P. G., Burner, U, Jantschko, W, Regelsberger, G & Obinger, C. Two-electron reduction and one-electron oxidation of organic hydroperoxides by human myeloperoxidase. *FEBS Letters* **484,** 139–143 (2000).

26. Davies, M. J. Myeloperoxidase-derived oxidation: mechanisms of biological damage and its prevention. *Journal of Clinical Biochemistry and Nutrition* **48,** 8–19 (2011).

27. Furtmuller, P. G., Burner, U. & Obinger, C. Reaction of myeloperoxidase compound I with chloride, bromide, iodide, and thiocyanate. *Biochemistry* **37,** 17923–17930 (1998).

28. Acharya, K. R. & Ackerman, S. J. Eosinophil granule proteins: form and function. *Journal of Biological Chemistry* **289,** 17406–17415 (2014).

29. Ihalin, R., Loimaranta, V. & Tenovuo, J. Origin, structure, and biological activities of peroxidases in human saliva. *Archives of Biochemistry and Biophysics* **445,** 261–268 (2006).

30. Van Dalen C Kettle A. Substrates and products of eosinophil peroxidase. *The Biochemical Journal* **358,** 233–239 (2001).

31. Winterbourn, C. C., Parsons-Mair, H. N., Gebicki, S., Gebicki, J. M. & Davies, M. J. Requirements for superoxide-dependent tyrosine hydroperoxide formation in peptides. *Biochemical Journal* **381,** 241–248 (2004).

32. Winterbourn, C. C. & Kettle, A. J. Redox Reactions and Microbial Killing in the Neutrophil Phagosome. *Antioxidants & Redox Signaling* **18,** 642–660 (2013).

33. Lau, D. & Baldus, S. Myeloperoxidase and its contributory role in inflammatory vascular disease. *Pharmacology and Therapeutics* **111,** 16–26 (2006).

34. Pitanga, T. *et al.* Neutrophil-derived microparticles induce myeloperoxidase-mediated damage of vascular endothelial cells. *BMC Cell Biology* **15,** 21 (2014).

35. Heinecke, J. W., Li, W., Francis, G. A. & Goldstein, J. A. Tyrosyl radical generated by myeloperoxidase catalyzes the oxidative cross-linking of proteins. *Journal of Clinical Investigation* **91,** 2866–2872 (1993).

36. Brennan, M. L. & Hazen, S. L. Amino acid and protein oxidation in cardiovascular disease. *Amino Acids* **25,** 365–374 (2003).

37. Ndrepepa, G. *et al.* Myeloperoxidase level in patients with stable coronary artery disease and acute coronary syndromes. *European Journal of Clinical Investigation* **38,** 90–96 (2008).

38. Zhang, R. *et al.* Association between myeloperoxidase levels and risk of coronary artery disease. *The Journal of the American Medical Association* **286,** 2136–2142 (2001).

39. Kutter, D *et al.* Consequences of total and subtotal myeloperoxidase deficiency: risk or benefit ? *Acta Haematologica* **104,** 10–5 (2000).

40. Ferrante, G. *et al.* High levels of systemic myeloperoxidase are associated with coronary plaque erosion in patients with acute coronary syndromes: A clinicopathological study. *Circulation* **122,** 2505–2513 (2010).

41. Niccoli, G., Dato, I. & Crea, F. Myeloperoxidase May Help to Differentiate Coronary Plaque Erosion From Plaque Rupture in Patients With Acute Coronary Syndromes. *Trends in Cardiovascular Medicine* **20,** 276–281 (2010).

42. Virmani, R., Burke, V. P. & Farb, A. Plaque rupture and plaque erosion. *Thrombosis and Haemostasis* **82,** 1–3 (1999).

43. Shah, P. K. Pathophysiology of coronary thrombosis: Role of plaque rupture and plaque erosion. *Progress in Cardiovascular Diseases* **44,** 357–368 (2002).

44. Lentner, C. Geigy Scientific Tables, volume 3: Physical Chemistry, Composition of Blood, Hematology, Somatometric Data. *Basel: Ciba-Geigy,* 325 (1984).

45. Albrich, J. M., Gilbaugh, J. H., Callahan, K. B. & Hurst, J. K. Effects of the putative neutrophil-generated toxin, hypochlorous acid, on membrane permeability and transport systems of Escherichia coli. *Journal of Clinical Investigation* **78,** 177–184 (1986).

46. Schraufstatter, I. U. *et al.* Mechanisms of hypochlorite injury of target cells. *Journal of Clinical Investigation* **85,** 554–562 (1990).

47. Prütz, W. A. Hypochlorous acid interactions with thiols, nucleotides, DNA, and other biological substrates. *Archives of Biochemistry and Biophysics* **332,** 110–120 (1996).

48. Winterbourn, C. C. Biological reactivity and biomarkers of the neutrophil oxidant, hypochlorous acid. *Toxicology* **181-182,** 223–227 (2002).

49. Hawkins, C. L., Pattison, D. I. & Davies, M. J. Hypochlorite-induced oxidation of amino acids, peptides and proteins. *Amino Acids* **25,** 259–274 (2003).

50. Pattison, D. I., Davies, M. J. & Hawkins, C. L. Reactions and reactivity of myeloperoxidase-derived oxidants: Differential biological effects of hypochlorous and hypothiocyanous acids. *Free Radical Research* **46,** 975–995 (2012).

51. Storkey, C., Davies, M. J. & Pattison, D. I. Reevaluation of the rate constants for the reaction of hypochlorous acid (HOCl) with cysteine, methionine, and peptide derivatives using a new competition kinetic approach. *Free Radical Biology and Medicine* **73,** 60–66. ISSN: 18734596 (2014).

52. Frijhoff, J. *et al.* Clinical Relevance of Biomarkers of Oxidative Stress. *Antioxidants & Redox Signaling* **23,** 1144–1170 (2015).

53. Mahler, H. C., Friess, W., Grauschopf, U. & Kiese, S. Protein aggregation: Pathways, induction factors and analysis. *Journal of Pharmaceutical Sciences* **98,** 2909–2934 (2009).

54. Amin, S., Barnett, G. V., Pathak, J. A., Roberts, C. J. & Sarangapani, P. S. Protein aggregation, particle formation, characterization & rheology. *Current Opinion in Colloid & Interface Science* **19,** 438–449 (2014).

55. Hazen, S. L., D'Avignon, A., Anderson, M. M., Hsu, F. F. & Heinecke, J. W. Human neutrophils employ the myeloperoxidase-hydrogen peroxide-chloride system to oxidize ??-amino acids to a family of reactive aldehydes: Mechanistic studies identifying labile intermediates along the reaction pathway. *Journal of Biological Chemistry* **273,** 4997–5005 (1998).

56. Winterbourn, C. C. & Kettle, A. J. Biomarkers of myeloperoxidase-derived hypochlorous acid. *Free Radical Biology and Medicine* **29,** 403–409 (2000).

57. Hawkins, C. L., Morgan, P. E. & Davies, M. J. Quantification of protein modification by oxidants. *Free Radical Biology and Medicine* **46,** 965–988 (2009).

58. Pattison, D. I., Hawkins, C. L. & Davies, M. J. Hypochlorous acid-mediated protein oxidation: How important are chloramine transfer reactions and protein tertiary structure? *Biochemistry* **46,** 9853–9864 (2007).

59. Chapman, A. L., Senthilmohan, R., Winterbourn, C. C. & Kettle, A. J. Comparison of Mono- and Dichlorinated Tyrosines with Carbonyls for Detection of Hypochlorous Acid Modified Proteins. *Archives of Biochemistry and Biophysics* **377,** 95–100 (2000).

60. Buss, H., Chan, T. P., Sluis, K. B., Domigan, N. M. & Winterbourn, C. C. Protein carbonyl measurement by a sensitive ELISA method. *Free Radical Biology and Medicine* **23,** 361–366 (1997).

61. Curtis, M. P., Hicks, A. J. & Neidigh, J. W. Kinetics of 3-chlorotyrosine formation and loss due to hypochlorous acid and chloramines. *Chemical Research in Toxicology* **24,** 418–428 (2011).

62. Curtis, M. P. & Neidigh, J. W. Kinetics of 3-nitrotyrosine modification on exposure to hypochlorous acid. *Free Radical Research* **48,** 1355–1362 (2014).

63. Malle, E *et al.* Immunologic Detection and Measurement of Hypochlorite-Modified LDL With Specific Monoclonal Antibodies. *Arteriosclerosis, Thrombosis, and Vascular Biology* **15,** 982–989 (1995).

64. WOODS, A. A., LINTON, S. M. & DAVIES, M. J. Detection of HOCl-mediated protein oxidation products in the extracellular matrix of human atherosclerotic plaques. *Biochemical Journal* **370,** 729–735 (2003).

65. Woods, A. a. & Davies, M. J. Fragmentation of extracellular matrix by hypochlorous acid. *Biochemical Journal* **376,** 219–227 (2003).

66. Fuchs, B. & Schiller, J. Glycosaminoglycan degradation by selected reactive oxygen species. *Antioxidants & Redox Signaling* **21,** 1044–1062 (2014).

67. Rees, M. D. *et al.* Myeloperoxidase-derived oxidants selectively disrupt the protein core of the heparan sulfate proteoglycan perlecan. *Matrix Biology* **29,** 63–73 (2010).

68. Rees, M. D., Pattison, D. I. & Davies, M. J. Oxidation of heparan sulphate by hypochlorite: role of N-chloro derivatives and dichloramine-dependent fragmentation. *Biochemical Journal* **391,** 125–134 (2005).

69. Akeel, A., Sibanda, S., Martin, S. W., Paterson, A. W. J. & Parsons, B. J. Chlorination and oxidation of heparin and hyaluronan by hypochlorous acid and hypochlorite anions: effect of sulfate groups on reaction pathways and kinetics. *Free Radical Biology and Medicine* **56,** 72–88 (2013).

70. Rees, M. D., Hawkins, C. L. & Davies, M. J. Hypochlorite-mediated fragmentation of hyaluronan, chondroitin sulfates, and related N-acetyl glycosamines: evidence for chloramide intermediates, free radical transfer reactions, and site-specific fragmentation. *Journal of the American Chemical Society* **125,** 13719–13733 (2003).

71. Rees, M. D., Hawkins, C. L. & Davies, M. J. Hypochlorite and superoxide radicals can act synergistically to induce fragmentation of hyaluronan and chondroitin sulphates. *Biochemical Journal* **381,** 175–184 (2004).

72. Vissers, M. C., Carr, A. C. & Winterbour, C. C. Fatty acid chlorohydrins and bromohydrins are cytotoxic to human endothelial cells. *Redox Report* **6,** 49–55 (2001).

73. Messner, M. C., Albert, C. J., McHowat, J. & Ford, D. A. Identification of lysophosphatidylcholine-chlorohydrin in human atherosclerotic lesions. *Lipids* **43,** 243–249 (2008).

74. Dever, G., Stewart, L.-J., Pitt, A. R. & Spickett, C. M. Phospholipid chlorohydrins cause ATP depletion and toxicity in human myeloid cells. *FEBS Letters* **540,** 245–250 (2003).

75. Leopold, J. A. & Loscalzo, J. Oxidative risk for atherothrombotic cardiovascular disease. *Free Radical Biology and Medicine* **47,** 1673–1706 (2009).

76. Forstermann, U., Xia, N. & Li, H. Roles of Vascular Oxidative Stress and Nitric Oxide in the Pathogenesis of Atherosclerosis. *Circulation Research* **120,** 713–735 (2017).

77. Steffen, Y. *et al.* Protein modification elicited by oxidized low-density lipoprotein (LDL) in endothelial cells: Protection by (-)-epicatechin. *Free Radical Biology and Medicine* **42,** 955–970. ISSN: 08915849 (2007).

78. Fleming, A. M., Alshykhly, O., Zhu, J., Muller, J. G. & Burrows, C. J. Rates of chemical cleavage of DNA and RNA oligomers containing guanine oxidation products. *Chemical Research in Toxicology* **28,** 1292–1300 (2015).

79. Gajewski, E., Rao, G., Nackerdien, Z. & Dizdaroglu, M. Modification of DNA bases in mammalian chromatin by radiation-generated free radicals. *Biochemistry* **29,** 7876–7882 (1990).

80. Hawkins, C. L. & Davies, M. J. Hypochlorite-induced damage to DNA, RNA, and polynucleotides: formation of chloramines and nitrogen-centered radicals. *Chemical Research in Toxicology* **15,** 83–92 (2002).

81. Kong, Q. & Lin, C.-L. G. Oxidative damage to RNA: mechanisms, consequences, and diseases. *Cellular and Molecular Life sciences : CMLS* **67,** 1817–1829 (2010).

82. Neeley, W. L. & Essigmann, J. M. Mechanisms of formation, genotoxicity, and mutation of guanine oxidation products. *Chemical Research in Toxicology* **19,** 491–505 (2006).

83. Martinet, W., Knaapen, M. W. M., De Meyer, G. R. Y., Herman, A. G. & Kockx, M. M. Elevated Levels of Oxidative DNA Damage and DNA Repair Enzymes in Human Atherosclerotic Plaques. *Circulation* **106,** 927 LP –932 (2002).

84. Martinet, W, de Meyer, G. R. Y., Herman, A. G. & Kockx, M. M. Reactive oxygen species induce RNA damage in human atherosclerosis. *European Journal of Clinical Investigation* **34,** 323–327 (2004).

85. Martinet, W., De Meyer, G. R. Y., Herman, A. G. & Kockx, M. M. Amino acid deprivation induces both apoptosis and autophagy in murine C2C12 muscle cells. *Biotechnology letters* **27,** 1157–1163 (2005).

86. Salvayre, R, Negre-Salvayre, A & Camare, C. Oxidative theory of atherosclerosis and antioxidants. *Biochimie* **125,** 281–296 (2016).

87. Peskin, A. V. & Winterbourn, C. C. Kinetics of the reactions of hypochlorous acid and amino acid chloramines with thiols, methionine, and ascorbate. *Free Radical Biology and Medicine* **30,** 572–579 (2001).

88. Carr, A. C. & Winterbourn, C. C. Oxidation of neutrophil glutathione and protein thiols by myeloperoxidase-derived hypochlorous acid. *Biochemical Journal* **327,** 275–281 (1997).

89. Pullar, J. M., Winterbourn, C. C. & Vissers, M. C. Loss of GSH and thiol enzymes in endothelial cells exposed to sublethal concentrations of hypochlorous acid. *The American Journal of Pathology* **277,** H1505–12 (1999).

90. Rodriguez-Mateos, A. *et al.* Bioavailability, bioactivity and impact on health of dietary flavonoids and related compounds: an update. *Archives of Toxicology* **88,** 1803–1853 (2014).

91. Krych-Madej, J., Stawowska, K. & Gebicka, L. Oxidation of flavonoids by hypochlorous acid: reaction kinetics and antioxidant activity studies. *Free Radical Research* **50,** 898–908 (2016).

92. Ashby, M. T., Carlson, A. C. & Scott, M. J. Redox buffering of hypochlorous acid by thiocyanate in physiologic fluids. *Journal of the American Chemical Society* **126,** 15976–15977 (2004).

93. Xu, Y., Szep, S. & Lu, Z. The antioxidant role of thiocyanate in the pathogenesis of cystic fibrosis and other inflammation-related diseases. *Proceedings of the National Academy of Sciences of the United States of America* **106,** 20515–20519 (2009).

94. Hawkins, C. L. The role of hypothiocyanous acid (HOSCN) in biological systems. *Free Radical Research* **43,** 1147–1158 (2009).

95. Chandler, J. D. & Day, B. J. Thiocyanate: A potentially useful therapeutic agent with host defense and antioxidant properties. *Biochemical Pharmacology* **84,** 1381–1387 (2012).

96. Tsuge, K., Kataoka, M. & Seto, Y. Cyanide and Thiocyanate Levels in Blood and Saliva of Healthy Adult Volunteers. *Journal of Health Science* **46,** 343–350 (2000).

97. A Rubab, Z. & Rahman, M. A. Serum thiocyanate levels in smokers, passive smokers and never smokers. *The Journal of the Pakistan Medical Association* **56,** 323–326 (2006).

98. Morgan, P. E. *et al.* High plasma thiocyanate levels in smokers are a key determinant of thiol oxidation induced by myeloperoxidase. *Free Radical Biology and Medicine* **51,** 1815–1822 (2011).

99. Nedoboy, P. E. *et al.* High plasma thiocyanate levels are associated with enhanced myeloperoxidase-induced thiol oxidation and long-term survival in subjects following a first myocardial infarction. *Free Radical Research* **48,** 1256–1266 (2014).

100. Thomas, E. L. & Aune, T. M. Lactoperoxidase, peroxide, thiocyanate antimicrobial system: correlation of sulfhydryl oxidation with antimicrobial action. *Infection and Immunity* **20,** 456–463 (1978).

101. Nagy, P., Jameson, G. N. L. & Winterbourn, C. C. Kinetics and mechanisms of the reaction of hypothiocyanous acid with 5-thio-2-nitrobenzoic acid and reduced glutathione. *Chemical Research in Toxicology* **22,** 1833–1840 (2009).

102. Hawkins, C. L., Pattison, D. I., Stanley, N. R. & Davies, M. J. Tryptophan residues are targets in hypothiocyanous acid-mediated protein oxidation. *Biochemical Journal* **414,** 271–280 (2008).

103. Barrett, T. J. & Hawkins, C. L. Hypothiocyanous acid: benign or deadly? *Chemical Research in Toxicology* **25,** 263–273 (2012).

104. Alguindigue Nimmo, S. L., Lemma, K. & Ashby, M. T. Reactions of cysteine sulfenyl thiocyanate with thiols to give unsymmetrical disulfides. *Heteroatom Chemistry* **18,** 467–471 (2007).

105. Winterbourn, C. C. & Hampton, M. B. Thiol chemistry and specificity in redox signaling. *Free Radical Biology and Medicine* **45,** 549–561 (2008).

106. Barrett, T. J. *et al.* Inactivation of thiol-dependent enzymes by hypothiocyanous acid: Role of sulfenyl thiocyanate and sulfenic acid intermediates. *Free Radical Biology and Medicine* **52,** 1075–1085 (2012).

107. Poole, L. B. The basics of thiols and cysteines in redox biology and chemistry. *Free Radical Biology and Medicine* **80,** 148–157. ISSN: 1873-4596 (Electronic) (2015).

108. Lane, A. E., Tan, J. T. M., Hawkins, C. L., Heather, A. K. & Davies, M. J. The myeloperoxidase-derived oxidant HOSCN inhibits protein tyrosine phosphatases and modulates cell signalling via the mitogen-activated protein kinase (MAPK) pathway in macrophages. *Biochemical Journal* **430,** 161–169 (2010).

109. Bozonet, S. M., Scott-Thomas, A. P., Nagy, P. & Vissers, M. C. M. Hypothiocyanous acid is a potent inhibitor of apoptosis and caspase 3 activation in endothelial cells. *Free Radical Biology and Medicine* **49,** 1054–1063 (2010).

110. Van Dalen, C. J., Whitehouse, M. W., Winterbourn, C. C. & Kettle, A. J. Thiocyanate and chloride as competing substrates for myeloperoxidase. *Biochemical Journal* **327 (Pt 2,** 487–492 (1997).

111. Scanlon, C. E., Berger, B, Malcom, G & Wissler, R. W. Evidence for more extensive deposits of epitopes of oxidized low density lipoprotein in aortas of young people with elevated serum thiocyanate levels. PDAY Research Group. *Atherosclerosis* **121,** 23–33 (1996).

112. Wang, Z. *et al.* Protein carbamylation links inflammation, smoking, uremia and atherogenesis. *Nature Medicine* **13,** 1176–1184 (2007).

113. Holzer, M. *et al.* Protein carbamylation renders high-density lipoprotein dysfunctional. *Antioxidants & Redox Signaling* **14,** 2337–2346 (2011).

114. Morgan, P. E., Laura, R. P., Maki, R. A., Reynolds, W. F. & Davies, M. J. Thiocyanate supplementation decreases atherosclerotic plaque in mice expressing human myeloperoxidase. *Free Radical Research* **49,** 743–749 (2015).

115. Vissers, M. C. & Winterbourn, C. C. Oxidative damage to fibronectin. II. The effect of H2O2 and the hydroxyl radical. *Archives of Biochemistry and Biophysics* **285,** 357–364 (1991).

116. Morgan, P. E., Pattison, D. I. & Davies, M. J. Quantification of hydroxyl radical-derived oxidation products in peptides containing glycine, alanine, valine, and proline. *Free Radical Biology and Medicine* **52,** 328–339 (2012).

117. Klebanoff, S. J. Myeloperoxidase: friend and foe. *Journal of Leukocyte Biology* **77,** 598–625 (2005).

118. Nauseef, W. M. Detection of superoxide anion and hydrogen peroxide production by cellular NADPH oxidases. *Biochimica et Biophysica Acta* **1840,** 757–767 (2014).

119. Winterbourn, C. C. The biological chemistry of hydrogen peroxide. *Methods in Enzymology* **528,** 3–25 (2013).

120. Josephson, R. A., Silverman, H. S., Lakatta, E. G., Stern, M. D. & Zweier, J. L. Study of the mechanisms of hydrogen peroxide and hydroxyl free radical-induced cellular injury and calcium overload in cardiac myocytes. *Journal of Biological Chemistry* **266,** 2354–2361 (1991).

121. Imlay, J. A. Cellular defenses against superoxide and hydrogen peroxide. *Annual Review of Biochemistry* **77,** 755–776 (2008).

122. Attri, P. *et al.* Generation mechanism of hydroxyl radical species and its lifetime prediction during the plasma-initiated ultraviolet (UV) photolysis. *Scientific Reports* **5,** 9332 (2015).

123. Winterbourn, C. C. Comparative reactivities of various biological compounds with myeloperoxidase-hydrogen peroxide-chloride, and similarity of oxidant to hypochlorite. *Biochimica et Biophysica Acta - General Subjects* **840,** 204–210 (1985).

124. Kettle, A. J. & Winterbourn, C. C. Myeloperoxidase: a key regulator of neutrophil oxidant production. *Redox Report* **3,** 3–15 (1997).

125. Pattison, D. I. & Davies, M. J. Kinetic analysis of the reactions of hypobromous acid with protein components: implications for cellular damage and use of 3-bromotyrosine as a marker of oxidative stress. *Biochemistry* **43,** 4799–4809 (2004).

126. Pattison, D. I. & Davies, M. J. Reactions of myeloperoxidase-derived oxidants with biological substrates: gaining chemical insight into human inflammatory diseases. *Current Medicinal Chemistry* **13,** 3271–3290 (2006).

127. Rees, M. D., McNiven, T. N. & Davies, M. J. Degradation of extracellular matrix and its components by hypobromous acid. *Biochemical Journal* **401,** 587–596 (2007).

128. Suzuki, T. & Ohshima, H. *Modification by Fluoride, Bromide, Iodide, Thiocyanate and Nitrite Anions of Reaction of a Myeloperoxidase-H2O2-Cl- System with Nucleosides* **3,** 301–304 (2003).

129. Ferrer-Sueta, G. *et al.* Biochemistry of Peroxynitrite and Protein Tyrosine Nitration. *Chemical Reviews* (2018).

130. Degendorfer, G. *et al.* Peroxynitrite-mediated oxidation of plasma fibronectin. *Free Radical Biology and Medicine* **97,** 602–615 (2016).

131. Chuang, C. Y. *et al.* Oxidation modifies the structure and function of the extracellular matrix generated by human coronary artery endothelial cells. *Biochemical Journal* **459,** 313–322 (2014).

132. Degendorfer, G., Chuang, C. Y., Hammer, A., Malle, E. & Davies, M. J. Peroxynitrous acid induces structural and functional modifications to basement membranes and its key component, laminin. *Free Radical Biology and Medicine* **89,** 721–733 (2015).

133. Leopold, J. A. Antioxidants and coronary artery disease: from pathophysiology to preventive therapy. *Coronary Artery Disease* **26,** 176–183 (2015).

134. Lubrano, V. & Balzan, S. Enzymatic antioxidant system in vascular inflammation and coronary artery disease. *World Journal of Experimental Medicine* **5,** 218–224 (2015).

135. Chandler, J. D., Nichols, D. P., Nick, J. A., Hondal, R. J. & Day, B. J. Selective metabolism of hypothiocyanous acid by mammalian thioredoxin reductase promotes lung innate immunity and antioxidant defense. *Journal of Biological Chemistry* **288,** 18421–18428 (2013).

136. Nordberg, J & Arner, E. S. Reactive oxygen species, antioxidants, and the mammalian thioredoxin system. *Free Radical Biology and Medicine* **31,** 1287–1312 (2001).

137. Snider, G. W., Ruggles, E., Khan, N. & Hondal, R. J. Selenocysteine confers resistance to inactivation by oxidation in thioredoxin reductase: comparison of selenium and sulfur enzymes. *Biochemistry* **52,** 5472–5481 (2013).

138. Skaff, O. *et al.* Selenium-containing amino acids are targets for myeloperoxidase-derived hypothiocyanous acid: determination of absolute rate constants and implications for biological damage. *Biochemical Journal* **441,** 305–316 (2012).

139. Badylak, S. F., Freytes, D. O. & Gilbert, T. W. Extracellular matrix as a biological scaffold material: Structure and function. *Acta Biomaterialia* **5,** 1–13 (2009).

140. Mouw, J. K., Ou, G. & Weaver, V. M. Extracellular matrix assembly: a multiscale deconstruction. *Nature Reviews Molecular Cell Biology* **15,** 771–785 (2014).

141. Lukashev, M. E. & Werb, Z. ECM signalling: Orchestrating cell behaviour and misbehaviour. *Trends in Cell Biology* **8,** 437–441 (1998).

142. LeBleu, V. S., MacDonald, B. & Kalluri, R. Structure and Function of Basement Membranes. *Experimental Biology and Medicine* **232,** 1121–1129 (2007).

143. Badylak, S. F. The extracellular matrix as a scaffold for tissue reconstruction. *Seminars in Cell and Developmental Biology* **13,** 377–383 (2002).

144. Schultz, G. S. & Wysocki, A. Interactions between extracellular matrix and growth factors in wound healing. *Wound Repair and Regeneration* **17,** 153–162 (2009).

145. Dobaczewski, M., Gonzalez-Quesada, C. & Frangogiannis, N. G. The extracellular matrix as a modulator of the inflammatory and reparative response following myocardial infarction. *Journal of Molecular and Cellular Cardiology* **48,** 504–511 (2010).

146. Sorokin, L. The impact of the extracellular matrix on inflammation. *Nature Reviews Immunology* **10,** 712–723 (2010).

147. Chiang, H. Y., Korshunov, V. A., Serour, A., Shi, F. & Sottile, J. Fibronectin is an important regulator of flow-induced vascular remodeling. *Arteriosclerosis, Thrombosis, and Vascular Biology* **29,** 1074–1079 (2009).

148. Xu, J. & Shi, G.-P. Vascular wall extracellular matrix proteins and vascular diseases. *Biochimica et Biophysica Acta - Molecular Basis of Disease* **1842,** 2106–2119 (2014).

149. Singh, P., Carraher, C. & Schwarzbauer, J. E. Assembly of fibronectin extracellular matrix. *Annual Review of Cell and Developmental Biology* **26,** 397–419 (2010).

150. Lu, P., Takai, K., Weaver, V. M. & Werb, Z. Extracellular Matrix degradation and remodeling in development and disease. *Cold Spring Harbor Perspectives in Biology* **3** (2011).

151. Bonnans, C., Chou, J. & Werb, Z. Remodelling the extracellular matrix in development and disease. *Nature Reviews Molecular Cell Biology* **15,** 786–801 (2014).

152. Rees, M. D., Kennett, E. C., Whitelock, J. M. & Davies, M. J. Oxidative damage to extracellular matrix and its role in human pathologies. *Free Radical Biology and Medicine* **44,** 1973–2001 (2008).

153. Noble, P. W. & Jiang, D. Matrix regulation of lung injury, inflammation, and repair: the role of innate immunity. *Proceedings of the American Thoracic Society* **3,** 401–404 (2006).

154. Karsdal, M. A. *et al.* Extracellular Matrix Remodeling: The Common Denominator in Connective Tissue Diseases Possibilities for Evaluation and Current Understanding of the Matrix as More Than a Passive Architecture, but a Key Player in Tissue Failure. *ASSAY and Drug Development Technologies* **11,** 70–92 (2013).

155. Yurdagul, A., Finney, A. C., Woolard, M. D. & Orr, A. W. The arterial microenvironment: the where and why of atherosclerosis. *Biochemical Journal* **473,** 1281–1295 (2016).

156. Gandhi, N. S. & Mancera, R. L. The structure of glycosaminoglycans and their interactions with proteins. *Chemical Biology & Drug Design* **72,** 455–482 (2008).

157. Iozzo, R. V. & Schaefer, L. Proteoglycan form and function: A comprehensive nomenclature of proteoglycans. *Matrix Biology* **42,** 11–55 (2015).

158. Pantazaka, E. & Papadimitriou, E. Chondroitin sulfate-cell membrane effectors as regulators of growth factor-mediated vascular and cancer cell migration. *Biochimica et Biophysica Acta* **1840,** 2643–2650 (2014).

159. Monneau, Y., Arenzana-Seisdedos, F. & Lortat-Jacob, H. The sweet spot: how GAGs help chemokines guide migrating cells. *Journal of Leukocyte Biology* **99,** 935–953 (2016).

160. Gallagher, J. T. Multiprotein signalling complexes: regional assembly on heparan sulphate. *Biochemical Society tTansactions* **34,** 438–441 (2006).

161. Xu, X., Jha, A. K., Harrington, D. A., Farach-Carson, M. C. & Jia, X. Hyaluronic acid-based hydrogels: from a natural polysaccharide to complex networks. *Soft Matter* **8,** 3280 (2012).

162. Farach-Carson, M. C. & Carson, D. D. Perlecan - A multifunctional extracellular proteoglycan scaffold. *Glycobiology* **17,** 897–905 (2007).

163. Lord, M. S. *et al.* The role of vascular-derived perlecan in modulating cell adhesion, proliferation and growth factor signaling. *Matrix Biology* **35,** 112–122 (2014).

164. Woods, A, Longley, R. L., Tumova, S & Couchman, J. R. Syndecan-4 binding to the high affinity heparin-binding domain of fibronectin drives focal adhesion formation in fibroblasts. *Archives of biochemistry and biophysics* **374,** 66–72 (2000).

165. Bass, M. D., Morgan, M. R. & Humphries, M. J. Integrins and syndecan-4 make distinct, but critical, contributions to adhesion contact formation. *Soft Matter* **3,** 372–376 (2007).

166. Marneros, A. G. & Olsen, B. R. Physiological role of collagen XVIII and endostatin. *FASEB Journal* **19,** 716–728 (2005).

167. Kiani, C., Chen, L., Wu, Y. J., Yee, A. J. & Yang, B. B. Structure and function of aggrecan. *Cell Research* **12,** 19–32 (2002).

168. Li, F. *et al.* Involvement of highly sulfated chondroitin sulfate in the metastasis of the Lewis lung carcinoma cells. *Journal of Biological Chemistry* **283,** 34294–34304 (2008).

169. Mizumoto, S. & Sugahara, K. Glycosaminoglycans are functional ligands for receptor for advanced glycation end-products in tumors. *The FEBS Journal* **280,** 2462–2470 (2013).

170. Mizumoto, S., Yamada, S. & Sugahara, K. Molecular interactions between chondroitin-dermatan sulfate and growth factors/receptors/matrix proteins. *Current Opinion in Structural Biology* **34,** 35–42 (2015).

171. Pomin, V. H. Keratan sulfate: an up-to-date review. *International Journal of Biological Macromolecules* **72,** 282–289 (2015).

172. Frenkel, J. S. The role of hyaluronan in wound healing. *International Wound Journal* **11,** 159–163 (2014).

173. Shoulders, M. D. & Raines, R. T. Collagen Structure and Stability. *Annual Review of Biochemistry* **78,** 929–958 (2009).

174. Rodriguez-Pascual, F. & Slatter, D. A. Collagen cross-linking: insights on the evolution of metazoan extracellular matrix. *Scientific Reports* **6,** 37374 (2016).

175. Khoshnoodi, J., Pedchenko, V. & Hudson, B. G. Mammalian collagen IV. *Microscopy Research and Technique* **71,** 357–370 (2008).

176. Adiguzel, E., Ahmad, P. J., Franco, C. & Bendeck, M. P. Collagens in the progression and complications of atherosclerosis. *Vascular Medicine* **14,** 73–89 (2009).

177. Keeley, F. W., Bellingham, C. M. & Woodhouse, K. A. Elastin as a self-organizing biomaterial: use of recombinantly expressed human elastin polypeptides as a model for investigations of structure and self-assembly of elastin. *Philosophical Transactions of the Royal Society Biological Sciences* **357,** 185–189 (2002).

178. Umeda, H, Takeuchi, M & Suyama, K. Two new elastin cross-links having pyridine skeleton. Implication of ammonia in elastin cross-linking in vivo. *Journal of Biological Chemistry* **276,** 12579–12587 (2001).

179. Davis, E. C. Stability of elastin in the developing mouse aorta: a quantitative radioautographic study. *Histochemistry* **100,** 17–26 (1993).

180. Avolio, A, Jones, D & Tafazzoli-Shadpour, M. Quantification of alterations in structure and function of elastin in the arterial media. *Hypertension* **32,** 170–175 (1998).

181. Sherratt, M. J. Tissue elasticity and the ageing elastic fibre. *Age* **31,** 305–325 (2009).

182. Tu, Y. & Weiss, A. S. Glycosaminoglycan-mediated coacervation of tropoelastin abolishes the critical concentration, accelerates coacervate formation, and facilitates spherule fusion: implications for tropoelastin microassembly. *Biomacromolecules* **9,** 1739–1744 (2008).

183. Yeo, G. C., Keeley, F. W. & Weiss, A. S. Coacervation of tropoelastin. *Advances in Colloid and Interface Science* **167,** 94–103 (2011).

184. Sato, F. *et al.* Distinct steps of cross-linking, self-association, and maturation of tropoelastin are necessary for elastic fiber formation. *Journal of Molecular Biology* **369,** 841–851 (2007).

185. Van der Donckt, C. *et al.* Elastin fragmentation in atherosclerotic mice leads to intraplaque neovascularization, plaque rupture, myocardial infarction, stroke, and sudden death. *European Heart Journal* **36,** 1049–1058 (2015).

186. Hamill, K. J., Kligys, K., Hopkinson, S. B. & Jones, J. C. R. Laminin deposition in the extracellular matrix: a complex picture emerges. *Journal of Cell Science* **122,** 4409–4417 (2009).

187. Petajaniemi, N. *et al.* Localization of laminin alpha4-chain in developing and adult human tissues. *Journal of Histochemistry and Cytochemistry* **50,** 1113–1130 (2002).

188. Wang, J. *et al.* Cardiomyopathy associated with microcirculation dysfunction in laminin $\alpha 4$ chain-deficient mice. *Journal of Biological Chemistry* **281,** 213–220 (2006).

189. Rauch, U. *et al.* Laminin isoforms in atherosclerotic arteries from mice and man. *Histology and Histopathology* **26,** 711–724 (2011).

190. Pike, M. C., Wicha, M. S., Yoon, P, Mayo, L & Boxer, L. A. Laminin promotes the oxidative burst in human neutrophils via increased chemoattractant receptor expression. *Journal of Immunology* **142,** 2004–2011 (1989).

191. Robert, L. Aging of the vascular wall and atherogenesis: Role of the elastin-laminin receptor. *Atherosclerosis* **123,** 169–179 (1996).

192. Peterszegi, G, Mandet, C, Texier, S, Robert, L & Bruneval, P. Lymphocytes in human atherosclerotic plaque exhibit the elastin-laminin receptor: Potential role in atherogenesis. *Atherosclerosis* **135,** 103–107 (1997).

193. Kostidou, E. *et al.* Enhanced laminin carbonylation by monocytes in diabetes mellitus. *Clinical Biochemistry* **40,** 671–679 (2007).

194. Kostidou, E., Topouridou, K., Daniilidis, A., Kaloyianni, M. & Koliakos, G. Oxidized laminin-1 induces increased monocyte attachment and expression of ICAM-1 in endothelial cells. *International Journal of Experimental Pathology* **90,** 630–637 (2009).

195. Mosher, D. F. Assembly of fibronectin into extracellular matrix. *Current Opinion in Structural Biology* **3,** 214–222 (1993).

196. Pankov, R. Fibronectin at a glance. *Journal of Cell Science* **115,** 3861–3863 (2002).

197. To, W. S. & Midwood, K. S. Plasma and cellular fibronectin: distinct and independent functions during tissue repair. *Fibrogenesis & Tissue Repair* **4,** 21 (2011).

198. Paci, E., Clarke, J., Steward, A., Vendruscolo, M. & Karplus, M. Self-consistent determination of the transition state for protein folding: application to a fibronectin type III domain. *Proceedings of the National Academy of Sciences of the United States of America* **100,** 394–399 (2003).

199. Han, J.-H., Batey, S., Nickson, A. A., Teichmann, S. A. & Clarke, J. The folding and evolution of multidomain proteins. *Nature Reviews Molecular Cell Biology* **8,** 319 (2007).

200. White, E. S. & Muro, A. F. Fibronectin splice variants: Understanding their multiple roles in health and disease using engineered mouse models. *IUBMB Life* **63,** 538–546 (2011).

201. Wang, X.-Q. *et al.* An earthworm protease cleaving serum fibronectin and decreasing HBeAg in HepG2.2.15 cells. *BMC Biochemistry* **9,** 30 (2008).

202. Maurer, L. M., Ma, W. & Mosher, D. F. Dynamic structure of plasma fibronectin. *Critical reviews in Biochemistry and Molecular Biology* **51,** 213–227 (2015).

203. Takahashi, S *et al.* The RGD motif in fibronectin is essential for development but dispensable for fibril assembly. *Journal of Cell Science* **178,** 167–178 (2007).

204. Sechler, J. L., Corbett, S. A. & Schwarzbauer, J. E. Modulatory roles for integrin activation and the synergy site of fibronectin during matrix assembly. *Molecular Biology of the Cell* **8,** 2563–2573 (1997).

205. Nagae, M. *et al.* Crystal structure of alpha5beta1 integrin ectodomain: atomic details of the fibronectin receptor. *Journal of Cell Biology* **197,** 131–140 (2012).

206. Barkalow, F. J. & Schwarzbauer, J. E. Interactions between fibronectin and chondroitin sulfate are modulated by molecular context. *Journal of Biological Chemistry* **269,** 3957–3962 (1994).

207. Bloom, L, Ingham, K. C. & Hynes, R. O. Fibronectin regulates assembly of actin filaments and focal contacts in cultured cells via the heparin-binding site in repeat III13. *Molecular Biology of the Cell* **10,** 1521–1536 (1999).

208. Raitman, I. *et al.* Heparin-fibronectin interactions in the development of extracellular matrix insolubility. *Matrix Biology* (2017).

209. Mostafavi-Pour, Z, Askari, J. A., Whittard, J. D. & Humphries, M. J. Identification of a novel heparin-binding site in the alternatively spliced IIICS region of fibronectin: roles of integrins and proteoglycans in cell adhesion to fibronectin splice variants. *Matrix Biology* **20,** 63–73 (2001).

210. Napper, C. E., Drickamer, K. & Taylor, M. E. Collagen binding by the mannose receptor mediated through the fibronectin type II domain. *Biochemical Journal* **395,** 579–586 (2006).

211. Schwarzbauer, J. E. Identification of the fibronectin sequences required for assembly of a fibrillar matrix. *Journal of Cell Biology* **113,** 1463–1473 (1991).

212. Sottile, J & Mosher, D. F. N-terminal type I modules required for fibronectin binding to fibroblasts and to fibronectin's III1 module. *Biochemical Journal* **323 (Pt 1),** 51–60. ISSN: 0264-6021 (Print) (1997).

213. Wu, Y. J., La Pierre, D. P., Wu, J., Yee, A. J. & Yang, B. B. The interaction of versican with its binding partners. *Cell Research* **15,** 483–494 (2005).

214. Chung, H., Multhaupt, H. A. B., Oh, E.-S. & Couchman, J. R. Minireview: Syndecans and their crucial roles during tissue regeneration. *FEBS Letters* **590,** 2408–2417 (2016).

215. Sotoodehnejadnematalahi, F. & Burke, B. Structure, function and regulation of versican: the most abundant type of proteoglycan in the extracellular matrix. *Acta Medica Iranica* **51,** 740–750 (2013).

216. Yang, W. & Yee, A. J. Versican V2 isoform enhances angiogenesis by regulating endothelial cell activities and fibronectin expression. *FEBS Letters* **587,** 185–192 (2013).

217. Erat, M. C., Sladek, B., Campbell, I. D. & Vakonakis, I. Structural analysis of collagen type I interactions with human fibronectin reveals a cooperative binding mode. *Journal of Biological Chemistry* **288,** 17441–17450 (2013).

218. Zollinger, A. J. & Smith, M. L. Fibronectin, the extracellular glue. *Matrix Biology* **60-61.** Special issue on Provisional Matrix, 27 –37. ISSN: 0945-053X (2017).

219. Stahl, P. D. & Ezekowitz, R. A. The mannose receptor is a pattern recognition receptor involved in host defense. *Current Opinion in Immunology* **10,** 50–55 (1998).

220. Gazi, U. & Martinez-Pomares, L. Influence of the mannose receptor in host immune responses. *Immunobiology* **214,** 554–561 (2009).

221. Sottile, J. *et al.* Fibronectin-dependent collagen I deposition modulates the cell response to fibronectin. *American Journal of Physiology: Cell physiology* **293,** C1934–46 (2007).

222. Sgarioto, M. *et al.* Collagen type I together with fibronectin provide a better support for endothelialization. *Comptes Rendus Biologies* **335,** 520–528 (2012).

223. Sevilla, C. A., Dalecki, D. & Hocking, D. C. Regional fibronectin and collagen fibril co-assembly directs cell proliferation and microtissue morphology. *PLoS One* **8,** e77316 (2013).

224. Velling, T., Risteli, J., Wennerberg, K., Mosher, D. F. & Johansson, S. Polymerization of type I and III collagens is dependent on fibronectin and enhanced by integrins alpha 11beta 1 and alpha 2beta 1. *Journal of Biological Chemistry* **277,** 37377–37381 (2002).

225. Sottile, J. & Hocking, D. C. Fibronectin Polymerization Regulates the Composition and Stability of Extracellular Matrix Fibrils and Cell-Matrix Adhesions. *Molecular Biology of the Cell* **14,** 3546–3559 (2002).

226. Zhang, Y. *et al.* Disentangling the multifactorial contributions of fibronectin, collagen and cyclic strain on MMP expression and extracellular matrix remodeling by fibroblasts. *Matrix Biology* **40,** 62–72 (2014).

227. Duplaa, C *et al.* The integrin very late antigen-4 is expressed in human smooth muscle cell. Involvement of alpha 4 and vascular cell adhesion molecule-1 during smooth muscle cell differentiation. *Circulation Research* **80,** 159–169 (1997).

228. Davis, G. E., Bayless, K. J., Davis, M. J. & Meininger, G. A. Regulation of tissue injury responses by the exposure of matricryptic sites within extracellular matrix molecules. *The American Journal of Pathology* **156,** 1489–1498 (2000).

229. Kaiura, T. L. *et al.* The effect of growth factors, cytokines, and extracellular matrix proteins on fibronectin production in human vascular smooth muscle cells. *Journal of Vascular Surgery* **31,** 577–584 (2000).

230. Zhou, X. *et al.* Fibronectin fibrillogenesis regulates three-dimensional neovessel formation. *Genes & Development* **22,** 1231–1243 (2008).

231. Astrof, S. & Hynes, R. O. Fibronectins in vascular morphogenesis. *Angiogenesis* **12,** 165–175 (2009).

232. Woods, A, Couchman, J. R., Johansson, S & Hook, M. Adhesion and cytoskeletal organisation of fibroblasts in response to fibronectin fragments. *The EMBO Journal* **5,** 665–670 (1986).

233. Kim, S, Bell, K, Mousa, S. A. & Varner, J. A. Regulation of angiogenesis in vivo by ligation of integrin alpha5beta1 with the central cell-binding domain of fibronectin. *The American Journal of Pathology* **156,** 1345–1362 (2000).

234. Keselowsky, B. G., Collard, D. M. & Garcia, A. J. Surface chemistry modulates fibronectin conformation and directs integrin binding and specificity to control cell adhesion. *Journal of Biomedical Materials Research* **66,** 247–259 (2003).

235. Cornelissen, C. G. *et al.* Fibronectin coating of oxygenator membranes enhances endothelial cell attachment. *Biomedical Engineering Online* **12,** 7 (2013).

236. Hendel, A. & Granville, D. J. Granzyme B cleavage of fibronectin disrupts endothelial cell adhesion, migration and capillary tube formation. *Matrix Biology* **32,** 14–22 (2013).

237. Mercurius, K. O. & Morla, A. O. Inhibition of vascular smooth muscle cell growth by inhibition of fibronectin matrix assembly. *Circulation Research* **82,** 548–556 (1998).

238. Costell, M. *et al.* Hyperplastic conotruncal endocardial cushions and transposition of great arteries in perlecan-null mice. *Circulation Research* **91,** 158–164 (2002).

239. Vikramadithyan, R. K. *et al.* Atherosclerosis in perlecan heterozygous mice. *Journal of Lipid Research* **45,** 1806–12 (2004).

240. Kennett, E. C. *et al.* Peroxynitrite modifies the structure and function of the extracellular matrix proteoglycan perlecan by reaction with both the protein core and the heparan sulfate chains. *Free Radical Biology and Medicine* **49,** 282–293 (2010).

241. Wagsater, D., Zhu, C., Bjorkegren, J., Skogsberg, J. & Eriksson, P. MMP-2 and MMP-9 are prominent matrix metalloproteinases during atherosclerosis development in the Ldlr(-/-)Apob(100/100) mouse. *International Journal of Molecular Medicine* **28,** 247–253 (2011).

242. Nagase, H & Woessner, J. F. J. Matrix metalloproteinases. *Journal of Biological Chemistry* **274,** 21491–21494 (1999).

243. Bigg, H. F., Rowan, A. D., Barker, M. D. & Cawston, T. E. Activity of matrix metalloproteinase-9 against native collagen types I and III. *FEBS Journal* **274,** 1246–1255 (2007).

244. Klysik, A. B., Naduk-Kik, J, Hrabec, Z, Gos, R & Hrabec, E. Intraocular matrix metalloproteinase 2 and 9 in patients with diabetes mellitus with and without diabetic retinopathy. *Archives of Medical Science* **6,** 375–381 (2010).

245. Tamarat, R. *et al.* Blockade of advanced glycation end-product formation restores ischemia-induced angiogenesis in diabetic mice. *Proceedings of the National Academy of Sciences of the United States of America* **100,** 8555–60 (2003).

246. Guilbert, M. *et al.* Probing non-enzymatic glycation of type i collagen: A novel approach using Raman and infrared biophotonic methods. *Biochimica et Biophysica Acta - General Subjects* **1830,** 3525–3531 (2013).

247. Fu, M. X. *et al.* Glycation, glycoxidation, and cross-linking of collagen by glucose: Kinetics, mechanisms, and inhibition of late stages of the Maillard reaction. *Diabetes* **43,** 676–683 (1994).

248. Olszowski, S., Mak, P., Olszowska, E. & Marcinkiewicz, J. Collagen type II modification by hypochlorite. *Acta Biochimica Polonica* **50,** 471–479 (2003).

249. Gonzales, M *et al.* Structure and function of a vimentin-associated matrix adhesion in endothelial cells. *Molecular Biology of the Cell* **12,** 85–100 (2001).

250. Mann, K *et al.* Amino acid sequence of mouse nidogen, a multidomain basement membrane protein with binding activity for laminin, collagen IV and cells. *The EMBO Journal* **8,** 65–72 (1989).

251. Kohfeldt, E, Sasaki, T, Göhring, W & Timpl, R. Nidogen-2: a new basement membrane protein with diverse binding properties. *Journal of Molecular Biology* **282,** 99–109 (1998).

252. Mokkapati, S. *et al.* Basement membranes in skin are differently affected by lack of nidogen 1 and 2. *Journal of Investigative Dermatology* **128,** 2259–67 (2008).

253. George, E. L., Georges-Labouesse, E. N., Patel-King, R. S., Rayburn, H & Hynes, R. O. Defects in mesoderm, neural tube and vascular development in mouse embryos lacking fibronectin. *Development* **119,** 1079–1091 (1993).

254. Yang, J. T., Rayburn, H & Hynes, R. O. Embryonic mesodermal defects in alpha 5 integrin-deficient mice. *Development* **119,** 1093–1105 (1993).

255. George, E. L., Baldwin, H. S. & Hynes, R. O. Fibronectins are essential for heart and blood vessel morphogenesis but are dispensable for initial specification of precursor cells. *Blood* **90,** 3073–3081 (1997).

256. Yang, J. T. *et al.* Overlapping and independent functions of fibronectin receptor integrins in early mesodermal development. *Developmental Biology* **215,** 264–77 (1999).

257. Dzamba, B. J. & Peters, D. M. Arrangement of cellular fibronectin in noncollagenous fibrils in human fibroblast cultures. *Journal of Cell Science* **100 (Pt 3,** 605–12 (1991).

258. McDonald, J. A., Kelley, D. G. & Broekelmann, T. J. Role of fibronectin in collagen deposition: Fab' to the gelatin-binding domain of fibronectin inhibits both fibronectin and collagen organization in fibroblast extracellular matrix. *Journal of Cell Biology* **92,** 485–492 (1982).

259. Hielscher, A., Ellis, K., Qiu, C., Porterfield, J. & Gerecht, S. Fibronectin Deposition Participates in Extracellular Matrix Assembly and Vascular Morphogenesis. *PLoS One* **11,** e0147600 (2016).

260. Vissers, M. C. & Winterbourn, C. C. Oxidative damage to fibronectin. I. The effects of the neutrophil myeloperoxidase system and HOCl. *Archives of Biochemistry and Biophysics* **285,** 53–59 (1991).

261. Vissers, M. C. M. & Thomas, C. Hypochlorous acid disrupts the adhesive properties of subendothelial matrix. *Free Radical Biology and Medicine* **23,** 401–411 (1997).

262. Kan, M & Shi, E. G. Fibronectin, not laminin, mediates heparin-dependent heparin- binding growth factor type I binding to substrata and stimulation of endothelial cell growth. *In Vitro Cell Development Biology* **26,** 1151–1156 (1990).

263. Lawler, J. The functions of thrombospondin-1 and -2. *Current Opinion in Cell Biology* **12,** 634–640 (2000).

264. Rohwedder, I. *et al.* Plasma fibronectin deficiency impedes atherosclerosis progression and fibrous cap formation. *EMBO Molecular Medicine* **4,** 564–576 (2012).

265. Tabas, I., Williams, K. J. & Borén, J. Subendothelial lipoprotein retention as the initiating process in atherosclerosis: Update and therapeutic implications. *Circulation* **116,** 1832–1844 (2007).

266. Doherty, D. E., Henson, P. M. & Clark, R. A. F. Fibronectin fragments containing the RGDS cell-binding domain mediate monocyte migration into the rabbit lung. A potential mechanism for C5 fragment-induced monocyte lung accumulation. *Journal of Clinical Investigation* **86,** 1065–1075 (1990).

267. Everitt, E. A., Malik, A. B. & Hendey, B. Fibronectin enhances the migration rate of human neutrophils in vitro. *Journal of Leukocyte Biology* **60,** 199–206 (1996).

268. Wachtfogel, Y. T. *et al.* Fibronectin degradation products containing the cytoadhesive tetrapeptide stimulate human neutrophil degranulation. *Journal of Clinical Investigation* **81,** 1310–1316 (1988).

269. Yurdagul, A. *et al.* alpha5beta1 Integrin Signaling Mediates Oxidized Low-Density Lipoprotein-Induced Inflammation and Early Atherosclerosis. *Arteriosclerosis, Thrombosis, and Vascular Biology* **34,** 1362–1373 (2014).

270. Kubala, L. *et al.* The potentiation of myeloperoxidase activity by the glycosaminoglycan-dependent binding of myeloperoxidase to proteins of the extracellular matrix. *Biochimica et Biophysica Acta* **1830,** 4524–4536 (2013).

271. Olszowski, S., Olszowska, E., Kusior, D., Piwowarczyk, M. & Stelmaszynska, T. Hypochlorite Action on Plasma Fibronectin Promotes Its Extended Conformation in Complexes with Antibodies. *Journal of Protein Chemistry* **22,** 449–456 (2003).

272. Tan, M. H. *et al.* Deletion of the alternatively spliced fibronectin EIIIA domain in mice reduces atherosclerosis. *Blood* **104,** 11–18 (2004).

273. Babaev, V. R. *et al.* Absence of regulated splicing of fibronectin EDA exon reduces atherosclerosis in mice. *Atherosclerosis* **197,** 534–540 (2008).

274. Akiyama, S. K., Yamada, S. S., Chen, W. T. & Yamada, K. M. Analysis of fibronectin receptor function with monoclonal antibodies: Roles in cell adhesion, migration, matrix assembly, and cytoskeletal organization. *Journal of Cell Biology* **109,** 863–875 (1989).

275. Hahn, C. & Schwartz, M. A. Mechanotransduction in vascular physiology and atherogenesis. *Nature Reviews Molecular Cell Biology* **10,** 53–62 (2009).

276. Hahn, C., Orr, A. W., Sanders, J. M., Jhaveri, K. A. & Schwartz, M. A. The subendothelial extracellular matrix modulates JNK activation by flow. *Circulation Research* **104,** 995–1003 (2009).

277. Orr, A. W. *et al.* The subendothelial extracellular matrix modulates NF-κB activation by flow: A potential role in atherosclerosis. *Journal of Cell Biology* **169,** 191–202 (2005).

278. Song, K. S., Kim, H. K., Shim, W. & Jee, S. H. Plasma fibronectin levels in ischemic heart disease. *Atherosclerosis* **154,** 449–453 (2001).

279. Orem, C. *et al.* Plasma fibronectin level and its association with coronary artery disease and carotid intima-media thickness. *Coronary Artery Disease* **14,** 219–224 (2003).

280. Lemańska-Perek, A. *et al.* Analysis of Soluble Molecular Fibronectin-Fibrin Complexes and EDA-Fibronectin Concentration in Plasma of Patients with Atherosclerosis. *Inflammation* **39,** 1059–1068 (2016).

281. Zhang, Y. *et al.* Association study between fibronectin and coronary heart disease. *Clinical Chemistry and Laboratory Medicine : CCLM / FESCC* **44,** 37–42 (2006).

282. Vavalle, J. P., Wu, S. S., Hughey, R, Madamanchi, N. R. & Stouffer, G. a. *Plasma fibronectin levels and coronary artery disease.* 2007.

283. Daugherty, A, Dunn, J. L., Rateri, D. L. & Heinecke, J. W. Myeloperoxidase, a catalyst for lipoprotein oxidation, is expressed in human atherosclerotic lesions. *Journal of Clinical Investigation* **94,** 437–444 (1994).

284. Summers, F. A., Morgan, P. E., Davies, M. J. & Hawkins, C. L. Identification of plasma proteins that are susceptible to thiol oxidation by hypochlorous acid and N-chloramines. *Chemical Research in Toxicology* **21,** 1832–1840 (2008).

285. Cory, A. H., Owen, T. C., Barltrop, J. A. & Cory, J. G. Use of an aqueous soluble tetrazolium/formazan assay for cell growth assays in culture. *Cancer Communications* **3,** 207–212 (1991).

286. Ichiroh Manabe, R., Oh-e, N. & Sekiguchi, K. Alternatively spliced EDA segment regulates fibronectin-dependent cell cycle progression and mitogenic signal transduction. *Journal of Biological Chemistry* **274,** 5919–5924 (1999).

287. Khan, Z. A. *et al.* EDB fibronectin and angiogenesis - A novel mechanistic pathway. *Angiogenesis* **8,** 183–196 (2005).

288. Kohan, M., Muro, A. F., White, E. S. & Berkman, N. EDA-containing cellular fibronectin induces fibroblast differentiation through binding to 4 7 integrin receptor and MAPK/Erk 1/2-dependent signaling. *The FASEB Journal* **24,** 4503–4512 (2010).

289. Reddie, K. G. & Carroll, K. S. Expanding the functional diversity of proteins through cysteine oxidation. *Current Opinion in Chemical Biology* **12,** 746–754 (2008).

290. Roos, G. & Messens, J. Protein sulfenic acid formation: From cellular damage to redox regulation. *Free Radical Biology and Medicine* **51,** 314–326 (2011).

291. Kato, Y. *et al.* Immunochemical Detection of Protein Dityrosine in Atherosclerotic Lesion of Apo-E-Deficient Mice Using a Novel Monoclonal Antibody. *Biochemical and Biophysical Research Communications* **275,** 11–15 (2000).

292. Leeuwenburgh, C. *et al.* Mass spectrometric quantification of markers for protein oxidation by tyrosyl radical, copper, and hydroxyl radical in low density lipoprotein isolated from human atherosclerotic plaques. *Journal of Biological Chemistry* **272,** 3520–3526 (1997).

293. Colombo, G. *et al.* Thiol oxidation and di-tyrosine formation in human plasma proteins induced by inflammatory concentrations of hypochlorous acid. *Journal of Proteomics* **152,** 22–32 (2017).

294. Lane, L. C. A simple method for stabilizing protein-sulfhydryl groups during SDS-gel electrophoresis. *Analytical Biochemistry* **86,** 655 –664. ISSN: 0003-2697 (1978).

295. Cleland, W. Dithiothreitol, a New Protective Reagent for SH Groups *. *Biochemistry* **3,** 480–2 (May 1964).

296. Smith, D. E., Mosher, D. F., Johnson, R. B. & Furcht, L. T. Immunological identification of two sulfhydryl-containing fragments of human plasma fibronectin. *Journal of Biological Chemistry* **257,** 5831–5838 (1982).

297. H, L. C.O.T. E. Probing the folded state of fibronectin type III domains in stretched fibrils by measuring buried cysteine accessibility. *The Journal of Biological Chemistry* **286,** 26375–26382 (2011).

298. Stadtman, E. R., Van Remmen, H., Richardson, A., Wehr, N. B. & Levine, R. L. Methionine oxidation and aging. *Biochimica et Biophysica Acta - Proteins and Proteomics* **1703,** 135–140 (2005).

299. Stadtman, E. R. Protein oxidation and aging. *Free Radical Research* **40,** 1250–1258 (2006).

300. Levine, R. L., Mosoni, L, Berlett, B. S. & Stadtman, E. R. Methionine residues as endogenous antioxidants in proteins. *Proceedings of the National Academy of Sciences of the United States of America* **93,** 15036–40 (1996).

301. Levine, R. L., Moskovitz, J. & Stadtman, E. R. Oxidation of methionine in proteins: Roles in antioxidant defense and cellular regulation. *IUBMB Life* **50,** 301–307 (2000).

302. Drazic, A. & Winter, J. The physiological role of reversible methionine oxidation. *Biochimica et Biophysica Acta - Proteins and Proteomics* **1844,** 1367–1382 (2014).

303. Moskovitz, J. & Oien, D. B. Protein carbonyl and the methionine sulfoxide reductase system. *Antioxidants & Redox Signaling* **12,** 405–15 (2010).

304. Schöneich, C. Methionine oxidation by reactive oxygen species: Reaction mechanisms and relevance to Alzheimer's disease. *Biochimica et Biophysica Acta - Proteins and Proteomics* **1703,** 111–119 (2005).

305. Matheson, N. R. & Travis, J. Differential effects of oxidizing agents on human plasma alpha 1-proteinase inhibitor and human neutrophil myeloperoxidase. *Biochemistry* **24,** 1941–1945 (1985).

306. Teng, N. *et al.* The roles of myeloperoxidase in coronary artery disease and its potential implication in plaque rupture. *Redox Report* **22,** 51–73 (2017).

307. Hawkins, C. L. & Davies, M. J. Hypochlorite-induced oxidation of proteins in plasma: formation of chloramines and nitrogen-centred radicals and their role in protein fragmentation. *Biochemical Journal* **340,** 539 (1999).

308. Domigan, N. M., Charlton, T. S., Duncan, M. W., Winterbourn, C. C. & Kettle, A. J. Chlorination of tyrosyl residues in peptides by myeloperoxidase and human neutrophils. *Journal of Biological Chemistry* **270,** 16542–16548 (1995).

309. Bergt, C., Fu, X., Huq, N. P., Kao, J. & Heinecke, J. W. Lysine residues direct the chlorination of tyrosines in YXXK motifs of apolipoprotein A-I when hypochlorous acid oxidizes high density lipoprotein. *Journal of Biological Chemistry* **279,** 7856–7866 (2004).

310. Thomas, E. L., Grisham, M. B. & Margaret Jefferson, M. Preparation and Characterization of Chloramines. *Methods in Enzymology* **132,** 569–585 (1986).

311. Hawkins, C. L. & Davies, M. J. *Hypochlorite-induced damage to proteins: formation of nitrogen-centred radicals from lysine residues and their role in protein fragmentation.* 1998.

312. Hazen, S. L. & Heinecke, J. W. *3-Chlorotyrosine, a specific marker of myeloperoxidase-catalyzed oxidation, is markedly elevated in low density lipoprotein isolated from human atherosclerotic intima* 1997.

313. Delporte, C. *et al.* Impact of myeloperoxidase-LDL interactions on enzyme activity and subsequent posttranslational oxidative modifications of apoB-100. *Journal of Lipid Research* **55,** 747–757 (2014).

314. Kato, Y. *et al.* Quantification of Modified Tyrosines in Healthy and Diabetic Human Urine using Liquid Chromatography/Tandem Mass Spectrometry. *Journal of Clinical Biochemistry and Nutrition* **44,** 67–78 (2009).

315. Beal, M. F. Oxidatively modified proteins in aging and disease. *Free Radical Biology and Medicine* **32,** 797–803 (2002).

316. Carroll, L. *et al.* Formation and detection of oxidant-generated tryptophan dimers in peptides and proteins. *Free Radical Biology and Medicine* **113,** 132–142 (2017).

317. Sharma, A, Askari, J. A., Humphries, M. J., Jones, E. Y. & Stuart, D. I. *Crystal structure of a heparin- and integrin-binding segment of human fibronectin.* 1999.

318. Doddapattar, P. *et al.* Fibronectin Splicing Variants Containing Extra Domain A Promote Atherosclerosis in Mice Through Toll-Like Receptor 4. *Arteriosclerosis, Thrombosis, and Vascular Biology* **35,** 2391–2400 (2015).

319. Kuzuya, M. *et al.* Effect of MMP-2 deficiency on atherosclerotic lesion formation in apoE-deficient mice. *Arteriosclerosis, Thrombosis, and Vascular Biology* **26,** 1120–1125 (2006).

320. Li, Z *et al. Increased expression of 72-kd type IV collagenase (MMP-2) in human aortic atherosclerotic lesions.* 1996.

321. Heo, S. H. *et al.* Plaque rupture is a determinant of vascular events in carotid artery atherosclerotic disease: Involvement of matrix metalloproteinases 2 and 9. *Journal of Clinical Neurology* **7,** 69–76 (2011).

322. Schonbeck, U *et al.* Expression of stromelysin-3 in atherosclerotic lesions: regulation via CD40-CD40 ligand signaling in vitro and in vivo. *Journal of Experimental Medicine* **189,** 843–853 (1999).

323. Rajavashisth, T. B. *et al.* Membrane type 1 matrix metalloproteinase expression in human atherosclerotic plaques: evidence for activation by proinflammatory mediators. *Circulation* **99,** 3103–9 (1999).

324. Lijnen, H. R. *et al.* Accelerated neointima formation after vascular injury in mice with stromelysin-3 (MMP-11) gene inactivation. *Arteriosclerosis, Thrombosis, and Vascular Biology* **19,** 2863–2870 (1999).

325. Matziari, M., Dive, V. & Yiotakis, A. Matrix metalloproteinase 11 (MMP-11; stromelysin-3) and synthetic inhibitors. *Medicinal Research Reviews* **27,** 528–552 (2007).

326. Shofuda, T *et al.* Cleavage of focal adhesion kinase in vascular smooth muscle cells overexpressing membrane-type matrix metalloproteinases. *Arteriosclerosis, Thrombosis, and Vascular Biology* **24,** 839–844 (2004).

327. Newby, A. C. Matrix metalloproteinases regulate migration, proliferation, and death of vascular smooth muscle cells by degrading matrix and non-matrix substrates. *Cardiovascular Research* **69,** 614–624 (2006).

328. Ries, C. *et al.* MMP-2, MT1-MMP, and TIMP-2 are essential for the invasive capacity of human mesenchymal stem cells: Differential regulation by inflammatory cytokines. *Blood* **109,** 4055–4063 (2007).

329. Vandenbroucke, R. E. & Libert, C. Is there new hope for therapeutic matrix metalloproteinase inhibition? *Nature Reviews Drug Discovery* **13,** 904–927 (2014).

330. Esparza, J *et al.* Fibronectin upregulates gelatinase B (MMP-9) and induces coordinated expression of gelatinase A (MMP-2) and its activator MT1-MMP (MMP-14) by human T lymphocyte cell lines. A process repressed through RAS/MAP kinase signaling pathways. *Blood* **94,** 2754–2766 (1999).

331. Fu, X., Kassimm, S. Y., Parks, W. C. & Heinecke, J. W. Hypochlorous Acid Oxygenates the Cysteine Switch Domain of Pro-matrilysin (MMP-7): A mechanism for matrix metalloproteinase activation and atherosclerotic plaque rupture by myeloperoxidase. *Journal of Biological Chemistry* **276,** 41279–41287 (2001).

332. Halpert, I. *et al.* Matrilysin is expressed by lipid-laden macrophages at sites of potential rupture in atherosclerotic lesions and localizes to areas of versican deposition, a proteoglycan substrate for the enzyme. *Proceedings of the National Academy of Sciences of the United States of America* **93,** 9748–9753 (1996).

333. Bourboulia, D. & Stetler-Stevenson, W. G. *Matrix metalloproteinases (MMPs) and tissue inhibitors of metalloproteinases (TIMPs): Positive and negative regulators in tumor cell adhesion* 2010.

334. Morgunova, E., Tuuttila, A., Bergmann, U., Tryggvason, K. & Huber, R. *Structural insight into the complex formation of latent matrix metalloproteinase 2 with tissue inhibitor of metalloproteinase 2* 2002.

335. Zaltsman, A. B., George, S. J. & Newby, A. C. Increased Secretion of Tissue Inhibitors of Metalloproteinases 1 and 2 From the Aortas of Cholesterol Fed Rabbits Partially Counterbalances Increased Metalloproteinase Activity. *Arteriosclerosis, Thrombosis, and Vascular Biology* **19,** 1012–1700 (1999).

336. Sternlicht, M. D. & Werb, Z. *How Matrix Metalloproteinases Regulate Cell Behavior* 2001. doi:10.1146/annurev.cellbio.17.1.463. arXiv: NIHMS150003. http://www.annualreviews.org/doi/10.1146/annurev.cellbio.17.1.463.

337. Galis, Z. S., Sukhova, G. K., Lark, M. W. & Libby, P. Increased expression of matrix metalloproteinases and matrix degrading activity in vulnerable regions of human atherosclerotic plaques. *Journal of Clinical Investigation* **94,** 2493–503 (1994).

338. Baker, A. H., Zaltsman, A. B., George, S. J. & Newby, A. C. Divergent effects of tissue inhibitor of metalloproteinase-1, -2, or -3 overexpression on rat vascular smooth muscle cell invasion, proliferation, and death in vitro. *Journal of Clinical Investigation* **101,** 1478–1487 (1998).

339. Johnson, J. L. *et al.* Suppression of atherosclerotic plaque progression and instability by tissue inhibitor of metalloproteinase-2: Involvement of macrophage migration and apoptosis. *Circulation* **113,** 2435–2444 (2006).

340. Nikkari, S. T. *et al.* Expression of collagen, interstitial collagenase, and tissue inhibitor of metalloproteinases-1 in restenosis after carotid endarterectomy. *The American Journal of Pathology* **148,** 777–83 (1996).

341. Lijnen, H. R., Soloway, P & Collen, D. Tissue inhibitor of matrix metalloproteinases-1 impairs arterial neointima formation after vascular injury in mice. *Circulation Research* **85,** 1186–1191 (1999).

342. Feng, Y. *et al.* ADAMTS13: more than a regulator of thrombosis. *International Journal of Hematology* **104,** 534–539 (2016).

343. Ruggeri, Z. M. The role of von Willebrand factor in thrombus formation. *Thrombosis Research* **120 Suppl,** S5–9 (2007).

344. Wang, X. *et al.* Endothelial Function, Inflammation, Thrombosis, and Basal Ganglia Perivascular Spaces in Patients with Stroke. *Journal of Stroke and Cerebrovascular Diseases* **25,** 2925–2931 (2016).

345. Kawecki, C, Lenting, P. J. & Denis, C. V. von Willebrand factor and inflammation. *Journal of Thrombosis and Haemostasis* **15,** 1285–1294 (2017).

346. Chauhan, A. K. *et al.* ADAMTS13: a new link between thrombosis and inflammation. *Journal of Experimental Medicine* **205,** 2065–2074 (2008).

347. Gandhi, C., Khan, M. M., Lentz, S. R. & Chauhan, A. K. ADAMTS13 reduces vascular inflammation and the development of early atherosclerosis in mice. *Blood* **119,** 2385–2391 (2012).

348. Bongers, T. N. *et al.* Lower levels of ADAMTS13 are associated with cardiovascular disease in young patients. *Atherosclerosis* **207,** 250–254 (2009).

349. Maino, A *et al.* Plasma ADAMTS-13 levels and the risk of myocardial infarction: an individual patient data meta-analysis. *Journal of Thrombosis and Haemostasi* **13,** 1396–1404 (2015).

350. Blankenberg, S., Barbaux, S. & Tiret, L. Adhesion molecules and atherosclerosis. *Atherosclerosis* **170,** 191–203 (2003).

351. García, A. J. & Boettiger, D. Integrin-fibronectin interactions at the cell-material interface: Initial integrin binding and signaling. *Biomaterials* **20,** 2427–2433 (1999).

352. Schiller, H. B. *et al.* β1- and αv-class integrins cooperate to regulate myosin II during rigidity sensing of fibronectin-based microenvironments. *Nature Cell Biology* **15,** 625–636 (2013).

353. Schwartz, E. A., Bizios, R., Medow, M. S. & Gerritsen, M. E. Exposure of Human Vascular Endothelial Cells to Sustained Hydrostatic Pressure Stimulates Proliferation : Involvement of the V Integrins. *Circulation Research* **84,** 315–322 (1999).

354. Winter, P. M. *et al.* Molecular Imaging of Angiogenesis in Early-Stage Atherosclerosis With ??v??3-Integrin-Targeted Nanoparticles. *Circulation* **108,** 2270–2274 (2003).

355. Hoshiga, M., Alpers, C. E., Smith, L. L., Giachelli, C. M. & Schwartz, S. M. αvβ3 Integrin Expression in Normal and Atherosclerotic Artery. *Circulation Research* **77,** 1129–1135 (1995).

356. Yang, J. T., Rayburn, H & Hynes, R. O. Cell adhesion events mediated by alpha 4 integrins are essential in placental and cardiac development. *Development* **121,** 549–60 (1995).

357. Patel, S. S., Thiagarajan, R., Willerson, J. T. & Yeh, E. T. H. Inhibition of α4 Integrin and ICAM-1 Markedly Attenuate Macrophage Homing to Atherosclerotic Plaques in ApoE-Deficient Mice. *Circulation* **97,** 75–81 (1998).

358. Morigi, M *et al.* Fluid shear stress modulates surface expression of adhesion molecules by endothelial cells. *Blood* **85,** 1696–703 (1995).

359. Labow, M. a. *et al.* Characterization of E-selectin-deficient mice: demonstration of overlapping function of the endothelial selectins. *Immunity* **1,** 709–20 (1994).

360. O'Brien, K. D., McDonald, T. O., Chait, A., Allen, M. D. & Alpers, C. E. Neovascular Expression of E-Selectin, Intercellular Adhesion Molecule-1, and Vascular Cell Adhesion Molecule-1 in Human Atherosclerosis and Their Relation to Intimal Leukocyte Content. *Circulation* **93,** 672–682 (1996).

361. Wyble, C. W. *et al.* TNF-alpha and IL-1 upregulate membrane-bound and soluble E-selectin through a common pathway. *The Journal of surgical research* **73,** 107–112 (1997).

362. O'Carroll, S. J. *et al.* Pro-inflammatory TNFα and IL-1β differentially regulate the inflammatory phenotype of brain microvascular endothelial cells. *Journal of Neuroinflammation* **12,** 131 (2015).

363. Dong, Z. M., Brown, A. a. & Wagner, D. D. Prominent Role of P-Selectin in the Development of Advanced Atherosclerosis in ApoE-Deficient Mice. *Circulation* **101,** 2290–2295 (2000).

364. Bielinski, S. J. *et al.* P-selectin and subclinical and clinical atherosclerosis: The Multi-Ethnic Study of Atherosclerosis (MESA). *Atherosclerosis* **240,** 3–9 (2015).

365. Reiner, A. P. *et al.* Soluble P-selectin, SELP polymorphisms, and atherosclerotic risk in European-American and African-African young adults the coronary artery risk development in young adults (CARDIA) study. *Arteriosclerosis, Thrombosis, and Vascular Biology* **28,** 1549–1555 (2008).

366. Frenette, P. S. & Wagner, D. D. Insights into selectin function from knockout mice. *Thrombosis and Haemostasis* **78,** 60–64 (1997).

367. Talib, J., Pattison, D. I., Harmer, J. A., Celermajer, D. S. & Davies, M. J. High plasma thiocyanate levels modulate protein damage induced by myeloperoxidase and perturb measurement of 3-chlorotyrosine. *Free Radical Biology and Medicine* **53,** 20–29 (2012).

368. Vetter, J. Plant cyanogenic glycosides. *Toxicon* **38,** 11–36 (2000).

369. Vesey, C. J. & Cole, P. V. Blood cyanide and thiocyanate concentrations produced by long-term therapy with sodium nitroprusside. *British Journal of Anaesthesia* **57,** 148–155 (1985).

370. Aune, T. M. & Thomas, E. L. Oxidation of protein sulfhydryls by products of peroxidase-catalyzed oxidation of thiocyanate ion. *Biochemistry* **17,** 1005–1010 (1978).

371. Ismael, F. O. *et al.* Comparative reactivity of the myeloperoxidase-derived oxidants HOCl and HOSCN with low-density lipoprotein (LDL): Implications for foam cell formation in atherosclerosis. *Archives of Biochemistry and Biophysics* **573,** 40–51 (2015).

372. Moriarty-Craige, S. E. & Jones, D. P. Extracellular thiols and thiol/disulfide redox in metabolism. *Annual Review of Nutrition* **24,** 481–509 (2004).

373. Ashfaq, S. *et al.* The relationship between plasma levels of oxidized and reduced thiols and early atherosclerosis in healthy adults. *Journal of the American College of Cardiology* **47,** 1005–1011 (2006).

374. Lloyd, M. M., van Reyk, D. M., Davies, M. J. & Hawkins, C. L. Hypothiocyanous acid is a more potent inducer of apoptosis and protein thiol depletion in murine macrophage cells than hypochlorous acid or hypobromous acid. *Biochemical Journal* **414,** 271–80 (2008).

375. Gilbert, H. F. Molecular and cellular aspects of thiol-disulfide exchange. *Advances in enzymology and related areas of molecular biology* **63,** 69–172 (1990).

376. Yi, M. C. & Khosla, C. Thiol-Disulfide Exchange Reactions in the Mammalian Extracellular Environment. *Annual Review of Chemical and Biomolecular Engineering* **7,** 197–222 (2016).

377. Sulkala, M. *et al.* Matrix metalloproteinase-8 (MMP-8) is the major collagenase in human dentin. *Archives of Oral Biology* **52,** 121–127 (2007).

378. Nwomeh, B. C., Liang, H. X., Cohen, I. K. & Yager, D. R. MMP-8 is the predominant collagenase in healing wounds and nonhealing ulcers. *The Journal of Surgical Research* **81,** 189–195 (1999).

379. Nordskog, B. K., Blixt, A. D., Morgan, W. T., Fields, W. R. & Hellmann, G. M. Matrix-degrading and pro-inflammatory changes in human vascular endothelial cells exposed to cigarette smoke condensate. *Cardiovascular Toxicology* **3,** 101–117 (2003).

380. Laxton, R. C. *et al.* A role of matrix metalloproteinase-8 in atherosclerosis. *Circulation Research* **105,** 921–929 (2009).

381. Quillard, T. *et al.* Selective inhibition of matrix metalloproteinase-13 increases collagen content of established mouse atherosclerosis. *Arteriosclerosis, Thrombosis, and Vascular Biology* **31,** 2464–2472 (2011).

382. Quillard, T., Araujo, H. A., Franck, G., Tesmenitsky, Y. & Libby, P. Matrix metalloproteinase-13 predominates over matrix metalloproteinase-8 as the functional interstitial collagenase in mouse atheromata. *Arteriosclerosis, Thrombosis, and Vascular Biology* **34,** 1179–1186 (2014).

383. Bermudez, E. A., Rifai, N., Buring, J. E., Manson, J. E. & Ridker, P. M. Relation between markers of systemic vascular inflammation and smoking in women. *The American Journal of Cardiology* **89,** 1117–1119 (2002).

384. Perlstein, T. S. & Lee, R. T. Smoking, metalloproteinases, and vascular disease. *Arteriosclerosis, Thrombosis, and Vascular Biology* **26,** 250–256 (2006).

385. Wang, J.-G., Mahmud, S. a., Nguyen, J. & Slungaard, A. Thiocyanate-dependent induction of endothelial cell adhesion molecule expression by phagocyte peroxidases: a novel HOSCN-specific oxidant mechanism to amplify inflammation. *Journal of Immunology* **177,** 8714–22 (2006).

386. Bradshaw, A. D. & Sage, E. H. SPARC, a matricellular protein that functions in cellular differentiation and tissue response to injury. *Journal of Clinical Investigation* **107,** 1049–1054 (2001).

387. Brekken, R. A. & Sage, E. H. SPARC, a matricellular protein: at the crossroads of cell-matrix communication. *Matrix Biology* **19,** 816–827 (2001).

388. Lane, T. F., Iruela-Arispe, M. L. & Sage, E. H. Regulation of gene expression by SPARC during angiogenesis in vitro. Changes in fibronectin, thrombospondin-1, and plasminogen activator inhibitor-1. *Journal of Biological Chemistry* **267,** 16736–16745 (1992).

389. Peixoto, E *et al.* SPARC (secreted protein acidic and rich in cysteine) knockdown protects mice from acute liver injury by reducing vascular endothelial cell damage. *Gene Therapy* **22,** 9–19 (2015).

390. Atorrasagasti, C. *et al.* Lack of the Matricellular Protein SPARC (Secreted Protein, Acidic and Rich in Cysteine) Attenuates Liver Fibrogenesis in Mice. *PLoS One* **8,** 1–17 (2013).

391. Kubow, K. E. *et al.* Mechanical forces regulate the interactions of fibronectin and collagen I in extracellular matrix. *Nature Communications* **6,** 8026 (2015).

392. Mangge, H., Becker, K., Fuchs, D. & Gostner, J. M. Antioxidants, inflammation and cardiovascular disease. *World Journal of Cardiology* **6,** 462–477 (2014).

393. Pisoschi, A. M. & Pop, A. The role of antioxidants in the chemistry of oxidative stress: A review. *European Journal of Medicinal Chemistry* **97,** 55–74 (2015).

394. Birben, E., Sahiner, U. M., Sackesen, C., Erzurum, S. & Kalayci, O. Oxidative stress and antioxidant defense. *The World Allergy Organization journal* **5,** 9–19 (2012).

395. Baldus, S. *et al.* Spatial mapping of pulmonary and vascular nitrotyrosine reveals the pivotal role of myeloperoxidase as a catalyst for tyrosine nitration in inflammatory diseases. *Free Radical Biology and Medicine* **33,** 1010–1019 (2002).

396. Nussbaum, C., Klinke, A., Adam, M., Baldus, S. & Sperandio, M. Myeloperoxidase: a leukocyte-derived protagonist of inflammation and cardiovascular disease. *Antioxidants & Redox Signaling* **18,** 692–713 (2013).

397. Tiruppathi, C. *et al.* Albumin mediates the transcytosis of myeloperoxidase by means of caveolae in endothelial cells. *Proceedings of the National Academy of Sciences of the United States of America* **101,** 7699–7704 (2004).

398. Sugiyama, S. *et al.* Macrophage Myeloperoxidase Regulation by Granulocyte Macrophage Colony-Stimulating Factor in Human Atherosclerosis and Implications in Acute Coronary Syndromes. *The American Journal of Pathology* **158,** 879–891 (2001).

399. Heinecke, J. W., Li, W., Daehnke, H. L. & Goldstein, J. A. Dityrosine, a specific marker of oxidation, is synthesized by the myeloperoxidase-hydrogen peroxide system of human neutrophils and macrophages. *Journal of Biological Chemistry* **268,** 4069–4077 (1993).

400. Reynolds, J. A. & Tanford, C. Binding of dodecyl sulfate to proteins at high binding ratios. Possible implications for the state of proteins in biological membranes. *Proceedings of the National Academy of Sciences of the United States of America* **66,** 1002–1007 (1970).

401. Griffith, I. P. The effect of cross-links on the mobility of proteins in dodecyl sulphate-polyacrylamide gels. *Biochemical Journal* **126,** 553–560 (1972).

402. Rath, A., Glibowicka, M., Nadeau, V. G., Chen, G. & Deber, C. M. Detergent binding explains anomalous SDS-PAGE migration of membrane proteins. *Proceedings of the National Academy of Sciences of the United States of America* **106,** 1760–1765 (2009).

403. Han, S. W. & Roman, J. Fibronectin induces cell proliferation and inhibits apoptosis in human bronchial epithelial cells: pro-oncogenic effects mediated by PI3-kinase and NF-kappa B. *Oncogene* **25,** 4341–4349 (2006).

404. Wang, J. & Milner, R. Fibronectin promotes brain capillary endothelial cell survival and proliferation through alpha5beta1 and alphavbeta3 integrins via MAP kinase signalling. *Journal of Neurochemistry* **96,** 148–159 (2006).

405. Cao, Y. *et al.* Fibronectin promotes cell proliferation and invasion through mTOR signaling pathway activation in gallbladder cancer. *Cancer Letters* **360,** 141–150 (2015).

406. Ingber, D. E. Fibronectin controls capillary endothelial cell growth by modulating cell shape. *Proceedings of the National Academy of Sciences of the United States of America* **87,** 3579–3583 (1990).

407. Malle, E., Marsche, G., Arnhold, J. & Davies, M. J. Modification of low-density lipoprotein by myeloperoxidase-derived oxidants and reagent hypochlorous acid. *Biochimica et Biophysica Acta - Molecular and Cell Biology of Lipids* **1761,** 392–415 (2006).

408. Klebanoff, S. J., Kettle, A. J., Rosen, H., Winterbourn, C. C. & Nauseef, W. M. Myeloperoxidase: a front-line defender against phagocytosed microorganisms. *Journal of Leukocyte Biology* **93,** 185–198 (2013).

409. Wagner, B. A. *et al.* Role of thiocyanate, bromide and hypobromous acid in hydrogen peroxide-induced apoptosis. *Free Radical Research* **38,** 167–175 (2004).

410. Cook, N. L., Moeke, C. H., Fantoni, L. I., Pattison, D. I. & Davies, M. J. The myeloperoxidase-derived oxidant hypothiocyanous acid inhibits protein tyrosine phosphatases via oxidation of key cysteine residues. *Free Radical Biology and Medicine* **90,** 195–205 (2016).

411. Kettle, A. J. & Winterbourn, C. C. The mechanism of myeloperoxidase-dependent chlorination of monochlorodimedon. *Biochimica et Biophysica Acta (BBA) - Protein Structure and Molecular Enzymology* **957,** 185 –191. ISSN: 0167-4838 (1988).

412. Pulakazhi Venu, V. K. *et al.* Fibronectin extra domain A stabilises atherosclerotic plaques in apolipoprotein E and in LDL-receptor-deficient mice. *Thrombosis and Haemostasis* **114,** 186–197 (2015).

413. Yasuda, T. & Poole, A. R. A fibronectin fragment induces type II collagen degradation by collagenase through an interleukin-1-mediated pathway. *Arthritis and Rheumatism* **46,** 138–148 (2002).

414. Leikina, E, Mertts, M. V., Kuznetsova, N & Leikin, S. Type I collagen is thermally unstable at body temperature. *Proceedings of the National Academy of Sciences of the United States of America* **99,** 1314–1318 (2002).

415. Brodsky, B. & Persikov, A. V. Molecular structure of the collagen triple helix. *Advances in Protein Chemistry* **70,** 301–339 (2005).

416. Dzamba, B. J., Wu, H., Jaenisch, R. & Peters, D. M. Fibronectin binding site in type I collagen regulates fibronectin fibril formation. *Journal of Cell Biology* **121,** 1165–1172 (1993).

417. Li, S., Van Den Diepstraten, C., D'Souza, S. J., Chan, B. M. C. & Pickering, J. G. Vascular smooth muscle cells orchestrate the assembly of type I collagen via alpha2beta1 integrin, RhoA, and fibronectin polymerization. *The American Journal of Pathology* **163,** 1045–1056 (2003).

418. Filla, M. S., Dimeo, K. D., Tong, T. & Peters, D. M. Disruption of fibronectin matrix affects type IV collagen, fibrillin and laminin deposition into extracellular matrix of human trabecular meshwork (HTM) cells. *Experimental Eye Research* **165,** 7–19 (2017).

419. Canty, E. G. & Kadler, K. E. Procollagen trafficking, processing and fibrillogenesis. *Journal of Cell Science* **118,** 1341–1353 (2005).

420. Humphries, S. M., Lu, Y., Canty, E. G. & Kadler, K. E. Active negative control of collagen fibrillogenesis in vivo. Intracellular cleavage of the type I procollagen propeptides in tendon fibroblasts without intracellular fibrils. *Journal of Biological Chemistry* **283,** 12129–12135 (2008).

421. Clark, R. A. F. Fibrin is a many splendored thing. *Journal of Investigative Dermatology* **121,** xxi–xxii (2003).

422. Corbett, S. A., Lee, L, Wilson, C. L. & Schwarzbauer, J. E. Covalent cross-linking of fibronectin to fibrin is required for maximal cell adhesion to a fibronectin-fibrin matrix. *Journal of Biological Chemistry* **272,** 24999–25005 (1997).

423. Watson, S. P. Platelet activation by extracellular matrix proteins in haemostasis and thrombosis. *Current Pharmaceutical Design* **15,** 1358–1372 (2009).

424. Clark, R. A. F., An, J.-Q., Greiling, D., Khan, A. & Schwarzbauer, J. E. Fibroblast migration on fibronectin requires three distinct functional domains. *Journal of Investigative Dermatology* **121,** 695–705 (2003).

425. Clark, R. A. Fibronectin matrix deposition and fibronectin receptor expression in healing and normal skin. *Journal of Investigative Dermatology* **94,** 128S–134S (1990).

426. Ni, H. *et al.* Plasma fibronectin promotes thrombus growth and stability in injured arterioles. *Proceedings of the National Academy of Sciences of the United States of America* **100,** 2415–2419 (2003).

427. Matuskova, J. *et al.* Decreased plasma fibronectin leads to delayed thrombus growth in injured arterioles. *Arteriosclerosis, Thrombosis, and Vascular Biology* **26,** 1391–1396 (2006).

428. Sato, Y *et al.* Proportion of fibrin and platelets differs in thrombi on ruptured and eroded coronary atherosclerotic plaques in humans. *Heart (British Cardiac Society)* **91,** 526–530 (2005).

429. Badimon, L & Vilahur, G. Thrombosis formation on atherosclerotic lesions and plaque rupture. *Journal of Internal Medicine* **276,** 618–632 (2014).

430. Chung, C. Y. & Erickson, H. P. Glycosaminoglycans modulate fibronectin matrix assembly and are essential for matrix incorporation of tenascin-C. *Journal of Cell Science* **110 (Pt 1,** 1413–1419 (1997).

431. Ingham, K. C., Brew, S. A. & Atha, D. H. Interaction of heparin with fibronectin and isolated fibronectin domains. *Biochemical Journal* **272,** 605–611 (1990).

432. Ingham, K. C., Brew, S. A., Migliorini, M. M. & Busby, T. F. Binding of heparin by type III domains and peptides from the carboxy terminal hep-2 region of fibronectin. *Biochemistry* **32,** 12548–12553 (1993).

433. Johansson, S & Hook, M. Heparin enhances the rate of binding of fibronectin to collagen. *Biochemical Journal* **187,** 521–524 (1980).

434. Ambesi, A., Klein, R. M., Pumiglia, K. M. & McKeown-Longo, P. J. Anastellin, a fragment of the first type III repeat of fibronectin, inhibits extracellular signal-regulated kinase and causes G(1) arrest in human microvessel endothelial cells. *Cancer Research* **65,** 148–156 (2005).

435. Ohashi, T. & Erickson, H. P. Domain unfolding plays a role in superfibronectin formation. *Journal of Biological Chemistry* **280,** 39143–39151 (2005).

436. Morla, A, Zhang, Z & Ruoslahti, E. Superfibronectin is a functionally distinct form of fibronectin. *Nature* **367,** 193–196 (1994).

437. Akerman, M. E., Pilch, J., Peters, D. & Ruoslahti, E. Angiostatic peptides use plasma fibronectin to home to angiogenic vasculature. *Proceedings of the National Academy of Sciences of the United States of America* **102,** 2040–2045 (2005).

438. Klein, R. M., Zheng, M., Ambesi, A., Van De Water, L. & McKeown-Longo, P. J. Stimulation of extracellular matrix remodeling by the first type III repeat in fibronectin. *Journal of cell science* **116,** 4663–4674 (2003).

439. Liao, Y.-F., Gotwals, P. J., Koteliansky, V. E., Sheppard, D. & Van De Water, L. The EIIIA segment of fibronectin is a ligand for integrins alpha 9beta 1 and alpha 4beta 1 providing a novel mechanism for regulating cell adhesion by alternative splicing. *Journal of Biological Chemistry* **277,** 14467–14474 (2002).

440. Sechler, J. L. *et al.* A novel fibronectin binding site required for fibronectin fibril growth during matrix assembly. *Journal of Cell Biology* **154,** 1081–1088 (2001).

441. Ohashi, T., Lemmon, C. A. & Erickson, H. P. Fibronectin Conformation and Assembly: Analysis of Fibronectin Deletion Mutants and Fibronectin Glomerulopathy (GFND) Mutants. *Biochemistry* **56,** 4584–4591 (2017).

442. Shinde, A. V. *et al.* Identification of the peptide sequences within the EIIIA (EDA) segment of fibronectin that mediate integrin alpha9beta1-dependent cellular activities. *Journal of Biological Chemistry* **283,** 2858–2870 (2008).

443. Magnuson, V. L. *et al.* The alternative splicing of fibronectin pre-mRNA is altered during aging and in response to growth factors. *Journal of Biological Chemistry* **266,** 14654–14662 (1991).

444. Chauhan, A. K., Iaconcig, A., Baralle, F. E. & Muro, A. F. Alternative splicing of fibronectin: a mouse model demonstrates the identity of in vitro and in vivo systems and the processing autonomy of regulated exons in adult mice. *Gene* **324,** 55–63 (2004).

445. Grazioli, A., Alves, C. S., Konstantopoulos, K. & Yang, J. T. Defective blood vessel development and pericyte/pvSMC distribution in $\alpha 4$ integrin-deficient mouse embryos. *Developmental Biology* **293,** 165–177 (2006).

446. Astrof, S., Crowley, D. & Hynes, R. O. Multiple cardiovascular defects caused by the absence of alternatively spliced segments of fibronectin. *Developmental Biology* **311,** 11–24 (2007).

447. Fukuda, T. *et al.* Mice lacking the EDB segment of fibronectin develop normally but exhibit reduced cell growth and fibronectin matrix assembly in vitro. *Cancer Research* **62,** 5603–5610 (2002).

448. Nybo, T., Rogowska-Wrzesinska, A. & Davies, M. J. YO-08 - Detection and Characterization of Oxidative Modifications to Extracellular Matrix Proteins. *Free Radical Biology and Medicine* **108,** S17 (2017).

449. Phizicky, E. M. & Fields, S. Protein-protein interactions: methods for detection and analysis. *Microbiological Reviews* **59,** 94–123. ISSN: 0146-0749 (Print) (1995).

450. Rao, V. S., Srinivas, K, Sujini, G. N. & Kumar, G. N. S. Protein-protein interaction detection: methods and analysis. *International Journal of proteomics* **2014,** 147648 (2014).

451. Hartl, J., Peschel, A., Johannsmann, D. & Garidel, P. Characterizing protein-protein-interaction in high-concentration monoclonal antibody systems with the quartz crystal microbalance. *Physical Chemistry Chemical Chysics* **19,** 32698–32707 (2017).

452. Leonard, P., Hearty, S. & O'Kennedy, R. Measuring protein-protein interactions using Biacore. *Methods in Molecular Biology* **681,** 403–418 (2011).

453. Justus, C. R., Leffler, N., Ruiz-Echevarria, M. & Yang, L. V. In vitro Cell Migration and Invasion Assays. *Journal of Visualized Experiments* **1** (2014).

454. Liang, C.-C., Park, A. Y. & Guan, J.-L. In vitro scratch assay: a convenient and inexpensive method for analysis of cell migration in vitro. *Nature Protocols* **2,** 329–333 (2007).

455. Chen, H.-C. Boyden chamber assay. *Methods in Molecular Biology* **294,** 15–22 (2005).

456. Frantz, C., Stewart, K. M. & Weaver, V. M. The extracellular matrix at a glance. *Journal of Cell Science* **123,** 4195–4200 (2010).

457. Bezie, Y *et al.* Fibronectin expression and aortic wall elastic modulus in spontaneously hypertensive rats. *Arteriosclerosis, Thrombosis, and Vascular Biology* **18,** 1027–1034 (1998).

458. Martinez-Lemus, L. A., Hill, M. A. & Meininger, G. A. The plastic nature of the vascular wall: a continuum of remodeling events contributing to control of arteriolar diameter and structure. *Physiology* **24,** 45–57 (2009).

459. Ikari, Y, Yee, K. O. & Schwartz, S. M. Role of a5b1 and avb3 Integrins on Smooth Muscle Cell Spreading and Migration in Fibrin Gels. *Thrombosis and Haemostasis* **84,** 701–705 (2000).

460. Pickering, J. G. *et al.* alpha5beta1 integrin expression and luminal edge fibronectin matrix assembly by smooth muscle cells after arterial injury. *The American Journal of Pathology* **156,** 453–465 (2000).

461. Hedin, U, Bottger, B. A., Forsberg, E, Johansson, S & Thyberg, J. Diverse effects of fibronectin and laminin on phenotypic properties of cultured arterial smooth muscle cells. *Journal of Cell Biology* **107,** 307–319 (1988).

462. Hedin, U, Bottger, B. A., Luthman, J, Johansson, S & Thyberg, J. A substrate of the cell-attachment sequence of fibronectin (Arg-Gly-Asp-Ser) is sufficient to promote transition of arterial smooth muscle cells from a contractile to a synthetic phenotype. *Developmental Biology* **133,** 489–501 (1989).

463. Brown, S. L., Lundgren, C. H., Nordt, T & Fujii, S. Stimulation of migration of human aortic smooth muscle cells by vitronectin: implications for atherosclerosis. *Cardiovascular Research* **28,** 1815–1820 (1994).

464. Yue, T. L. *et al.* Osteopontin-stimulated vascular smooth muscle cell migration is mediated by beta 3 integrin. *Experimental Cell Research* **214,** 459–464 (1994).

465. Srivatsa, S. S. *et al.* Selective alpha v beta 3 integrin blockade potently limits neointimal hyperplasia and lumen stenosis following deep coronary arterial stent injury: evidence for the functional importance of integrin alpha v beta 3 and osteopontin expression during neointi. *Cardiovascular Research* **36,** 408–428 (1997).

466. Choi, E. T. *et al.* Inhibition of neointimal hyperplasia by blocking alpha V beta 3 integrin with a small peptide antagonist GpenGRGDSPCA. *Journal of Vascular Surgery* **19,** 125–134 (1994).

467. Slepian, M. J., Massia, S. P., Dehdashti, B, Fritz, A & Whitesell, L. Beta3-integrins rather than beta1-integrins dominate integrin-matrix interactions involved in postinjury smooth muscle cell migration. *Circulation* **97,** 1818–1827 (1998).

468. Hartman, C. D., Isenberg, B. C., Chua, S. G. & Wong, J. Y. Vascular smooth muscle cell durotaxis depends on extracellular matrix composition. *Proceedings of the National Academy of Sciences of the United States of America* **113,** 11190–11195 (2016).

469. Carraher, C. L. & Schwarzbauer, J. E. Regulation of matrix assembly through rigidity-dependent fibronectin conformational changes. *Journal of Biological Chemistry* **288,** 14805–14814 (2013).

470. Roy, J. *et al.* Fibronectin promotes cell cycle entry in smooth muscle cells in primary culture. *Experimental Cell Research* **273,** 169–177 (2002).

471. Asahara, T *et al.* Synergistic effect of vascular endothelial growth factor and basic fibroblast growth factor on angiogenesis in vivo. *Circulation* **92,** II365–71 (1995).

472. Fercana, G. R. *et al.* Perivascular extracellular matrix hydrogels mimic native matrix microarchitecture and promote angiogenesis via basic fibroblast growth factor. *Biomaterials* **123,** 142–154 (2017).

473. Missirlis, D., Haraszti, T., Kessler, H. & Spatz, J. P. Fibronectin promotes directional persistence in fibroblast migration through interactions with both its cell-binding and heparin-binding domains. *Scientific Reports* **7,** 3711 (2017).

474. Hartman, C. D., Isenberg, B. C., Chua, S. G. & Wong, J. Y. Extracellular matrix type modulates cell migration on mechanical gradients. *Experimental Cell Research* **359,** 361–366 (2017).

475. Shinde, A. V. *et al.* The alpha4beta1 integrin and the EDA domain of fibronectin regulate a profibrotic phenotype in dermal fibroblasts. *Matrix Biology* **41,** 26–35 (2015).

476. Desmouliere, A, Geinoz, A, Gabbiani, F & Gabbiani, G. Transforming growth factor-beta 1 induces alpha-smooth muscle actin expression in granulation tissue myofibroblasts and in quiescent and growing cultured fibroblasts. *Journal of Cell Biology* **122,** 103–111 (1993).

477. Serini, G *et al.* The fibronectin domain ED-A is crucial for myofibroblastic phenotype induction by transforming growth factor-beta1. *Journal of Cell Biology* **142,** 873–881 (1998).

478. Shih, P. T. *et al.* Minimally modified low-density lipoprotein induces monocyte adhesion to endothelial connecting segment-1 by activating beta1 integrin. *Journal of Clinical Investigation* **103,** 613–625 (1999).

479. Dutta, B. *et al.* Monocyte adhesion to atherosclerotic matrix proteins is enhanced by Asn-Gly-Arg deamidation. *Scientific Reports* **7,** 5765 (2017).

480. Huo, Y, Hafezi-Moghadam, A & Ley, K. Role of vascular cell adhesion molecule-1 and fibronectin connecting segment-1 in monocyte rolling and adhesion on early atherosclerotic lesions. *Circulation Research* **87,** 153–159 (2000).

481. Barringhaus, K. G. *et al.* Alpha4beta1 integrin (VLA-4) blockade attenuates both early and late leukocyte recruitment and neointimal growth following carotid injury in apolipoprotein E (-/-) mice. *Journal of Vascular Research* **41,** 252–260 (2004).

482. Yakubenko, V. P. *et al.* The role of integrin alpha D beta2 (CD11d/CD18) in monocyte/macrophage migration. *Experimental Cell Research* **314,** 2569–2578 (2008).

483. Oakes, P. W. *et al.* Neutrophil morphology and migration are affected by substrate elasticity. *Blood* **114,** 1387–1395 (2009).

484. Stroka, K. M. & Aranda-Espinoza, H. Neutrophils display biphasic relationship between migration and substrate stiffness. *Cell Motility and the Cytoskeleton* **66,** 328–341 (2009).

485. Spring, B. *et al.* Healthy lifestyle change and subclinical atherosclerosis in young adults: Coronary Artery Risk Development in Young Adults (CARDIA) study. *Circulation* **130,** 10–17 (2014).

486. Ornish, D *et al.* Can lifestyle changes reverse coronary heart disease? The Lifestyle Heart Trial. *Lancet* **336,** 129–133 (1990).

487. Ye, Y., Li, J. & Yuan, Z. Effect of antioxidant vitamin supplementation on cardiovascular outcomes: a meta-analysis of randomized controlled trials. *PLoS One* **8,** e56803 (2013).

488. Wilson, J. Cyanide in human disease: a review of clinical and laboratory evidence. *Fundamental and Applied Toxicology* **3,** 397–399 (1983).

489. Cipollone, R., Ascenzi, P., Tomao, P., Imperi, F. & Visca, P. Enzymatic detoxification of cyanide: clues from Pseudomonas aeruginosa Rhodanese. *Journal of Molecular Microbiology and Diotechnology* **15,** 199–211 (2008).

490. Botti, T. P., Amin, H, Hiltscher, L & Wissler, R. W. A comparison of the quantitation of macrophage foam cell populations and the extent of apolipoprotein E deposition in developing atherosclerotic lesions in young people: high and low serum thiocyanate groups as an indication of smoking. PDAY Research Grou. *Atherosclerosis* **124,** 191–202 (1996).

491. Kamceva, G. *et al.* Cigarette Smoking and Oxidative Stress in Patients with Coronary Artery Disease. *Open access Macedonian Journal of Medical Sciences* **4,** 636–640 (2016).

492. Hadfield, K. A. *et al.* Myeloperoxidase-derived oxidants modify apolipoprotein A-I and generate dysfunctional high-density lipoproteins: comparison of hypothiocyanous acid (HOSCN) with hypochlorous acid (HOCl). *Biochemical Journal* **449,** 531–542 (2013).

493. Requejo, R., Hurd, T. R., Costa, N. J. & Murphy, M. P. Cysteine residues exposed on protein surfaces are the dominant intramitochondrial thiol and may protect against oxidative damage. *The FEBS Journal* **277,** 1465–1480 (2010).

494. Burns, C. B. & Godwin, I. R. A comparison of the effects of inorganic and alkyllead compounds on human erythrocytic delta-aminolevulinic acid dehydratase (ALAD) activity in vitro. *Journal of Applied Toxicology* **11,** 103–110 (1991).

495. Davies, M. J. The oxidative environment and protein damage. *Biochimica et Biophysica Acta - Proteins and Proteomics* **1703,** 93–109 (2005).

496. Levine, G. N. *et al.* 2011 ACCF/AHA/SCAI Guideline for Percutaneous Coronary Intervention: a report of the American College of Cardiology Foundation/American Heart Association Task Force on Practice Guidelines and the Society for Cardiovascular Angiography and Interventions. *Circulation* **124,** e574–651 (2011).

497. Alexander, J. H. & Smith, P. K. Coronary-Artery Bypass Grafting. *The New England Journal of Medicine* **374,** 1954–1964 (2016).

498. Carroll, L. *et al.* Reactivity of selenium-containing compounds with myeloperoxidase-derived chlorinating oxidants: Second-order rate constants and implications for biological damage. *Free Radical Biology and Medicine* **84,** 279–288 (2015).

499. Frangogiannis, N. G., Smith, C. W. & Entman, M. L. The inflammatory response in myocardial infarction. *Cardiovascular Research* **53,** 31–47 (2002).

500. Nahrendorf, M. *et al.* Dual channel optical tomographic imaging of leukocyte recruitment and protease activity in the healing myocardial infarct. *Circulation Research* **100,** 1218–1225 (2007).

501. Iwata, A., Morrison, M. L. & Roth, M. B. Iodide protects heart tissue from reperfusion injury. *PLoS One* **9,** e112458 (2014).

502. Storkey, C., Davies, M. J., White, J. M. & Schiesser, C. H. Synthesis and antioxidant capacity of 5-selenopyranose derivatives. *Chemical Communications* **47,** 9693–9695 (2011).

503. Assmann, A, Briviba, K & Sies, H. Reduction of methionine selenoxide to selenomethionine by glutathione. *Archives of Biochemistry and Biophysics* **349,** 201–203 (1998).

504. Krause, R. J. & Elfarra, A. A. Reduction of L-methionine selenoxide to seleno-L-methionine by endogenous thiols, ascorbic acid, or methimazole. *Biochemical Pharmacology* **77,** 134–140 (2009).

505. Kumakura, F., Mishra, B., Priyadarsini, K. I. & Iwaoka, M. A Water-Soluble Cyclic Selenide with Enhanced Glutathione Peroxidase-Like Catalytic Activities. *European Journal of Organic Chemistry* **2010,** 440–445 (2010).

506. Forbes, L. V. *et al.* Potent reversible inhibition of myeloperoxidase by aromatic hydroxamates. *Journal of Biological Chemistry* **288,** 36636–36647 (2013).

507. Zheng, W. *et al.* PF-1355, a mechanism-based myeloperoxidase inhibitor, prevents immune complex vasculitis and anti-glomerular basement membrane glomerulonephritis. *Journal of Pharmacology and Experimental Therapeutics* **353,** 288–298 (2015).

508. Lazarevic-Pasti, T., Leskovac, A. & Vasic, V. Myeloperoxidase Inhibitors as Potential Drugs. *Current Drug Metabolism* **16,** 168–190 (2015).

509. Desikan, R., Narasimhulu, C. A., Khan, B., Rajagopalan, S. & Parthasarathy, S. in *Mechanisms of Vascular Defects in Diabetes Mellitus* 535–571 (2017).

510. Kettle, A. J., Gedye, C. A., Hampton, M. B. & Winterbourn, C. C. Inhibition of myeloperoxidase by benzoic acid hydrazides. *Biochemical Journal* **308 (Pt 2,** 559–563 (1995).